UNC-WRRI-2000-328

GEOCHEMICAL TRACERS OF GROUNDWATER MOVEMENT BETWEEN THE CASTLE HAYNE AND ASSOCIATED COASTAL PLAIN AQUIFERS

by
Terri L. Woods, E. Glynn Beck, Delynda T. Tolen-Mehlhop, Rae Troiano and
J. Kevin Whitley

Department of Geology
East Carolina University
Greenville, NC 27858-4353

The research on which this report is based was financed by the Water Resources Research Institute of The University of North Carolina.

WRRI Project No. 70148

February 2000

One hundred fifty copies of this report were printed at a cost of $1677.95 or $10.83 per copy.

ACKNOWLEDGMENT

This project could not have been completed without the help of a great many people besides the graduate student coauthors. Jim Watson and John Woods provided invaluable technical help throughout the past 3 years. Steve Campbell, Curtis Consolvo, Paul Fullagar, Richard Mauger, Don Neal, Charles O'Rear, Stan Riggs, Art Spivak, Richard Spruill, and Lynn Sutton provided ideas, discussed problems and results, and reviewed parts of the proposal and this manuscript. The Geology Department contributed substantial financial, vehicular, equipment, and human resources. Without the guidance and patience of Debbie Daniels in the Environmental Chemistry Laboratory of the Biology Department at ECU, many of these analyses would never have been completed. I also wish to acknowledge the contributions of the following undergraduate students; Anna Hilting, Holly Land, Mark Rollog, and Allison DeBastiani. Finally, I am especially grateful to the WRRI staff and reviewers whose patient reading and careful comments have substantially improved the quality of this document.

ABSTRACT

Water from wells penetrating the Upper Castle Hayne (UCH), Yorktown (YK), Peedee (PD), and other aquifers was analyzed for major and minor elements, and Sr, C, and O isotopes. Dissolution of aquifer material and closer proximity to the saltwater/freshwater interface causes an eastward increase in many concentrations. Ion exchange with aquifer minerals and mixing with water from other aquifers and surface water also affect water chemistry.

$^{87}Sr/^{86}Sr$ ratios of water from the UCH, YK, and PD are 0.708104-0.709269, 0.709111-0.709200, and 0.708202-0.708752, respectively. Sr chemistry approaches that of the host aquifer downgradient. $\delta^{18}O$ of UCH groundwater varies from -5.28 o/oo to -3.12 o/oo reflecting the composition of groundwater recharged during the last glacial maximum. $\delta^{13}C$ in the UCH increases eastward (-16.29 o/oo to -3.36 o/oo) approaching the value for marine carbonates.

Chemical and mineralogical analysis of the Castle Hayne showed it to be a moldic, fossiliferous limestone dominated by calcite and quartz with minor Fe-rich glauconite, dolomite, and phosphate.

KEYWORDS: Castle Hayne aquifer, Yorktown aquifer, and Peedee aquifer, $^{87}Sr/^{86}Sr$ ratios, $\delta^{18}O$, $\delta^{13}C$, limestone aquifer, hydrogeochemistry

TABLE OF CONTENTS

LIST OF FIGURES

LIST OF TABLES

SUMMARY AND CONCLUSIONS

GROUNDWATER STUDY OF THE CASTLE HAYNE AQUIFER

Major and Minor Element Chemistry

Variation in water chemistry of the Castle Hayne Aquifer (CHAS) throughout the Coastal Plain south of Albemarle Sound was described by extending the previous study of Sutton and Woods (1995) southward to Jones, Carteret, Duplin, Onslow, Pender, New Hanover, and Brunswick Counties.

Sodium, Cl, and SO_4 generally increase from west to east.

Alkalinity increases from southwest to northeast with some distinctly higher values in the northeastern region.

Magnesium generally increases from west to east but decreases abruptly near Lake Phelps, where alkalinity is unusually high.

The pattern of Ca concentrations is complex, showing first an increase in the far western regions, then a decrease near Lake Phelps followed by increasing concentrations in the easternmost region.

Western wells in the Upper Castle Hayne Aquifer (U-CHAS) are Ca and bicarbonate rich and easternmost wells are alkali and Cl rich. Water from wells in the U-CHAS, affected by heavy pumping at Aurora, is dominated by mixed cations and bicarbonate. An U-CHAS well in the northeast is alkali and bicarbonate rich.

Graphs of various major ion concentrations versus Total Dissolved Solids (TDS) reveal three groups of groundwaters in the U-CHAS whose chemical compositions are determined by different geochemical and hydrologic processes. TDS ranges for low-, intermediate-, and high-TDS groups are 310-640 ppm, 950-970 ppm, and 1290-4690 ppm, respectively.

In the U-CHAS, the boundary of regions dominated by low-TDS, Ca and bicarbonate waters generally coincides with the eastern limit of the recharge area.

Isotopes

Investigation of the strontium chemistry of waters from the Castle Hayne and other aquifers in the Northern Coastal Plain indicates that strontium and its isotopes will be useful tracers of groundwater mixing and evolution.

Groundwater from the largely marine Coastal Plain aquifers shows an increase in $^{87}Sr/^{86}Sr$ ratio with decreasing age of the aquifers, as predicted by the evolution in seawater $^{87}Sr/^{86}Sr$ ratio through time.

$^{87}Sr/^{86}Sr$ ratios and Sr concentrations in the U-CHAS range from 0.708104 - 0.709263 and 0.242 - 3.095ppm, respectively. The general pattern of decreasing ratios from west to east suggests that dissolution of, or exchange with, aquifer minerals is gradually raising Sr contents and isotopic ratios to that of the host aquifer (≈0.70775).

The $^{87}Sr/^{86}Sr$ ratios of groundwater from the Castle Hayne, Yorktown, and Pungo River Aquifers plot above theoretical mixing lines calculated by combining strontium-poor recharge waters with aquifer strontium in various proportions, suggesting significant downward leakage of water. Groundwater from the western recharge area shows the most extensive geochemical influence of this leakage. Groundwater from the eastern, deeper portions of the aquifer shows less influence of downward leakage and more evidence of progressive acquisition of aquifer strontium, perhaps accompanied by mixing at the salt water/fresh water interface.

Preliminary analysis of C and O isotopes and organic carbon in groundwater from the Northern Coastal Plain suggests that these parameters will be very useful for unraveling the processes of groundwater evolution downgradient, and for identifying regions where leakage from other aquifers is affecting groundwater chemistry.

$\delta^{13}C$ values for the U-CHAS and L-CHAS vary from -3.36 to -16.29 o/oo and -2.61 to -12.00 o/oo, respectively. $\delta^{13}C$ values generally become more positive from west to east. The dissolved inorganic carbon in CHAS groundwater in the recharge area acquires its strongly negative $\delta^{13}C$ signature by incorporation of carbon released from decaying organic matter. The $\delta^{13}C$ of CHAS groundwater approaches the value for marine Phanerozoic

carbonates (≈0 o/oo) as residence time in the aquifer increases. Local disruption of this pattern appears to be related to leakage of water into the CHAS from the surface or from adjacent aquifers.

$\delta^{18}O$ values for the U-CHAS and L-CHAS vary from -3.12 to -5.28 o/oo and from -3.61 to -4.65 o/oo, respectively. In the CHAS the values generally become more positive to the east, but local interruptions of this trend occur. The general trend suggests that CHAS groundwater preserves the oxygen isotopic signature of meteoric water that recharged the aquifer during the last glacial maximum.

Total organic carbon in the U-CHAS and L-CHAS varies from 0.41-4.18 mgC/L and 1.78-3.28 mgC/L, respectively. The pattern of variation is complex and problematic.

Hydrologic and geochemical processes affecting CHAS groundwater chemistry

The major geochemical processes determining U-CHAS groundwater compositions are: (1) dissolution of aquifer minerals, (2) leakage of water from overlying aquifers and surface waters, (3) mixing along the salt water/fresh water interface, (4) intermixing of saltier groundwater from underlying aquifers, (5) exchange with aquifer minerals, (6) dissolution of salts from soils.

Western, low-TDS, Ca and bicarbonate rich waters are dominated by dissolution/precipitation reactions involving aquifer carbonates, mainly calcite.

Eastern, high-TDS, alkali and Cl rich waters are heavily influenced by mixing with saline formation waters, especially near heavily pumped wells supplying municipalities.

Along the coast old river channels such as that of the paleo-White Oak River under Bogue Banks appear to allow seawater to move inland more readily than other deposits.

Ion exchange reactions affect compositions throughout the study area, interacting complexly with other geochemical processes.

Dissolution of soil salts, ion exchange, and microbially mediated redox reactions in surficial materials add

small concentrations of Na, Cl, and Fe to recharge waters.

YORKTOWN AND PEEDEE GROUNDWATER CHEMISTRY STUDY

Preliminary chemical characterization of groundwater in the Yorktown and Peedee Aquifers suggest the following trends.

Yorktown

In general cation concentrations increase from west to east, however, contour lines are quite irregular and there are isolated highs and lows, especially in the center of the region between Albemarle Sound and the Pamlico River.

Alkalinity and Cl tend to increase towards the coast, but the pattern of sulfate variation is unclear.

Cations are mixed or dominated by alkalis and anions are mixed or, more frequently, dominated by HCO_3^-.

Contours seem to be significantly influenced by the locations of surface bodies of fresh water -- much more so than contours for the deeper aquifers.

Intermixed salt water dominates compositions to the east. Wells located where inlets used to be, such as at Bodie Island, can be extremely saline.

Strontium concentrations and $^{87}Sr/^{86}Sr$ ratios vary from 0.427-6.951 ppm and 0.709111-0.709200, respectively.

The pattern of variation in $\delta^{18}O$ is complex, but values vary from -3.74 o/oo to -5.04 o/oo.

Yorktown $\delta^{13}C$ values fall between -15.28 o/oo and -4.38 o/oo, becoming more positive from southwest to northeast.

Total organic carbon contents in the Yorktown range from 0.32-1.88 mg C/L, but the pattern of geographic variation is unclear.

Peedee

Concentrations of Ca show the most complex pattern of geographic variation with a region of high

concentrations near Kinston, between two regions of lower Ca.

Mg, Na, and K increase from southwest to northeast.

Major anion concentrations increase steadily from southwest to northeast, although Cl and sulfate increase abruptly halfway across the study area.

Peedee waters are either Ca rich and HCO_3 rich, alkali rich and HCO_3 rich, or alkali and Cl rich with the latter occurring farther to the east.

Strontium concentrations and $^{87}Sr/^{86}Sr$ ratios for waters vary from 0.141-6.157 ppm and 0.708202-0.708752, respectively.

CHAS ROCK MINERAL AND MINERAL CHEMISTRY STUDY

The information presented provides a preliminary description of the mineralogy and mineral chemistry of the CHAS in the Northern Coastal Plain. Mineral abundances, chemistries and patterns of variation will permit more realistic geochemical modeling of processes that affect water chemistry along flowpaths.

Lithology

The CHAS is dominantly composed of quartz glauconitic biomicrite and contains zones of quartz sand, glauconite, phosphate, dolomite, pyrite, feldspar, and minor zeolites.

Mollusks and echinoderm fragments are the dominant bioclasts while brachiopods, bryozoans, and foraminifera are present.

Fossils are frequently dissolved, leaving zones of high moldic porosity.

Diagenesis

The micrite matrix is commonly aggradding to microsparite due to burial and diagenesis.

Dolomite is found in low abundance in both the upper and lower portions of the CHAS, but is slightly more pervasive north of the Pamlico River.

The paucity of dolomite suggests that it is a secondary diagenetic mineral of replacement origin.

Some dolomite rhombohedra have been replaced by silica during diagenesis.

Lateral Trends

The dominant lateral trend in the study area is changing lithofacies and chemistry from southwest to northeast.

The total number of bioclasts increases from east to west and slightly from north to south in the study area.

Glauconite content generally increases from southwest to northeast.

Average octahedral Al and Mg content of glauconite increase from southwest to northeast while average octahedral Fe content decreases. Octahedral Al and Fe content are inversely related to each other while Mg content is less variable.

Vertical Trends

The dominant vertical trend in the study area is changing lithofacies from sandy, glauconitic limestone in the lower CHAS to shelly lime mud in the upper CHAS. The proposed boundary between the upper and lower CHAS is noted both lithologically and geochemically. More micrite mud, bioclasts and dolomite with minor amounts of glauconite, phosphate, and iron sulfide characterize the upper CHAS. The lower CHAS is arenaceous with glauconite and lesser amounts of phosphate, dolomite and iron sulfide.

Complete sections of the aquifer from the three northeastern wells, show very similar changes in lithology and glauconite chemistry with depth. In the two southwest wells, Fe content in glauconite increases initially in the upper CHAS before it decreases. Iron content in glauconite increases with depth in the lower CHAS in wells WH-T2-78 and BF-T5-67. Trends of increasing and decreasing Fe, Al, and Mg in the octahedral site of glauconite suggest similar geochemical environments with changing environments of deposition in the upper and lower CHAS.

Environment of Deposition

As indicated by the bioclast assemblage of mollusks, echinoderms, bryozoan, brachiopods, and foraminifera, CHAS sediments were deposited on the middle to outer shelf during sea level transgressions and regressions.

The occurrence of glaucony and phosphate in localized zones is suggestive of low sedimentation during sea level low-stands.

The southwest region was closer to shore with shallower, more agitated waters, indicated by the presence of more bioclasts and quartz sand and less glauconite.

The northeast region was further offshore in deeper water on the shelf, indicated by the presence of more micrite mud and glauconite and fewer bioclasts.

Quartz sand is most pervasive in the lower CHAS suggesting a stronger sediment influx during deposition of that unit. Micrite mud is more abundant in the upper CHAS possibly due to lower energy and higher sea level.

Data suggest that trends in glauconite chemistry correlate with changes in lithofacies. These trends are most likely related to the conditions and chemistries in the original environment of deposition.

RECOMMENDATIONS

In view of the rapidly increasing demand for water in the Coastal Plain of North Carolina the following topics need to be investigated:

-The regional variation in the chemistry of groundwater in the Yorktown, Peedee, Black Creek, and Cape Fear Aquifers needs to be elucidated.
For the Yorktown, special attention should be paid to the impact of bodies of surface water on groundwater chemistry.

-Underground storage of surface water is being suggested in some regions to help meet increasing demand. This will require preliminary information on the mineralogy and mineral chemistry of the Yorktown, Peedee, Black Creek, and Cape Fear aquifers. Such information is necessary in order to predict the effects on water quality of interactions between aquifer materials and stored water.

-Now that chemical and isotopic signatures are available for groundwater from the Castle Hayne and some other aquifers, studies of the extent of vertical mixing between aquifers should be pursued.

-In light of the expanding use of reverse osmosis for desalinization of water in coastal areas, sources of saline formation water leaking into coastal aquifers should be identified and quantified.

The North Carolina DEHNR could greatly facilitate collection of this information by:

-determining accurate latitudes and longitudes for their monitoring wells, as well as those in the USGS and other networks,

-evaluating the physical condition of wells in their monitoring network and repairing or reinstalling damaged wells located in critical areas,

-accurately determining the aquifers in which the wells in their monitoring network are screened in light of all the new lithologic and geophysical information that has been collected for Coastal Plain formations since the wells were installed,

Locations of paleo-river channels in coastal regions should be determined because these old river channels (such as the paleo-White Oak River under Bogue Banks) appear to allow seawater to move inland more readily than other deposits along the coast.

-For the same reason the locations of old tidal inlets (such as at Bodie Island) along the Outer Banks should be determined.

The possibility that recharge of acidic, organic-rich waters from swamps, lakes, and water-logged soils into deeper aquifers is occurring in some places should be investigated, as this process can significantly affect water quality.

High-iron content is one of the most expensive water quality issues to deal with. Therefore, the processes causing rapid changes in the iron content of aquifers in their recharge areas should be investigated.

To enhance economic development, a study of the effect of water quality on water-intensive industries such as fish farming should be undertaken.

Because of the now extensive chemical and strontium isotopic information available for the Castle Hayne Aquifer, the paleoclimate implications of carbon and oxygen isotopic data recently collected should be pursued.

INTRODUCTION

Rivers and the Cretaceous aquifers are currently major sources of water in the Coastal Plain of North Carolina (Figure 1) (Winner and Lyke 1989). Significant water-level declines in the Cretaceous aquifers (i.e., Peedee, Black Creek, and Cape Fear) (Lyke and Brockman 1990, Giese et al. 1991) will drive increased exploitation of the Castle Hayne and other Cenozoic aquifers. Adequate chemical and hydrologic data are necessary for prudent management of this resource. This investigation focused on the Castle Hayne Aquifer, the most productive in the area (Winner and Lyke 1986), already extensively developed for industrial uses, and fast-becoming an important source for public water supply. For convenience, and to avoid confusion, the Coastal Plain has been divided into three regions; Northeastern, Northwestern, and Southwestern (Figure 2).

A preliminary study provided basic chemical and strontium isotopic signatures for waters from the Castle Hayne, a marine limestone of Eocene-Oligocene age (Sutton and Woods 1994, Woods et al. 1994, and Sutton and Woods 1995). Concentrations of SO_4, Cl, Sr, Ca, and Mg, alkalinities, and strontium isotopic ratios could not be completely explained by dissolution of aquifer materials along flow paths. Leakage into the Castle Hayne from underlying and overlying units appears to have a significant impact on water chemistry. This study confirms previous results that indicate mixing within the Castle Hayne of freshwater and water with a dissolved salt composition similar to that of sea water [Lloyd and Daniel 1988, Harned et al. 1989, Sherwani 1980, Sutton and Woods 1995]. Sources of this salty water have not previously been identified. One major objective of this research was to identify and characterize the various waters entering the Castle Hayne so the chemical and strontium isotopic signature of groundwater from the Pliocene Yorktown and Upper Cretaceous Peedee were studied. There is very little open literature on the water chemistry of these aquifers, but previous data were evaluated along with samples collected for this study. By elucidating the chemical and Sr-isotopic signatures of groundwater from these formations, and studying paths of groundwater flow, mass balance calculations can ultimately be used to track water movement between aquifers.

HYDROGEOLOGIC FRAMEWORK

The Cenozoic and Upper Cretaceous formations of the North Carolina Coastal Plain include sands, silts, clays, and limestones that dip and thicken eastward (Figures 3 and 4). Sands and limestones are the aquifers and silt and clay layers

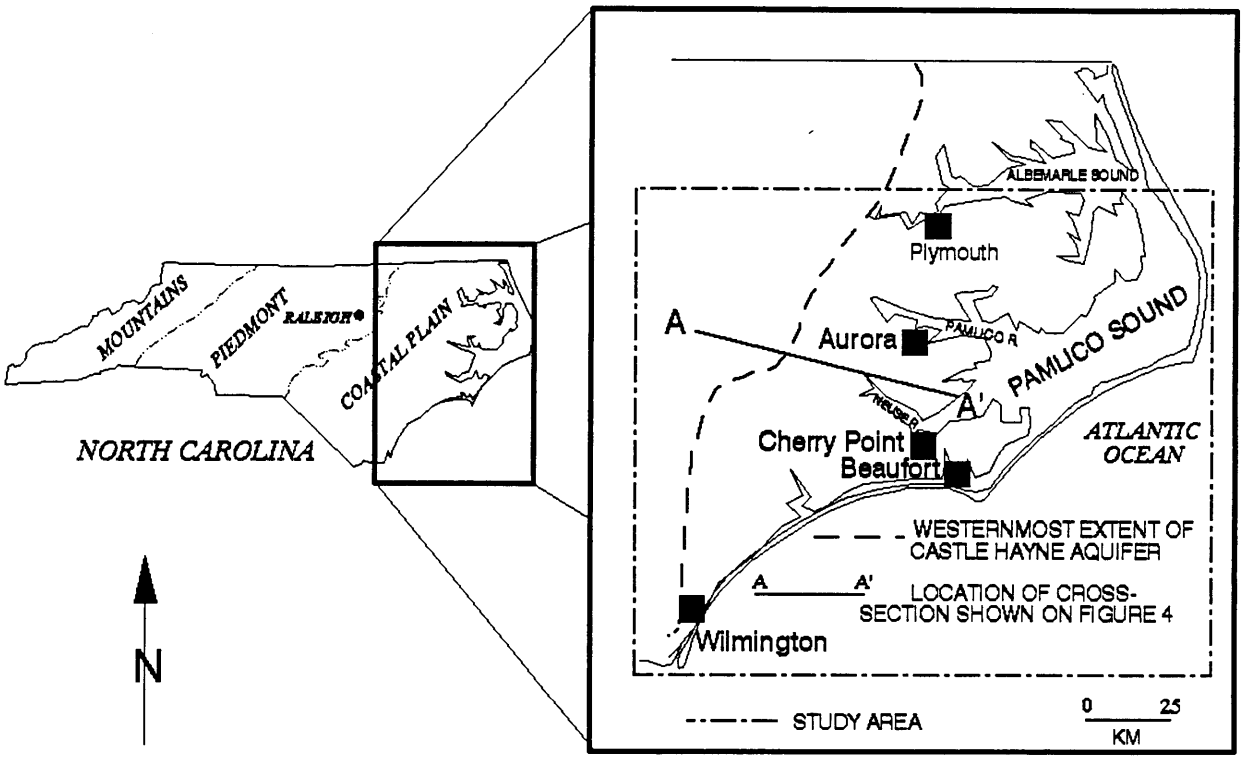

Figure 1. Location of study area and hydrogeologic cross-section shown in Figure 4

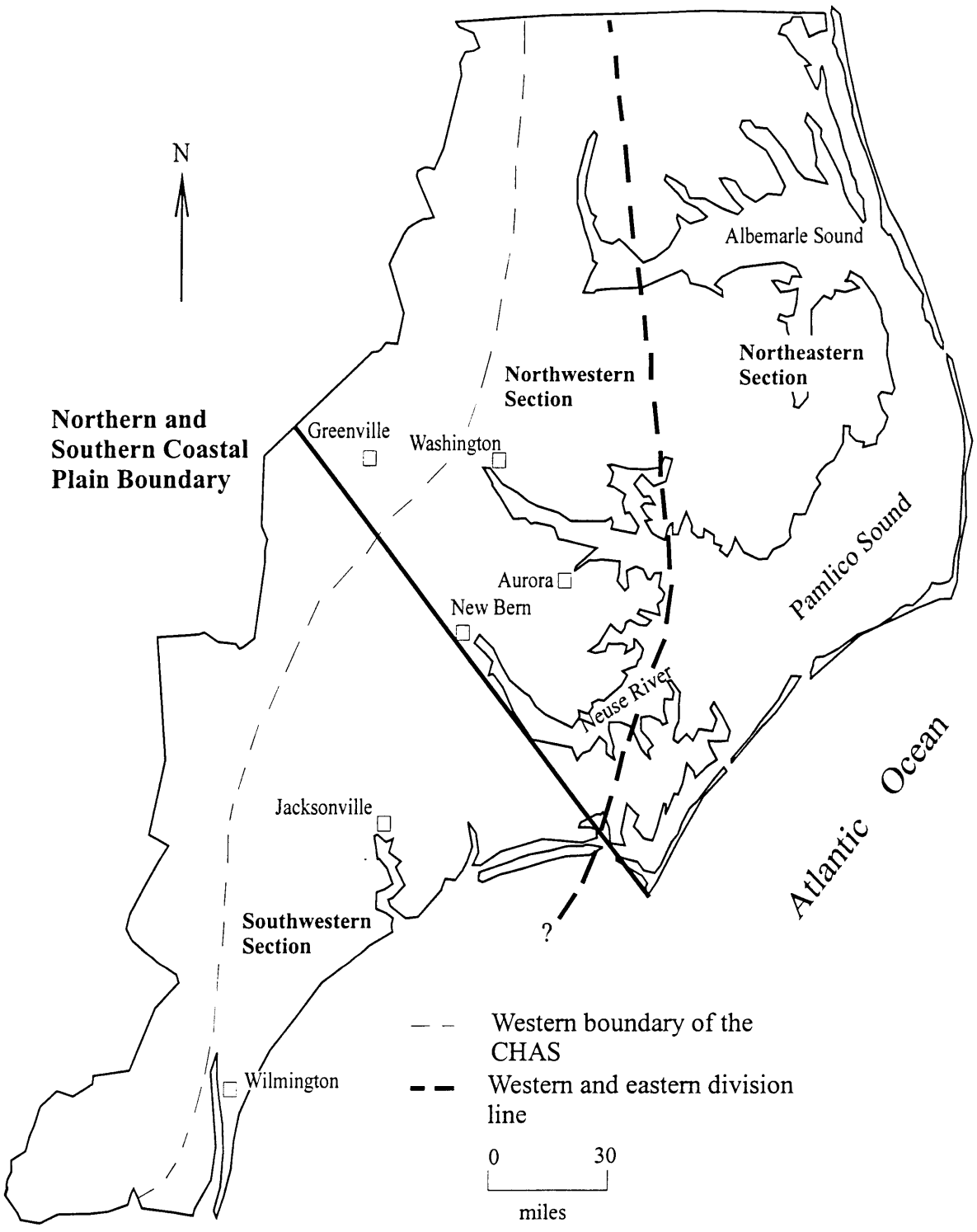

Figure 2. Areal extent of the CHAS and its subdivisions of the Coastal Plain [modified from Giese and others (1991)]

System	Series	Stratigraphic Units	Hydrogeologic Units		Description
Quaternary	Recent Pleistocene	Undifferentiated Unnamed Unit	Post-Miocene Unit		Sand, silt, shells, and some clay
Tertiary	Pliocene	Yorktown Formation	Yorktown Unit		Interbedded sand and clay with some shell beds
	Miocene	Pungo River Formation	Pungo River Unit		Phosphate and quartz sand, silt, clay, and limestone
	Oligocene	Belgrade Fm.	Castle Hayne Aquifer System	Upper Castle Hayne Unit	Permeable and porous shell limestone
		River Bend Fm.			
	Eocene	Castle Hayne Limestone		Lower Castle Hayne Unit	Shell limestone interbedded with calcareous sands
	Paleocene	Beaufort Formation		Beaufort Unit	Fine glauconitic sand, silty and clayey in part
Cretaceous	Upper Cretaceous	Peedee Formation	Peedee Unit		Sand interbedded with clay and silt
		Black Creek Formation	Black Creek Unit		Laminated clay with interbedded sand
		Cape Fear Formation	Upper Cape Fear Unit		Alternating beds of sand and clay
			Lower Cape Fear Unit		Fine sand
	Lower Cretaceous	Unnamed Formation	Lower Cretaceous Unit		Sand, shale, gravel and limestone
Basement					

Figure 3. Stratigraphy and hydrogeology of Coastal Plain formations [modified from Gamus (1972), Lloyd & Daniel (1988), and Winner & Coble (1996)]

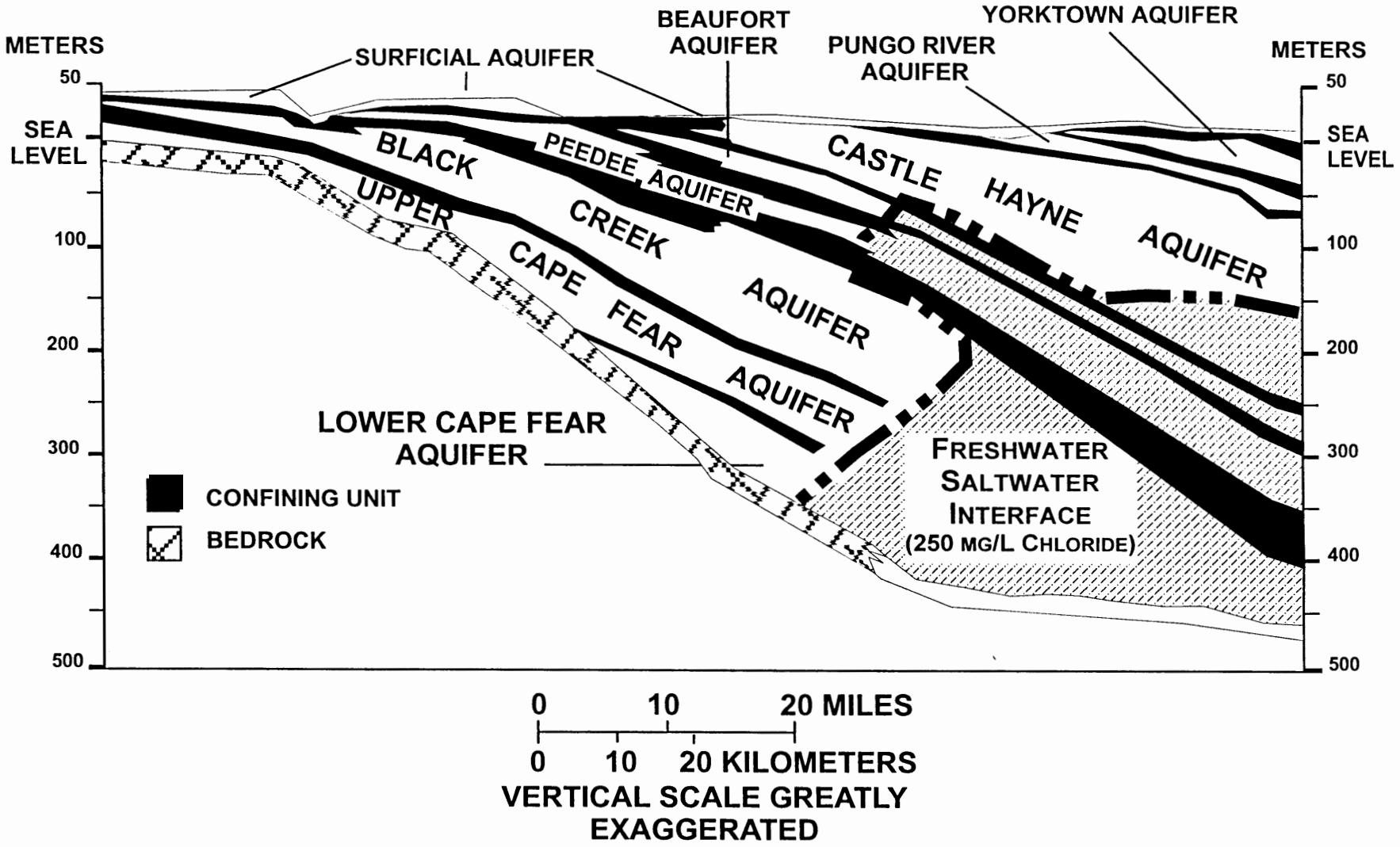

Figure 4. Hydrogeologic cross-section of the Neuse River area (Modified after Smith et al., 1996).
Location of cross-section is shown on Figure 1.

are the confining beds. The Pliocene Yorktown, Eocene-Oligocene Castle Hayne, and Upper Cretaceous Peedee are the main aquifer systems studied during this investigation.

The Castle Hayne is the most extensively developed aquifer in North Carolina (Lyke and Treece 1988). Withdrawals of 146 million gallons per day (mgd), are dominated by pumping at a large phosphate mine in Aurora (Figure 1). In the northern Coastal Plain the Upper Castle Hayne Aquifer (U-CHAS) is predominantly well-indurated mold and cast limestone with minor dolomite, quartz, and glauconite, whereas the Lower Castle Hayne Aquifer (L-CHAS) is a weakly consolidated, sandy limestone containing some dolomite (Gamus 1972). Other minerals include Ca phosphates, pyrite, zeolites, hematite, and limonite (Moran 1989; Otte 1981 and 1986; Ward et al. 1978). Amsbaugh (1996) described the U-CHAS in the central part of the study area as quartz-rich (40-60%), fossiliferous biosparrudite, with minor glauconitic and phosphatic sand. He found the L-CHAS to be a quartz-rich (20-60%), fossiliferous biomicrudite, with minor glauconitic and phosphatic sand and lime mud. A well sorted, fine-grained, calcareous, muddy-limy quartz sand wedge was used as the boundary between the U-CHAS and L-CHAS (Amsbaugh 1996). The CHAS in the Southwestern Coastal Plain is characterized as a moldic and bryozoan-rich limestone, grading to calcareous fine-grained sandstone in the deeper subsurface (Lautier 1994).

Gamus (1972) divided the CHAS into three hydrologic units: the U-CHAS, the L-CHAS, and the Beaufort; more recent workers (Winner and Coble 1996, Giese et al. 1991) consider the Beaufort to be a separate aquifer (Figure 3). The Beaufort differs significantly from the Castle Hayne and is dominated by fine- to medium-grained glauconitic sand, clayey sand and clay, with occasional shell and limestone beds (Gamus 1972, Harris and Zullo 1991). Few wells penetrate the L-CHAS and almost none penetrate the Beaufort, few data on their water chemistries are available and, therefore, for this report, the Beaufort will be considered part of the L-CHAS.

The hydrology of the Castle Hayne Aquifer is influenced by several other units (Giese et al. 1991) (Figure 4). In the study area, the Castle Hayne is typically overlain by the Pungo River or Yorktown Formations. Both units, especially the Pungo River, are characterized by much lower permeabilities than the Castle Hayne (Giese et al. 1991) and thus act as confining layers. In some areas the Castle Hayne is in direct contact with the Surficial Aquifer; (Warner 1993) and (Amsbaugh 1996) have noted downward leakage into the Castle Hayne. The upper lithologic unit of the U-CHAS acts as a confining layer but is thin and contains large amounts of sand which may allow significant leakage between the Castle Hayne and overlying aquifers. The

underlying Cretaceous aquifers are also possible sources of leakage into the Castle Hayne (Giese et al. 1991).

The CHAS is recharged downdip where the confining beds are thin, absent, or of higher hydraulic conductivity (Giese et al. 1991) as well as in the western region where the aquifer is essentially unconfined or reaches the surface. Outcrop locations (Otte 1986) and areas of thin or absent confining units (Giese et al. 1991, DeWiest 1969) were used in this study to estimate approximate boundaries for the recharge area (Figure 5). The recharge area in the Southwestern Coastal Plain extends out to sea which allows much more influx of saline water than in the Northwestern Coastal Plain. DeWiest (1969) suggested that the area of direct recharge covers approximately 290 square miles and roughly coincides with the subcrop pattern for the CHAS. Sherwani (1980) estimates that direct recharge to the aquifer is 20 mgd north of the Pamlico River and 45 mgd south of the Pamlico River.

The Yorktown is dominated by silty to clayey or shelly sands and fine sands; silts and shelly silts; and clays (Ward et al. 1991). The sand fraction is dominated by quartz and the clay fraction by glauconite; phosphatic sands and fossil debris are locally abundant. The Pungo River is composed of fine- to medium-grained marine sands, some highly phosphatic. The sand-sized fraction includes quartz, phosphate and carbonates. Locally beds of limestone, coarse sand, dolosilt, carbonate mud, glauconite, and fossils occur (Ames 1994, Riggs et al. 1982). The Peedee consists dominantly of calcareous muddy sands and calcareous muds (Sohl and Owens 1991). Less clayey sands and sandy limestones occur locally. Quartz dominates the sand fraction and feldspar makes up 10-20%. Clay minerals are kaolinite, illite, and smectite.

Winner and Coble (1996) and Giese et al. (1991) compiled and analyzed data on sedimentology, stratigraphy, and groundwater flow in the aquifers of the North Carolina Coastal Plain. Winner and Coble (1996) established a hydrogeologic framework for the system as part of the Regional Aquifer System Analysis conducted by the United States Geologic Survey (USGS). Giese et al. (1991) developed computer models to simulate groundwater flow and simulated water tables and potentiometric surfaces for prepumping (1900), 1980, and 2000. These maps were used to assess and predict changes in the groundwater flow system since the end of the prepumping period. Giese et al. (1991) determined that pumpage has only slightly changed the overall recharge and discharge to the aquifers, but has significantly altered vertical flow in areas where major pumping occurs. Heavy pumping caused groundwater in overlying units to move downward whereas it had moved upward in predevelopment times.

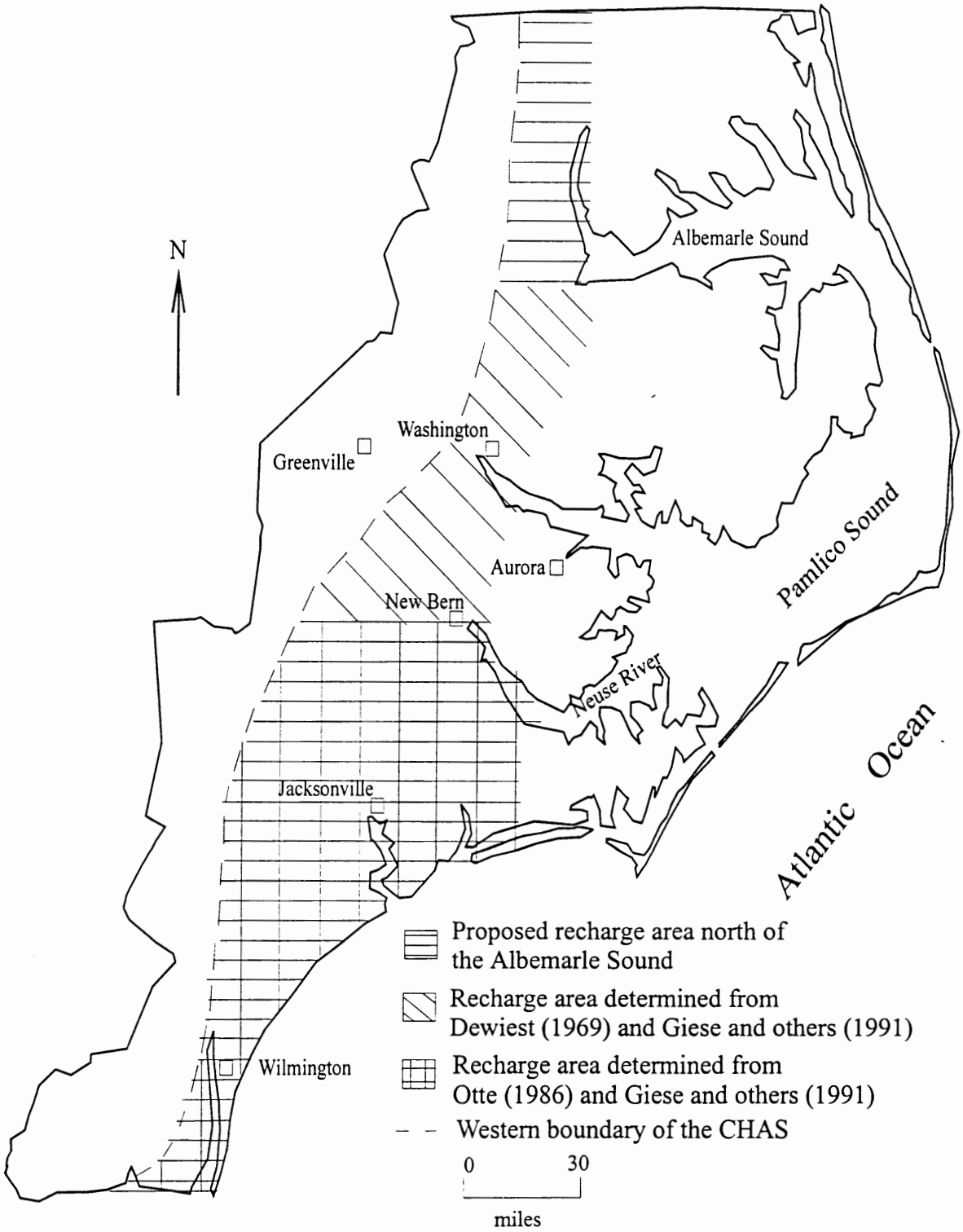

Figure 5. Proposed area of recharge to the CHAS

GROUNDWATER CHEMISTRY

Some chemical analyses of water from the Castle Hayne and other aquifers were available when this study was begun (Appendix A) (Knobel 1985, NCDEHNR database, 1981-1992, Sherwani 1980, Giese et al. 1987, Wilder et al. 1978, Lloyd and Daniel 1988). However, prior to work by Sutton and Woods (1995), there had been no thorough regional investigation of the chemistry of groundwater in any of these aquifers using up-to-date sampling, filtering, and on-site analytical techniques. Sutton and Woods (1995) sampled waters from 29 wells north and east of the Neuse River analyzing for major, and 25 minor species concentrations, Eh, pH, O_2, and $^{87}Sr/^{86}Sr$ ratios (Appendix B). They found that waters from the L-CHAS and easternmost wells in the U-CHAS are alkali and Cl rich, while waters from western wells in the U-CHAS are Ca and HCO_3 rich. Total dissolved solids (TDS) ranged from 310 to 10,900 mg/L. (Appendices A and B are available from the first author and WRRI.)

In the Castle Hayne Aquifer, freshwater mixes with water having a dissolved salt composition similar to sea water (Figure 6). Since pumping began at the phosphate mine in Aurora (Figure 5) in 1965, chemical analyses have shown that the Cl content of the Castle Hayne near the mine has increased (NCDNER 1976). In a study of groundwater chemistry at Cherry Point, Lloyd and Daniel (1988) concluded that recent increases in Cl are probably due to upward movement of water from the deeper parts of the Castle Hayne Aquifer induced by excessive pumping. According to Ralph Heath (hydrologist, USGS, pers. com. 1992), the increased Cl is due to upconing, but Sherwani (1980) contended that increasing Cl cannot be solely due to upward migration of brackish water and proposed five possible explanations for water-quality deterioration in the U-CHAS:

1) lateral movement of water from farther east in the CHAS,
2) downward movement of brackish water from the Pamlico Estuary,
3) downward movement of brackish groundwater from the Yorktown,
4) upconing of brackish water from the L-CHAS and Beaufort, and
5) westward movement of the sea water-freshwater interface along the coast.

Because these processes can not yet be differentiated from one another, all salty intermixed water will be referred to as "saline formation water" (SFW) in this paper.

GROUNDWATER GEOCHEMISTRY

Sutton and Woods (1995) observed that concentrations of major ions generally increase from west to east in the Northern

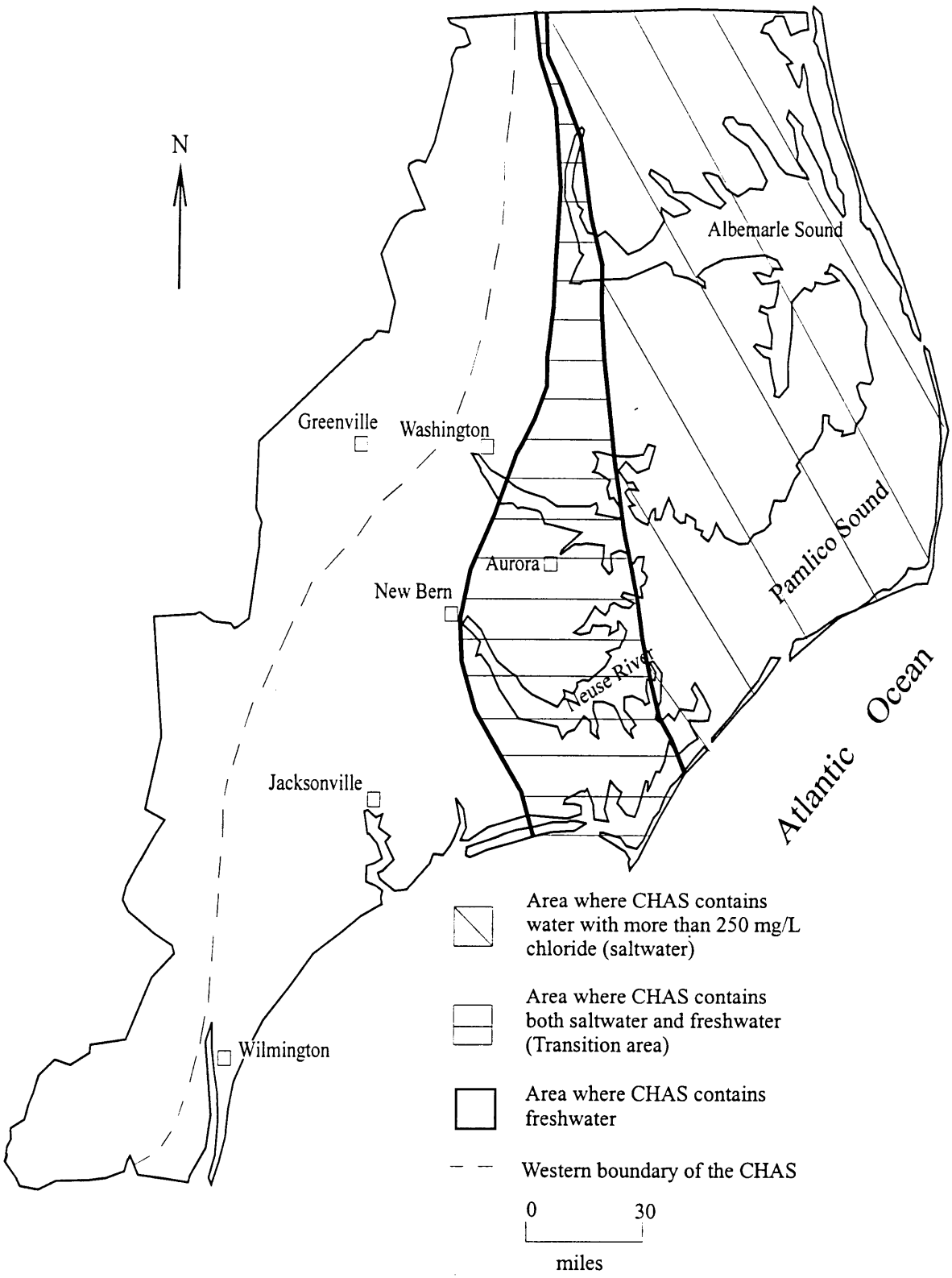

Figure 6. Freshwater and saltwater areas in the CHAS [modified from Harned and others (1989)].

Coastal Plain and that they are affected dominantly by four geochemical processes:

1) dissolution/precipitation of minerals,
2) mixing of groundwater with SFW,
3) chemical exchange between groundwater and aquifer ion exchange materials, and
4) dissolution of soil salts.

Meisler (1989) briefly discussed the groundwater geochemistry of coastal North Carolina in his study of salt water in the North Atlantic Coastal Plain.

San Juan and Sinha (1994) used $^{234}U/^{238}U$ ratios and uranium concentrations to study groundwater and surface waters north of Albemarle Sound. They concluded that it was possible to characterize some groundwater with these parameters, but that vertical mixing between aquifers presented complications. They suggested that the Surficial and Yorktown aquifers generally discharge downward into the Castle Hayne and that the Castle Hayne is probably discharging downward into the Black Creek. The potentiometric surface maps of Giese et al. (1991) suggest downward leakage from overlying aquifers throughout much of the Coastal Plain. Harned and Davenport (1990) estimated that 70% of the stream flow in the Albemarle/Pamlico region emanates from groundwater discharge in accord with San Juan and Sinha (1994) who observed that the uranium signature of the shallow aquifers and local streams is very similar. Wilder and Simons (1982) estimate that the mean dissolved solids load contributed by groundwater discharge is 35 ppm as compared to only 27 ppm from overland runoff.

STRONTIUM ISOTOPES AND GROUNDWATER STUDIES

Wickman (1948) first proposed that the temporal variation of the $^{87}Sr/^{86}Sr$ ratio in sea water could be used to determine the ages of marine chemical precipitates. Burke et al. (1982) and Denison et al. (1993), among others, have used $^{87}Sr/^{86}Sr$ ratios to date marine carbonates, evaporites, and phosphates. Edmond (1992), Raymo and Ruddiman (1992), Francois and Walker (1992), Palmer and Edmond (1989), Burke et al. (1982), Pitman (1978), Faure et al. (1965 and 1978), and Veizer and Compston (1974) investigated major causes of variation in sea water $^{87}Sr/^{86}Sr$ and the uniformity of $^{87}Sr/^{86}Sr$ ratios in coeval samples. Strontium isotopic analyses have also been applied to study the evolution, flow paths, and mixing of groundwaters; and diagenesis in carbonate aquifers (Sunwall and Pushkar 1979, Starinsky et al. 1983, Stueber et al. 1984, 1987, 1993a, 1993b; McNutt et al. 1984 and 1990, Chaudhuri et al. 1987, Banner et al. 1988, Collerson et al. 1988, Banner et al. 1989 and 1994, Cander 1994, Banner 1995).

DePaolo and Ingram (1985) and Hess et al. (1986) refined the curve describing temporal variations in the seawater $^{87}Sr/^{86}Sr$ ratio showing how ratios varied over Cenozoic and latest Cretaceous time. The rapid increase in sea water ratios during the late Cenozoic provides a particularly diagnostic tracer for groundwater that interacts chemically with Cenozoic marine formations (Figure 7). Denison et al. (1993) concluded that for Oligocene and younger marine chemical sediments, strontium isotope ratios determine the age of deposition to ± 1 million years or less. However, when seawater ratios remain constant or change very slowly, such as during the Eocene and Paleocene Epochs, only general age ranges can be determined. Recent work in the Southwestern Coastal Plain of North Carolina has described variations in the $^{87}Sr/^{86}Sr$ ratios, as well as $\delta^{18}O$ and $\delta^{13}C$ signatures, of important groundwater sources (Sirtariotis 1998).

GEOLOGY OF THE CASTLE HAYNE FORMATION

Macroscopic studies of the lithology and paleontology of the CHAS began in the early twentieth century (Clark 1909, Vaughan 1918). Early macroscopic studies focussed on lithology and paleontology. Textoris (1967 and 1969) provided preliminary petrographic data on the Castle Hayne Limestone, upper Oligocene beds, and carbonate-rich facies of the Cretaceous Peedee Formation. Detailed petrographic studies of the CHAS from the Superior and Martin Marietta Aggregates Quarries (10 miles north of Wilmington, NC) revealed major petrographic facies and diagenetic changes, and also related diagenetic features and permeability/porosity to pore-system development and original skeletal mineralogy (Cunliffe 1968, Cunliffe and Textoris 1969, Thayer and Textoris 1972, Textoris et al. 1972, Upchurch 1973).

Within the CHAS, Baum (1977) and Baum et al. (1978 and 1979a, b) recognized three dominant lithofacies of middle and upper Eocene age: a basal phosphate pebble biomicrudite, overlain by a bryozoan biosparrudite, overlain by a bryozoan biomicrudite. Ward (1977) and Ward et al. (1978) proposed a stratigraphic framework similar to Baum (1977) and Baum et al. (1978 and 1979a, b) for the CHAS. Their framework included three lithofacies of middle Eocene age: a phosphatic lithocalcirudite facies (the New Hanover Member), overlain by a bryozoan/echinoid biocalcarenite facies (the Comfort Member), overlain by a siliceous, molluscan-mold biocalcirudite facies (the Spring Garden Member). Otte (1981) interpreted the CHAS to include the New Hanover and Comfort Members and the phosphate pebble biomicrudite, bryozoan biosparrudite of Baum et al. (1978).

Zullo and Harris (1986) subdivided the CHAS into five lithostratigraphic sequences (0 through 4), which represent a

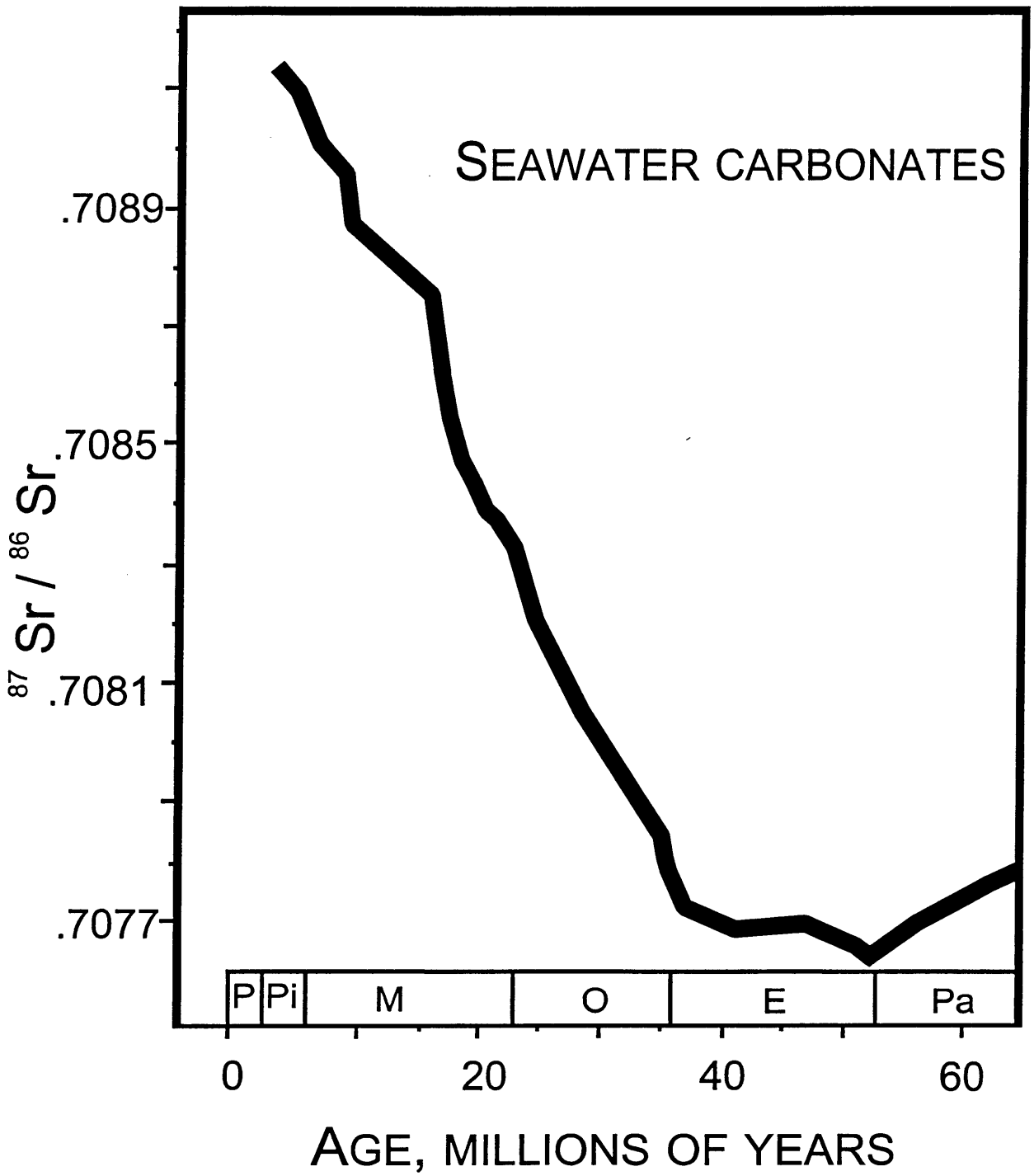

Figure 7. Variation of the $^{87}Sr/^{86}Sr$ ratio of Cenozoic marine carbonates and seawater. Based on measurements by DePaolo and Ingram (1985) whose ratios are higher than those in this report by 0.00006.

major transgressive and regressive sequence. Each sequence generally contains a basal phosphate-pebble biomicrudite overlain by a biosparrudite, a biomicrudite, and another biosparrudite. Moran (1989) separated the CHAS in southeastern North Carolina into forty-six stratigraphic units based on macroscopic, microscopic, and field observations. Four lithofacies occur among the stratigraphic units: a biomicrite/biomicrudite (indurated and unindurated), a pebble biomicrite/conglomerate (indurated), a biosparite/biosparrudite (indurated and unindurated), and a phosphorite (indurated).

GLAUCONITE FORMATION AND CHEMISTRY

Morton et al. (1984) suggest that the chemistry of glauconite is controlled by sedimentary environment, not the host material. Glauconite is thought to grow authigenically in a restricted microenvironment that is partially reducing/ partially oxidizing at or near the sediment-water interface under marine conditions (Odin and Matter 1981, Odin and Fullagar 1988, Weaver 1989, O'Brien et al. 1990). Traditionally, it was thought that the reducing conditions liberated Fe from either seawater or Fe-rich pore water for glauconite formation (Burst 1958a, b). It is now clear that the major source of iron for glauconite formation is the microbially-mediated reduction of Fe^{3+} oxide coatings on mineral grains in continental shelf sediments (Lovley et al. 1991). Weaver (1989) reported typical depths of glauconite formation on modern continental shelves and upper slopes are between 100 and 500 meters. For instance, glauconite internal molds commonly form on the deepest part of the present continental shelf off Morocco, Norway and the southeastern United States (Boichard et al. 1985). Other constraints on the formation of glauconite are: 1) presence of an initial substrate (e.g., fecal pellets, clay books, or mud lumps), 2) source of renewing ions (Fe and Al), 3) time for substrate to evolve in an area of low sedimentation (Odin and Matter 1981 and Odin and Stephan 1981).

METHODS

FIELD SAMPLING AND ANALYSIS

In accordance with guidelines for the USGS pilot National Water-Quality Assessment Program (Hardy et al. 1989) 89 wells were sampled between January, 1995 and May, 1997. The North Carolina Department of Environment, Health, and Natural Resources (NCDEHNR), Brunswick County Water Corporation, Hyde County Water Corporation, Onslow County Water Corporation, PCS Phosphate Corporation, and the cities of Atlantic Beach, Belhaven, Bogue Banks, Chinquapin, Columbia, Pink Hill, Rose Hill, Southport, Surf City, Wallace, Washington, and Waves provided access to the wells. Locations of sampled wells in the Upper and Lower Castle Hayne, Yorktown, Peedee, and other aquifers (i.e., Surficial, Pungo River, Beaufort, Black Creek, and Cape Fear) are indicated on Figures 8-12. Wells sampled and analyzed by Sutton and Woods (1995) are also plotted on the Upper and Lower Castle Hayne maps (Figures 8 and 9) because they have been collected very recently using the same sampling procedures as were employed for the current study. Previous data from sources other than Sutton and Woods (1995) have been used on many contour maps and are plotted with a different symbol.

In the interest of consistency, aquifer designations for wells sampled during this study were determined by comparing depths of screened intervals to the hydrogeologic framework developed by Winner and Coble (1996). As pointed out by a reviewer of this report, their framework was designed for regional reconnaissance and used only a small percent of the well data available. Therefore, it provides an oversimplified analysis and has probably resulted in some wells being assigned to the wrong aquifer. This is especially true for the siliclastic aquifers such as the Yorktown, Peedee, and Black Creek. This project was intended to provide only a preliminary characterization of groundwater chemistry in these siliclastic aquifers -- a detailed analysis of lithology was beyond the scope of the study. The focus of this study was the carbonate Castle Hayne Aquifer, which is usually readily distinguishable from the others. It is unlikely that wells have been incorrectly assigned to the Castle Hayne, so incorrect designations should not have a significant effect on the results.

Another source of error that has not yet been adequately addressed is that many wells in the USGS/NCDEHNR network are old, and in need of redevelopment and repair. Some of the wells undoubtedly have casing leaks. Some unusual patterns, such as those observed around M12l1 and L13i1 in the Northeastern Coastal Plain, may be a result of these problems. However, no significant generalizations or conclusions in this report are

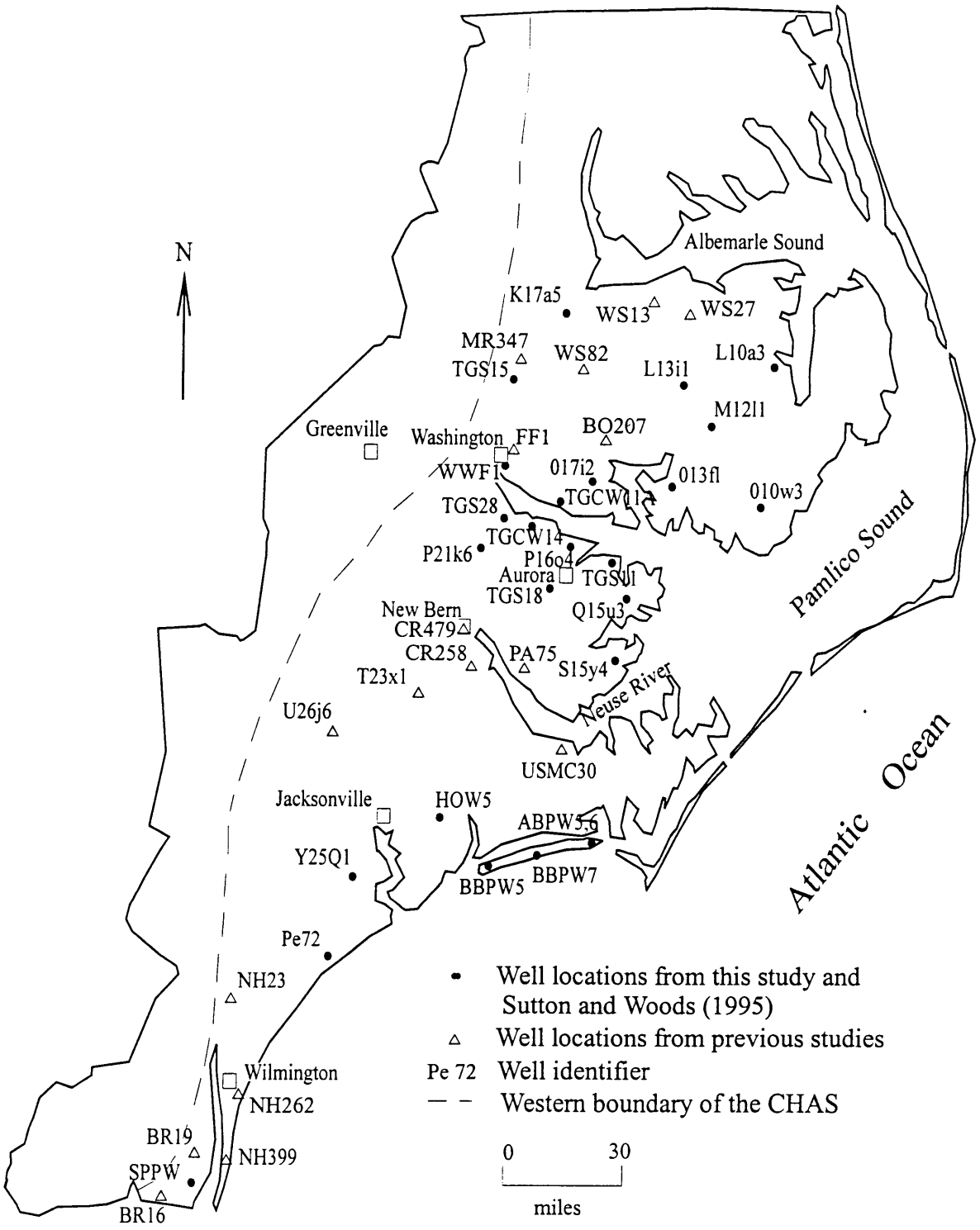

Figure 8. U-CHAS sample locations
[Previous studies are: Knobel (1985), NCDEHNR (1987), Sullivan's fish farm, and Lloyd and Daniel (1988).]

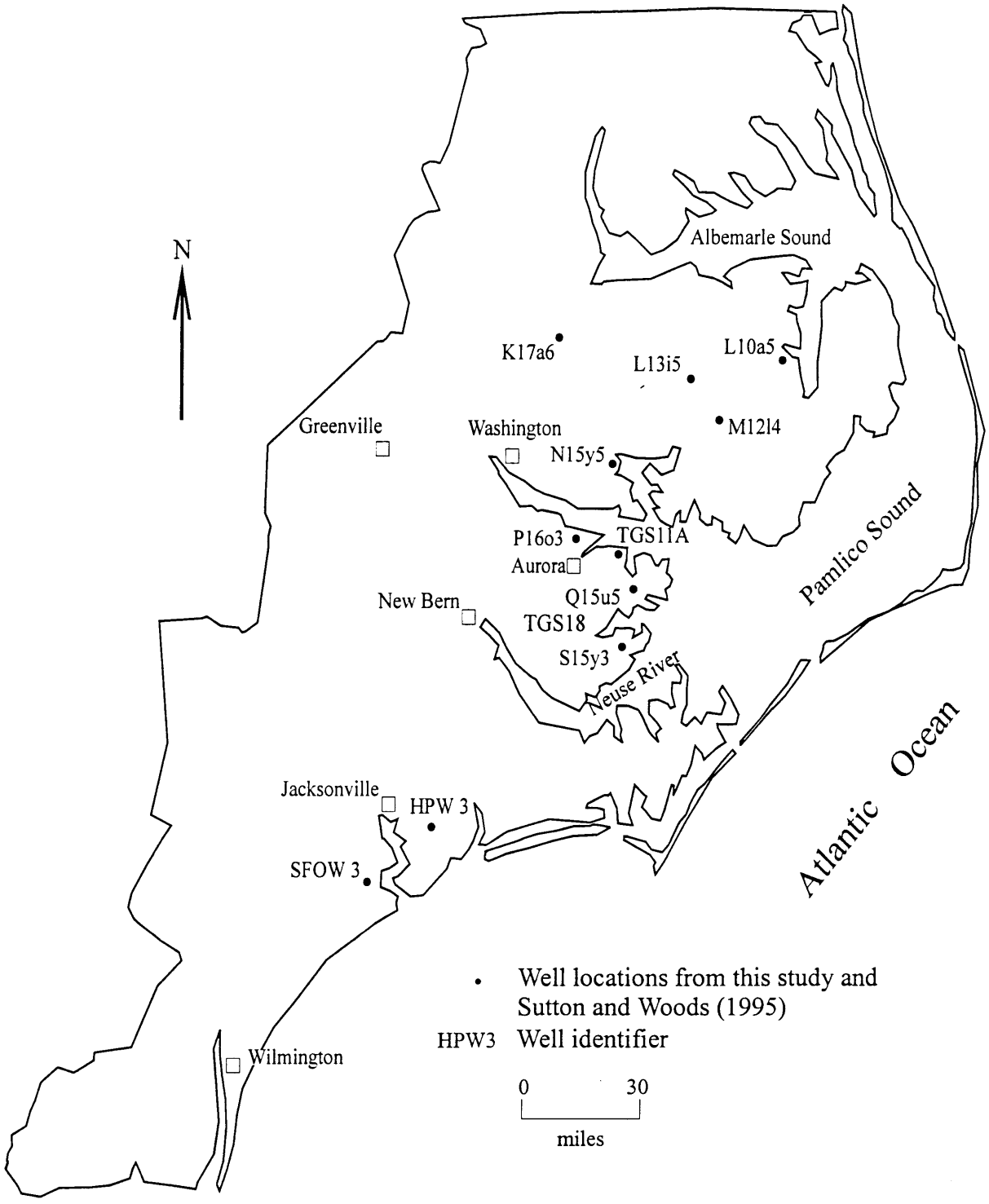

Figure 9. L-CHA sample locations

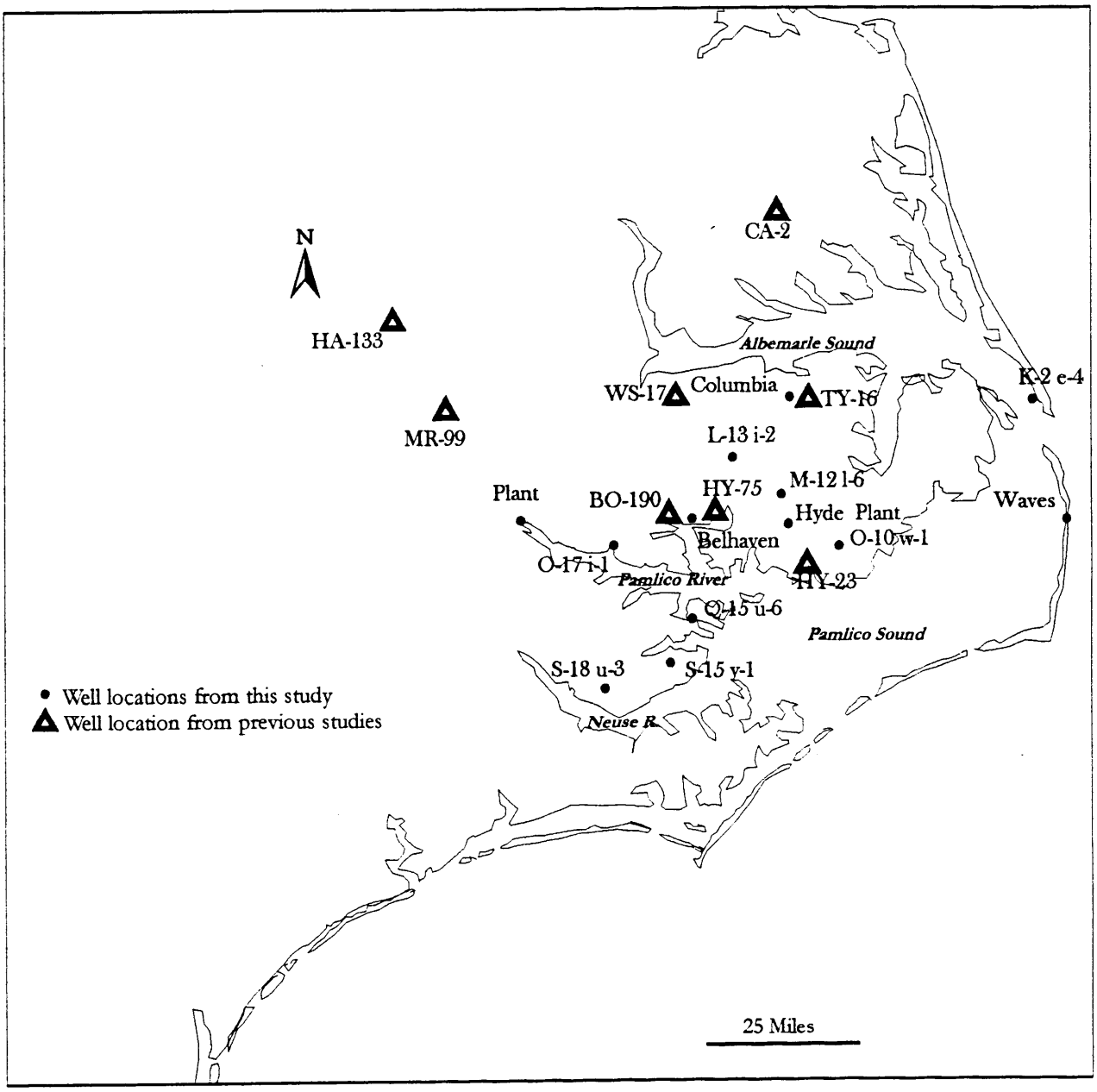

Figure 10. Yorktown Aquifer sample locations.

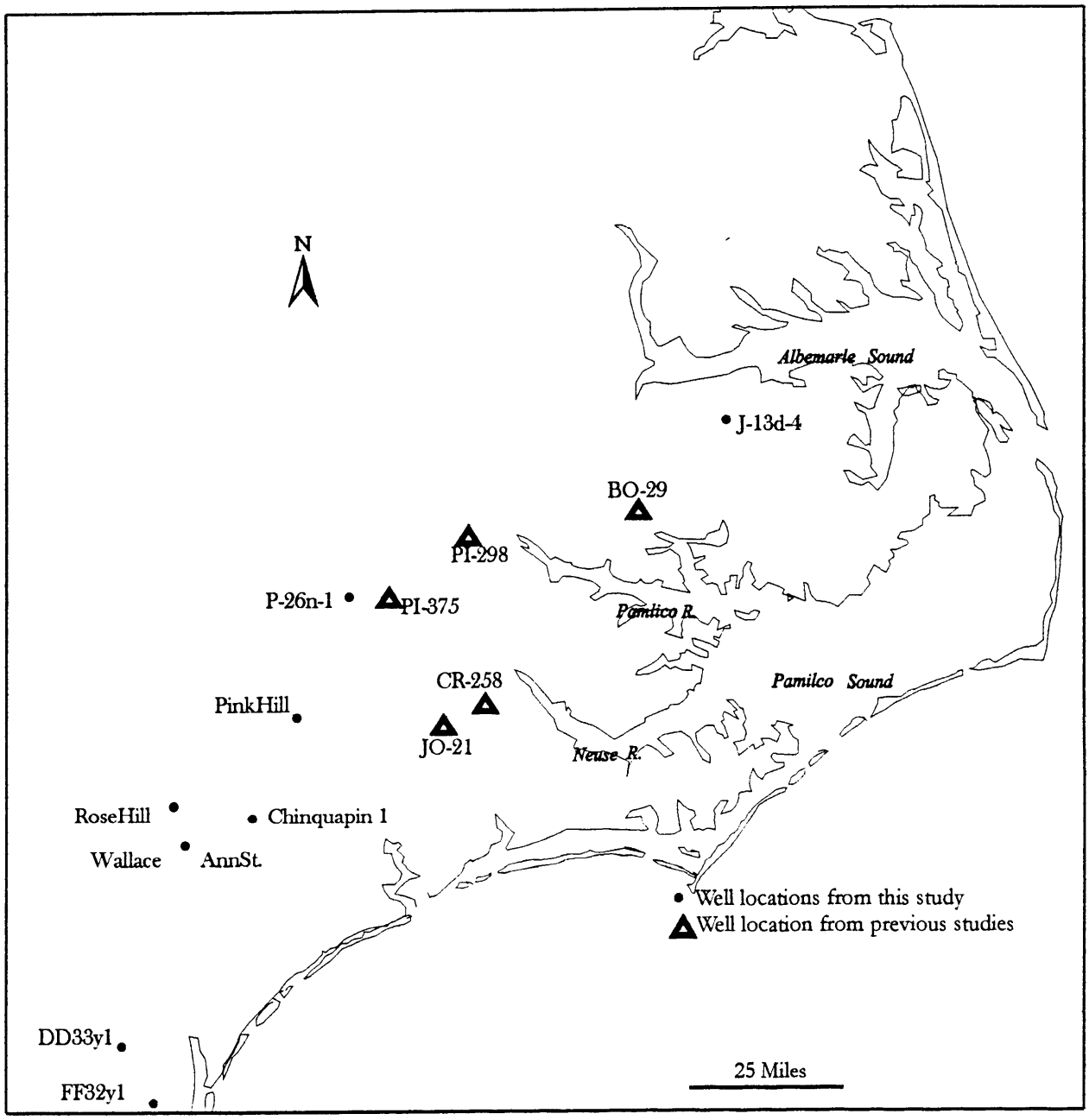

Figure 11. Peedee Aquifer sample locations.

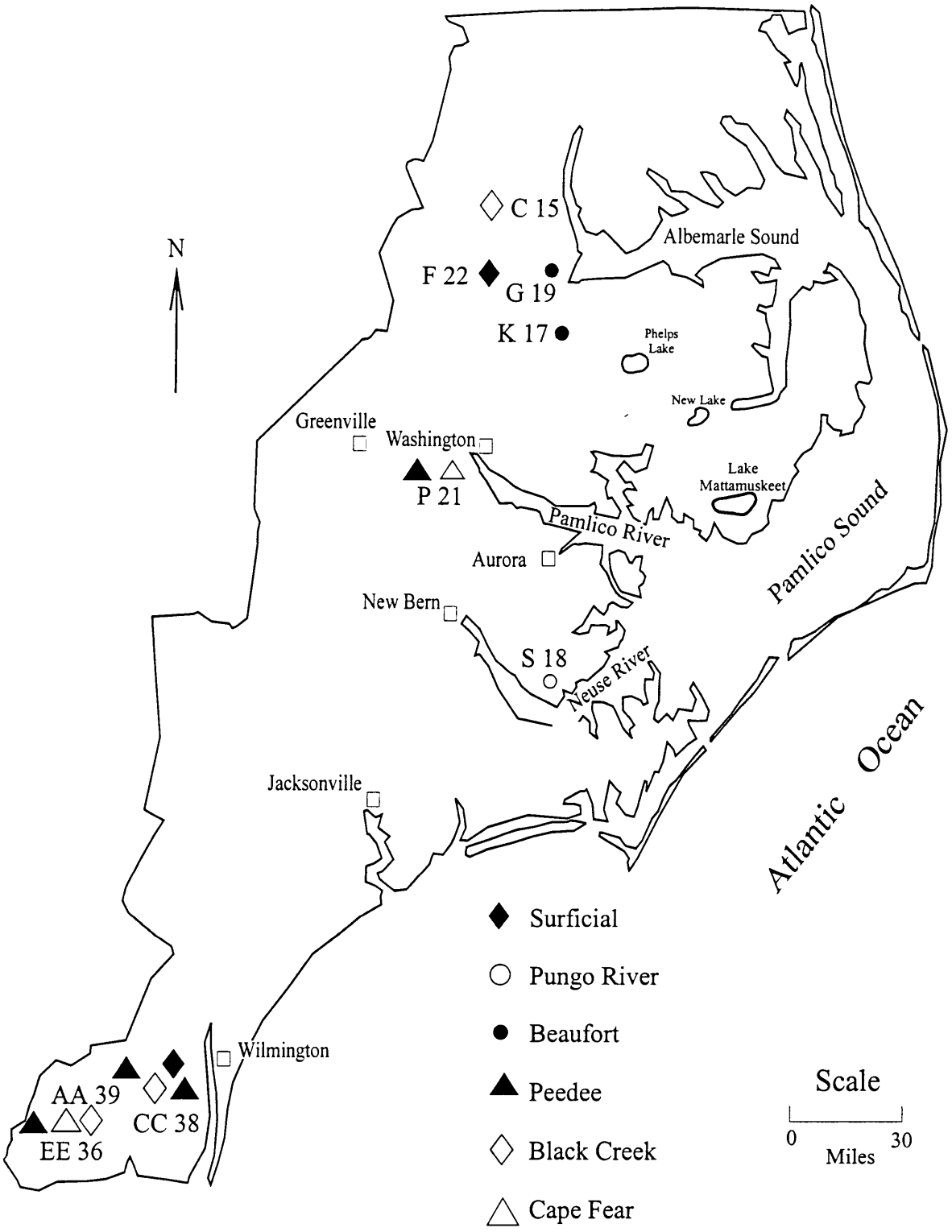

Figure 12. Sample locations from other aquifers.

based on just a single well analysis and the older data included on the contour maps are limited to the carefully screened values from the WATSTORE database of the USGS (Knobel 1985). Plans are being made to examine some wells using a downhole camera owned by Dr. Richard Spruill of the Geology Department at East Carolina University.

Sampled wells were purged a minimum of three well volumes, and up to as much as six well volumes, until chemical stability was achieved. Chemical stability was indicated by leveling off of pH and Eh readings continuously measured by electrodes in a flow-through beaker. Proper purging insures that the sample collected is representative of the water in the aquifer and not of the standing water in the well. Wells were purged and sampled using either a 230 Volt, 4" Grundfos submersible pump with a maximum flow rate of 7 gallons per minute (gpm), a 230 Volt, 2" Grundfos Redi-Flo2 submersible pump with a maximum flow rate of 7 gpm, or a 1 horsepower, 4" submersible Myers pump with a maximum flow rate of 35 gpm. The pump intake was placed between 5 to 10 feet below the drawdown water level in the well. All samples, except those collected for dissolved O_2 analysis, were passed through a 0.45 μm, in-line filter before sampling.

Concentrated HNO_3 was used to preserve 250-ml samples to be analyzed for cations by Atomic Absorption Spectrophotometry (AA). Another 250 mL of sample were collected for F^- analysis by ion selective electrode and Cl analysis by chloridometer. A 250-mL sample was collected for silica and sulfate analyses; silica by spectrophotometer and sulfate by turbidity meter. A 250-mL sample was frozen and later analyzed for ammonia, nitrate, nitrite, and phosphate using a colorimetric autoanalyzer. Samples were placed in an ice chest after collection. Water for dissolved oxygen determinations was collected in oxygen flasks and analyzed in the field by the Winkler method (Strickland and Parsons 1968). Two 50-mL samples for alkalinity determinations were titrated immediately using a Hach digital titrator (Wood 1976). Twenty-five mL of sample were collected to determine the concentration of sulfide in the field with a CHEMetrics test kit (CHEMetrics Inc. 1995). At some locations samples were collected for isotopic analysis ($^{87}Sr/^{86}Sr$, $\delta^{18}O$, $\delta^{13}C$) and determination of dissolved and particulate organic carbon. Dissolved organic carbon samples were filtered through a glass fiber filter and stored in 30-ml glass vials to which 2 drops of H_3PO_4 were added. Filters were stored in petri dishes for analysis of particulate organic carbon. An extra 500 mL were collected at each well and to evaluate analytical and sampling error, duplicate samples were collected at every third well.

Some wells equipped with permanent pumps were sampled from spigots using a specially designed fitting allowing the water to pass through the flow-through beaker. Wells at municipal water supply facilities were sampled by attaching a tygon sampling tube to their raw water outlet.

LABORATORY PROCEDURES

Spectrophotometry

Samples for silica analysis were kept refrigerated, then analyzed by the molybdosilicate method using a spectrophotometer within 48 hours of collection (Stainton et al. 1974). Six standards were used during each run and a correlation coefficient of at least 0.99 was obtained each time. All samples were diluted 1:50 before analysis.

Samples for nitrate, nitrite, phosphate, and ammonia analysis were frozen and then analyzed on a spectrophotometer within 3 months of collection (American Public Health Association 1992, Environmental Protection Agency 1979, Grasshoff et al. 1983, Jones 1984, Koroleff 1976, Solorzano 1969, Stanley 1987). The samples were thawed in a cold room 18 hours before analysis. Nitrate was reduced to nitrite with cadmium powder, and a solution of sulfanilamide and N- (1-naphthyl) ethylenediamine dihydrochloride was added as the color agent. The same color reagent was added to untreated samples to determine the amount of nitrite only; this concentration was subtracted from nitrate plus nitrite concentration to determine the concentration of nitrate. Phosphate was determined using an ascorbic acid method and ammonia concentrations were determined by the phenolhypochlorite method.

Ion Selective Electrode

The ion activity of F^- in solution was measured with an Orion combination F^- electrode (American Public Health Association 1992). TISAB III with CDTA was used as a buffer to provide a uniform ionic strength and background, adjust pH, and break up complexes. Use of the buffer allows the electrode to measure F^- concentration. Samples were refrigerated and then analyzed within one week of collection.

Chloridometer

A Buchler Digital chloridometer measured the concentration of Cl in solution by passing a fixed current between a pair of silver electrodes immersed in a glacial acetic acid solution (Buchler Instruments, Inc. 1981). The combination of silver ions and Cl ions results in an insoluble precipitate of silver chloride.

Samples were refrigerated and then analyzed within one week of collection.

Photometer

Sulfate ion is precipitated in an acetic acid medium with barium Cl to form barium sulfate crystals of uniform size (Rossum and Villarruz 1961, Sheen et al. 1935, Thomas and Cotton 1954). Light absorbance of the $BaSO_4$ suspension is measured by a photometer and the SO_4 concentration is determined by comparison of the reading with a standard curve. Samples were analyzed within 48 hours of collection.

Atomic Absorption

Samples for cation analysis by flame atomic absorption spectrometry (American Public Health Association 1995, Instrumentation Laboratory Inc. 1981, Sotera and Stux 1979) were preserved by adding 1 mL concentrated nitric acid to 250 mL of sample. Standards were made for each cation analyzed (Ca, K, Mg, Fe, and Na).

Total Organic Carbon

Dissolved organic carbon (DOC) samples were preserved in the field by the addition of H_2PO_3 to prevent conversion to CO_2 gas. Filter pads were frozen to preserve particulate organic carbon (POC). In the lab, thawed filters and DOC samples were placed in ampoules, treated with potassium persulfate and phosphoric acid, purged, sealed and autoclaved to oxidize organic matter to carbon dioxide. The quantity of carbon dioxide extracted from each ampoule (determined by an Analyzer Module) is equal to the organic carbon in mg C/L (American Public Health Association 1992).

Isotope Analysis

Samples to be analyzed for strontium isotopes were sent to laboratories at either the University of North Carolina-Chapel Hill (UNC-CH) or the University of North Carolina-Wilmington (UNC-W). The strontium isotopic compositions of the samples were measured by thermal ionization mass spectrometry on either a Micromass Sector 54 mass spectrometer at UNC-CH or a VG 336 mass spectrometer at UNC-W. All $^{87}Sr/^{86}Sr$ ratios are reported relative to a value of 0.710250 for NBS SRM 987. The isotopic analysis of oxygen and dissolved inorganic carbon was conducted by Mountain Mass Spectrometry in Evergreen, Colorado. All $\delta^{18}O$ and $\delta^{13}C$ values are reported relative to VSMOW and PDB, respectively.

STATISTICAL ANALYSIS OF GROUNDWATER DATA

Combined standard deviations calculated for duplicate CHAS samples from the Southwestern Coastal Plain are representative of the errors associated with our analyses. Combined standard deviations of duplicate samples analyzed for silica, ammonia, nitrate, nitrite, and phosphate are in Table 1; accuracy ranged from 89 - 98%. Fe, Ca, Mg, Na and K, analyzed by AA showed combined standard deviations of 0.08-9.78 ppm depending on concentration and ion (Table 2). Percent recovery ranged from 82 - 98%. Combined standard deviations for F^-, Cl, and sulfate were 0.09, 4.83, and 5.73, respectively. There was a 98 percent recovery for Cl (Buchler Instruments, Inc. 1981) and an 85 - 91% recovery for sulfate (American Public Health Association 1992).

Table 1. Statistical analysis of spectrophotometric data. Precision is expressed as combined standard deviation (sd) of "n" duplicate samples. Accuracy is expressed as % recovery of a known standard reference solution.

Ion	n	Combined sd	Range of	% Recovery
		ppm	Concen. (ppm)	
Silica	8	± 5.7	8.4 - 24	96 [1]
Ammonium	8	± 0.21	0.16 - 0.77	94 [2]
Nitrate	8	± 0.01	0 - 0.044	98 [3]
Nitrite	8	± 0.001	0.0013-0.0033	98 [3]
Phosphate	8	±0.08	0 - 0.23	89-96 [4]

1) as reported by Stainton et al. 1974
2) as reported by Solorzano 1969
3) as reported by Jones 1984
4) as reported by American Public Health Association 1992

Table 2. Statistical analysis of atomic absorption data. Precision is expressed as combined standard deviation of "n" duplicate samples. Accuracy is expressed as % recovery of a known standard reference solution.

Ion	n	Combined sd	Range of	% Recovery
		ppm	Concen. (ppm)	
Iron	4 4	± 0.18 ± 1.23	0.05 - 0.45 1.6 - 4.2	84
Magnesium	8	± 4.35	1.6 - 13.5	97
Sodium	7 1	± 2.4 ± 0.1	11.8 - 19.8 30.9 - 31.0	85
Potassium	8	± 4.8	5.1 - 19.0	82
Calcium	8	± 9.8	70.2 - 94.6	98

CASTLE HAYNE MINERALOGY AND MINERAL CHEMISTRY

The lithology, mineralogy, and oxide composition of rock samples of Castle Hayne Limestone from six wells (three cores and three sets of drill chips) (Figure 13, Table 3) were described. Samples were provided by the North Carolina Geologic Survey.

Table 3. Locations of wells providing core and drill chips

Well Name	Latitude	Longitude
WH-T2-78	35°43'30''	76°26'30''
TY-T1-76	35°50'59''	76°15'50''
BF-T5-67	35°33'30''	76°37'30''
BF-T1-69	35°26'30''	77°09'30''
PA-T2-XX	35°05'30''	76°50'30''
BF-T6-67	35°24'56''	76°48'30''

Petrographic Analysis

Three cores (wells BF-T1-69, PA-T2-XX, and BF-T6-67) were sampled at intervals determined by lithologic changes in the CHAS and fifteen thin sections were made from these samples. Lithologic determination for most was made by a point count of 200 points per thin section. One thin section representing the interval from 152 to 162 feet below sea level in well BF-T1-69, had only 142 points counted due to small sample area.

Thin sections were stained with a mixture of Alizarin Red-S and potassium ferricyanide in 0.2% hydrochloric acid to reveal the presence of dolomite (Lindholm and Finkelman 1972). Alizarin Red-S turns calcite red, while dolomite remains colorless. Potassium ferricyanide causes iron-poor calcite to turn mauve, iron-rich calcite to turn purple; ferroan dolomite turns light blue, and ankerite turns dark blue.

X-ray Diffraction Techniques (XRD)

Powder x-ray diffraction techniques were used on bulk rock samples from drill cuttings and one of the cores to distinguish areas within the CHAS containing minerals other than calcite and quartz. At the time of collection the drill cuttings were washed to remove driller's mud and, as a result, much of the fine material (e.g., clays, feldspars, zeolites) was also washed away. Mineral identification based on X-ray diffraction is tentative, because in bulk rock samples the dominant calcite and quartz peaks mask the generally low relative peak intensities of accessory minerals.

All depth intervals were analyzed by XRD in wells WH-T2-78, TY-T1-76, and BF-T5-67; however, in well BF-T1-69 only the

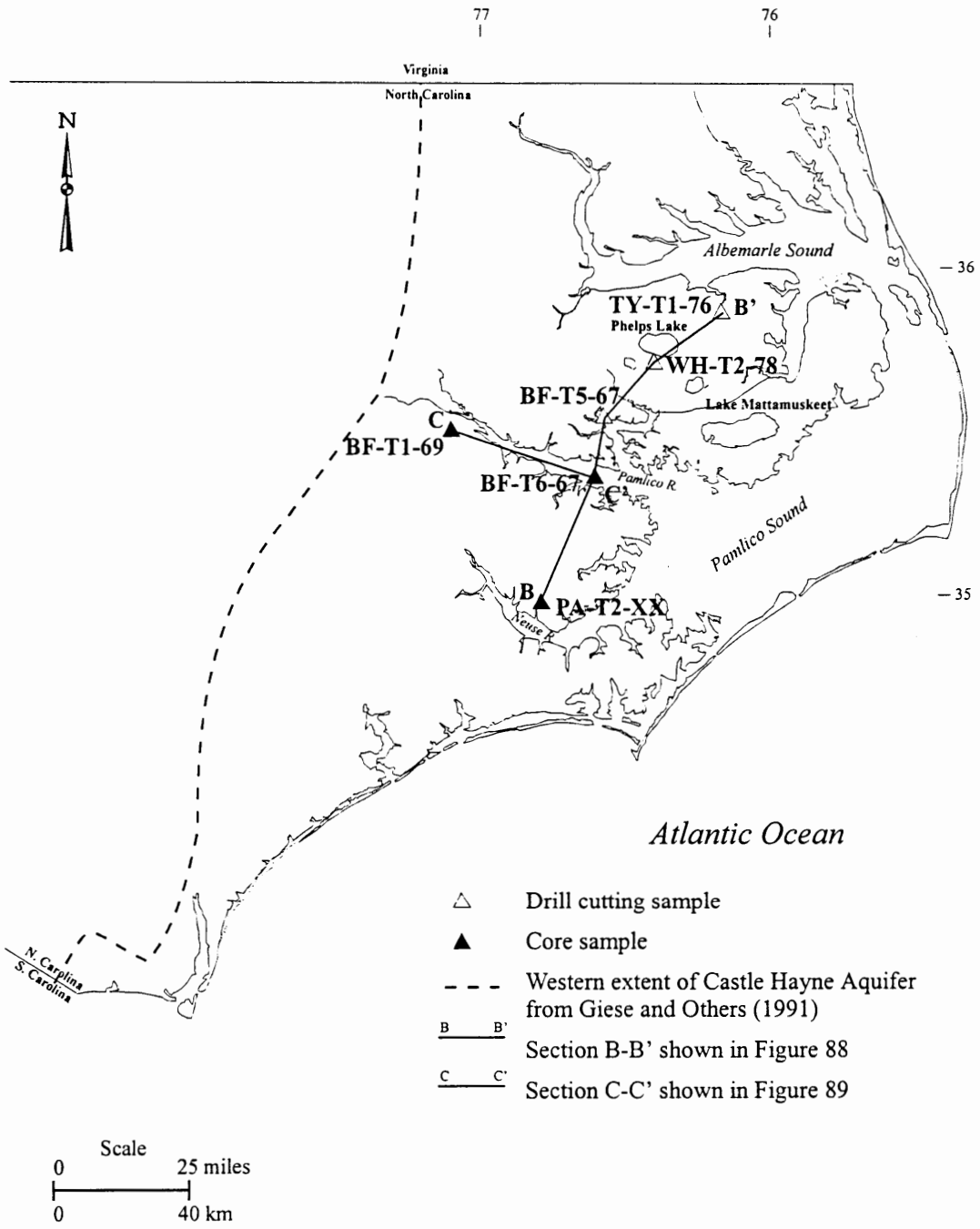

Figure 13. Location map of rock samples from the Castle Hayne Aquifer.

intervals with high point count for peloids were selected for XRD analysis. After petrographic analysis, it was decided that samples from wells BF-T6-67 and PA-T2-XX would not be X-rayed because they contained mostly calcite and quartz and minor concentrations of accessory minerals.

Sixty samples were analyzed by XRD to determine the mineralogy of the CHAS in the study area. Each sample was ground with a mortar and pestal and sieved (88 microns) to remove large pieces of rock before X-ray analysis. Samples were X-rayed from 5° 2θ to either 45° 2θ or 57° 2θ. The more restricted X-ray patterns were on preliminary samples, but the majority of the samples were X-rayed over the longer range. Samples representing each mineralogically distinct zone were chosen for EDX analyses.

Energy Dispersive X-ray Analysis (EDX)

A separate set of 45 polished sections from cores and drill cuttings was made for Scanning Electron Microscope (SEM) and EDX study. Sections were polished in a slurry of 0.05μm aluminum oxide and water for approximately 12 hours using a Vibromet Polisher (Heald-Wetlaufer et al. 1982). Each thin section was glued to an aluminum stub with silver paste, stripes of conductive graphite isopropanol base were painted on the top and bottom of the glass slide (not on the actual sample), and finally the thin section was coated with a thin layer of carbon. These procedures render the samples conductive, which helps reduce charging (bright lines or abnormal contrasts) when viewed with the SEM.

Each sample was analyzed using a Phillips SEM equipped with hardware and ZAP data reduction software from HNU Systems. The ZAP program is a standardless analysis that incorporates routine corrections based on background subtraction, peak overlap, characteristic line fluorescence, etc. and converts peak heights directly to weight percents. Each sample was analyzed at 0-10KeV for 200 seconds of Live Time. These parameters were chosen because they produced the best analyses of known standards similar in structure and chemistry to the unknown minerals. The majority of grains analyzed by EDX were chosen based on their morphology and grains appearing to be peloids (glauconite or phosphate) were analyzed most frequently. Spectra were collected for a total of approximately 500 grains, 250 to 300 of which were pure quartz or calcite. These were not analyzed further after identification. Because of the potential importance of cation exchange reactions in controlling groundwater composition, glauconite chemistry was investigated in detail. Carbonate matrix and cement were also chosen for analysis.

RESULTS

A previous study of the CHAS in the Northeastern Coastal Plain (Sutton and Woods 1995) has now been extended into the southern counties so maps describing the variation of CHAS groundwater chemistry south of Albemarle Sound have been drawn. Many U-CHAS and L-CHAS wells in the Northern Coastal Plain have also been resampled to analyze for carbon and oxygen isotopes and particulate and dissolved organic carbon. Major element chemistry was also reanalyzed and additional duplicate samples were collected to improve statistical control on the accuracy and precision of the results. This will permit meaningful statistical analysis of these data in the near future. Reanalyses (Appendix C) are as yet incomplete so these numbers are not included on figures or in the discussion, but are available from the first author and WRRI.

Study of the water chemistry of the Yorktown and Peedee is in the preliminary stages. Unlike the Castle Hayne work, which has been underway since the spring of 1993 and has been through two rounds of sampling, only a limited set of Peedee and Yorktown samples have been collected and analyzed. Also data available from the USGS and NCDEHNR have not yet been thoroughly analyzed. The lithologies of the Yorktown and Peedee are not as distinctive as that of the Upper Castle Hayne. Local drillers, hydrologists, and government officials have historically not had any trouble recognizing the U-CHAS except in the Southwestern Coastal Plain where it becomes very sandy. On the other hand, the sands, silts, and clays of other Coastal Plain formations can be very difficult to distinguish. Also, Winner and Coble (1996) reinterpreted the earlier stratigraphic and well-log data of workers such as Brown et al. (1972) and adopted different locations for some contacts between formations. As a result, when comparing the depths of wells sampled to the currently accepted hydrogeologic framework (Winner and Coble 1996), it was determined that many wells designated by the USGS and NCDEHNR as being in the Peedee and Yorktown Aquifers may actually be in other aquifers. Therefore, an adequate number of Peedee and Yorktown wells have not yet been sampled, however, data have been acquired from other formations such as the Black Creek, Pungo River, Beaufort, and Cape Fear.

Some contour maps include older data from the WATSTORE data base of the USGS (Knobel 1985), NCDEHNR (NCDEHNR 1981-1992) and Lloyd and Daniel (1988). On sample and contour maps these older data are designated by a different symbol than is used for wells sampled for this study. Knobel (1985) includes only analyses for which electrical neutrality balanced within 5% for samples with TDS > 5 milliequivalents per liter (meq/L), and within 10% for samples with TDS < 5 meq/L. Knobel (1985) contains many more

analyses than are included on these maps, but many of the analyses are from wells, which are geographically very close to each other or are chemically very similar. In this case, only a well with concentrations near the average was reported. When analyses of the same well water sampled at different times were available, only the most recent analysis was listed. In cases where it was very likely that a well had been drilled in an aquifer other than the one indicated, the analysis was rejected if it had significantly higher or lower TDS, Cl, SO_4, etc. than surrounding wells. Finally, wells were rejected if radically different results were reported for replicate sampling dates in the same year. On contour maps concentrations of dissolved species are designated as "0" when they are below the detection limit.

CASTLE HAYNE WATER CHEMISTRY AND ISOTOPES

Concentration ranges of aqueous species in CHAS waters, and any potentially anomalous values, are listed in Table 4, which includes data from Sutton and Woods (1995). A brief description of the chemical trends within the CHAS is given below and complete analyses of wells sampled for this study are in Appendix D, which is available from the first author and WRRI.

Major Elements

TDS, Cl, and sulfate (SO_4) in the CHAS north of the Neuse River generally increase from west to east (Figures 14-19). South of the Neuse River, TDS, Cl, and SO_4 increase from northwest to southeast, except southwest of Wilmington where TDS values decrease and then increase again from southwest to northeast. TDS, Cl, and SO_4 concentrations in the L-CHAS are generally higher than those in the U-CHAS at the same well site. TDS, Cl, and SO_4 in the L-CHAS increase from west to east. Alkalinity in the U-CHAS generally increases from southwest to northeast in the Northern Coastal Plain and from east to west near Wilmington, but no geographic trend for the L-CHAS is obvious (Figures 20 and 21). L-CHAS wells generally have higher Na, K, Ca, and Mg than U-CHAS wells at the same location. Potassium, Na, and Mg concentrations in the U-CHAS generally increase from west to east north of the Neuse River and from northwest to southeast south of the NeuseRiver (Figures 22-27). Calcium in the U-CHAS shows the most complex pattern of all the species analyzed and will be discussed in detail later (Figures 28 and 29). Silica concentrations increase, decrease, and then increase again between Albemarle Sound and Jacksonville, but south of Jacksonville, silica generally decreases from west to east (Figures 30 and 31). The two enclosed regions with silica concentrations greater than 40 ppm are defined by 3 water analyses from previous studies containing 50 ppm, 52 ppm,

Table 4. Concentration ranges of aqueous species in the CHAS

Dissolved species	Range of concentrations		Wells with anomalously low or high concentrations	
	U-CHAS	L-CHAS	Low	High
	ppm unless noted		Well ; Conc.	Well ; Conc.
TDS	170 - 4,693	340 - 10,600		SFOW3 (l) ; 854
				BB5 (u) ; 847
Cl^-	4 - 1,790	19 - 5,100	***L-13 (u) ; 55***	SFOW3 (l) ; 250
			L-13 (l) ; 510	BB5 (u) ; 360
				TGS 11a (l) ; 2,260
				M-12 (l) ; 5,100
SO_4^{2-}	0 - 336	0.3 - 1,120		***TGS 11a (l) ; 380***
				M-12 (l) ; 1,100
				Q-15 (l) ; 610
HCO_3^-	160 - 783	385 - 642	T23x1 (u) ; 160	***L-13 (u) ; 783***
F^-	0 - 3.2	0.08 - 1.71		***M-12 (l) ; 1.35***
				M-12 (u) ; 3.20
Na^+	3 - 1,690	11 - 3,360		SFOW3 (l) ; 50
				BB5 (u) ; 40
				TGS 11a (l) ; 1,470
				Q-15 (l) ; 920
K^+	0 - 82	5 - 124		SFOW3 (l) ; 27
Ca^{2+}	7 - 103	20 - 140		
Mg^{2+}	1 - 127	2 - 318		
Hardness	69 - 658	75 - 1,632		
SiO_2	7.0 - 78	7.0 - 26		
Fe	0.05 - 4.8	0.18 - 7.3		SFOW4 (l) ; 7.3
				Y25q1 (u) ; 4.1
NH_4^+	0.04 - 6.62	0.03 - 7.89		
S^{2-}	0 - 5.8	0 - 7.1		SFOW3 (l) ; 4.5
				BB5 (u) ; 1.5
				TGS 11a (u) ; 5.8
				P-16 (l) ; 7.1
NO_3^-	0 - 0.3	0 - 0.006		
PO_4^{3-}	0.003 - 0.22	0 - 0.12		
pH	6.92 - 8.2	6.8 - 7.67		T23x1 (u) ; 8.1
Eh (mV)	206 to -160	160 to -52	SFOW3 (l) ; -52	
			BB5 (u) ; -6	

(u), U-CHAS sample (l), L-CHAS sample
Hardness = mg equivalent CaCO3/L = 2.497 (Ca, mg/L) + 4.118 (Mg, mg/L)
(American Public Health Association 1992)
Bold = wells from Sutton and Woods (1995)

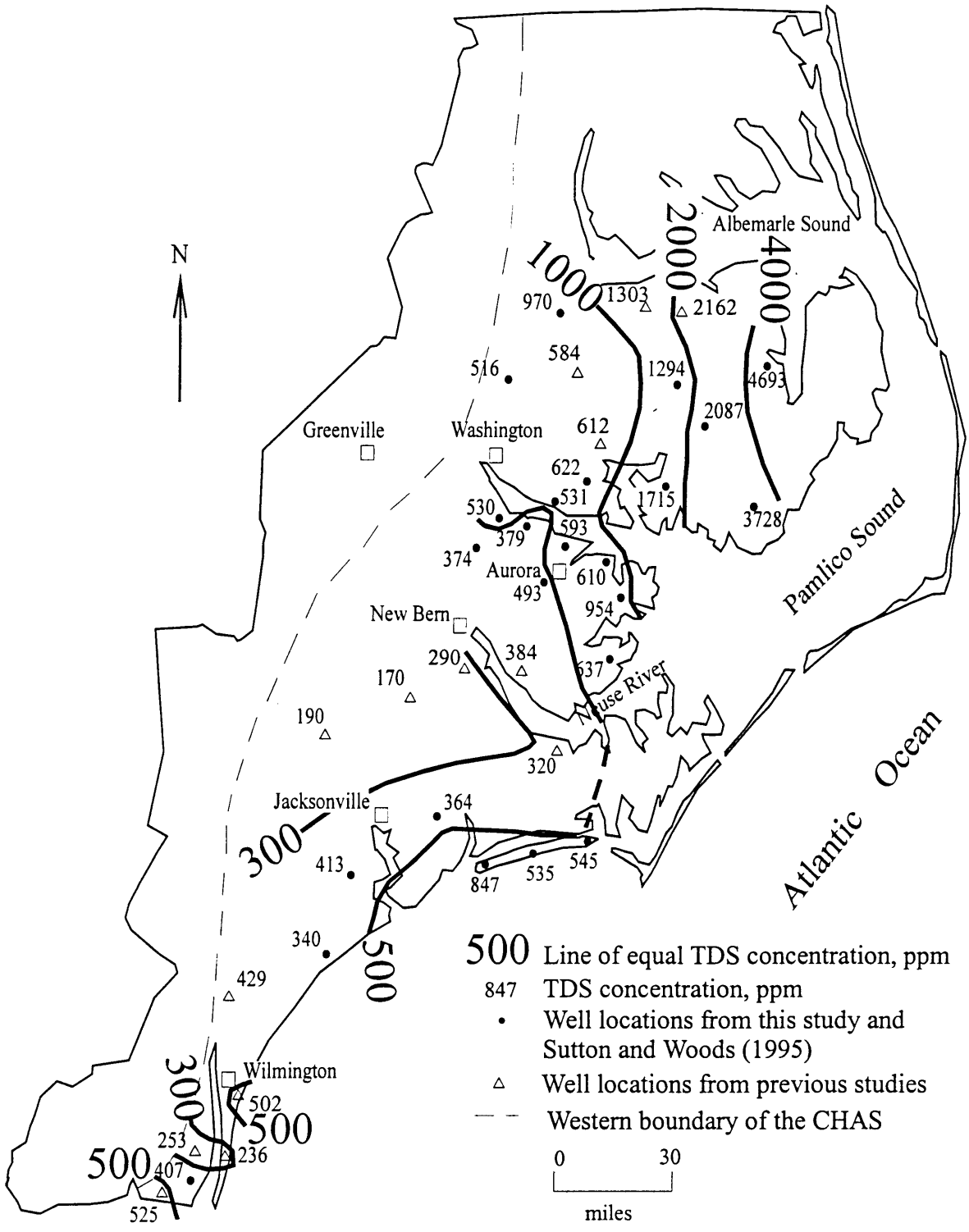

Figure 14. TDS in the U-CHAS

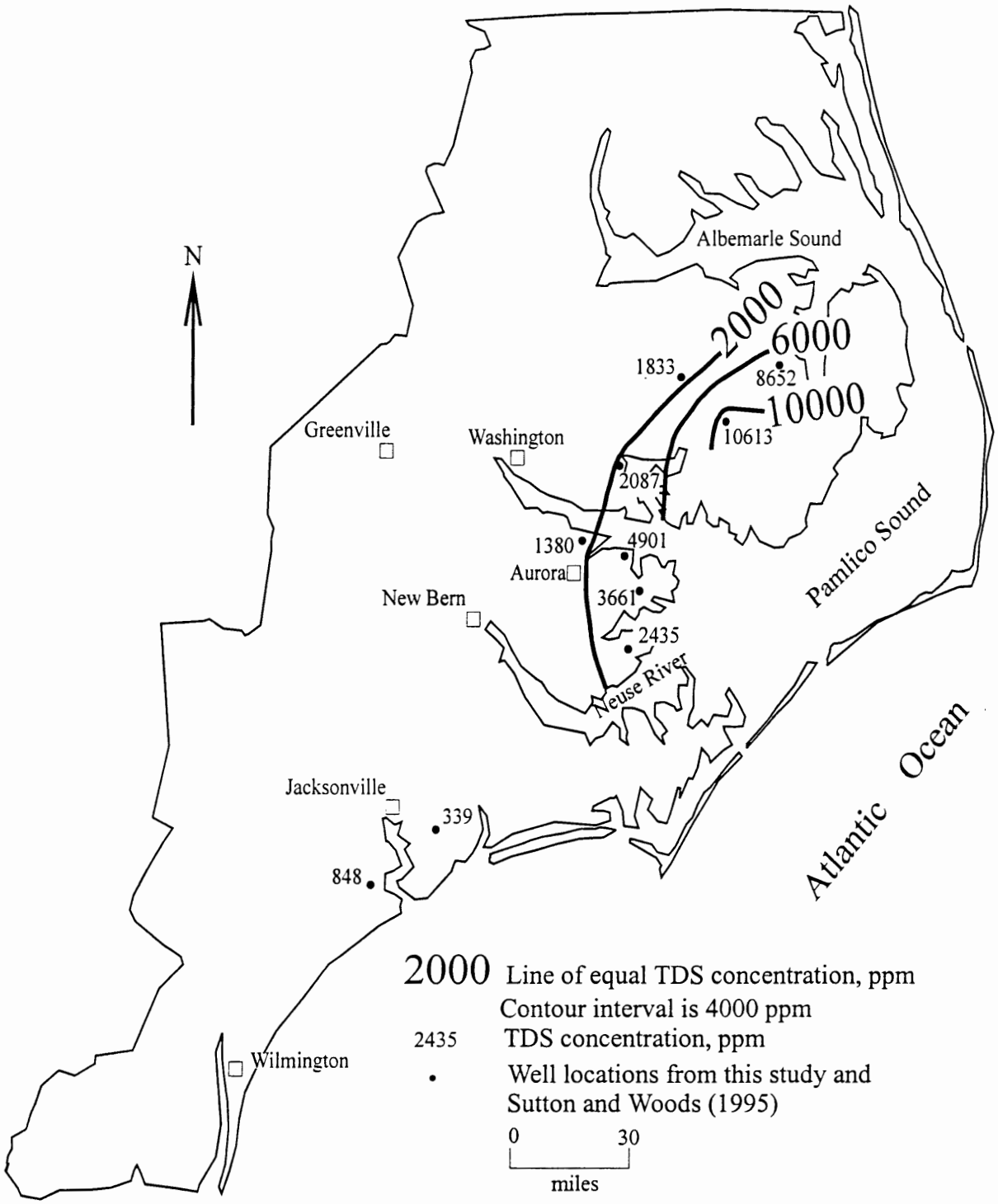

Figure 15. TDS in the L-CHAS

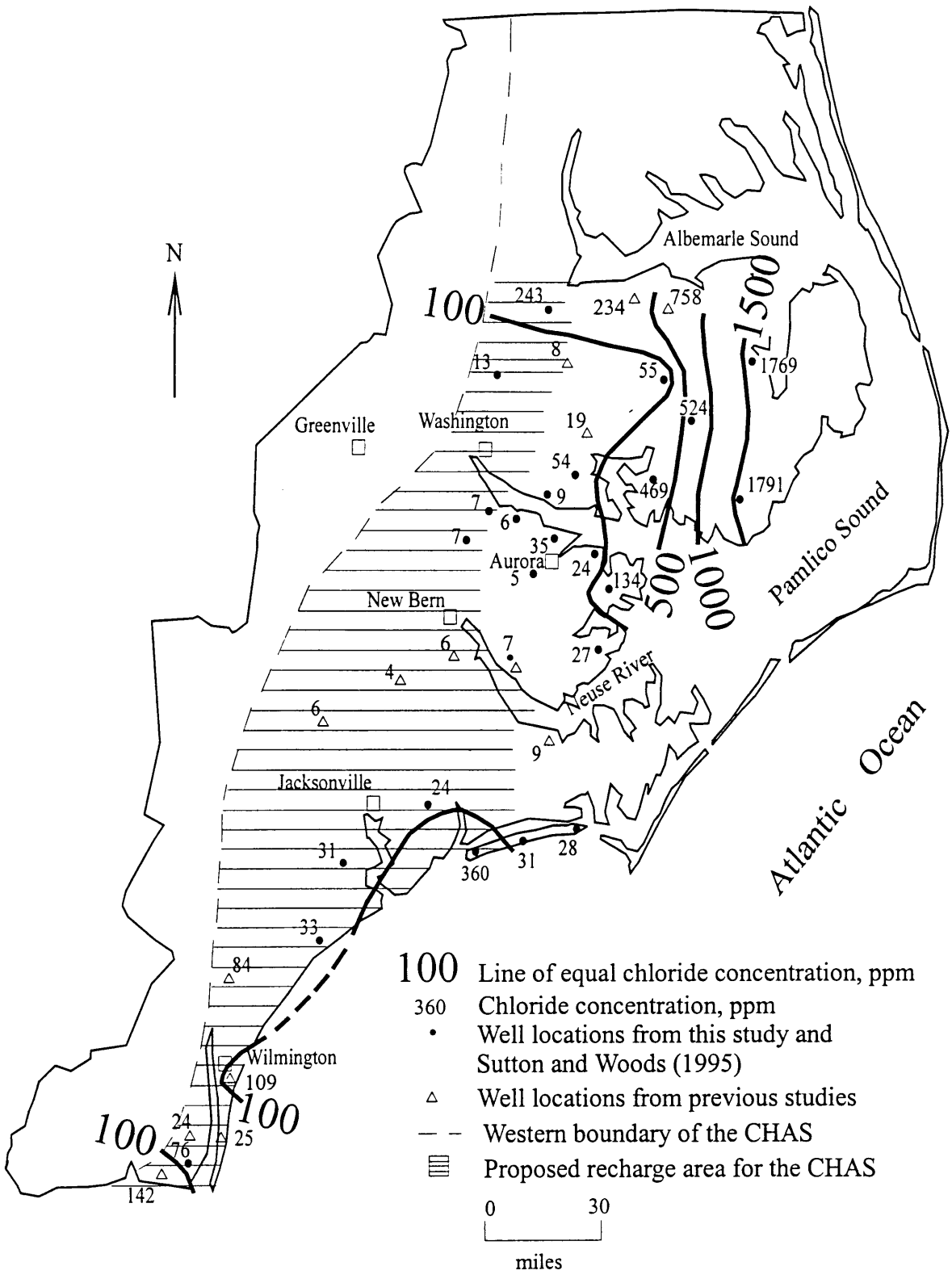

Figure 16. Chloride concentrations in the U-CHAS

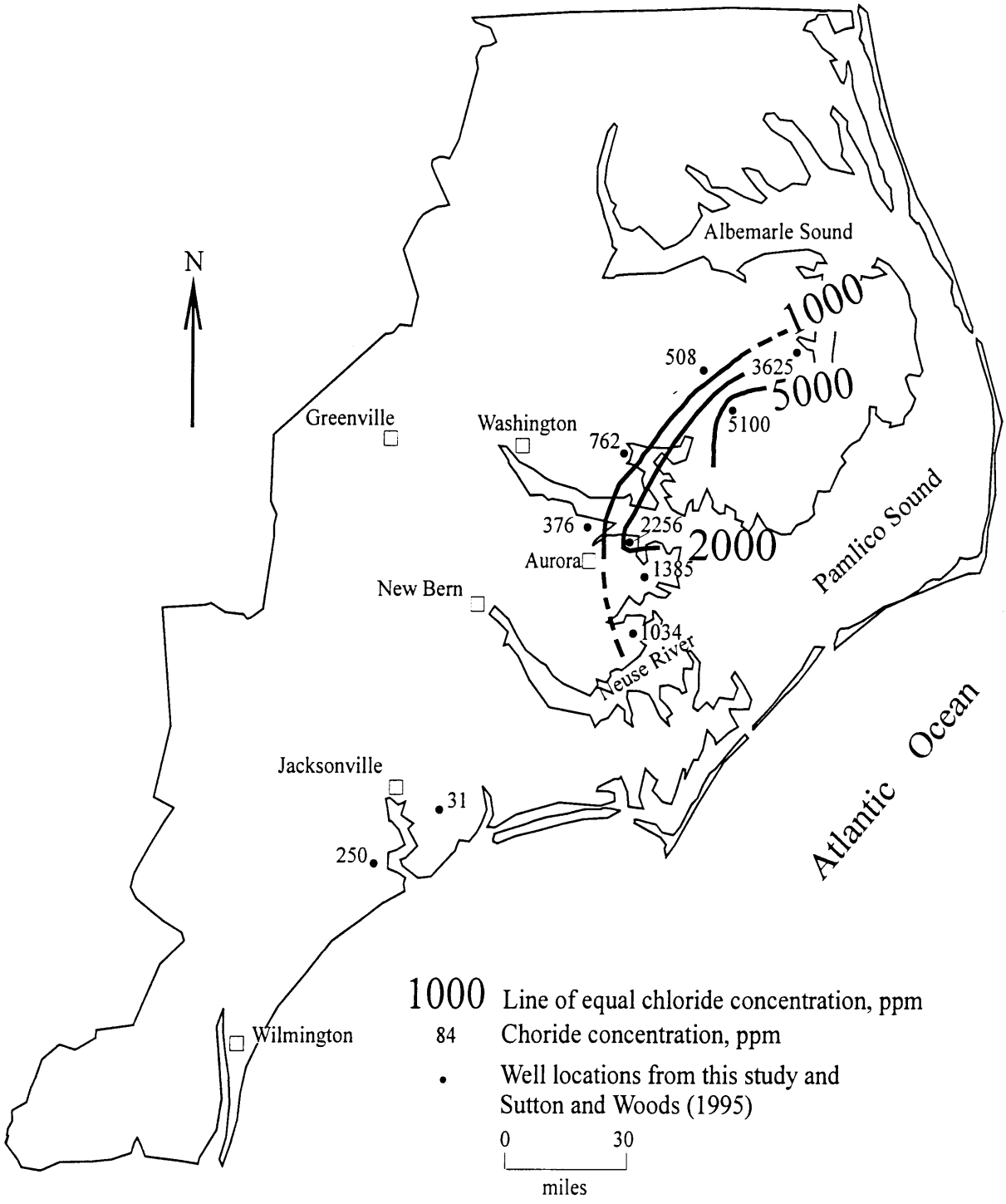

Figure 17. Chloride concentrations in the L-CHAS

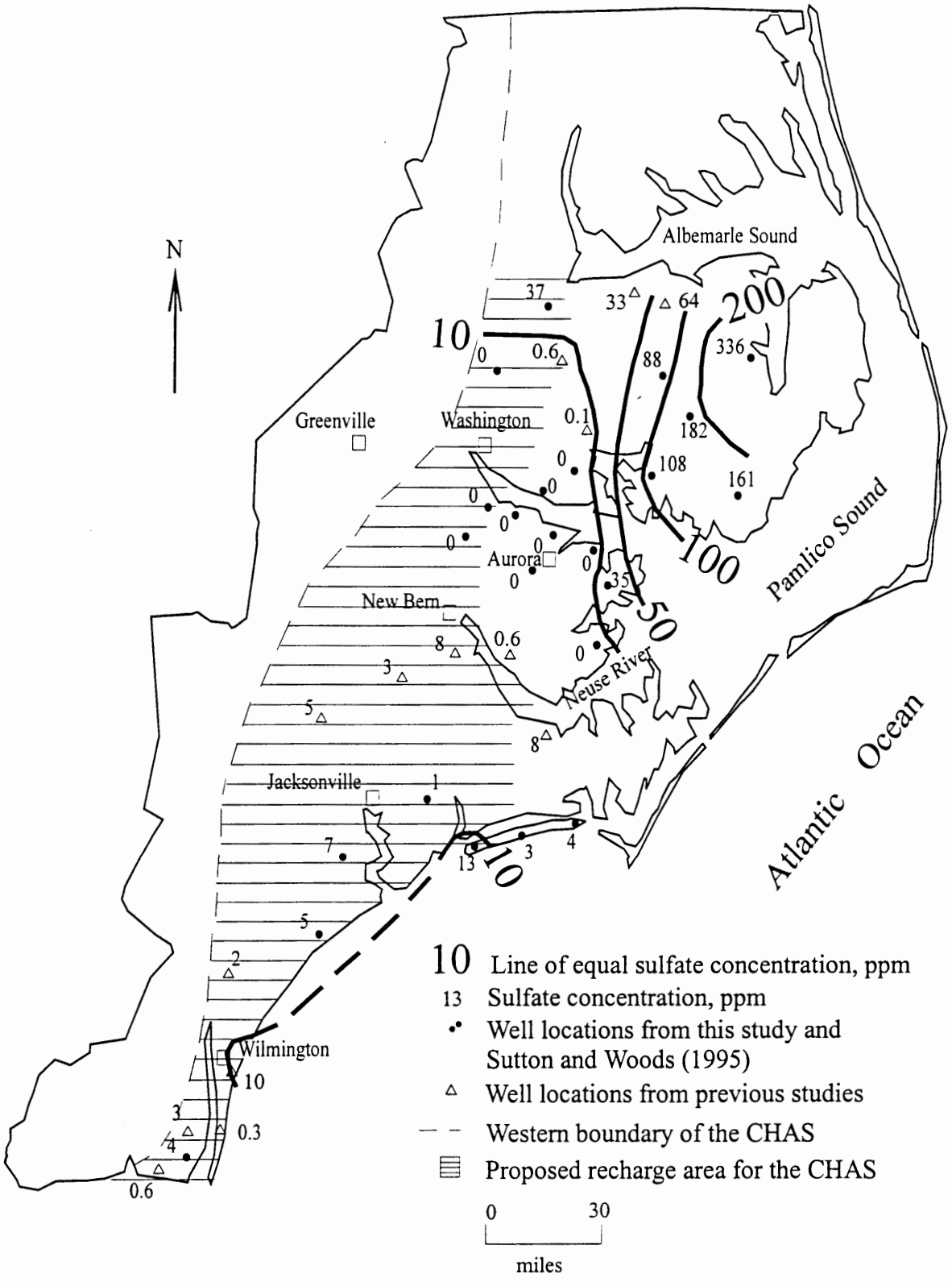

Figure 18. Sulfate concentrations in the U-CHAS

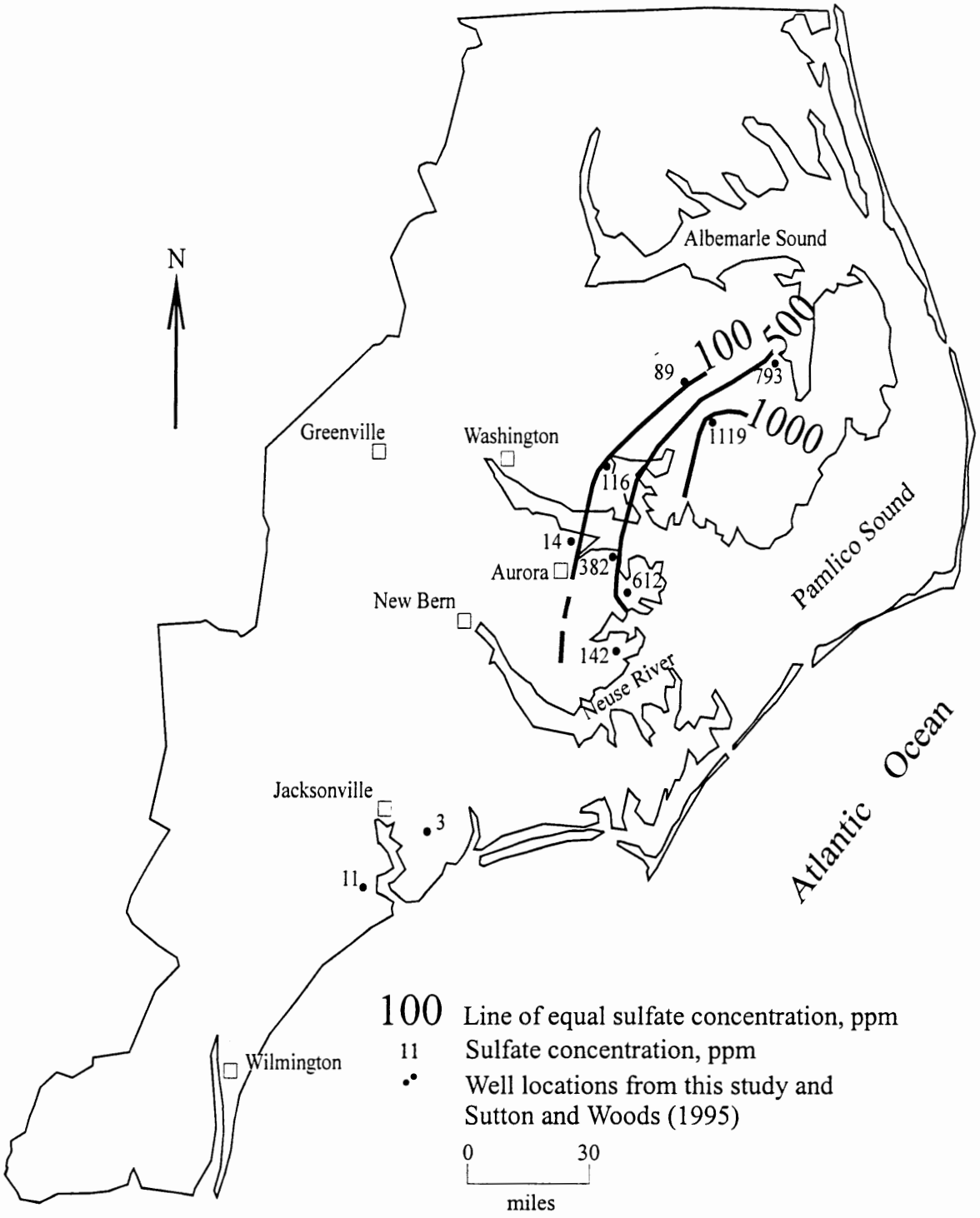

Figure 19. Sulfate concentrations in the L-CHAS

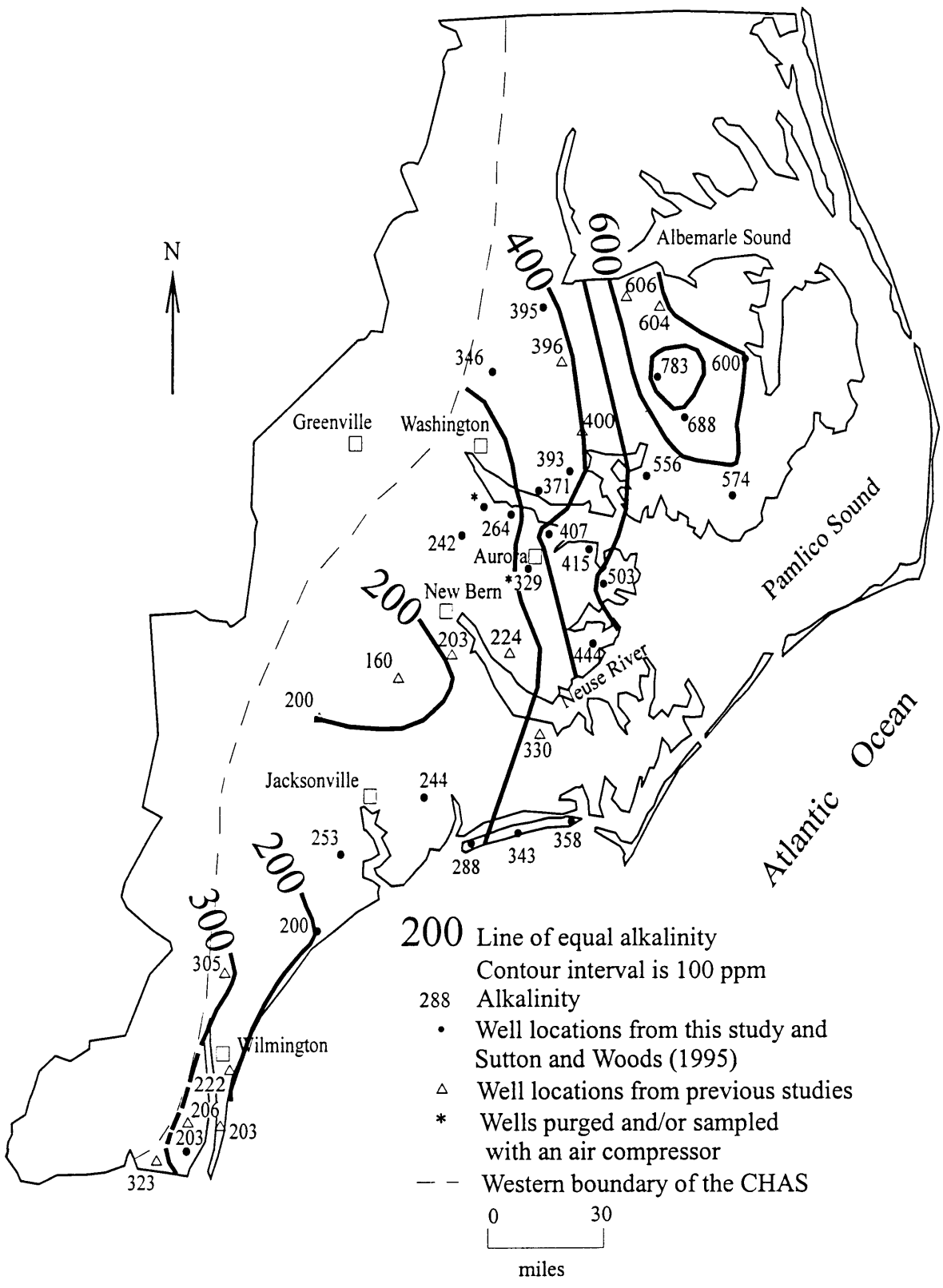

Figure 20. Alkalinity of the U-CHAS in ppm of HCO_3^- Concentrations were determined in the field.

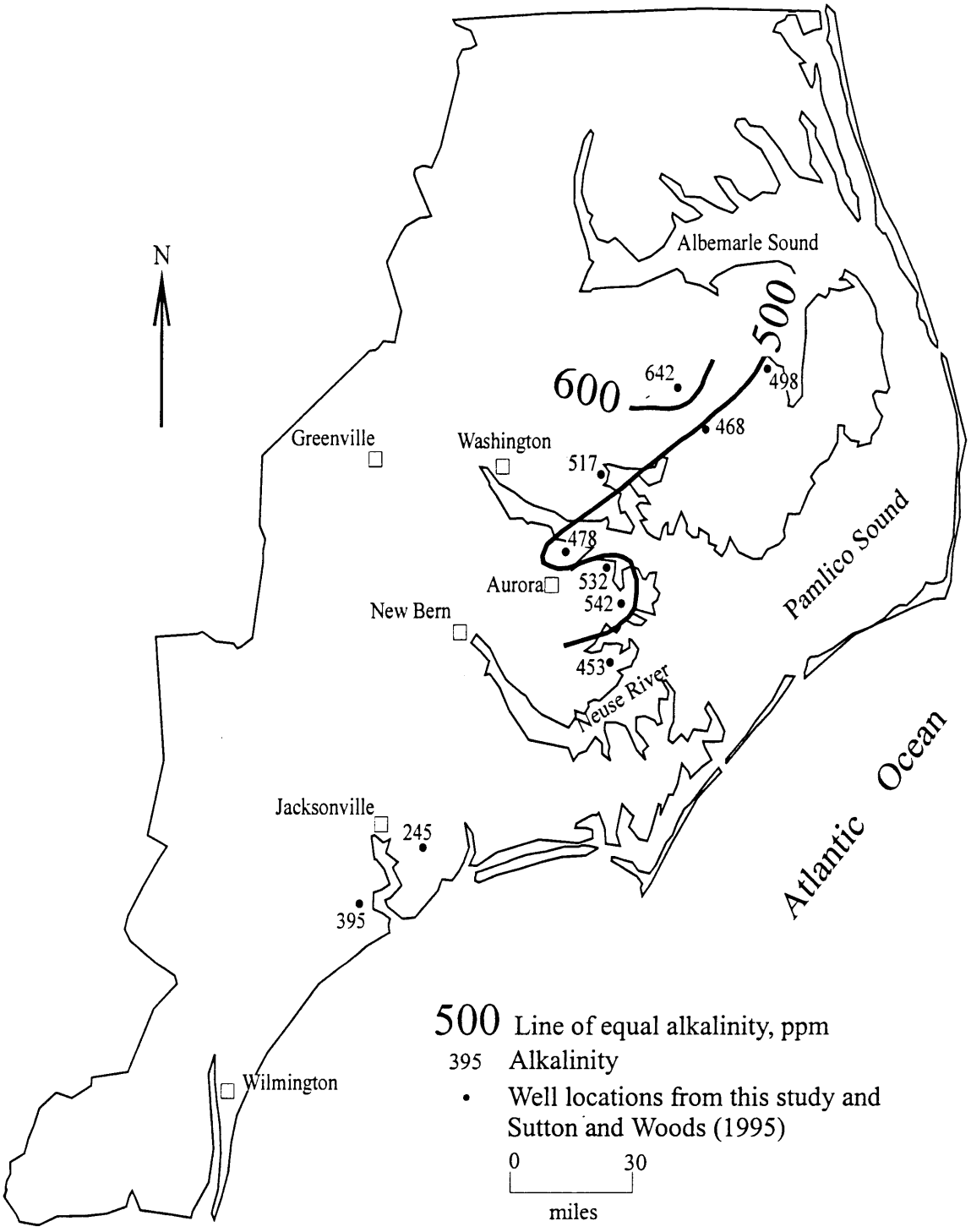

Figure 21. Alkalinity of the L-CHAS in ppm of HCO^-_3 Concentrations were determined in the field.

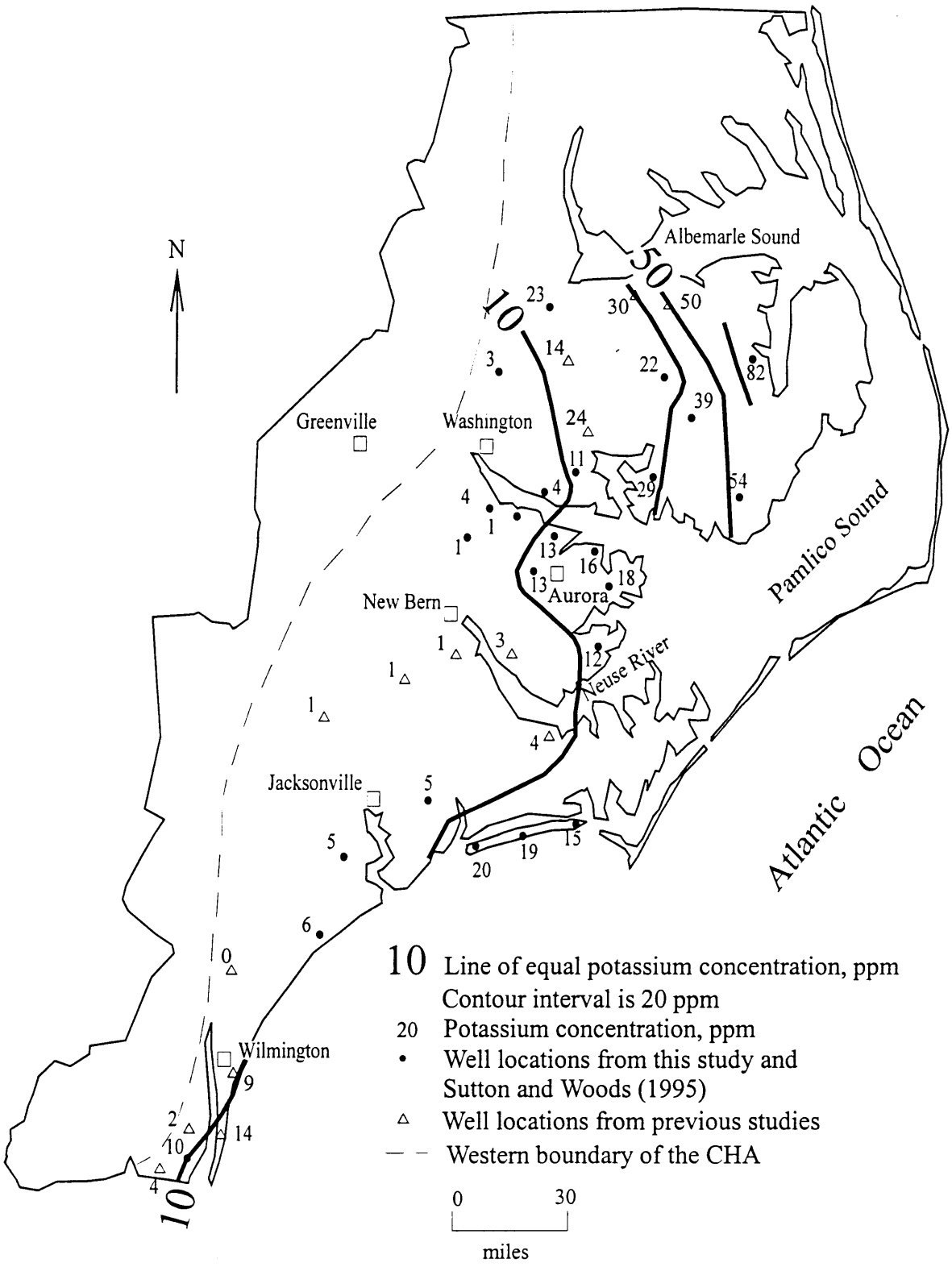

Figure 22. Potassium concentrations in the U-CHAS

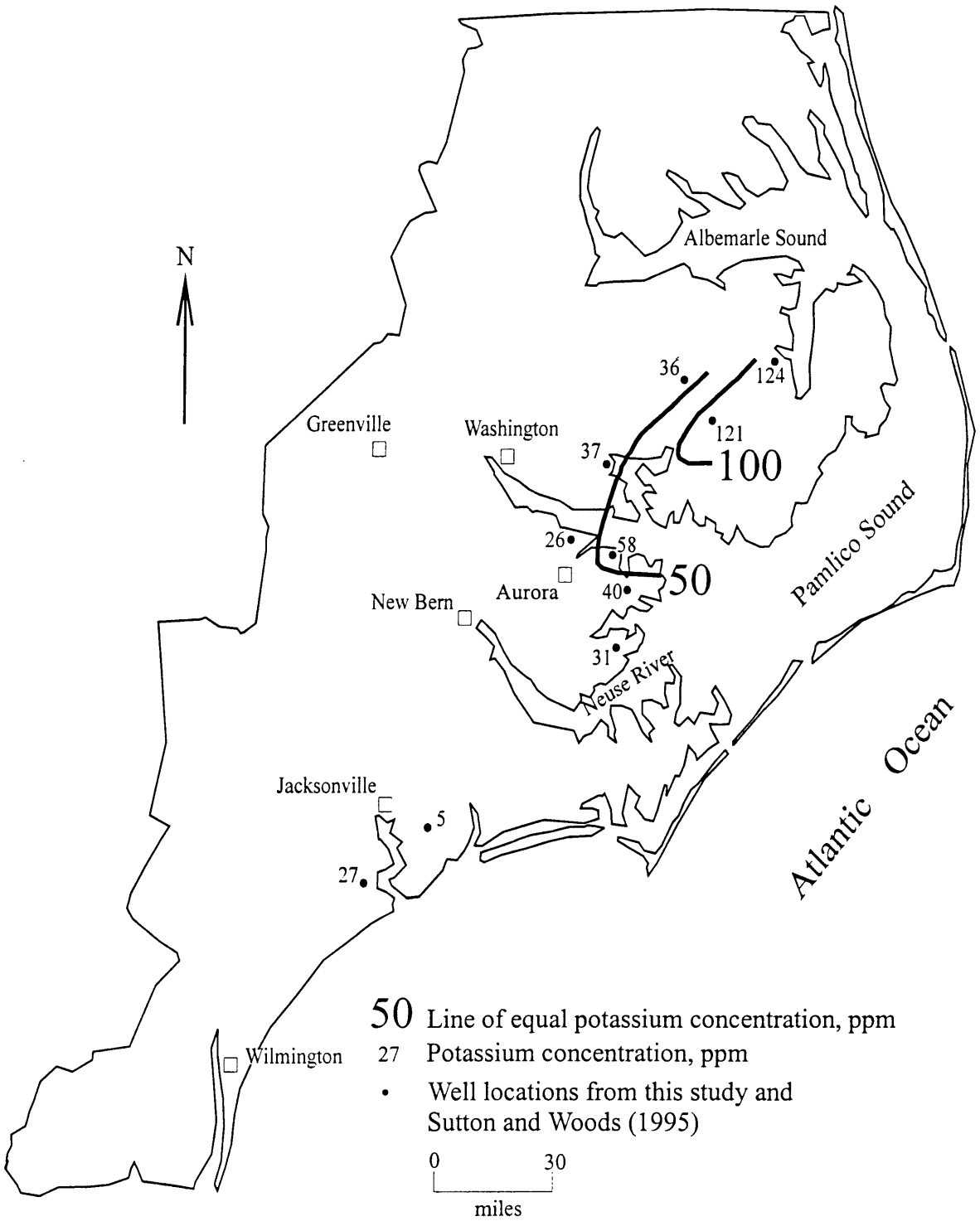

Figure 23. Potassium Concentrations in the L-CHAS

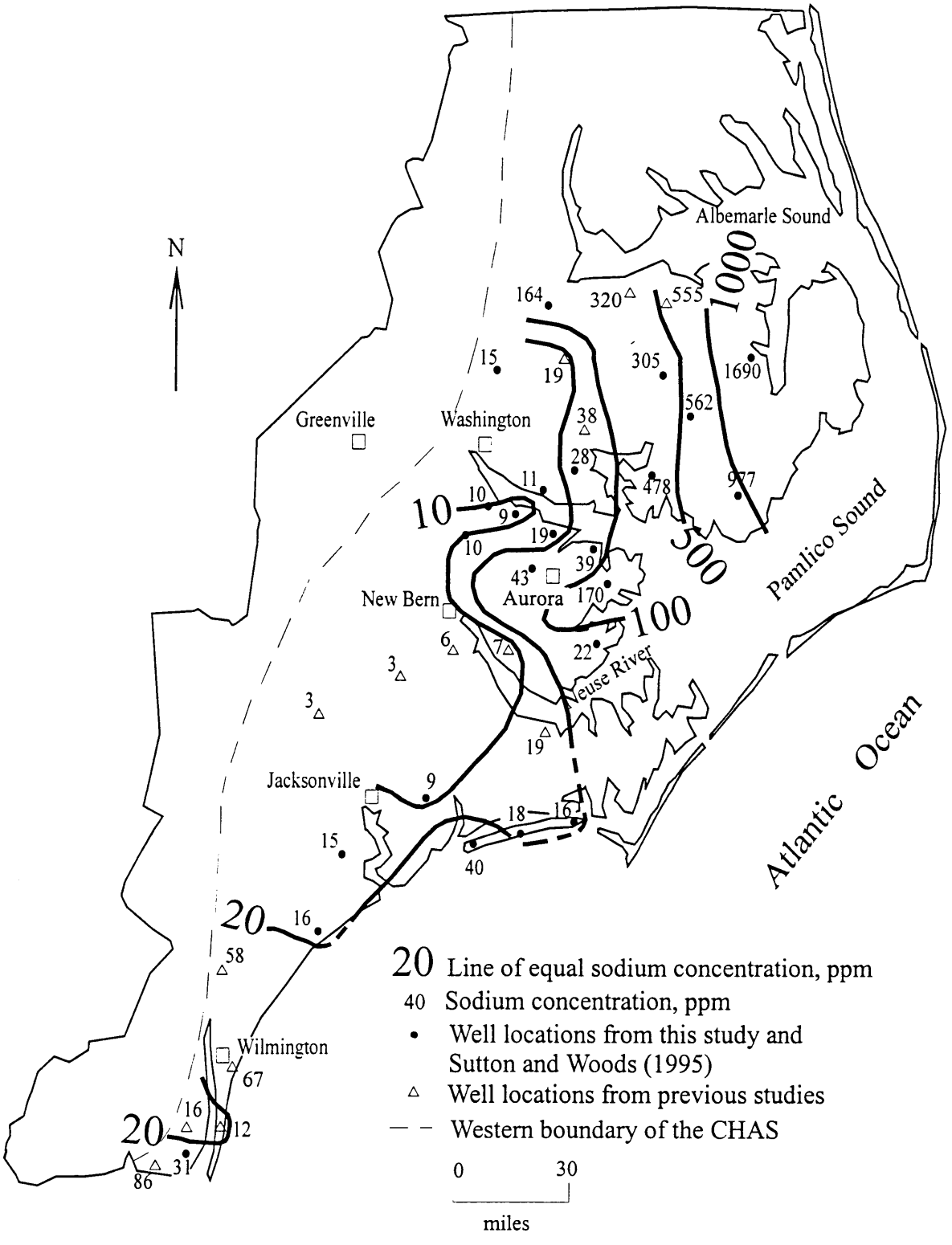

Figure 24. Sodium concentrations in the U-CHAS

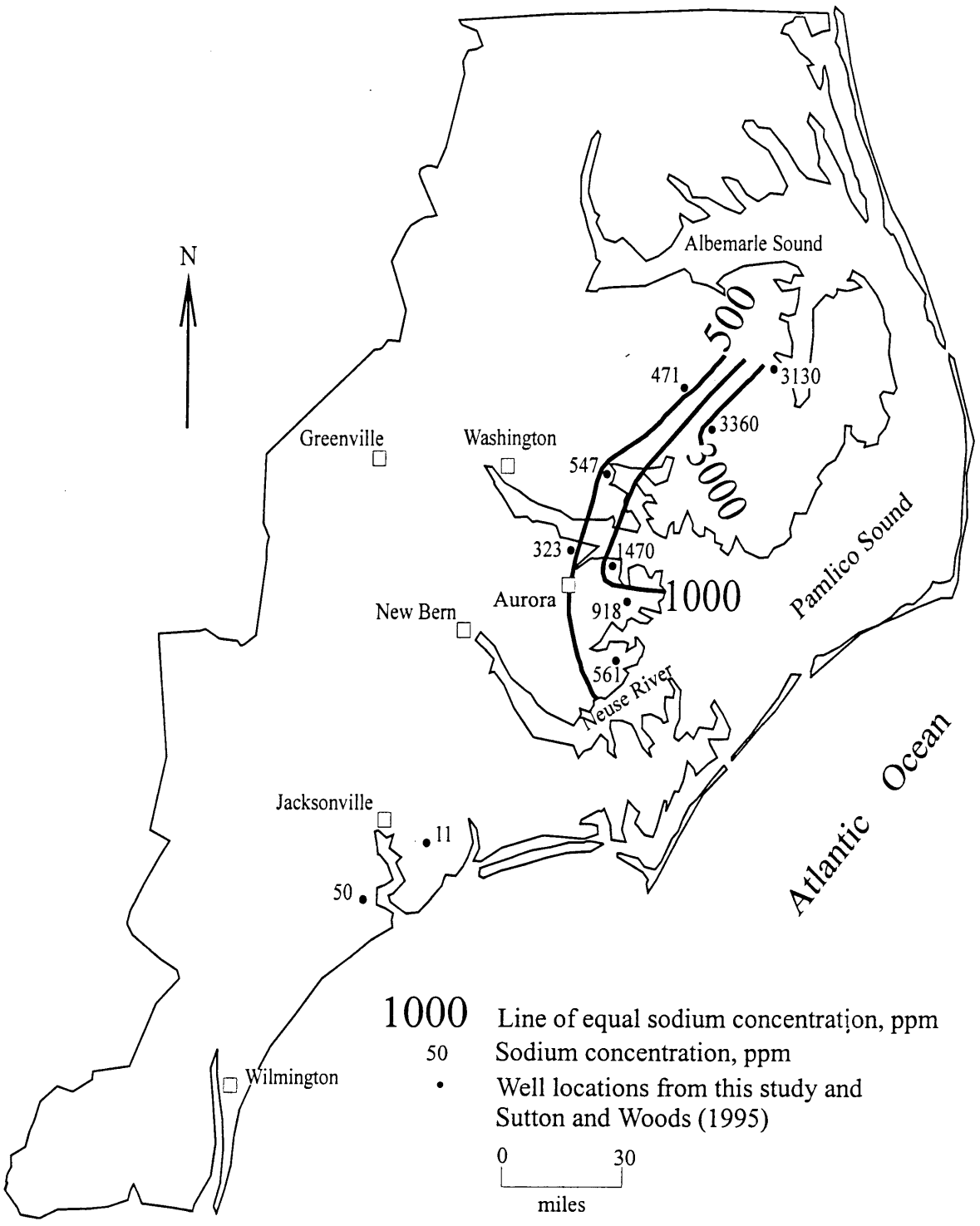

Figure 25. Sodium concentrations in the L-CHAS

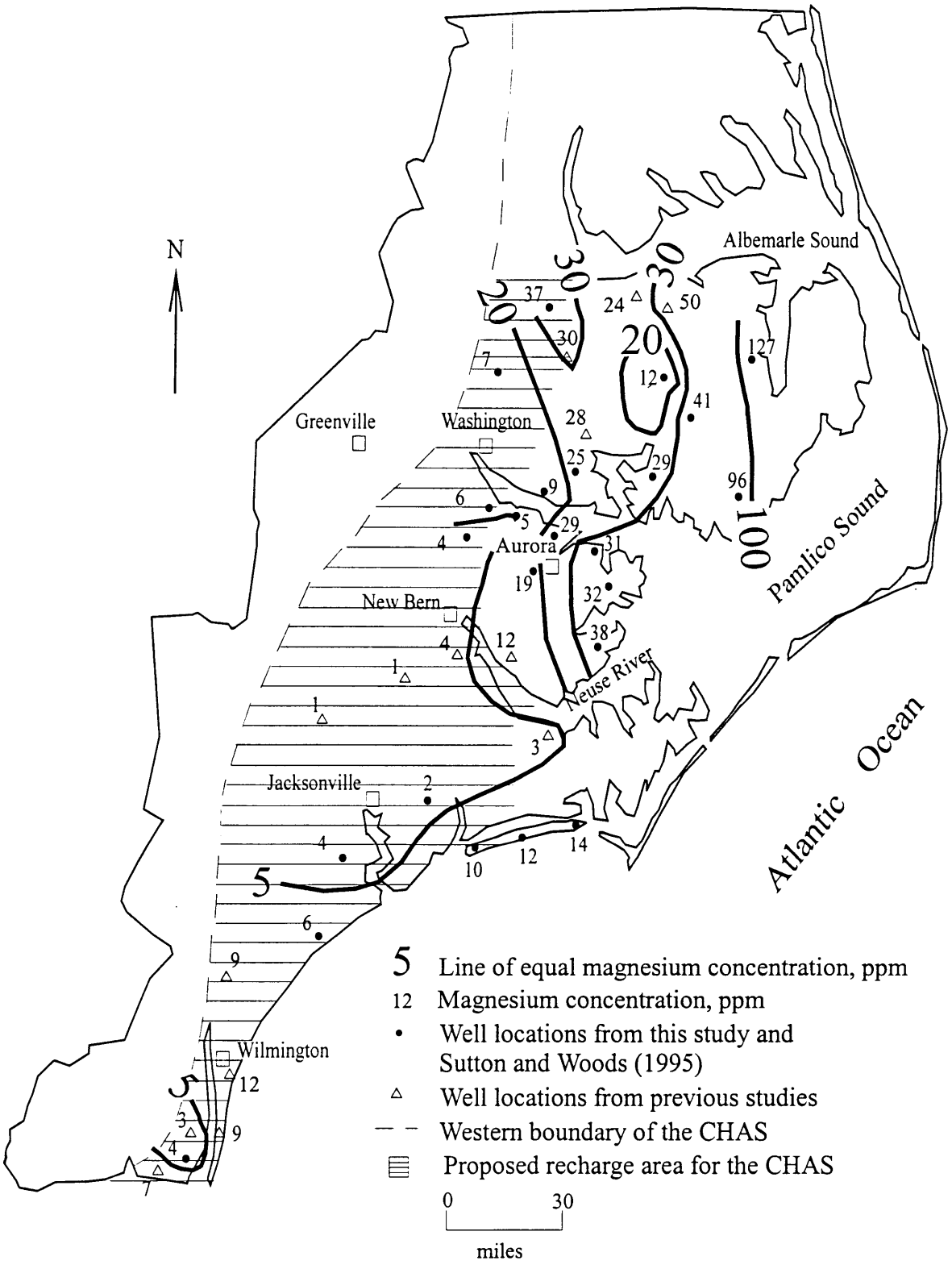

Figure 26. Magnesium concentrations in the U-CHAS

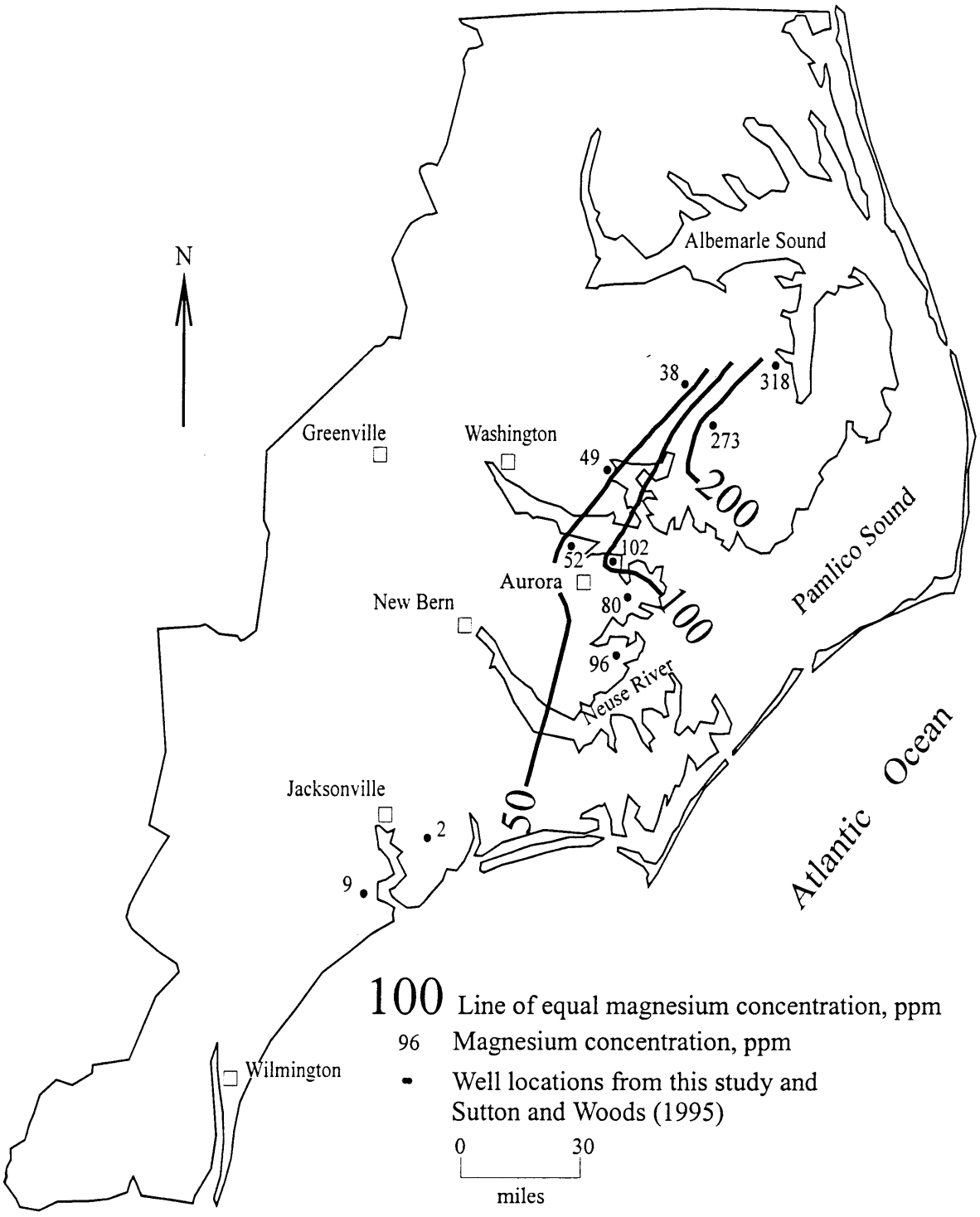

Figure 27. Magnesium concentrations in the L-CHAS

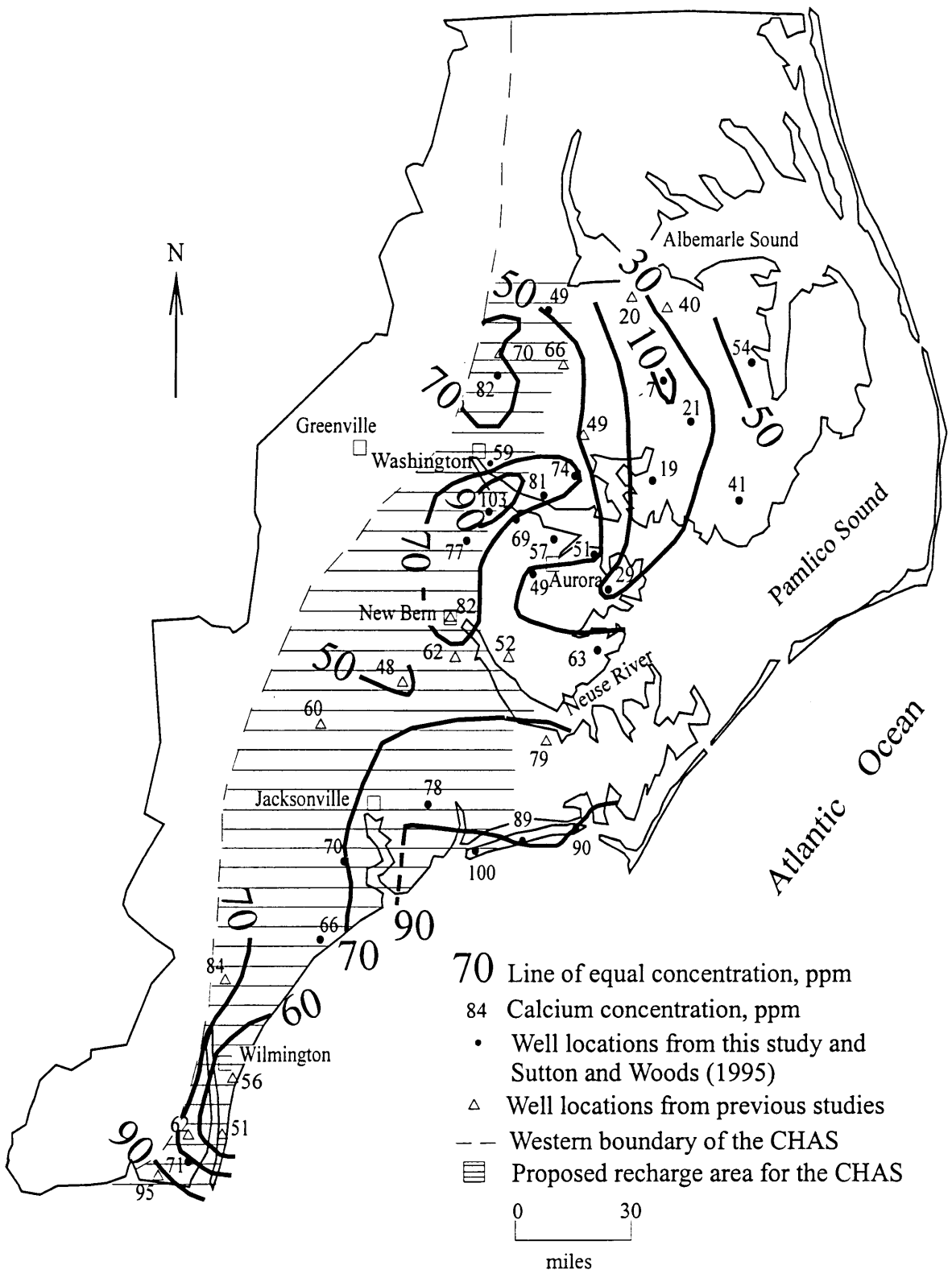

Figure 28. Calcium concentrations in the U-CHAS

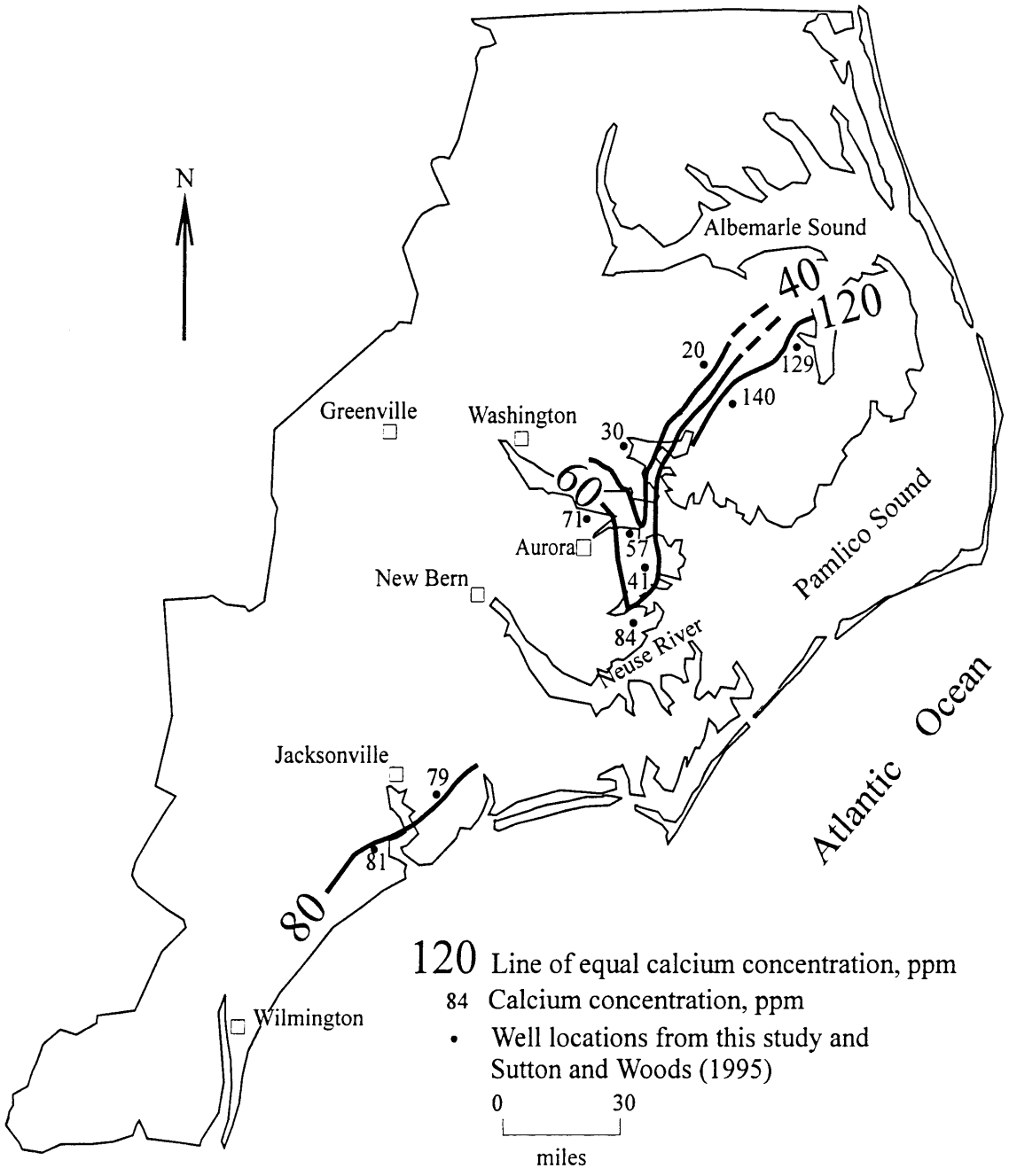

Figure 29. Calcium concentrations in the L-CHAS

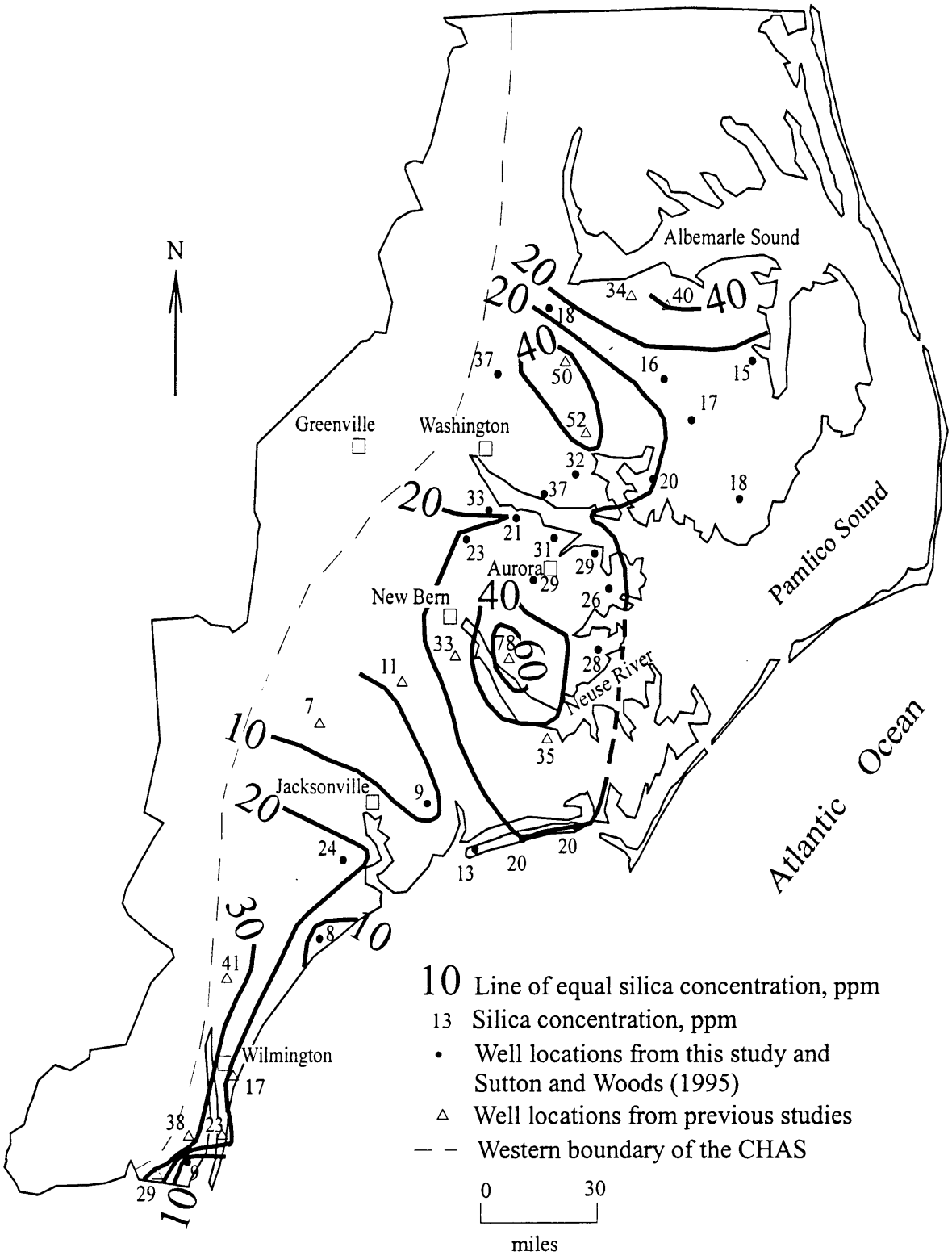

Figure 30. Silica concentrations in the U-CHAS

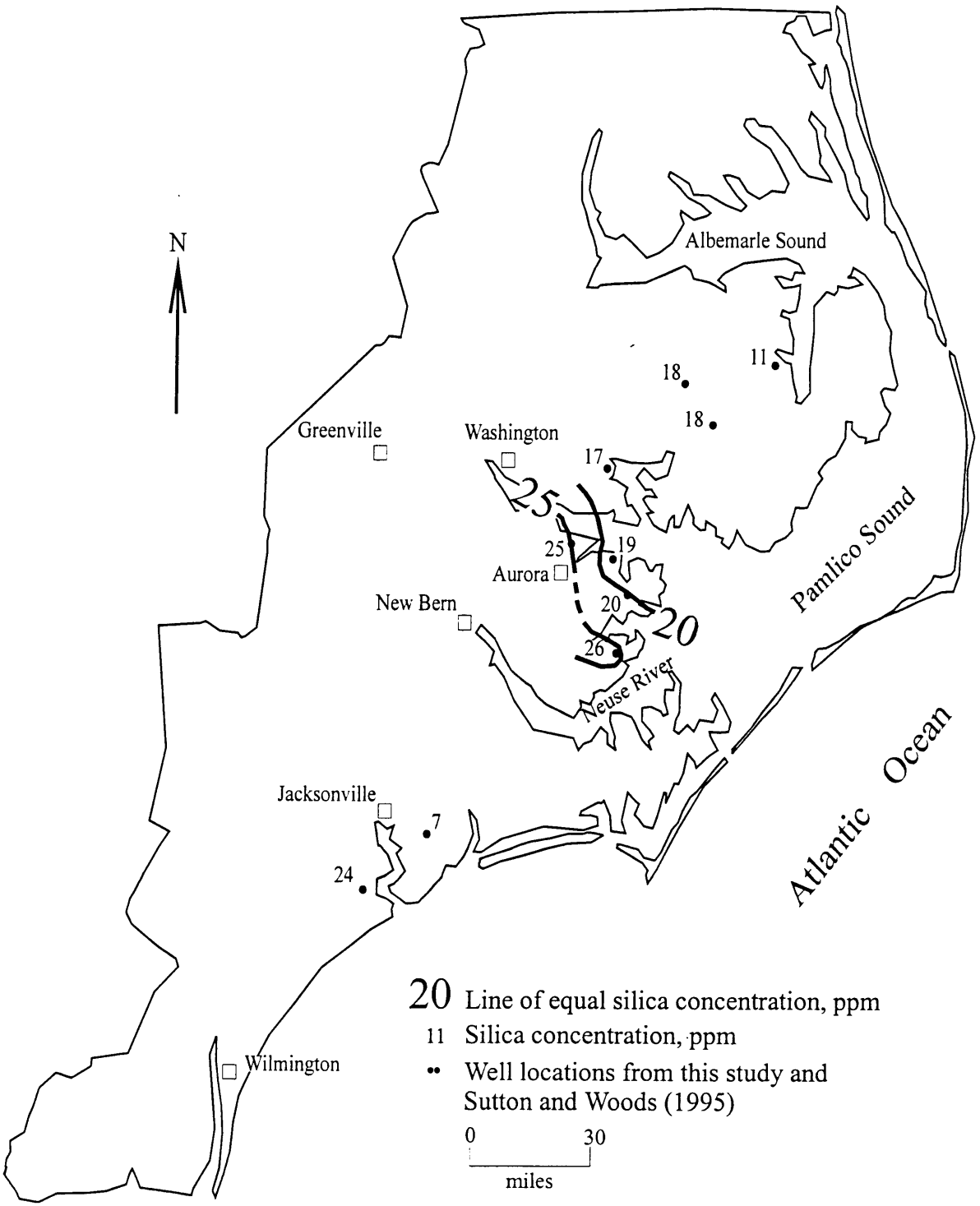

Figure 31. Silica concentrations in the L-CHAS

and 78 ppm of silica. These older analyses may be erroneous as silica values greater than about 40 ppm are quite rare (Sprinkle 1989).

Piper diagrams (1944) were used to delineate hydrochemical facies of groundwater in the Northern (Figures 32 and 33) and Southern (Figures 34 and 35) Coastal Plain. On Figure 36 calculated hydrochemical facies for all U-CHAS groundwater samples (including some from previous studies) are reported. In the western region (approximately coinciding with the recharge area) all waters are Ca rich (1) and bicarbonate rich (A), except wells BBPW5 and NH262 (Figure 8). Waters near Aurora are dominated by a mixture of cations and HCO_3 (4A) and the northeasternmost wells in the U-CHAS become alkali rich (3) and Cl rich (C), just like waters in the L-CHAS (Figure 37). Well L13i1 (Figure 8) is alkali rich (3) and bicarbonate rich (A).

Minor Elements

Ammonia concentrations increased from west to east in both the CHAS units (Figures 38 and 39) and were always higher in the L-CHAS than in the U-CHAS at the same site. No significantly high nitrite, nitrate, or phosphate concentrations were found and no clear patterns of geographic variation emerged, so contour maps for these constituents are not included. Very high dissolved sulfide values at TGCW14 (5.8ppm, Figure 8) in the U-CHAS and P16o3 (7.1ppm, Figure 9) in the L-CHAS complicate the pattern, but concentrations in the Northern Coastal Plain generally increase from west to east (Figures 40 and 41). Except for BBPW5 (1.5ppm) and BBPW7 (0.05ppm) in the U-CHAS (Figure 8) dissolved sulfide concentrations in the Southern Coastal Plain are below detection limits (Figure 40). There were no consistent differences between dissolved sulfide contents of waters from the Upper versus the Lower CHAS at the same site.

The pH for both the Upper and Lower CHAS ranged from 6.8 to 8.2 (Figures 42 and 43) with no consistent relationship observed between wells from the two aquifers at the same site (Sutton and Woods 1995). There are two distinct trends in pH in the U-CHAS (Figure 42). North of Jacksonville in two different areas separated by the Pamlico River, values generally increase and then decrease from west to east. South of Wilmington pH increases from southwest to northeast, which could be due to the lack of samples in the downdip part of the aquifer. No pH trend is apparent in the L-CHAS. Eh values (Figures 44 and 45) for the U-CHAS are generally more positive than those for the L-CHAS and values become more negative to the east in both aquifers.

Fluoride generally increases from west to east with some very high concentrations in the eastern portion of the Northeastern

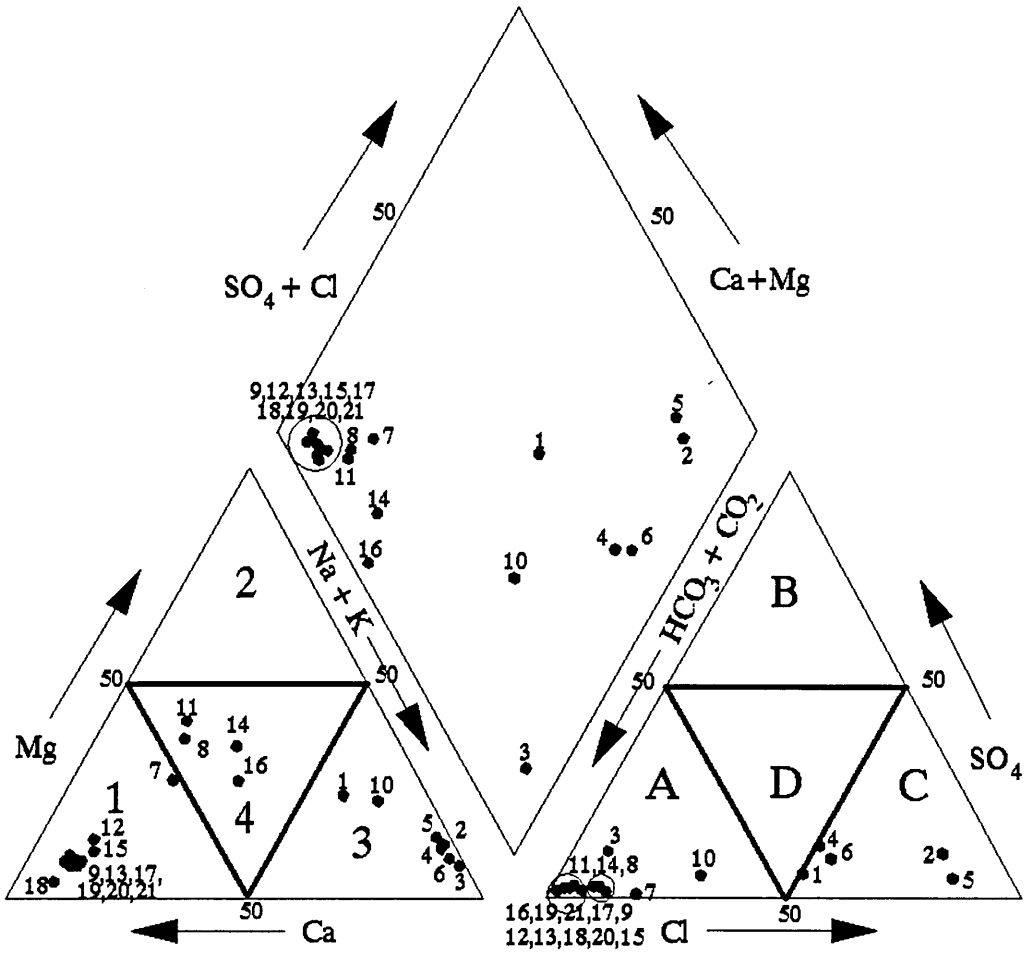

1. K-17 a-5
2. L-10 a-3
3. L-13 i-1
4. M-12 l-1
5. O-10 w-3
6. O-13 f-1
7. O-17 i-2
8. P-16 o-4
9. P-21 k-6
10. Q-15 u-3
11. S-15 y-4
12. TGCW-11A
13. TGCW-14
14. TGS-11
15. TGS-15
16. TGS-18
17. TGS-28
18. WWF-1
19. WWF-2
20. WWF-3
21. WWF-4

1. Ca-rich
2. Mg-rich
3. alkali-rich
4. mixed cations

A. bicarbonate-rich
B. sulfate-rich
C. chloride-rich
D. mixed anions

Figure 32. Piper diagram of the U-CHAS in the Northern Coastal Plain (Only includes wells sampled for this study.)

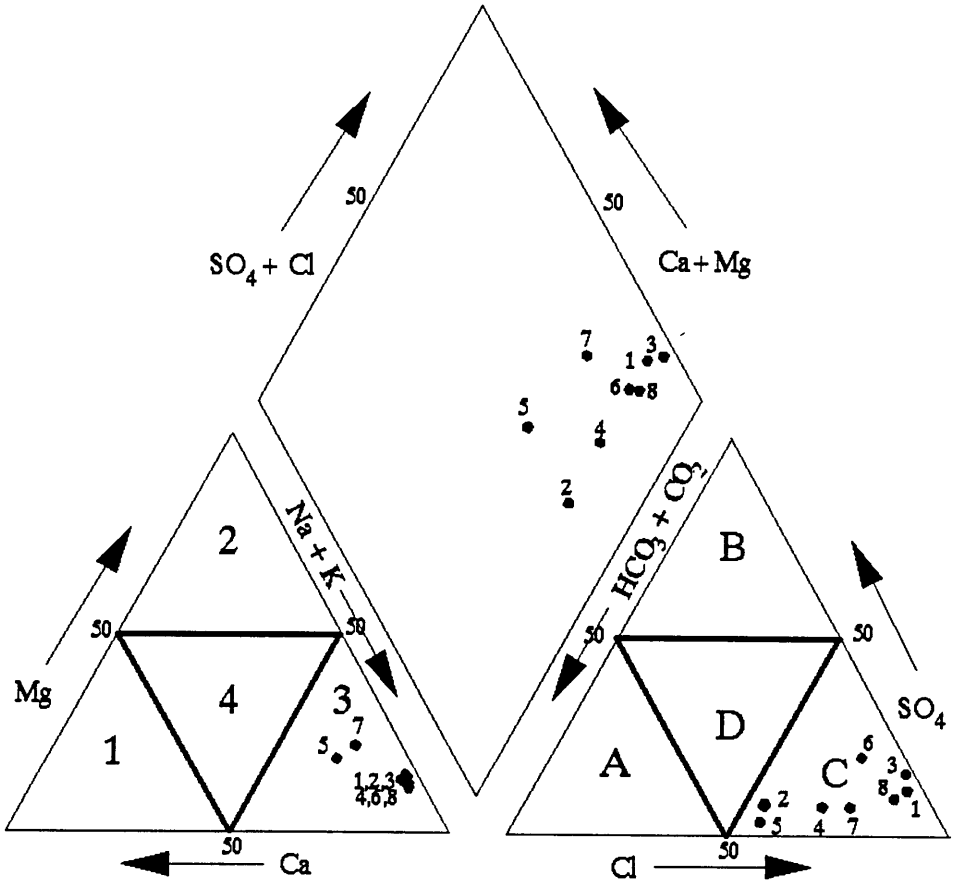

Figure 33. Piper diagram of the L-CHAS in the Northern Coastal Plain (Only includes wells sampled for this study.)

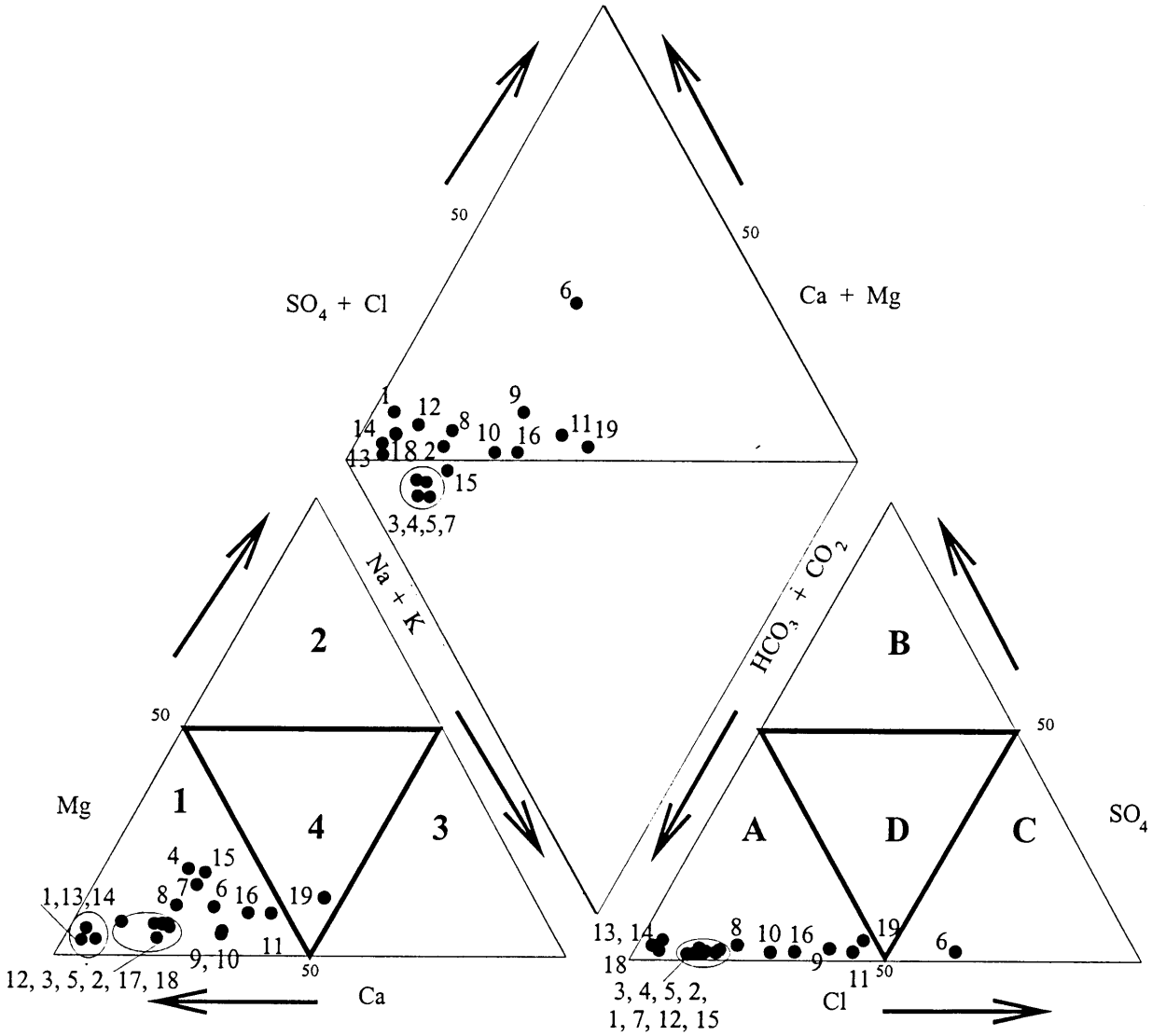

1. HOW 5
2. Y25Q1
3. ABPW 5
4. ABPW 6
5. BBPW 2
6. BBPW 5
7. BBPW 7
8. Pe 72
9. SPPW 002
10. SPPW 003
11. BR 16
12. BR 19
13. T23x1
14. U26j1
15. NH 399
16. NH 23
17. USMC 30
18. CR 258
19. NH 262

1. Ca-rich
2. Mg-rich
3. alkali-rich
4. mixed cations

A. bicarbonate-rich
B. sulfate-rich
C. chloride-rich
D. mixed anions

Figure 34. Piper Diagram of the U-CHAS in the Southern Coastal Plain. Only includes wells sampled for this study.

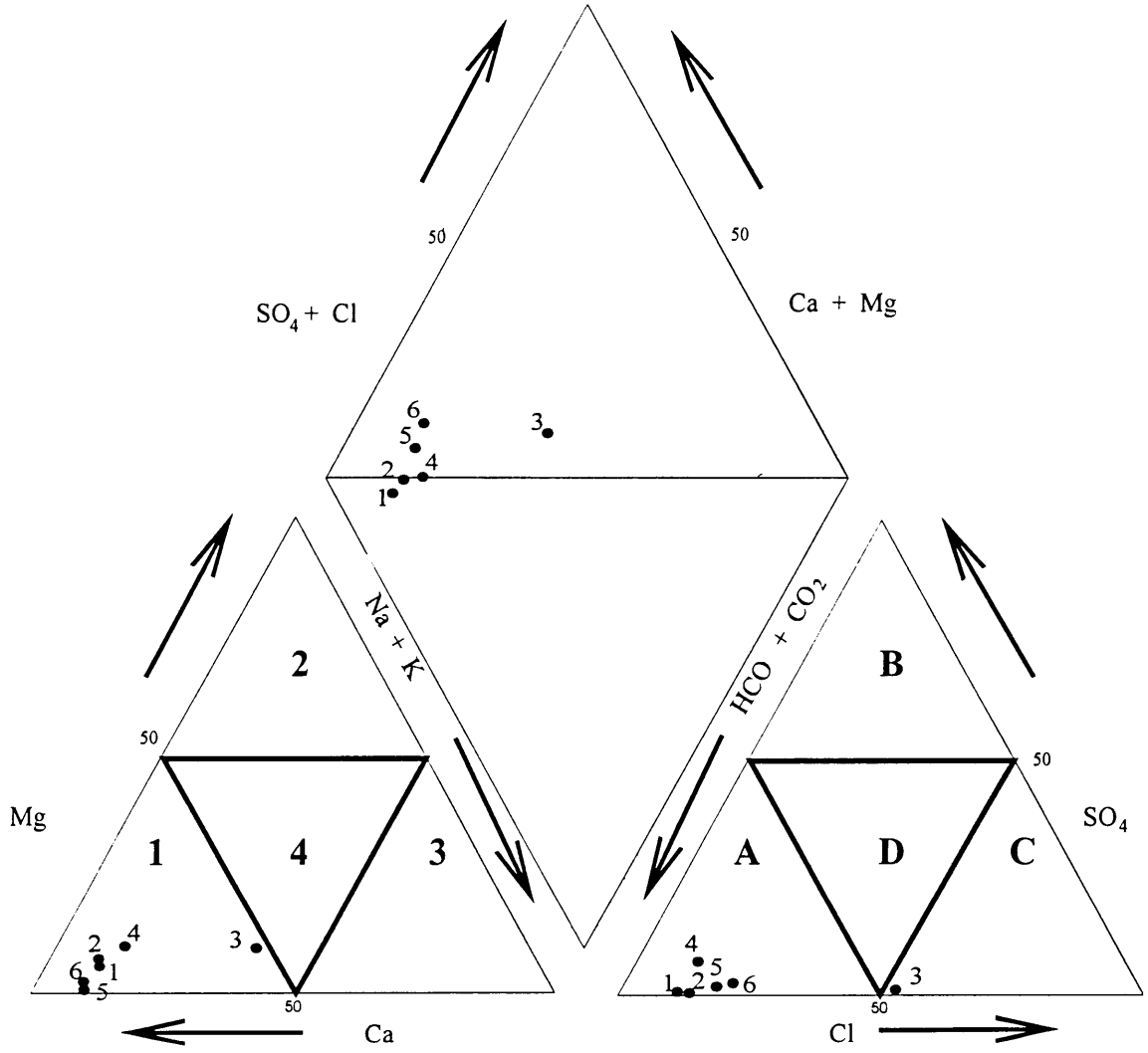

1. SFOW 1
2. SFOW 2
3. SFOW 3
4. SFOW 4
5. HPW 2
6. HPW 3

1. Ca-rich
2. Mg-rich
3. alkali-rich
4. mixed cations

A. bicarbonate-rich
B. sulfate-rich
C. chloride-rich
D. mixed anions

Figure 35. Piper Diagram of the L-CHAS in the Southern Coastal Plain. Only includes wells sampled for this study.

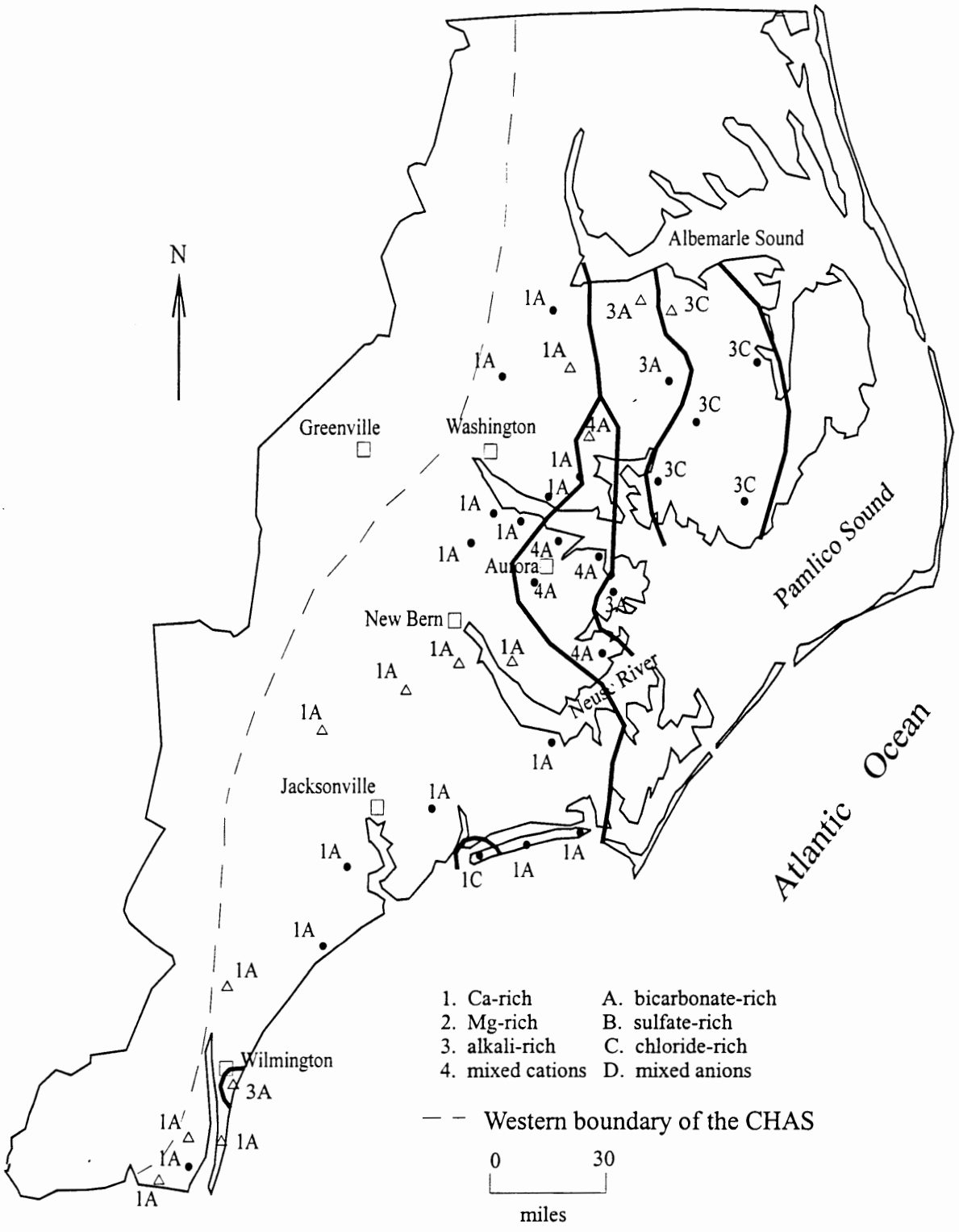

Figure 36. U-CHAS hydrochemical facies

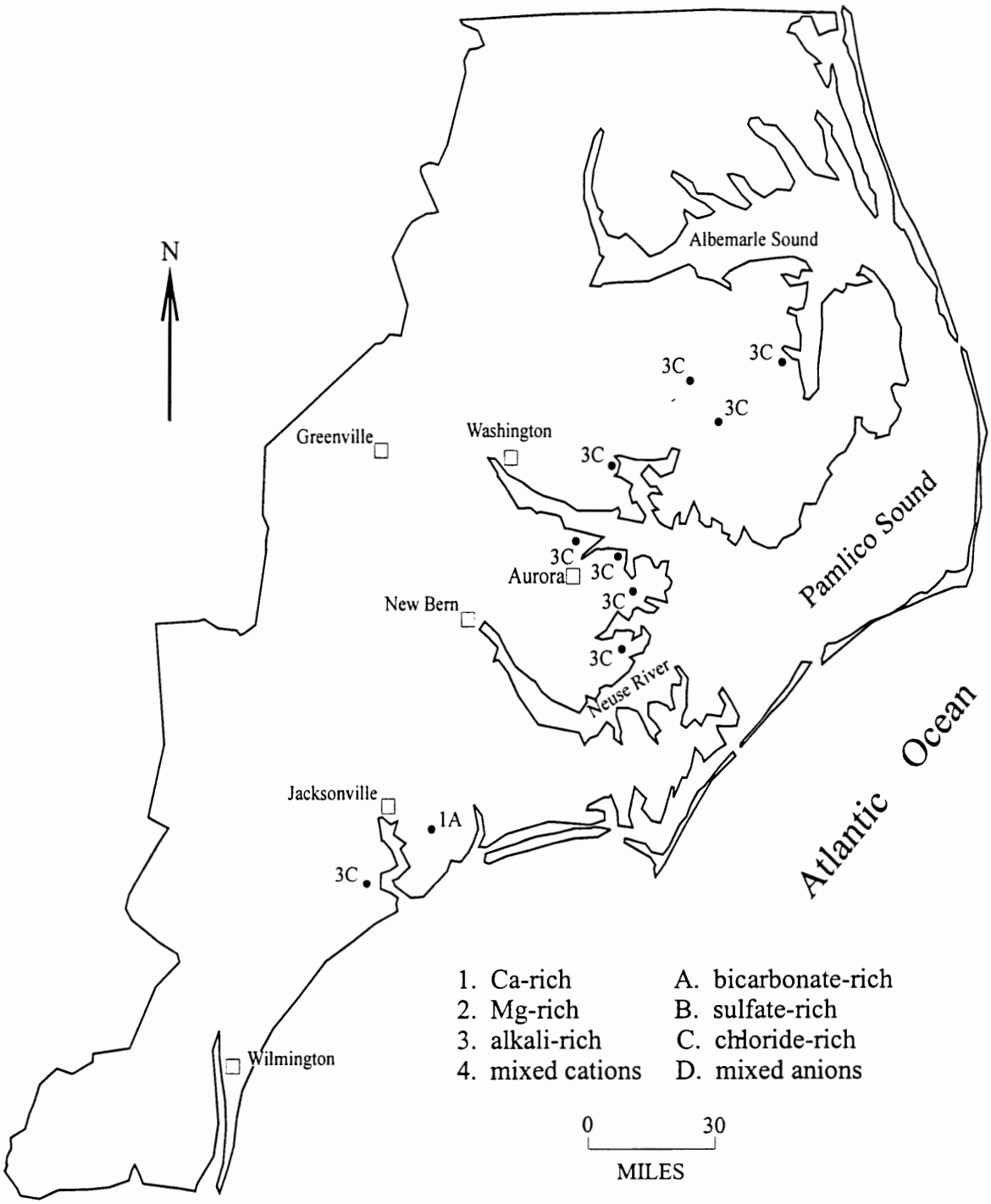

Figure 37. L-CHAS hydrochemical facies

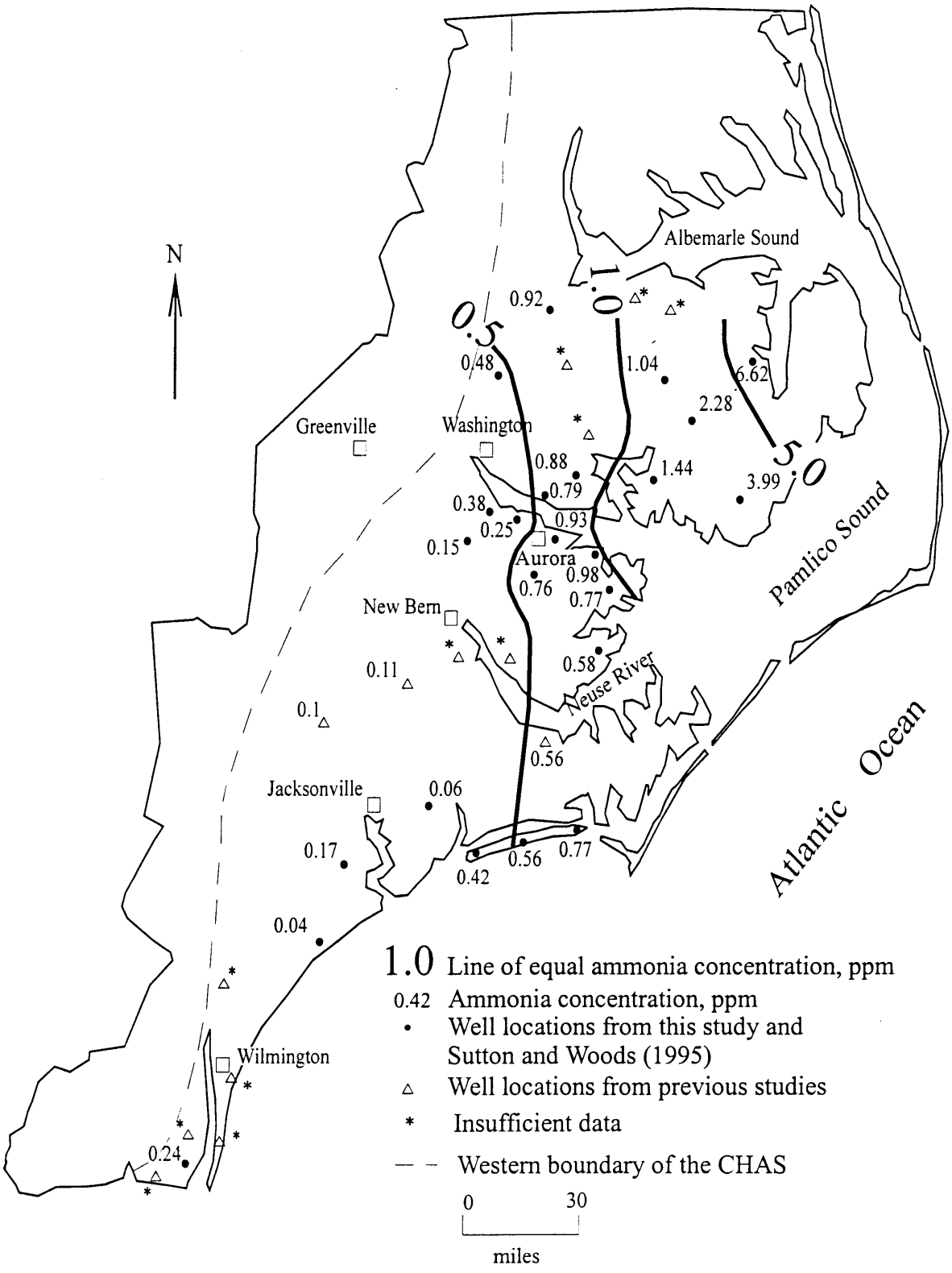

Figure 38. Ammonia concentrations in the U-CHAS
* Indicates that ammonia data were not available.

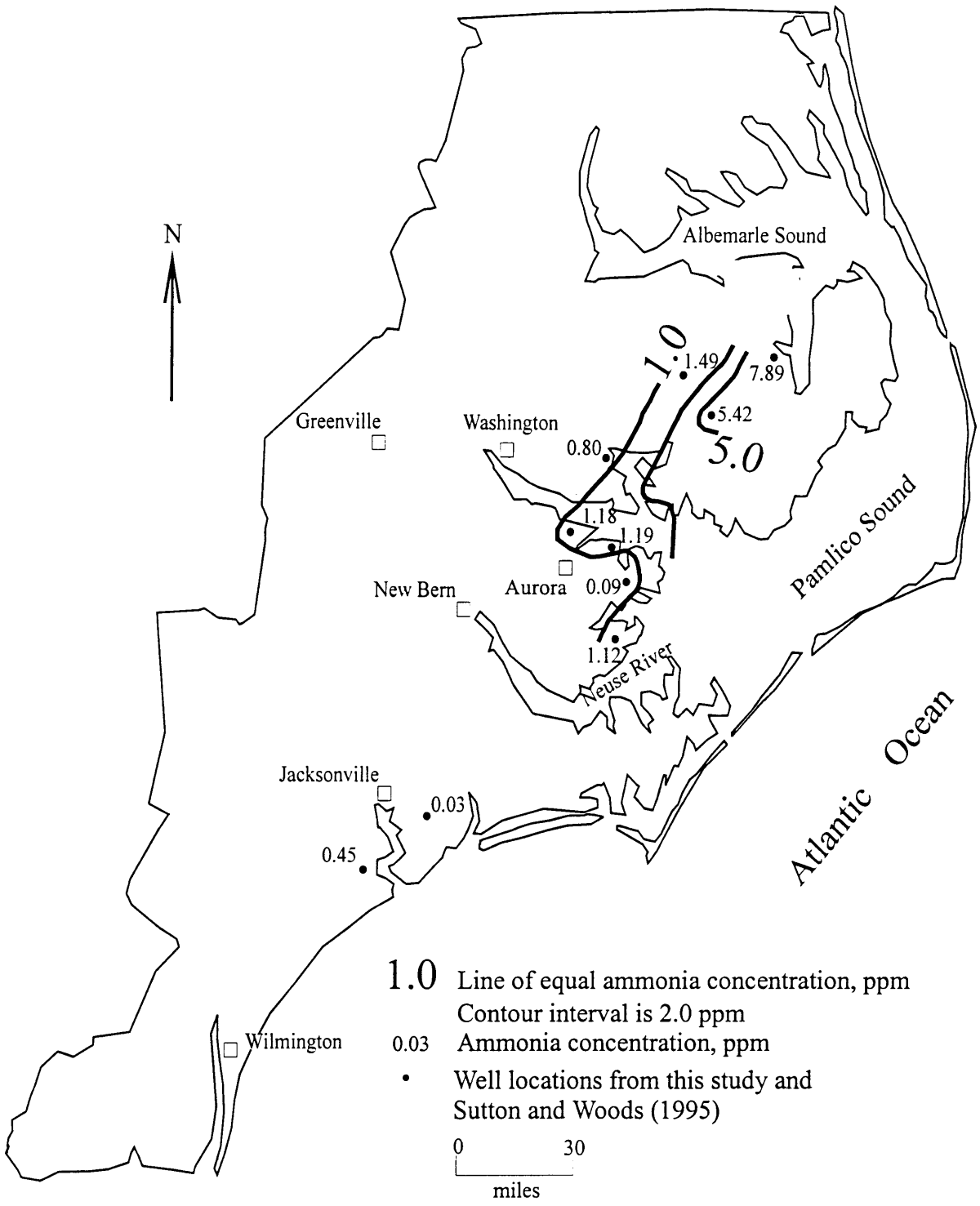

Figure 39. Ammonia concentrations in the L-CHAS

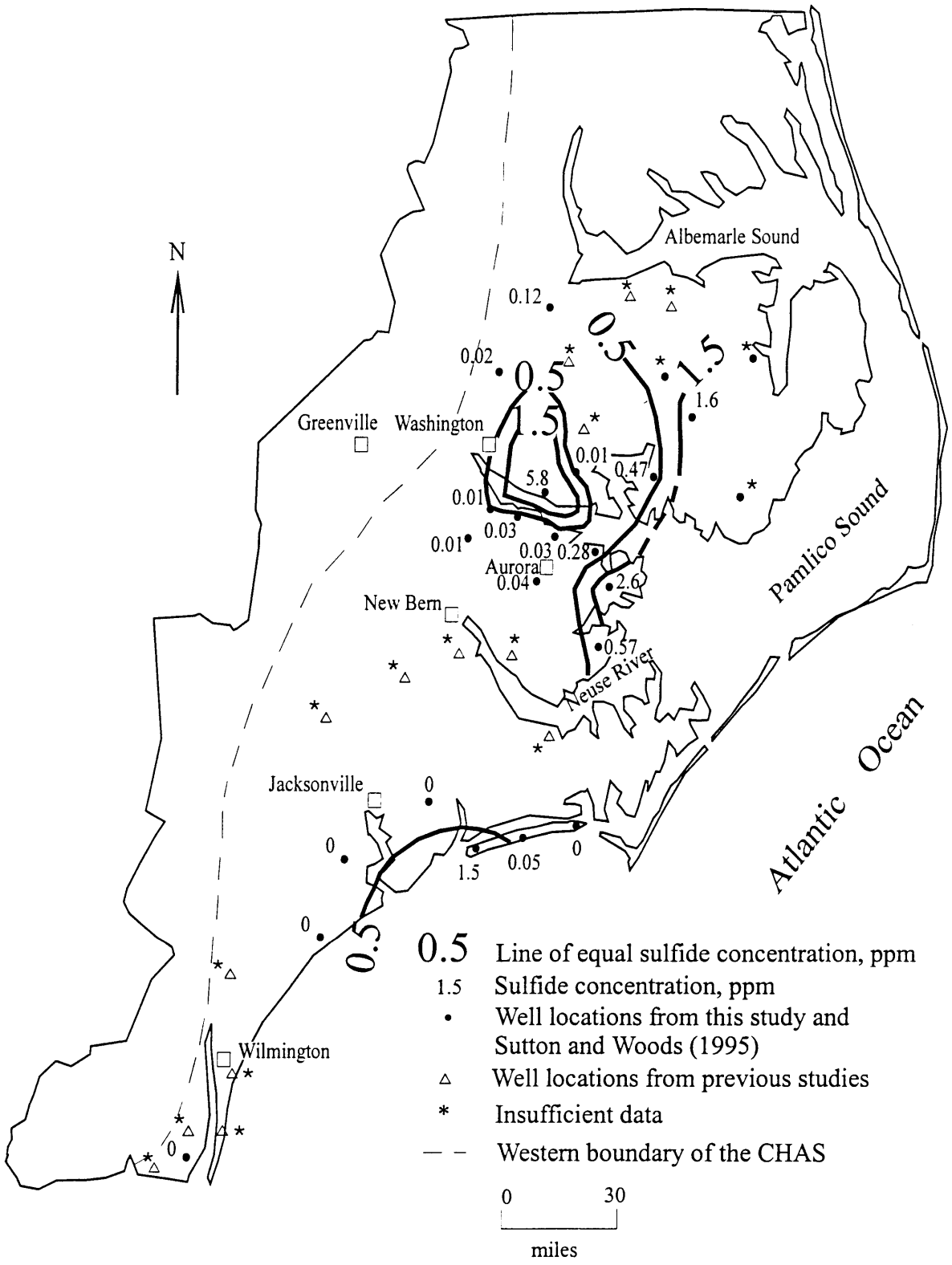

Figure 40. Sulfide concentrations in the U-CHAS
* Iindicates that sulfide data were not available.

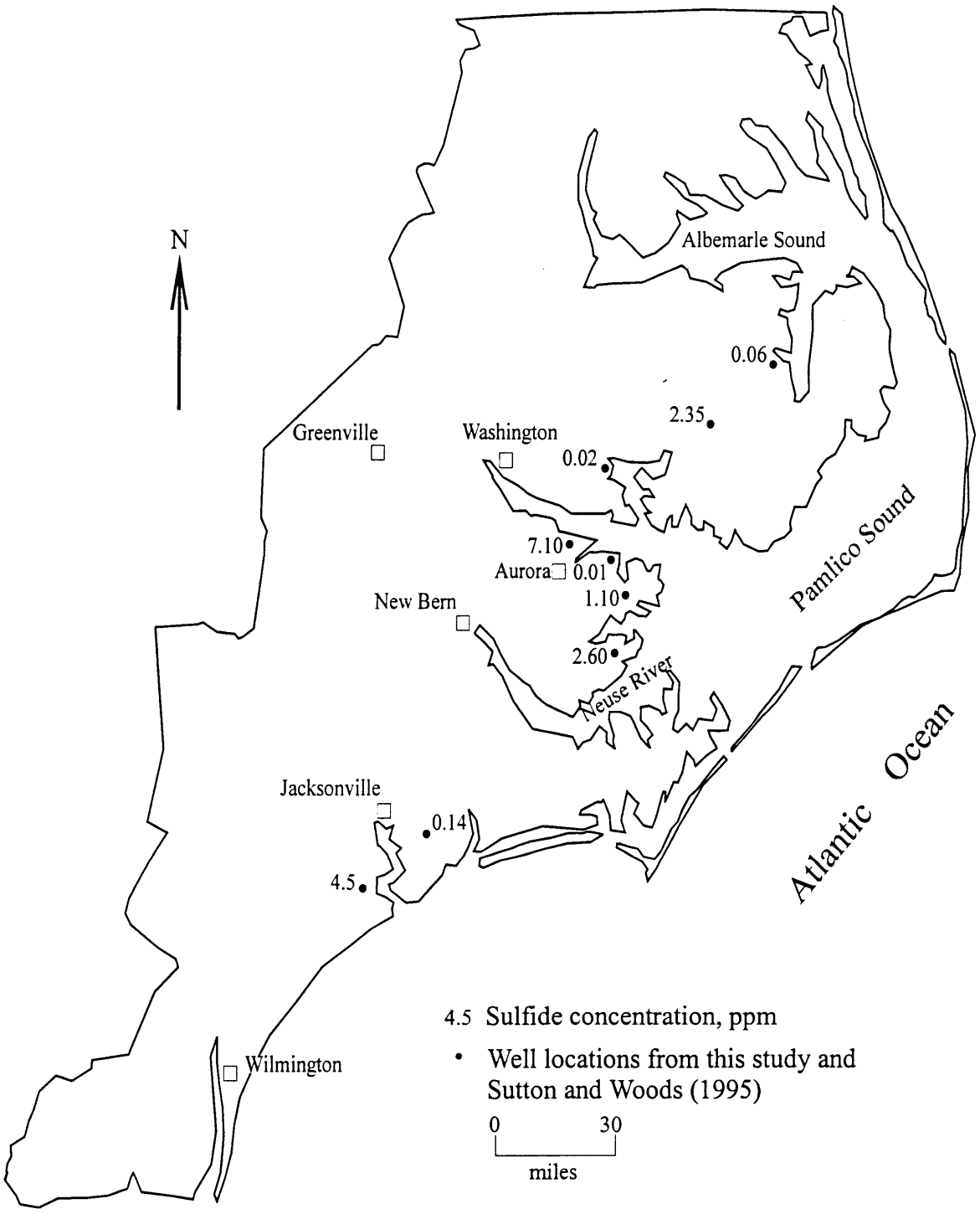

Figure 41. Sulfide Concentrations in the L-CHAS

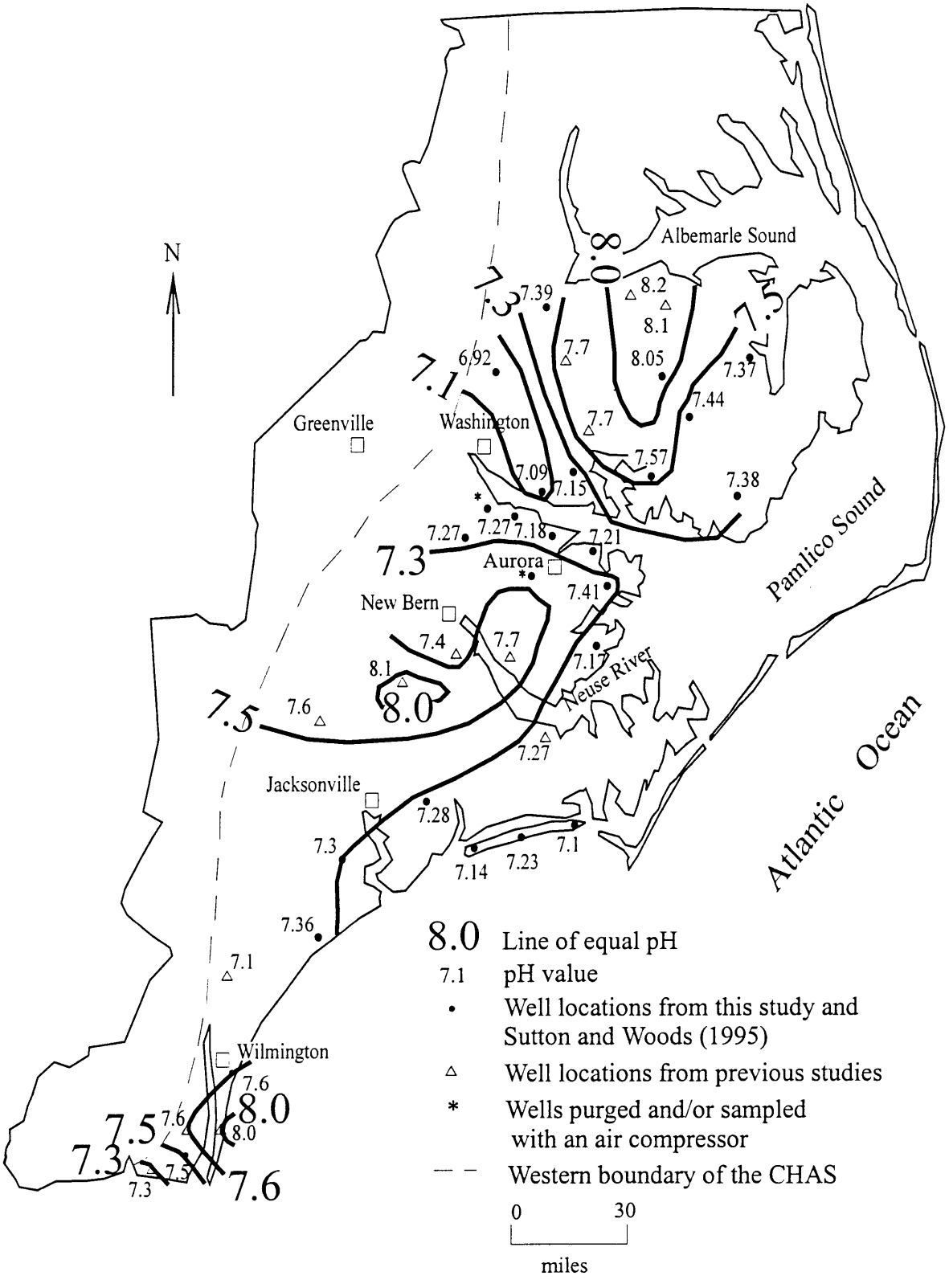

Figure 42. pH values in the U-CHAS

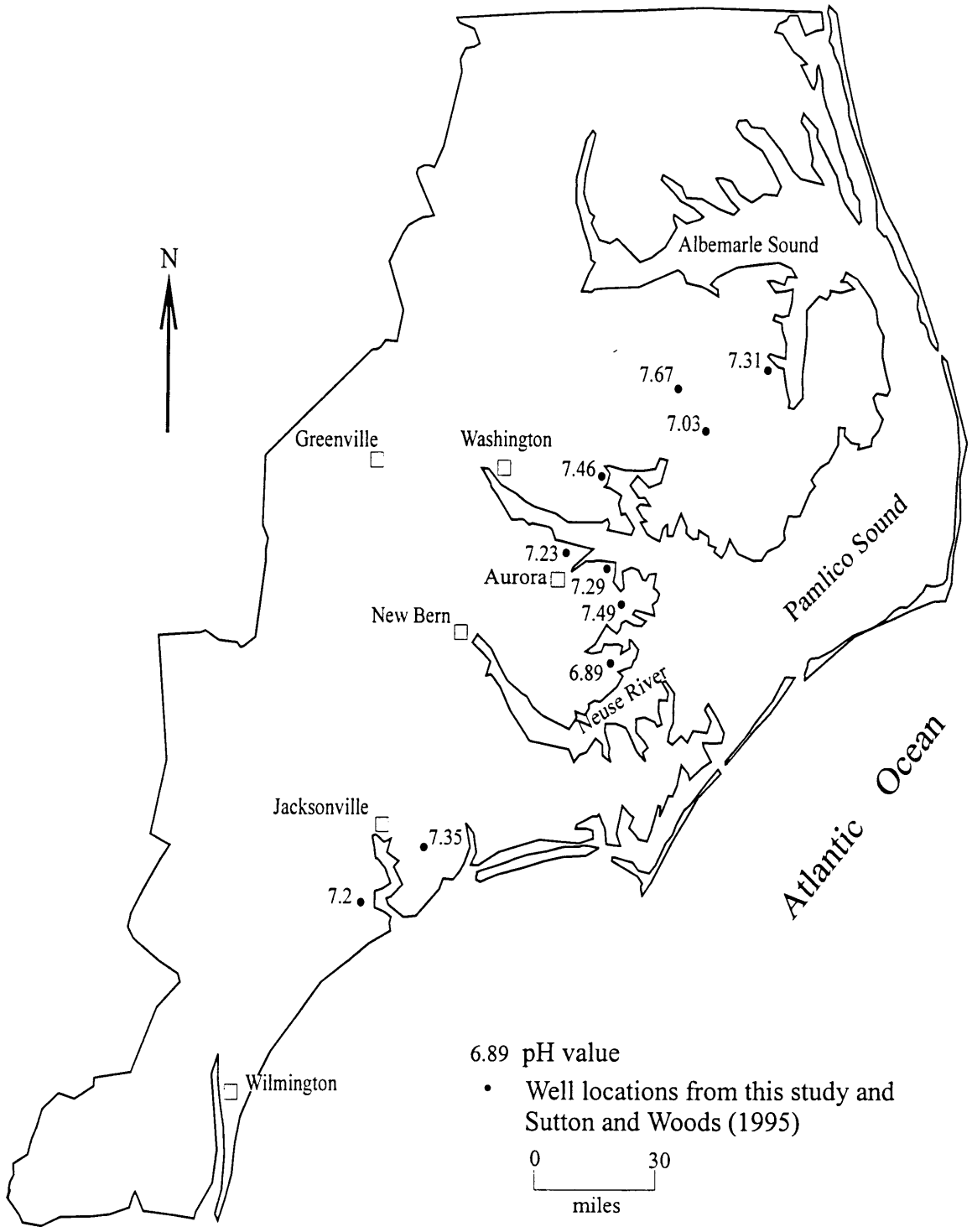

Figure 43. pH values in the L-CHAS

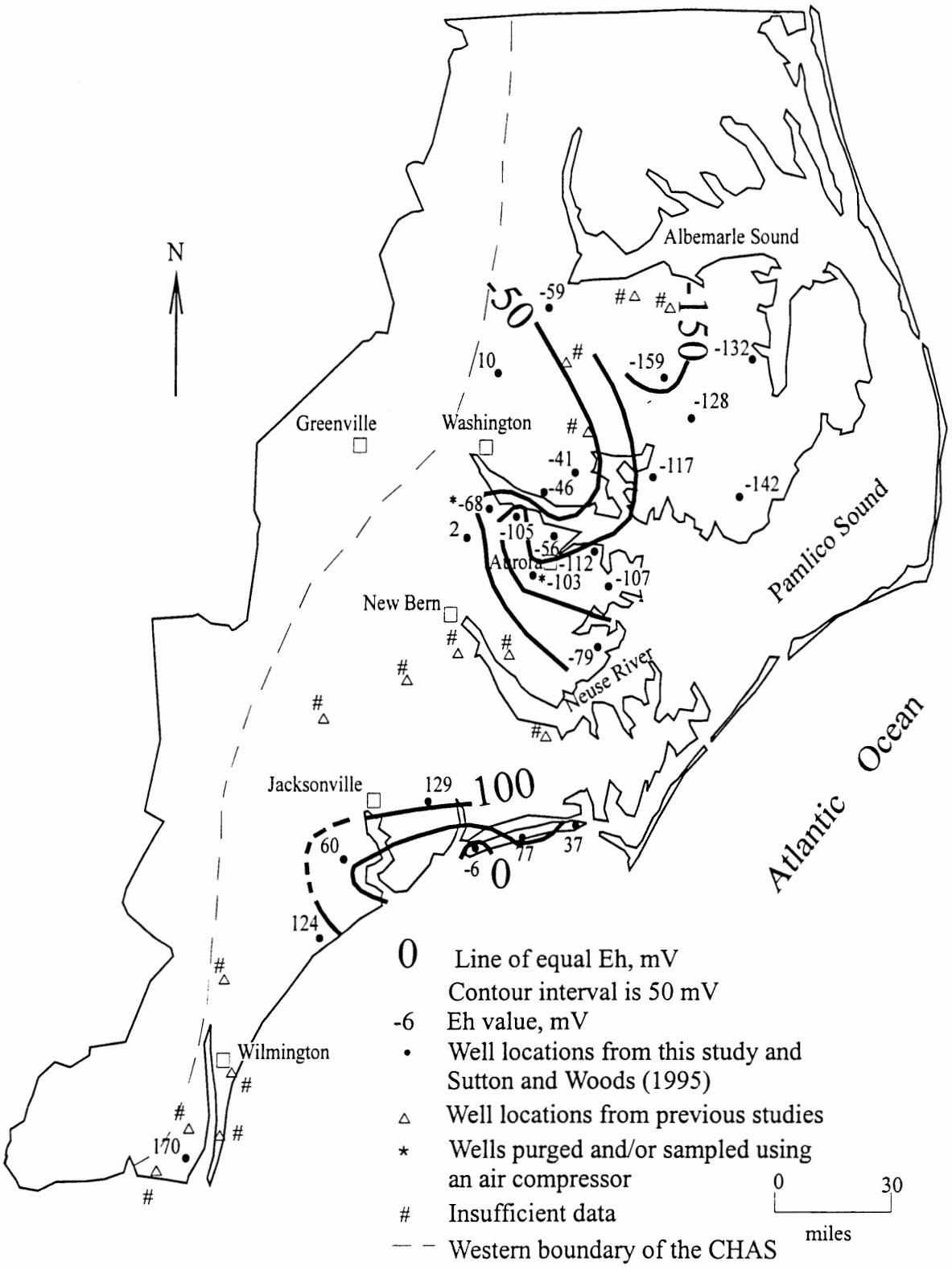

Figure 44. Eh values in the U-CHAS in millivolts (mV)

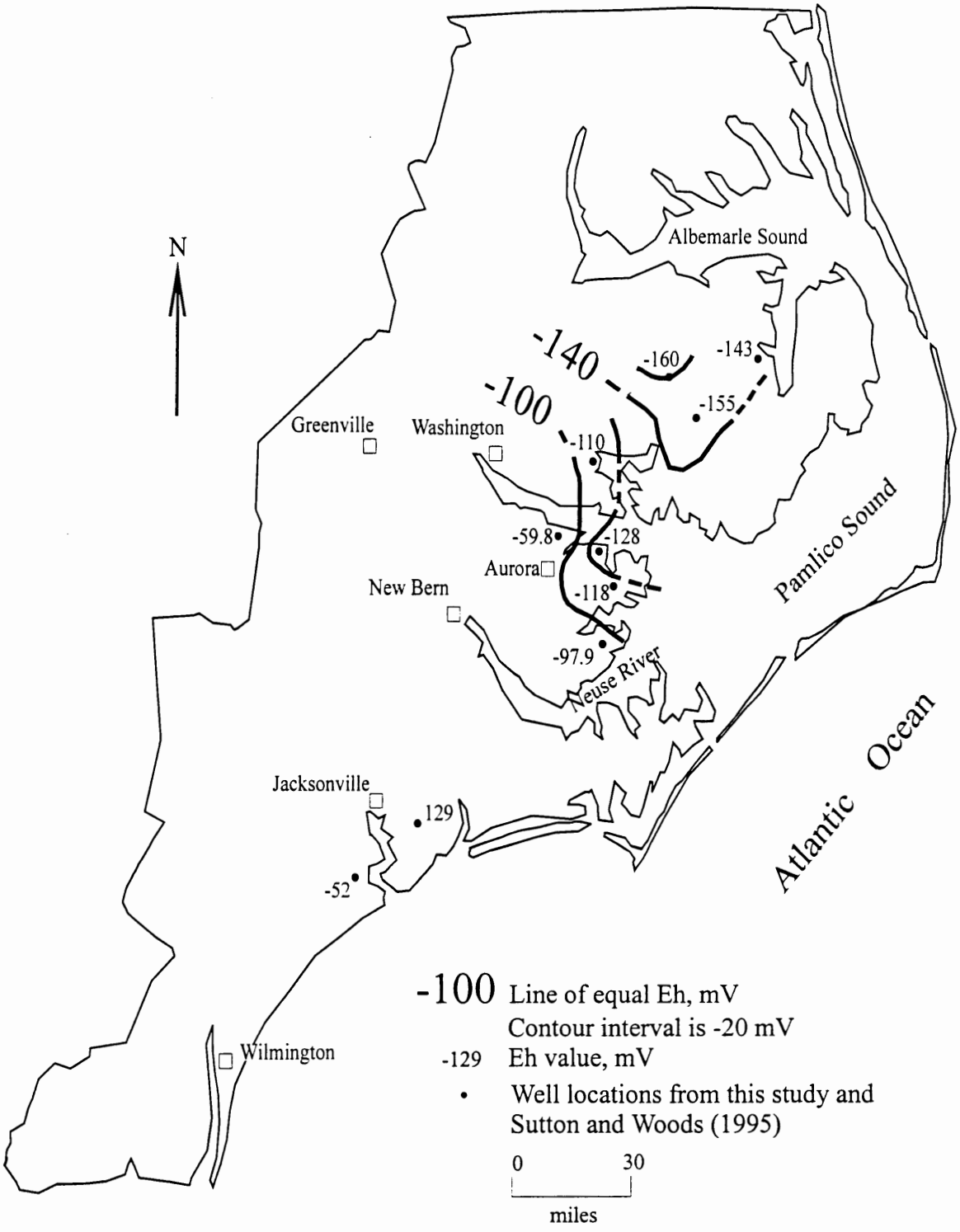

Figure 45. Eh values in the L-CHAS in millivolts (mV)

Coastal Plain (Figures 46 and 47). At the same site F is more concentrated in the U-CHAS than in the L-CHAS. Variation in Fe concentrations in both parts of the aquifer is complex, but in the U-CHAS values seem to decrease away from the recharge area (Figure 48). L-CHAS samples also show a complex pattern of first decreasing and then increasing Fe concentrations (Figure 49).

Strontium Content and Isotopic Signature

Isotopic ratios ($^{87}Sr/^{86}Sr$) and Sr concentrations determined for Northern Coastal Plain groundwater from the U-CHAS, L-CHAS, Yorktown, Peedee, Surficial, Pungo River, Black Creek, Beaufort, and Cape Fear aquifers, and of seawater and local river waters are given in Table 5. Analytical results for additional L-CHAS samples from the Northern Coastal Plain and groundwater samples from the Southwestern Coastal Plain were not received in time to be included on the maps or discussion, but these values are reported in Table 5. The results from the Southwestern Coastal Plain are described and discussed in a recent UNC-W thesis (Sirtariotis 1998). Values for rocks and fossils from Coastal Plain formations are from the work of Denison et al. 1993. Groundwater from the U-CHAS in the Northern Coastal Plain is the only subset of the data for which enough chemical and isotopic data exist to draw any significant conclusions, so the results and discussion below are largely limited to these samples.

The ratio of $^{87}Sr/^{86}Sr$ for groundwater in the U-CHAS steadily decreases from west to east across the study area, but strontium concentrations exhibit complex patterns in the central and northeastern regions (Figures 50 and 51). The geographic variation in strontium concentration in the northeast is similar to that observed for HCO_3, Mg, and Ca (Figures 20, 26, and 28). Except for wells K17a5 and K17a6 (Figures 8 and 9), L-CHAS samples have 2-7 times more strontium than samples from the U-CHAS at the same site. Also, for all sites but K17, L-CHAS samples have lower $^{87}Sr/^{86}Sr$ ratios than samples from the U-CHAS at the same site. Site K17 is near Albemarle Sound in a region where the CHAS confining unit is absent (Giese et al. 1991) and composition of groundwater at this location may be significantly affected by influx of surface water.

Carbon and Oxygen Isotopes and Organic Carbon

Results of analyses of carbon and oxygen isotopes and organic carbon concentration for groundwater from the Northern Coastal Plain are reported in Appendix C, which is available from the first author or WRRI. These results were only recently received so analysis will be incomplete compared to that for strontium isotopes.

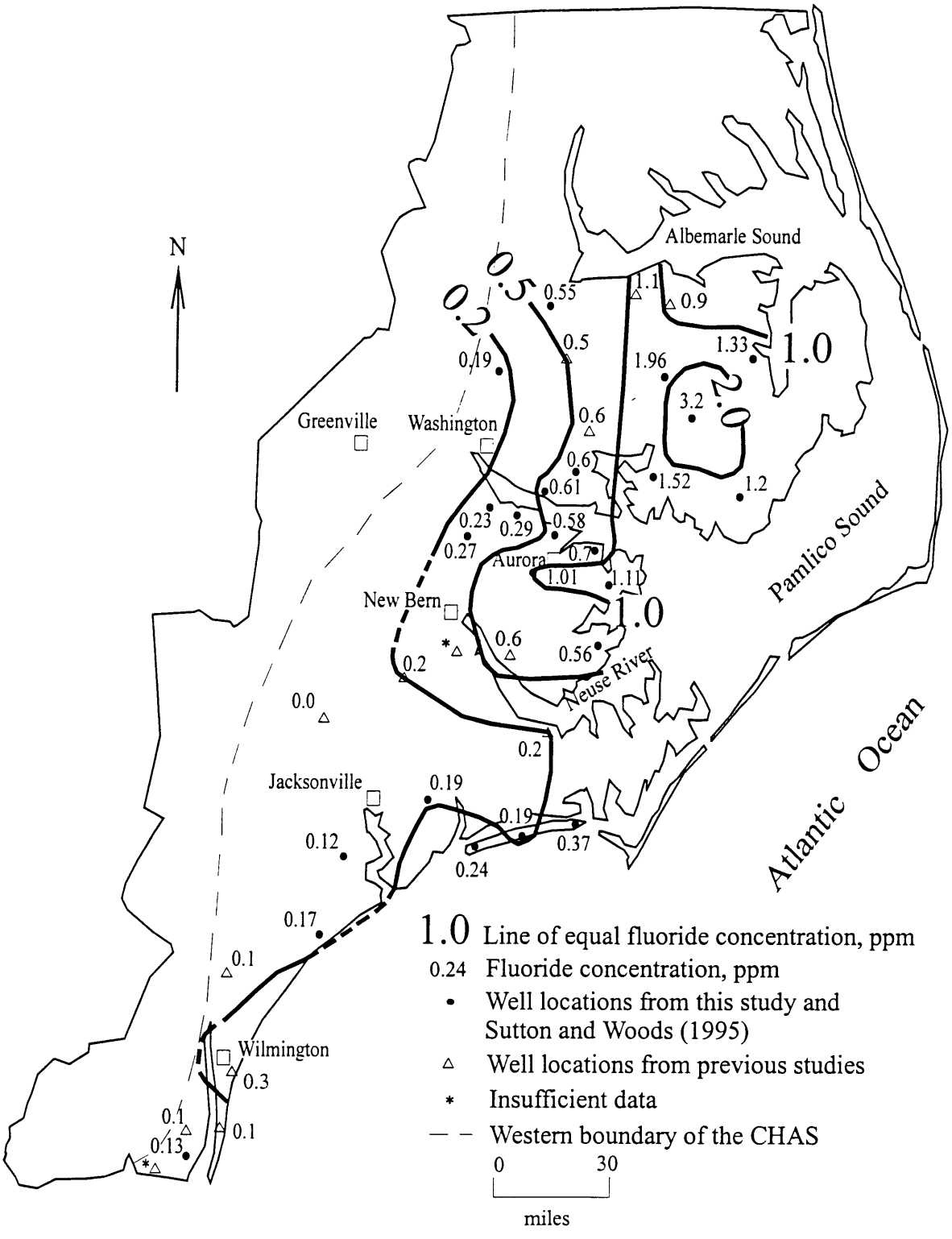

Figure 46. Fluoride concentrations in the U-CHAS
* Indicates that fluoride data were not available.

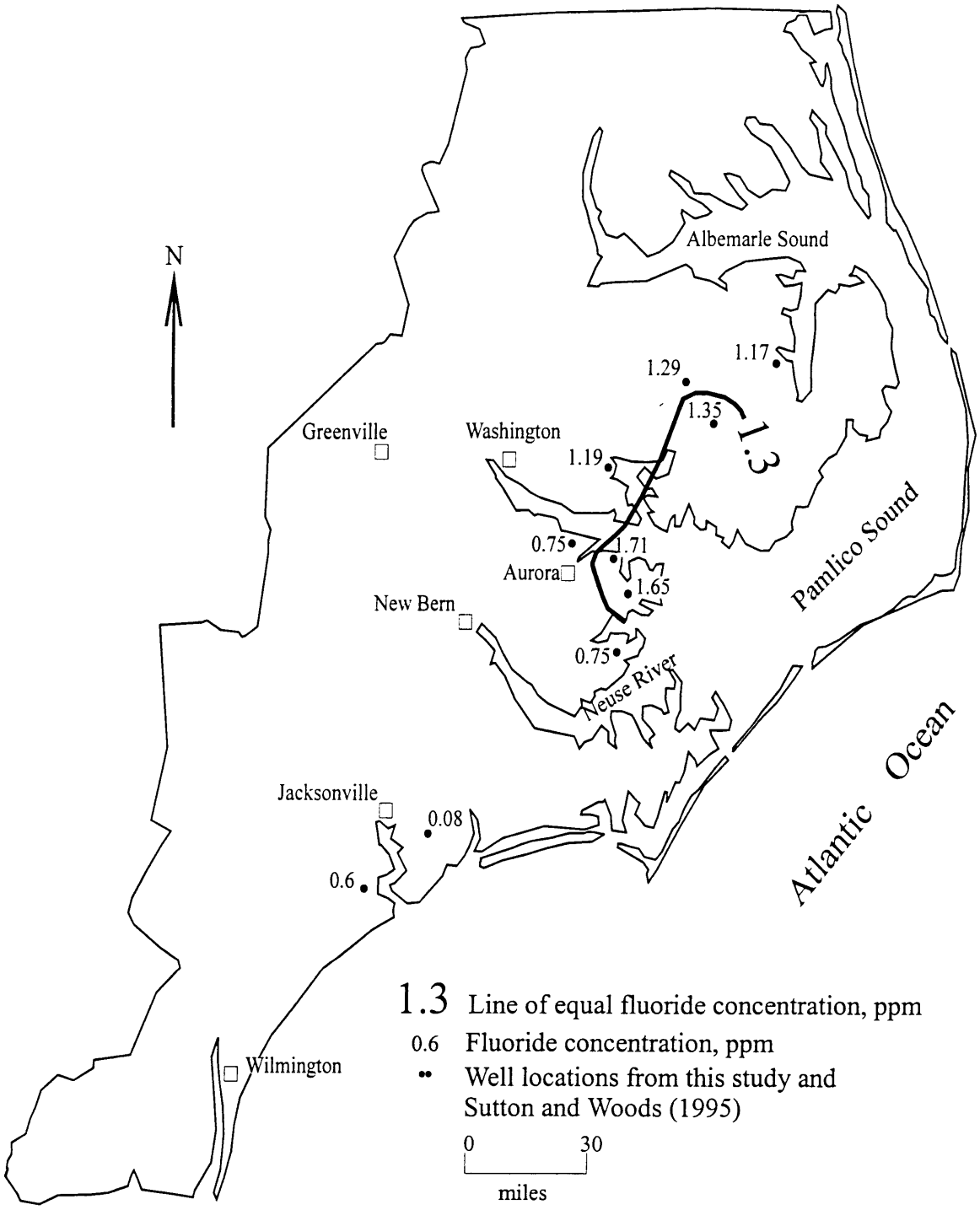

Figure 47. Fluoride concentrations in the L-CHAS

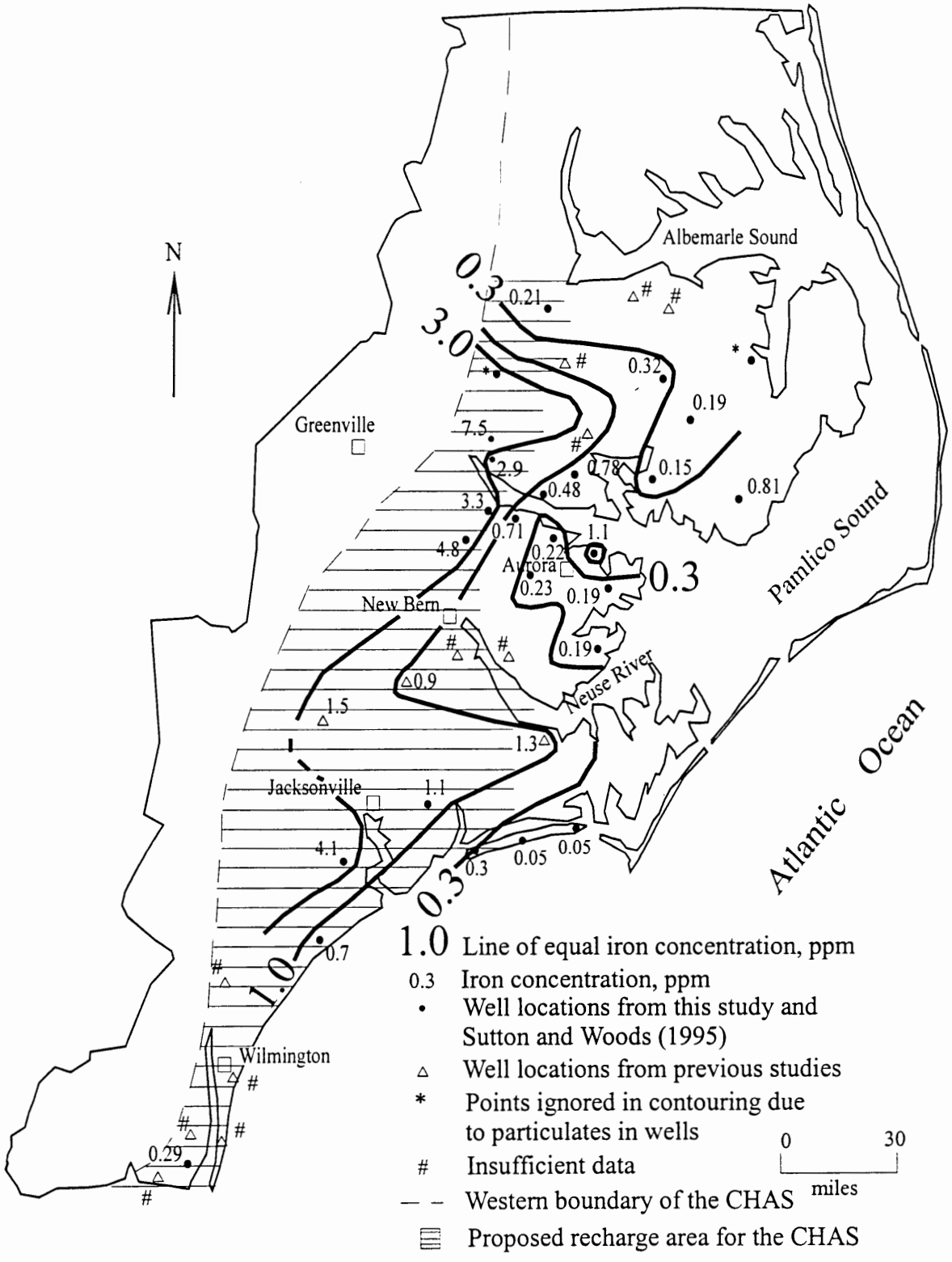

Figure 48. Iron concentrations in the U-CHAS

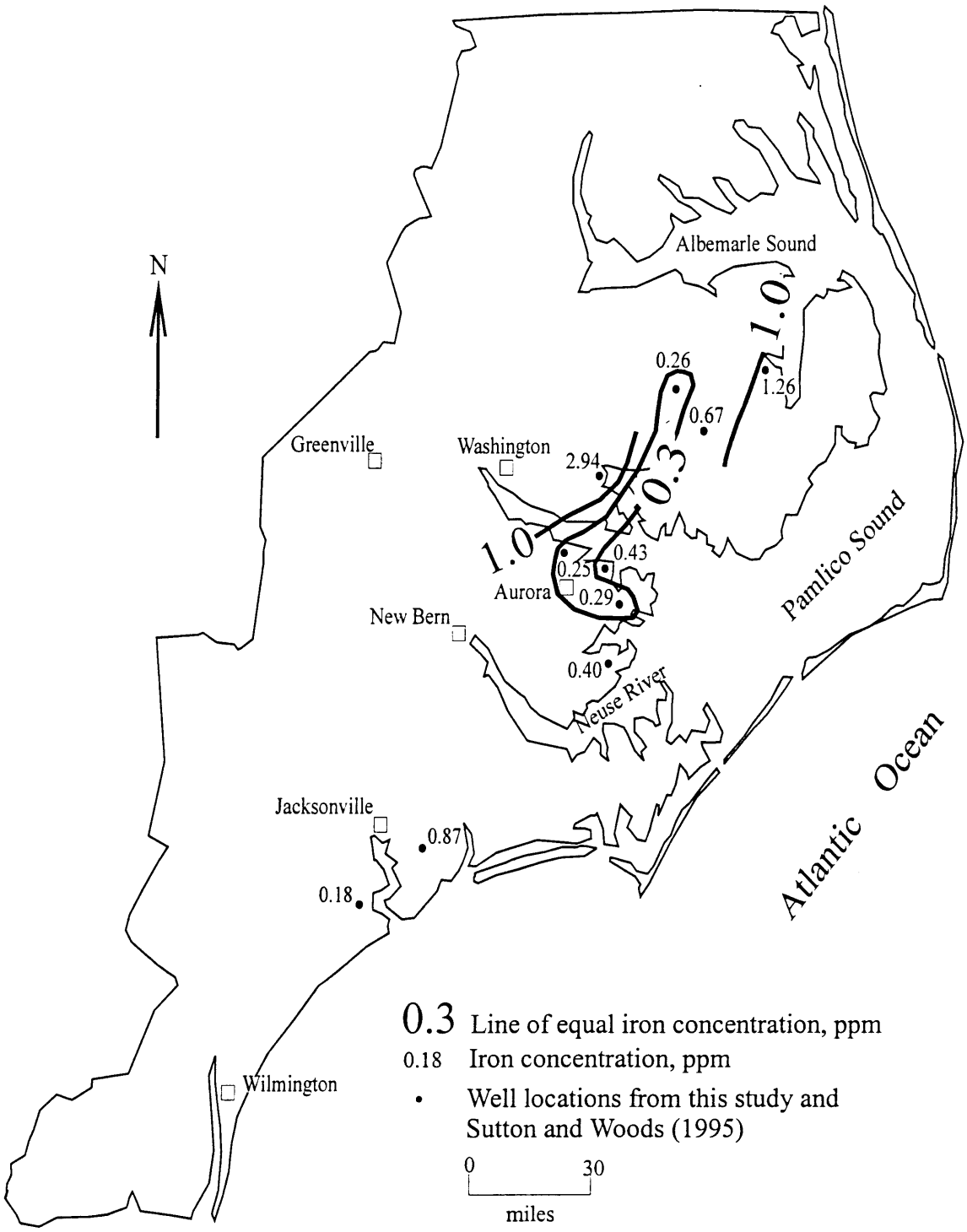

Figure 49. Iron concentrations in the L-CHAS

Table 5. Strontium composition of local waters					
Sample	Longitude	Latitude	PPM Sr	$^{87}Sr/^{86}Sr$	Date Run
Modern seawater			7.6	0.709180	
Rivers					
T-1-Tar			0.051	0.709500	1983
N-1-Neuse			0.044	0.709200	1983
Surficial					
CC 38 b5	-78.5291	34.3255	0.4820	0.709110	12/5/96
F-22 b-3	-77.1884	36.2325	0.0600	0.708464	3/8/97
FF 32 y2	-78.0805	34.0088	0.2200	0.710500	11/13/96
Yorktown					
K-2 e-4	-75.5543	35.8372	6.8400	0.709070	6/30/97
L-13 i-2	-76.5618	35.9360	0.7080	0.709200	1/6/97
Hyde Plant	-76.3500	35.6744	0.4270	0.709111	1/6/97
Pungo River					
S 18 u 7	-76.8370	35.0868	0.4130	0.709039	3/22/97
Castle Hayne					
WWF #2	-76.9469	35.5238	0.3000	0.709000	5/26/93
Upper Castle Hayne					
K-17 a-5	-76.8636	35.9106	0.6750	0.709006	5/23/93
L-13 i-1	-76.4347	35.7308	0.2420	0.708435	5/7/93
M-12 l-1	-76.3550	35.6222	0.8020	0.708302	7/9/93
O-10 w-3	-76.2086	35.4242	3.0950	0.708104	5/6/93
O-13 f-1	-76.4850	35.4833	0.8240	0.708308	5/10/93
O-17 i-2	-76.7831	35.4733	0.9580	0.708699	5/17/93
P-16 o-4	-76.7494	35.3775	0.9000	0.708547	5/27/93
P-21 k-6	-77.0886	35.3814	0.3010	0.708810	5/17/93
Q-15 u-3	-76.6022	35.3080	1.1180	0.708158	5/18/93
S-15 y-4	-76.6536	35.0964	0.8770	0.708605	5/18/93
TG S-11	-76.7083	35.3372	0.7170	0.708555	6/21/93
TG S-15	-76.9697	35.5872	0.6320	0.709263	3/14/98
FF 33 d1	-78.0125	34.0705	0.5200	0.709190	11/13/96
SPPW 002	-78.0172	33.9261	0.3670	0.709190	1997
SPPW 003	-78.0283	33.9280	0.4330	0.709320	1997
HOW 5	-77.2400	34.7377	0.2130	0.708590	1997
Y25Q1	-77.4830	34.6108	0.1690	0.708690	1997
ABPW 5	-76.7416	34.7013	0.5560	0.708970	1997
ABPW 6	-76.7086	34.7013	0.8040	0.708900	1997
BBPW 2	-77.0266	34.6672	0.5420	0.709160	1997
BBPW 5	-77.0691	34.6566	0.8470	0.708700	1997
BBPW 7	-76.8766	34.6891	0.4570	0.709230	1997
Pe 72	-77.5591	34.4444	0.1180	0.708460	1997
Lower Castle Hayne					
TG S-11A	-76.7083	35.3372	2.6540	0.708217	6/21/93
K 17a 6	-76.8636	35.9106	0.5870	0.709049	3/11/98
L 13 i 5	-76.4344	35.7307	0.8120	0.708258	3/11/98
M 12 l 4	-76.3540	35.6228	5.3670	0.708091	3/12/98
Q 15 u 5	-76.5959	35.2550	2.6430	0.708036	3/12/98

Table 5 contd.					
S15 y 3	-76.6557	35.0898	2.9370	0.708211	3/14/98
SFOW 1	-77.4847	34.5755	0.2360	0.709230	1997
SFOW 2	-77.4900	34.5680	0.1930	0.708400	1997
SFOW 3	-77.4938	34.5594	0.3640	0.708770	1997
SFOW 4	-77.4986	34.5488	0.2770	0.708780	1997
HPW 2	-77.2325	34.7194	0.2190	0.708520	1997
HPW 3	-77.2341	34.7255	0.1720	0.709100	1997
Beaufort					
G-19 b-3	-76.9203	36.2093	0.1760	0.708820	1/5/97
Peedee					
AA 39 v1	-78.5852	34.4166	0.2200	0.709440	12/10/96
CC 38 b6	-78.5291	34.3255	0.4830	0.708380	12/5/96
EE 36 k3	-78.3333	34.1327	0.0630	0.710230	12/10/96
EE 36 k4	-78.3333	34.1327	1.1700	0.708060	12/10/96
EE 36 k7	-78.3333	34.1327	0.3230	0.708770	12/9/96
P-26 n-1	-77.5216	35.3837	0.1410	0.708479	3/8/97
FF 32 Y1	-78.0805	34.0088	0.5900	0.709170	11/13/96
Pink Hill	-77.7322	35.0200	0.1450	0.708565	1/6/97
Wallace	-78.1000	34.7300	0.1290	0.708752	1/5/97
J-13 d-4	-76.4275	35.7383	6.1570	0.708202	1/6/97
Screened in both Castle Hayne and Peedee					
BCPW-2	-78.0861	33.9722	0.5560	0.709180	6/18/96
BCPW-5	-78.0847	33.9527	0.3670	0.709160	6/18/96
BCPW-7	-78.0936	33.9444	0.4390	0.709280	6/18/96
BCPW-15	-78.1025	33.9833	0.5920	0.709370	6/18/96
BCPW-18	-78.0652	33.9819	0.5510	0.709270	6/18/96
Black Creek					
AA 39 v4	-78.5852	34.4166	0.2900	0.708880	12/9/96
CC 38 b8	-78.5291	34.3255	0.0280	0.708170	12/4/96
EE 36 k5	-78.3333	34.1327	0.4710	0.707960	12/9/96
C-15 s-5	-76.5217	36.4593	0.0250	0.708342	1/6/97
Cape Fear					
CC 38 B7	-78.5291	34.3255	0.1850	0.708600	12/5/96
P-21 k-5	-76.0870	35.3871	0.0780	0.708113	1/6/97
EE 36 k2	-78.3333	34.1327	4.9400	0.707950	12/9/96

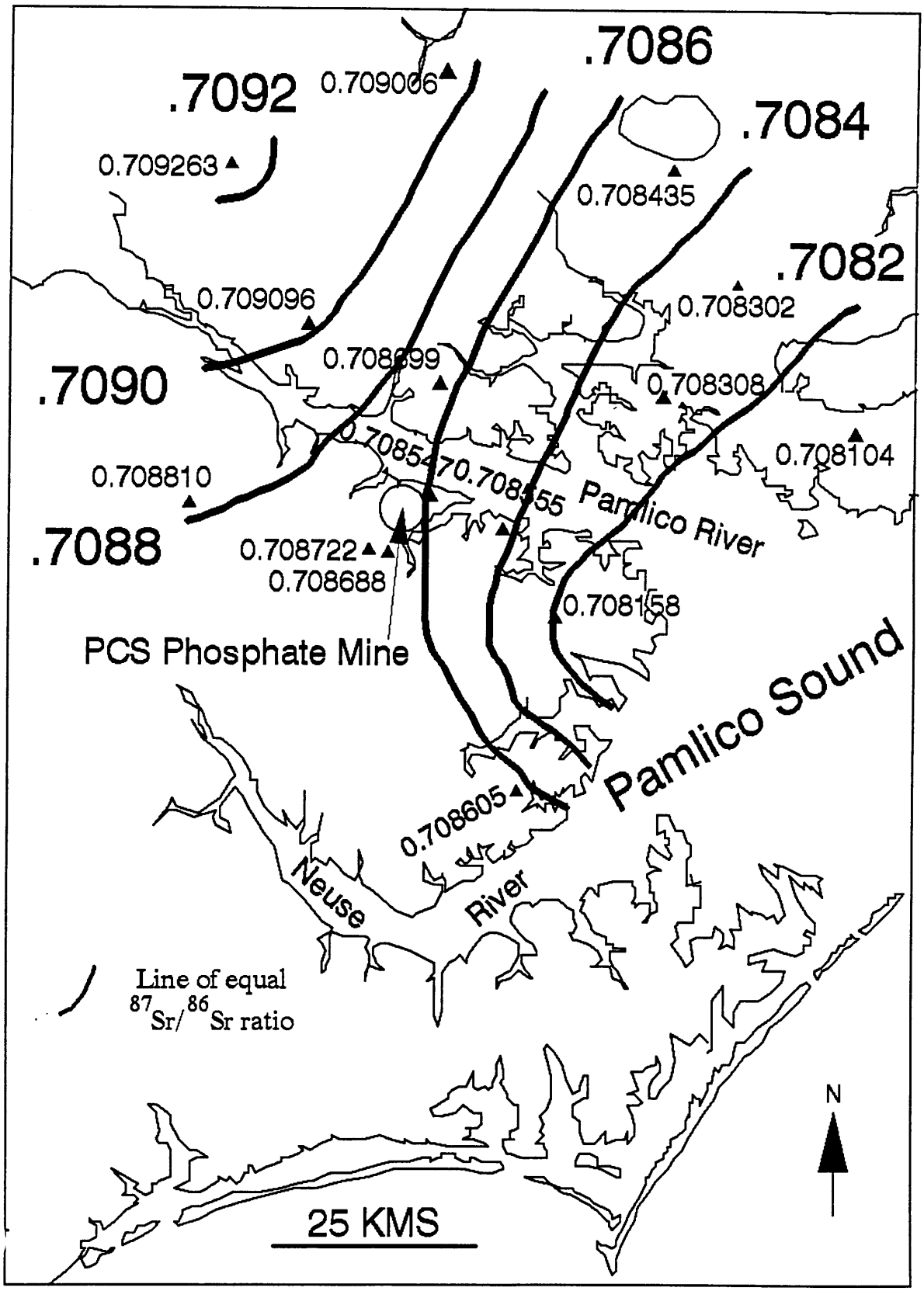

Figure 50. $^{87}Sr / ^{86}Sr$ ratios in the U-CHAS

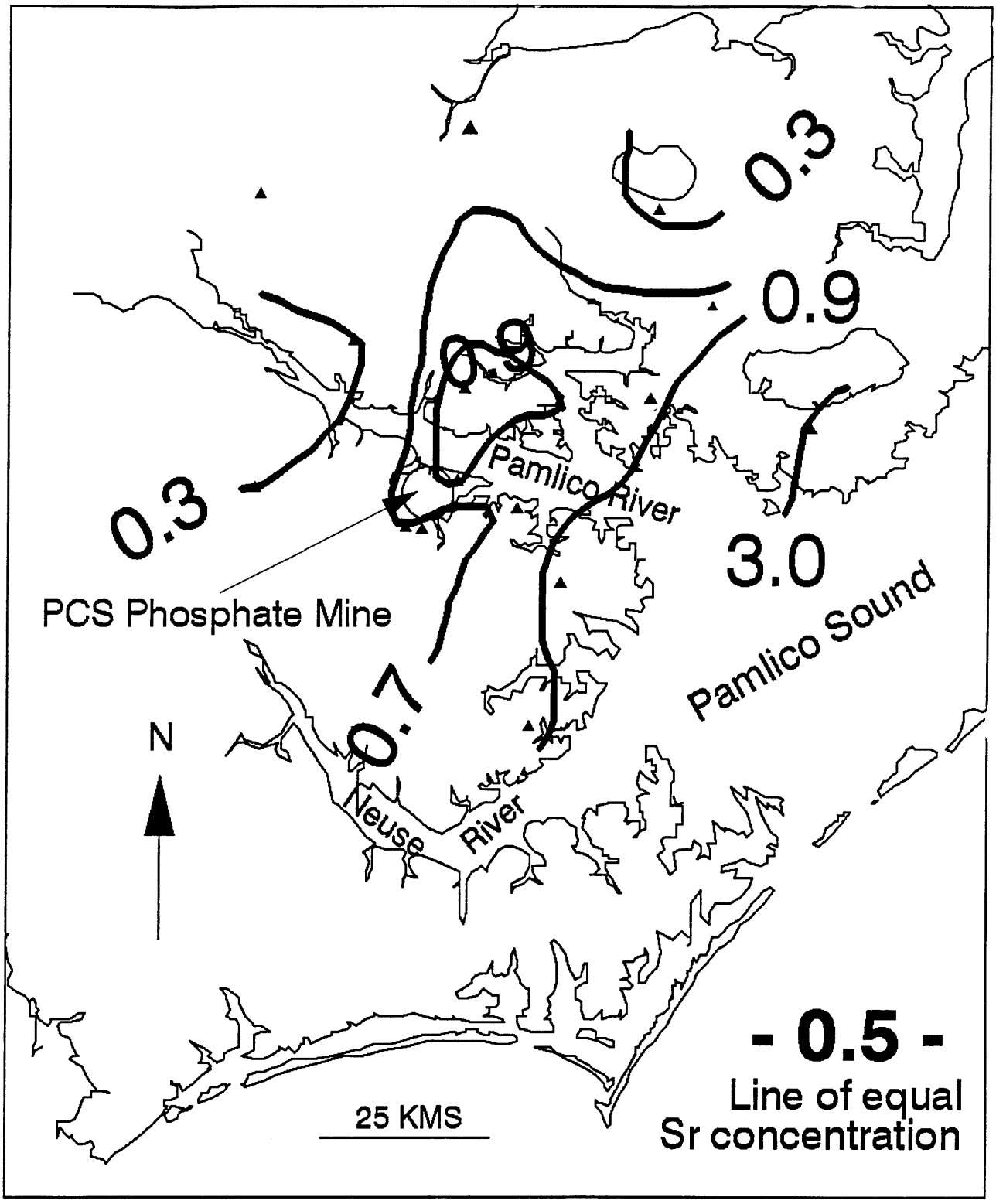

Figure 51. Strontium concentrations in the U-CHAS

$\delta^{13}C$ in the CHAS generally becomes more positive from west to east with values of -16.29°/$_{oo}$ to -3.36°/$_{oo}$ and -12.00°/$_{oo}$ to -2.61°/$_{oo}$ for the U-CHAS and the L-CHAS, respectively (Figures 52 and 53). At the same well site, values in the L-CHAS are more positive than those in the U-CHAS. $\delta^{18}O$ in the U-CHAS varies from-5.28°/$_{oo}$ to -3.12°/$_{oo}$ and generally becomes more positive to the east (Figure 54). In the central part of the study area, the pattern is more complex. In the L-CHAS, $\delta^{18}O$ first becomes more positive into the center of the region and then becomes more negative southeast varying from -3.61°/$_{oo}$ to -4.65°/$_{oo}$ (Figure 55). At the same site, $\delta^{18}O$ of water from the U-CHAS is very similar to or less than for the L-CHAS.

Variation of total organic carbon (TOC) in the U-CHAS is complex (Figure 56). In general, TOC decreases from west to east (2.61 to 0.41 $^{mgC}/_{L}$), but near Phelps Lake TOC content increases to the highest value in the study area (4.18 $^{mgC}/_{L}$). TOC values in the L-CHAS decrease from a high of 3.28 $^{mgC}/_{L}$ at Phelps Lake to low values ($\approx$ 1.8 $^{mgC}/_{L}$) near the Pamlico River. Then they increase again further south to a high of 2.14 $^{mgC}/_{L}$ (Figure 57).

YORKTOWN WATER CHEMISTRY AND ISOTOPES

Major elements

The electrical neutrality balance for well K2e4 was not within acceptable limits, so some of the values reported for this sample could be significantly in error. The problem appears to be with the analysis of highly concentrated samples for Na^+ by Atomic Absorption spectrometry because the chloridometer determinations of Cl^- have been verified by $AgNO_3$ titration. The Na^+ analyses are being repeated with an alternative procedure and the new measurements should be available soon. However, even considering a possible error of ± 25%, the concentrations at this location are still significantly higher than any other well, so the numbers were recorded on the maps and considered in the contouring. Concentrations of Ca, Mg, Na, and K range from 2-600, 1-600, 9-510, and 1-500 (ppm), respectively (Table 6). In general their concentrations increase from west to east, however, contour lines are quite irregular and there are isolated highs and lows, especially in the center of the region between Albemarle Sound and the Pamlico River (Figures 58-61). The contours seem to be significantly influenced by surface bodies of fresh water -- much more so than contours for the deeper aquifers. Alkalinity (10-560 ppm) and Cl (0-10000 ppm) (Figures 62 and 63) tend to increase towards the coast, but the pattern of sulfate variation (0-1400) (Figure 64) is unclear. A Piper diagram (Figure 65) reveals that cations in Yorktown waters are mixed or dominated by alkalis (3 or 4), and anions are mixed or, more frequently, dominated by HCO_3 (A or D).

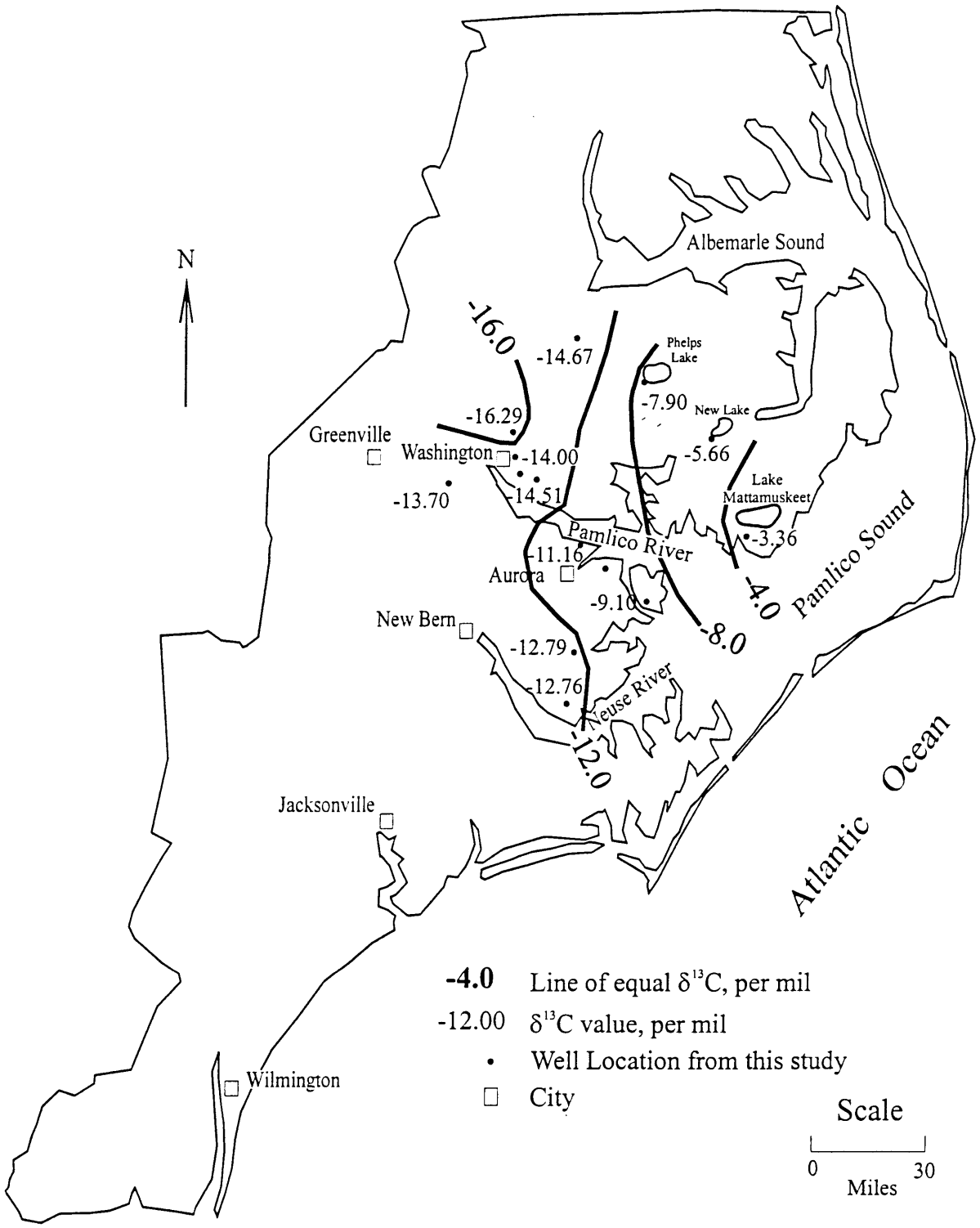

Figure 52. $\delta^{13}C$ of dissolved inorganic carbon in the U-CHAS

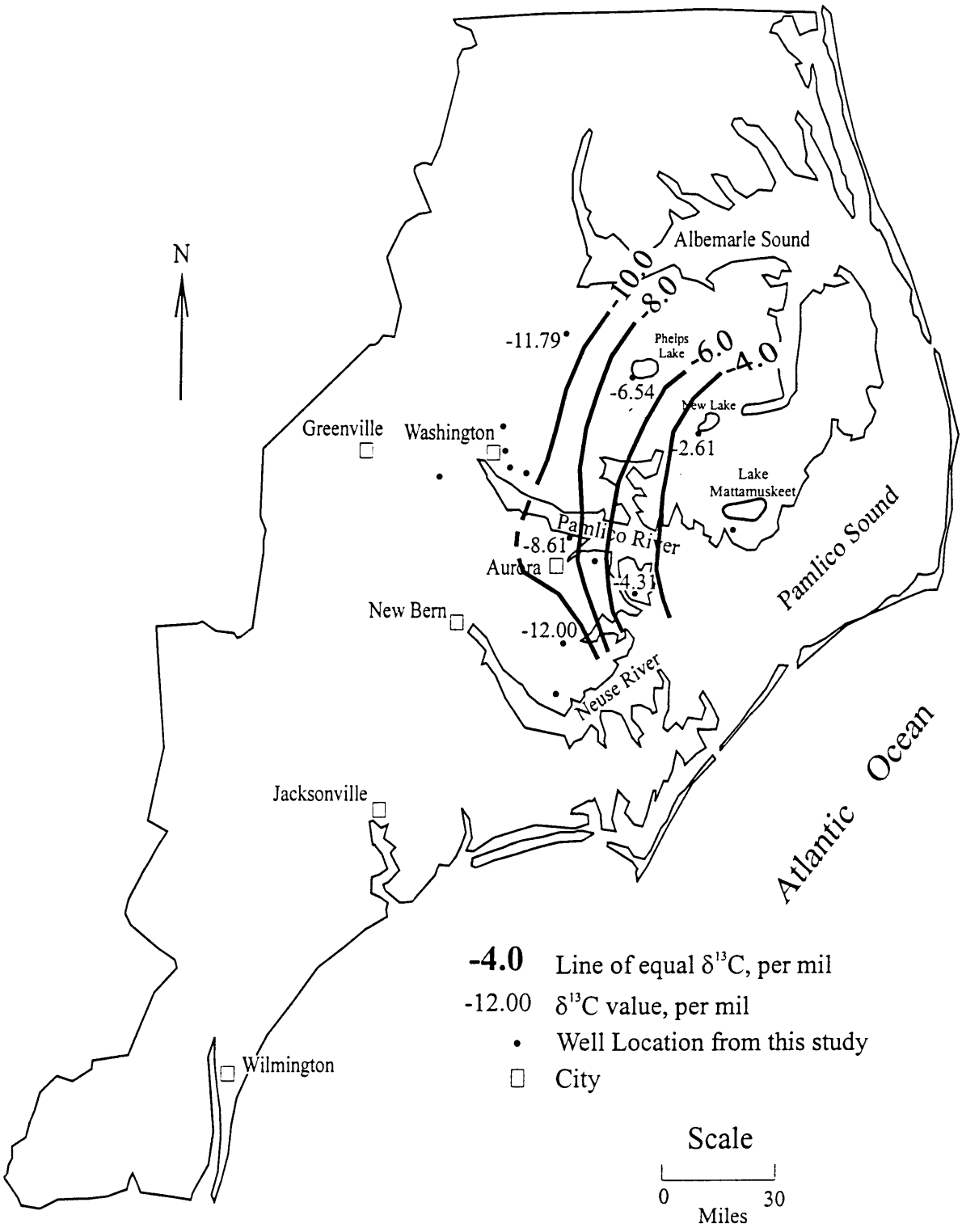

Figure 53. $\delta^{13}C$ of dissolved inorganic carbon in the L-CHAS

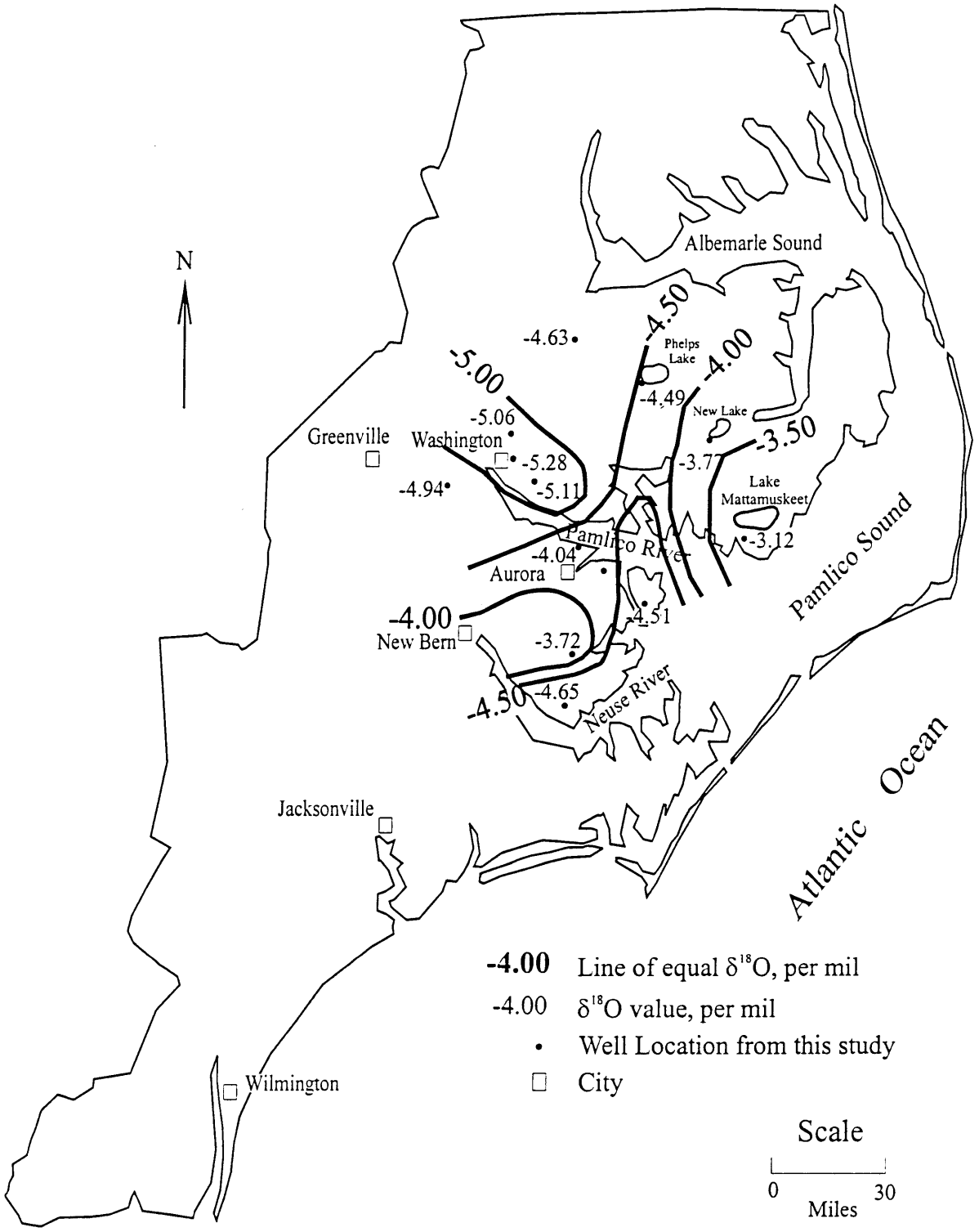

Figure 54. $\delta^{13}C$ in the U-CHAS

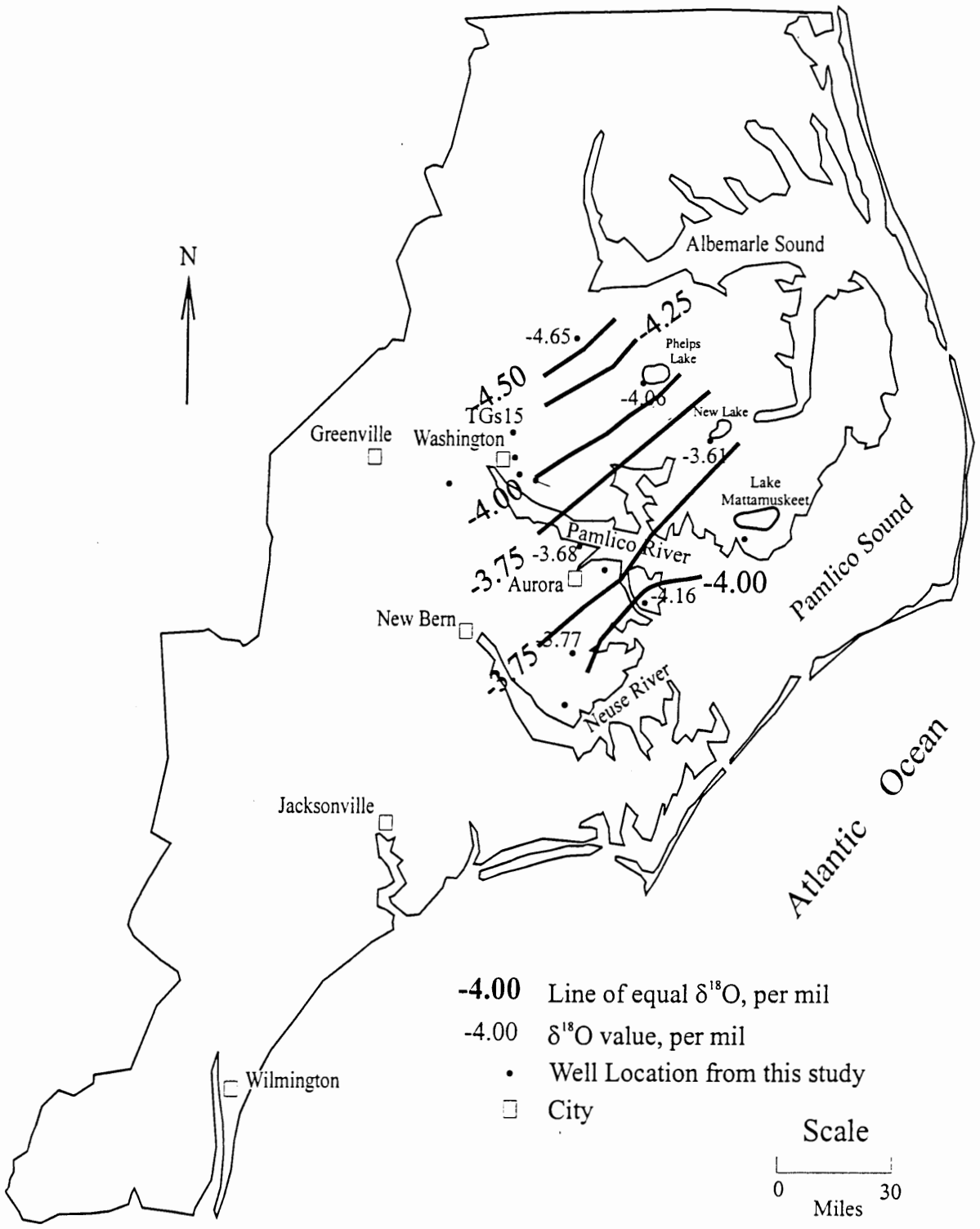

Figure 55. $\delta^{13}C$ in the L-CHAS

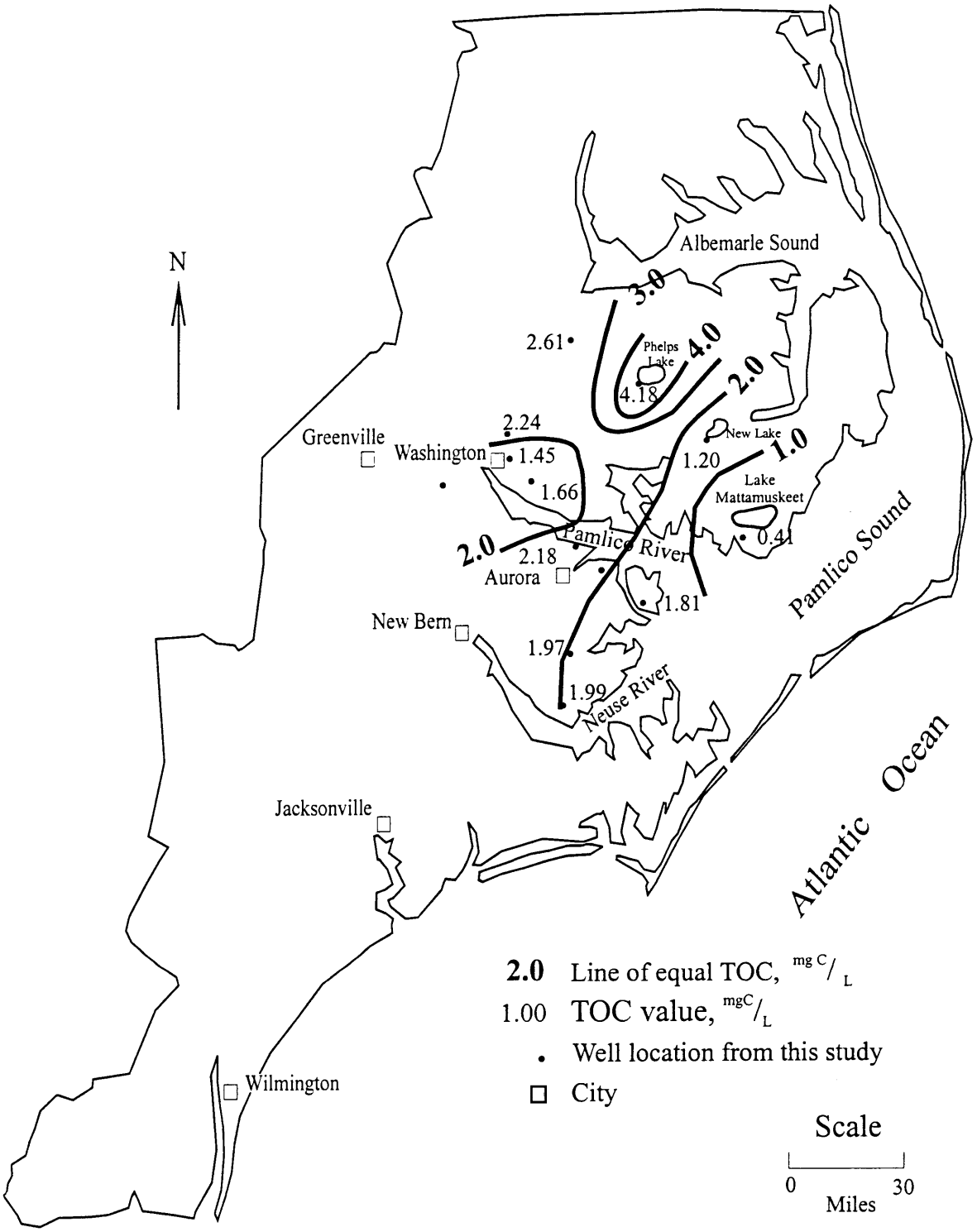

Figure 56. Total organic carbon concentrations in the U-CHAS ($^{mg\ C}/_{L}$)

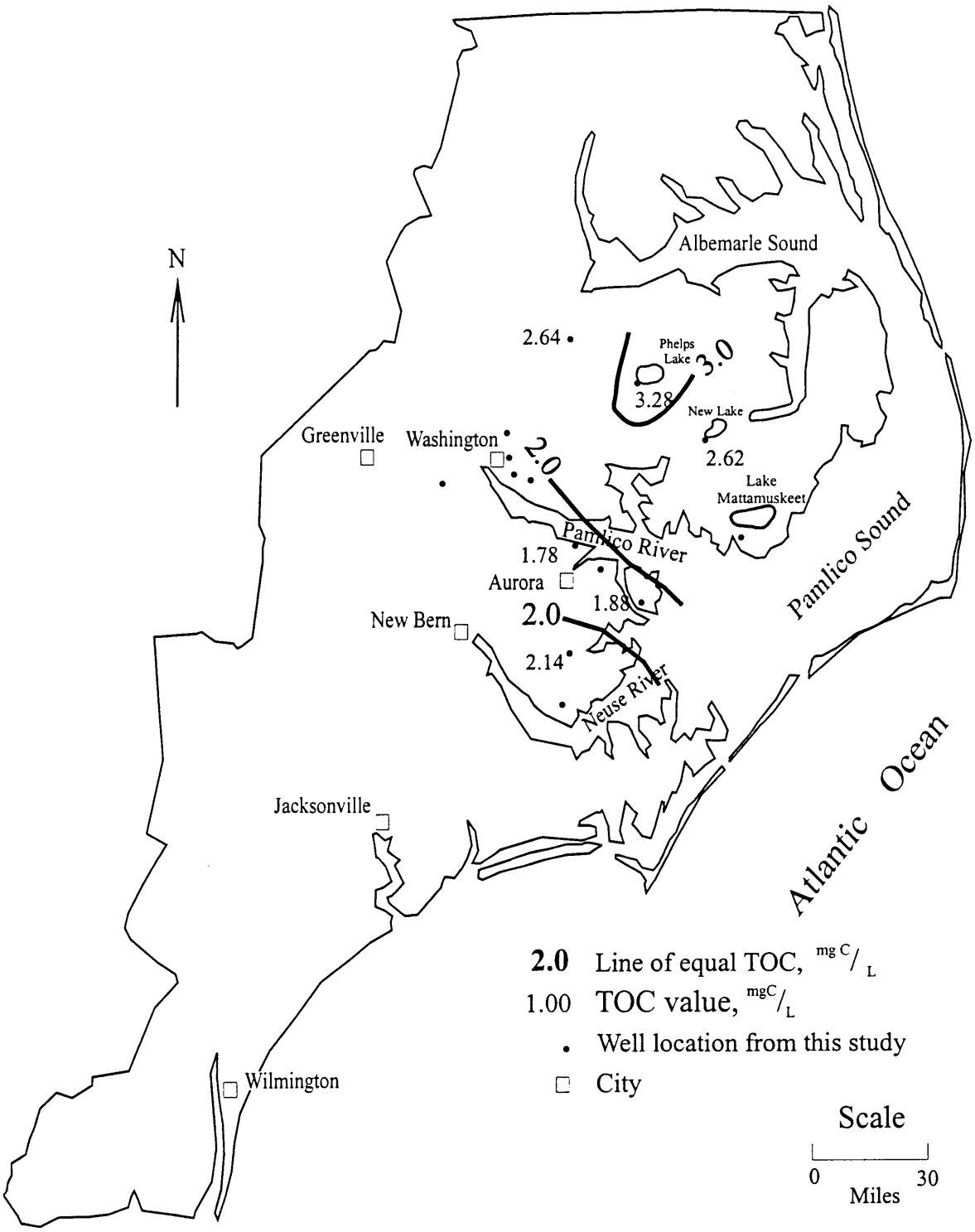

Figure 57. Total organic carbon concentrations in the L-CHAS ($^{mg\ C}/_{L}$)

Table 6. Chemical analyses of Yorktown groundwater. (Knobel 1985 data *)

Well Identifer	Temp (°C)	pH	Eh mv	TDS ppm	HCO_3 ppm	Cl^- ppm	SO_4^{2-} ppm	Na^+ ppm	K^+ ppm	Ca^{2+} ppm	SiO_2 ppm	Mg^{2+} ppm
O-17 i-1	17	6.7	174	663	450	0	7	44	31	84	30	17
K-2 e-4	18	7	154	13989	360	10000	1400	510	500	600	19	600
L-13 i-2	18	7	146	599	440	0	7	21	23	77	28	4
Hyde Plant	17	7.1	217	820	520	22	0	107	44	78	24	25
Columbia	16	7.2	195	762	330	130	24	140	47	73	9	9
Belhaven	18	7.2	89	735	500	0	23	71	39	80	6	16
Plant Yorktown	23	5.7	217	58	22	0	6	9	2	2	18	0
Waves	22.5	7.9	458	1645	740	400	5	430	45	9	14	1
CA-2*	No data	7.1	No data	456	195	99	2	72	10	31	34	13
BO-190*	No data	7.6	No data	680	448	18	4	80	16	56	43	15
HA-133*	No data	5.9	No data	70	11	16	11	13	2	5	11	1
HY-23*	No data	8.2	No data	784	547	17	2	70	30	32	31	55
HY-75*	No data	8.1	No data	820	560	26	1	20	20	100	46	47
TY-16*	No data	7.3	No data	649	308	113	23	66	8	57	45	29
WS-17*	No data	7.5	No data	669	413	41	1	54	18	71	48	23
MR-99*	No data	7.8	No data	202	148	6	3	No data	No data	44	No data	1
M-12 l-6	No data	No data	No data	No data	No data	24	2	No data	No data	No data	22	No data
O-10 w-1	18	7.5	No data	No data	No data	269	2	No data	No data	No data	9	No data
Q-15 u-6	19	7.0	No data	No data	No data	1	No data	No data	No data	No data	19	No data
S-15 y-1	18	7.2	No data	No data	272	24	No data	No data	No data	No data	14	No data
S-18 u-3	No data	7.7	No data	No data	No data	1	2	No data	No data	No data	13	No data
Relative Error %					4	8	2	2	8	4	3	4

Relative errors [as percent (%)] were calculated for each pair of duplicate analyses by 1) determining the average of the two concentrations, 2) determining the differences from the average of the pair of analyses, 3) dividing that difference by the average concentration, and 4) multiplying by 100. These percentages were then averaged over all pairs of duplicate anaylses to yield an estimate of relative error.

Table 6. (cont,d) Chemical analyses of Yorktown groundwater (Knobel 1985 data *)

Well Identifer	F^- ppm	S^{2-} ppm	NH_4^+ ppm	NO_3^- ppm	PO_4^{3-} ppm	Fe^{3+} ppm
O-17 i-1	0.16	0.0	0.800	0.058	0.030	6.17
K-2 e-4	0.07	0.15	5.000	0.003	0.040	9.63
L-13 i-2	0.21	0.0	0.700	0.000	0.010	3.67
Hyde Plant	0.19	0.0	1.200	0.000	0.130	1.21
Columbia	0.11	0.0	1.100	0.000	0.020	2.32
Belhaven	0.25	0.1	0.800	0.001	0.020	0.00
Plant Yorktown	0.06	0.0	0.060	0.000	0.220	0.00
Waves	1.47	0.0	2.000	0.024	0.070	0.00
CA-2*	0.2	0.0	No data	No data	0.7	No data
BO-190*	0.40	No data	No data	0.3	0.1	No data
HA-133*	No data	No data	No data	4.5	0.1	No data
HY-23*	0.40	No data	No data	1.4	No data	No data
HY-75*	0.20	No data	No data	0.8	0.1	No data
TY-16*	0.00	No data	No data	No data	No data	No data
WS-17*	0.00	No data	No data	0.5	0.1	No data
MR-99*	No data	No data	No data	No data	No data	No data
M-12 l-6	0.27	No data	1.35	0.00	0.17	No data
O-10 w-1	0.38	1.00	2.35	0.00	0.02	No data
Q-15 u-6	0.24	0.00	0.19	0.00	0.04	No data
S-15 y-1	0.12	0.00	0.09	0.00	0.09	No data
S-18 u-3	0.18	0.00	0.82	0.00	0.09	No data
Relative Error %	4		31		9	0

Relative errors [as percent (%)] were calculated for each pair of duplicate anaylses by 1) determining the average of the two concentrations, 2) detemining the differences from the average of the pair of analyses, 3) dividing that difference by the average concenrations, and 4) multiplying by 100. These percentages were then average over all pairs of duplicate anaylses to yield an estimate of relative error.

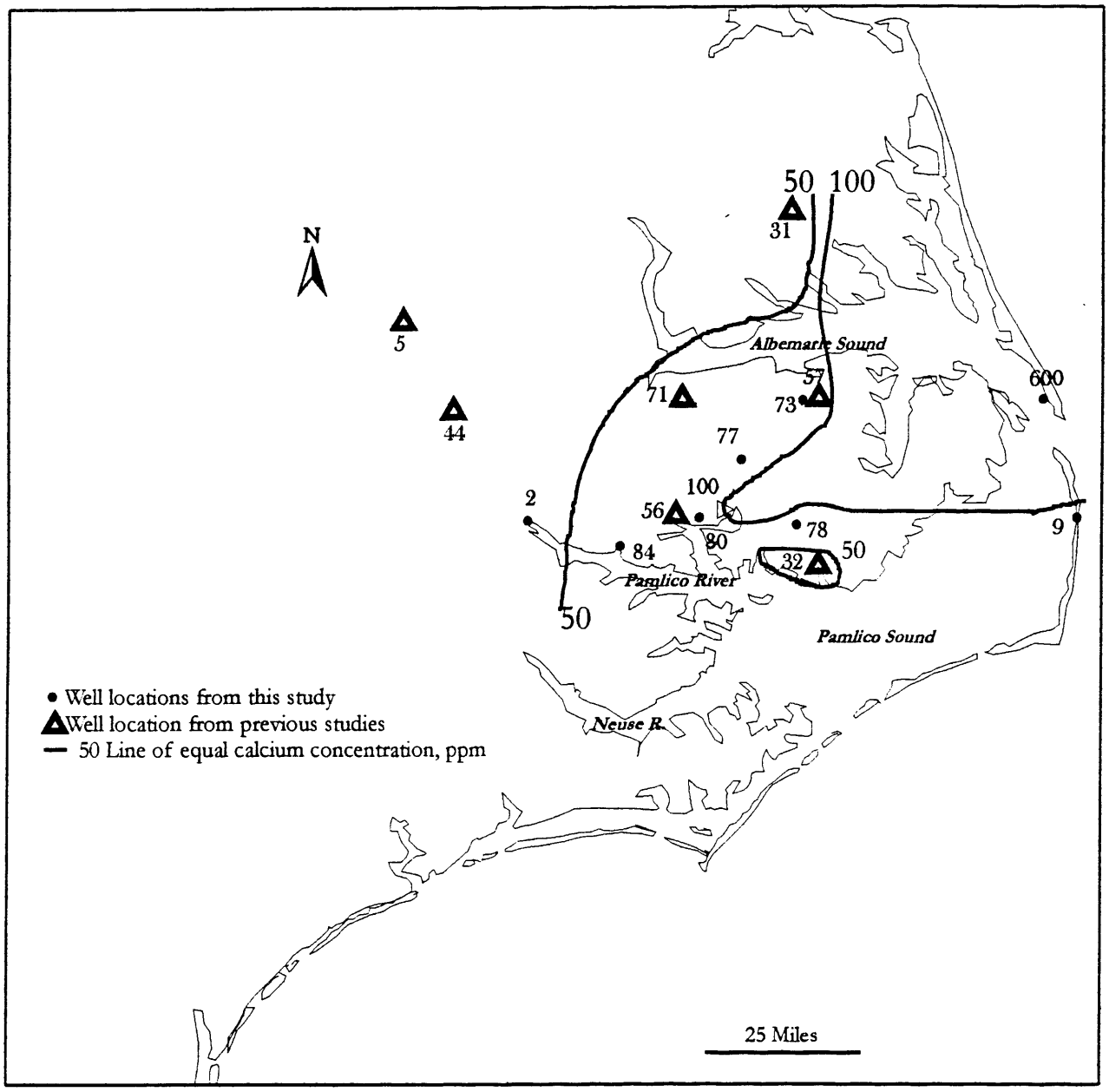

Figure 58. Calcium concentrations in the Yorktown Aquifer.

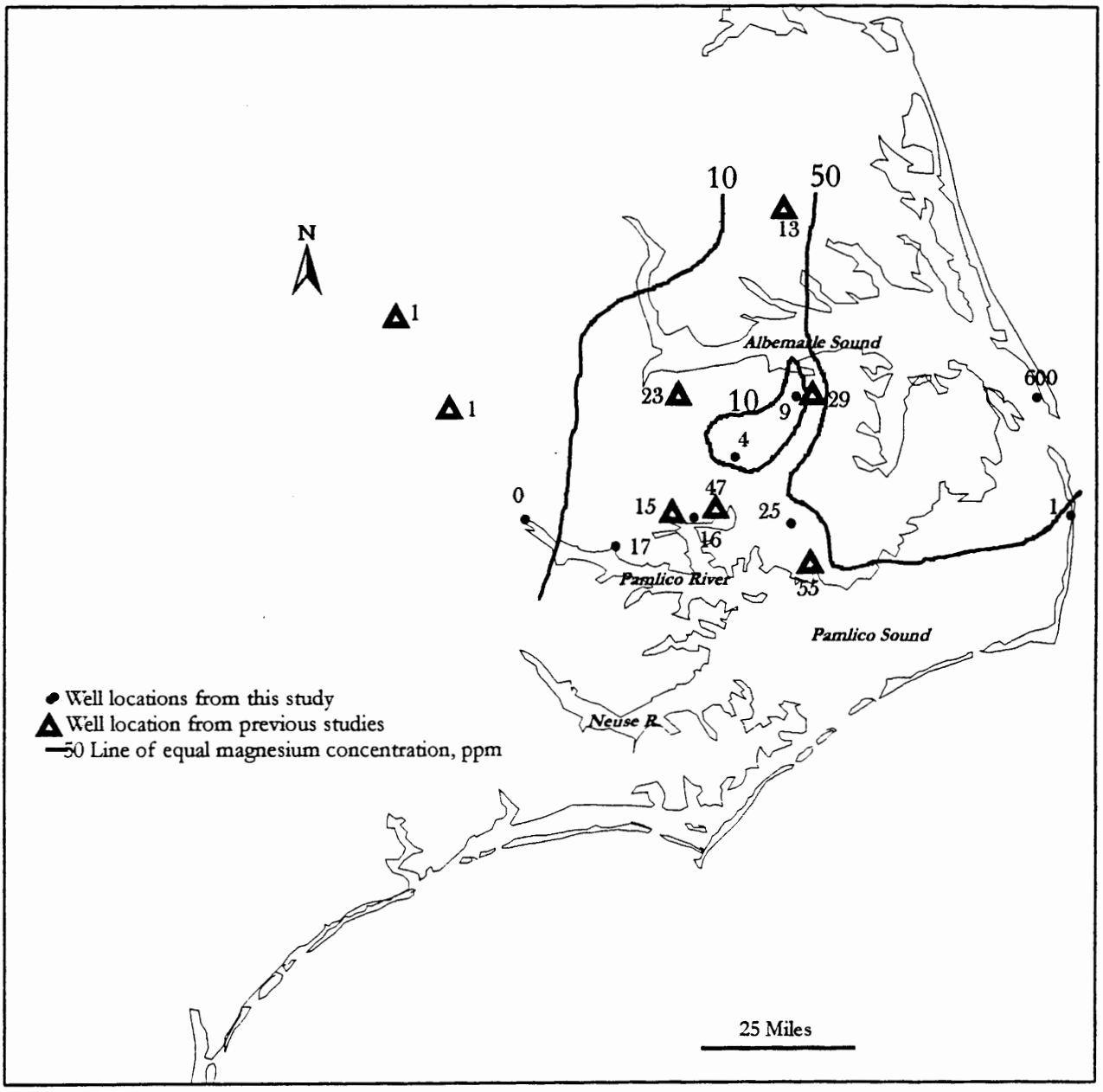

Figure 59. Magnesium concentrations in the Yorktown Aquifer.

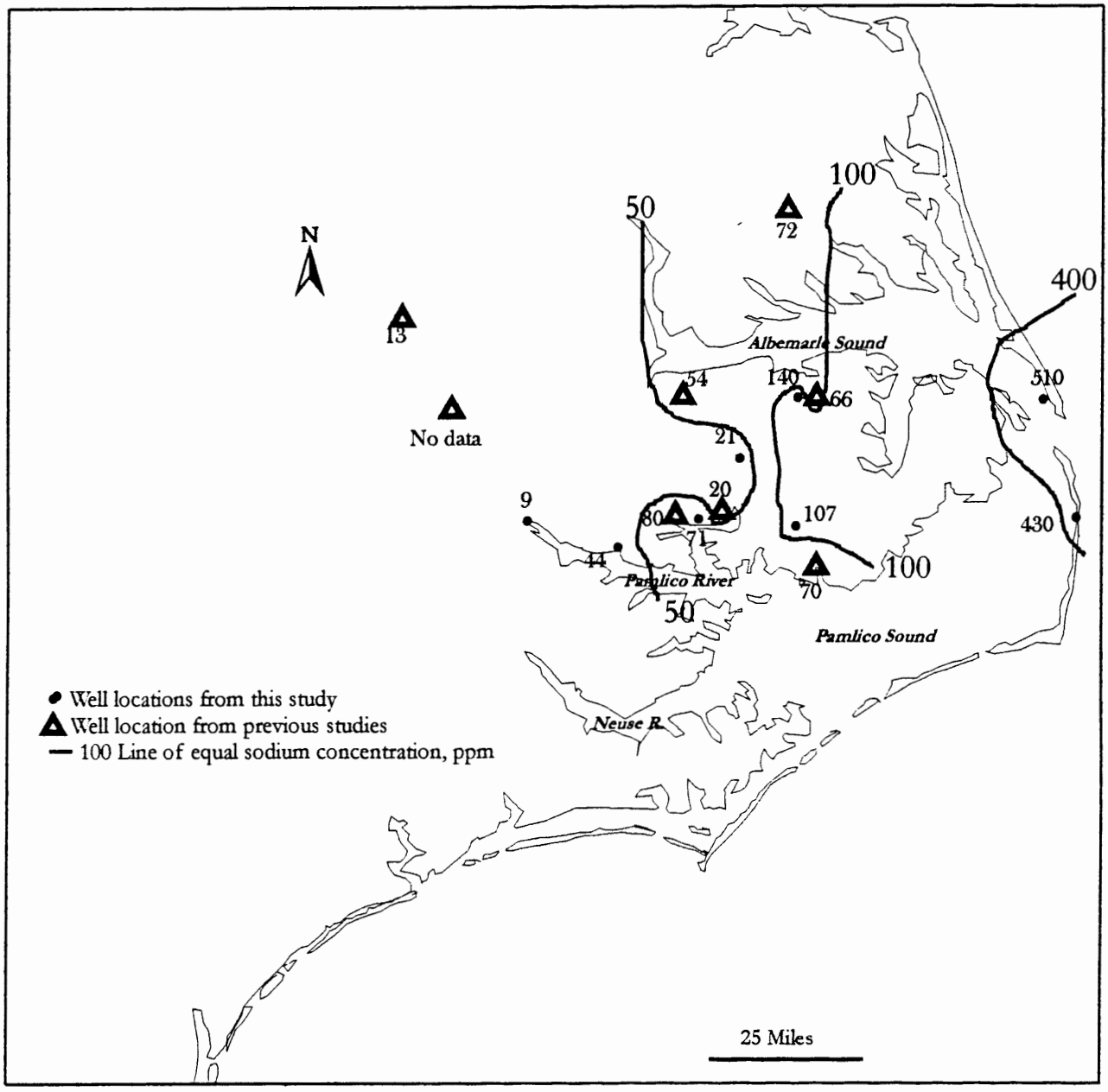

Figure 60. Sodium concentrations in the Yorktown Aquifer.

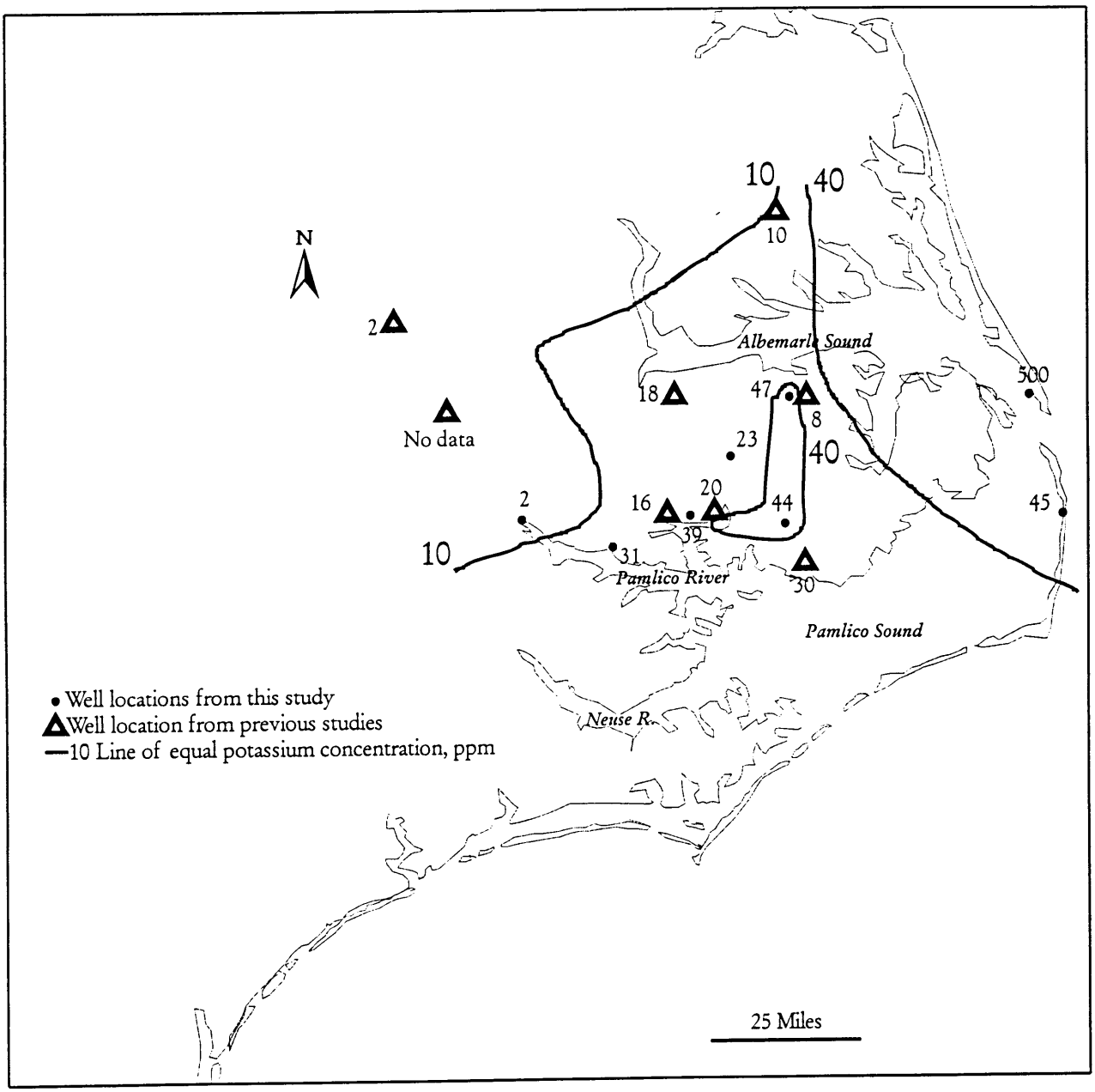

Figure 61. Potassium concentrations in the Yorktown Aquifer.

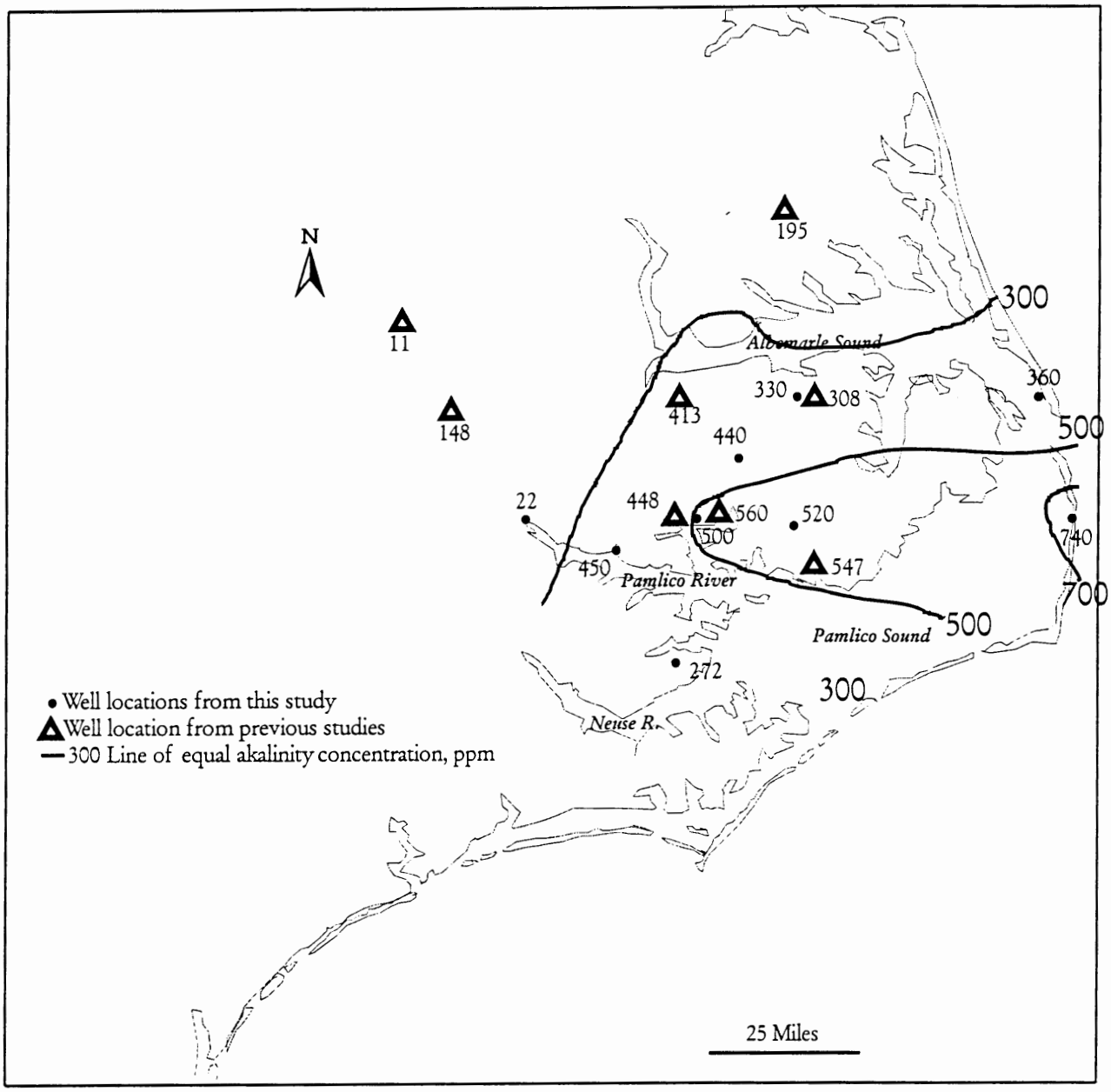

Figure 62. Alkalinity in the Yorktown Aquifer(as HCO_3 in ppm).

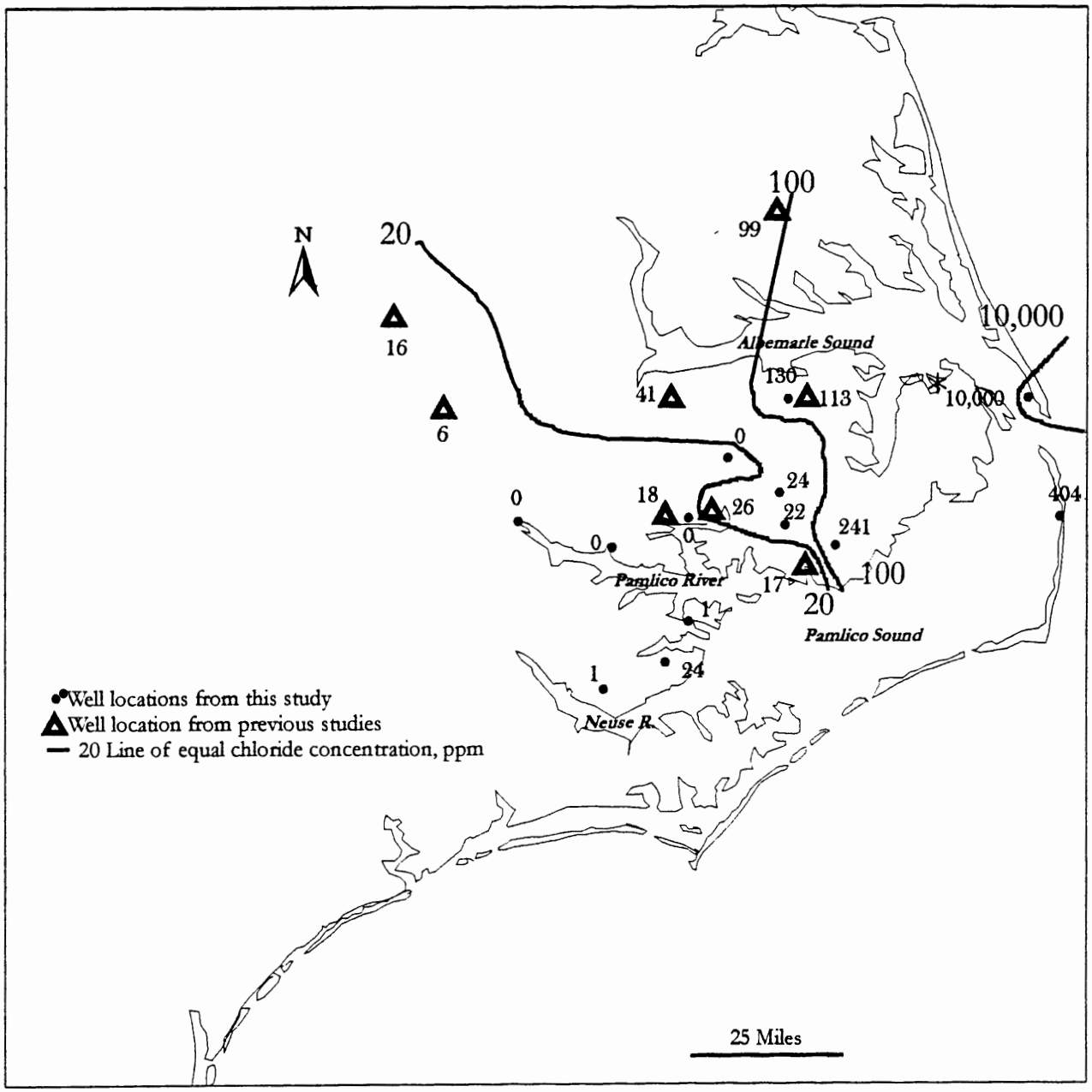

Figure 63. Chloride concentrations in the Yorktown Aquifer. (* See text:: Probably significantly lower than this, but still much higher than any of wells farther west.)

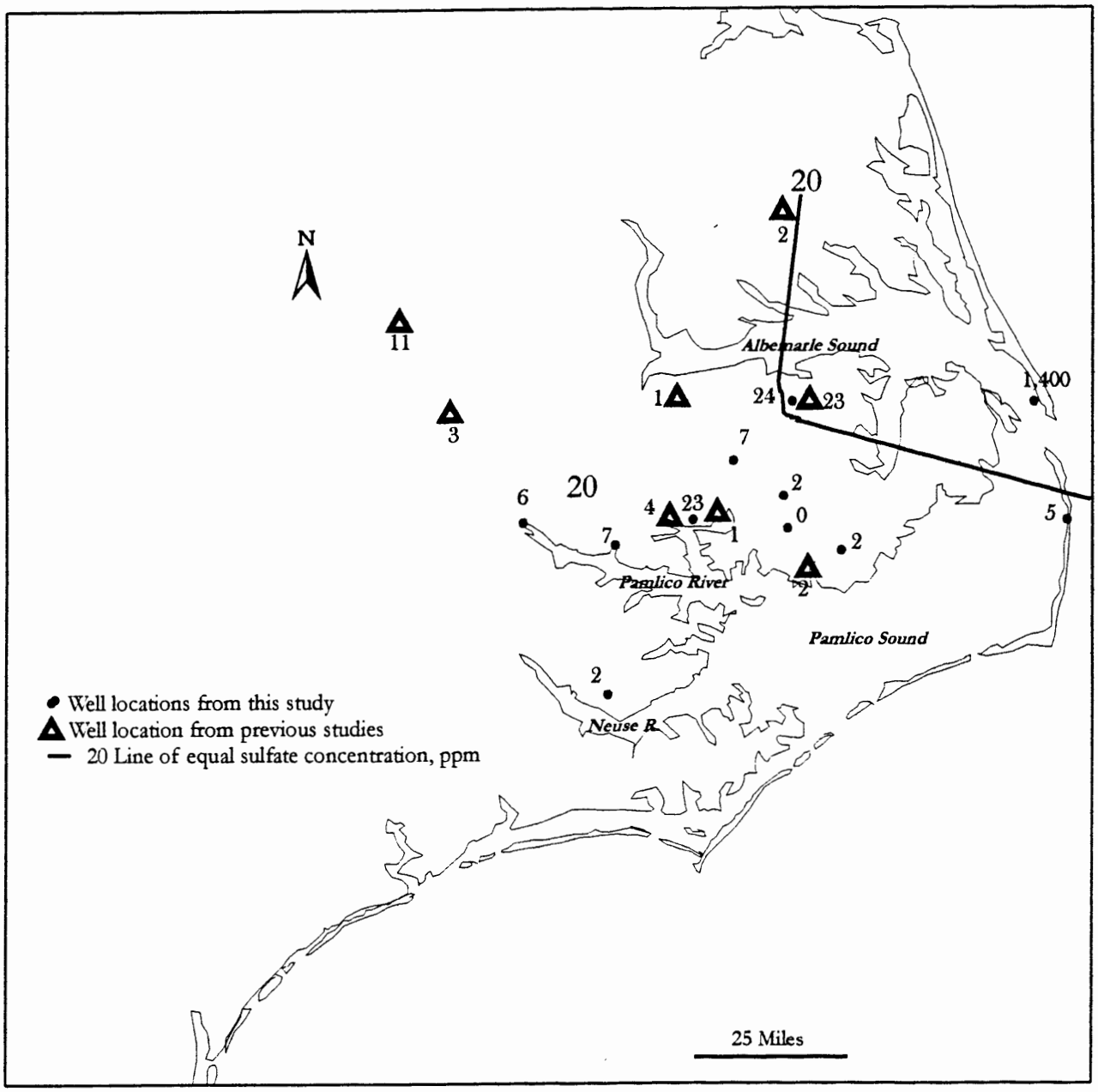

Figure 64. Sulfate concentrations in the Yorktown Aquifer.

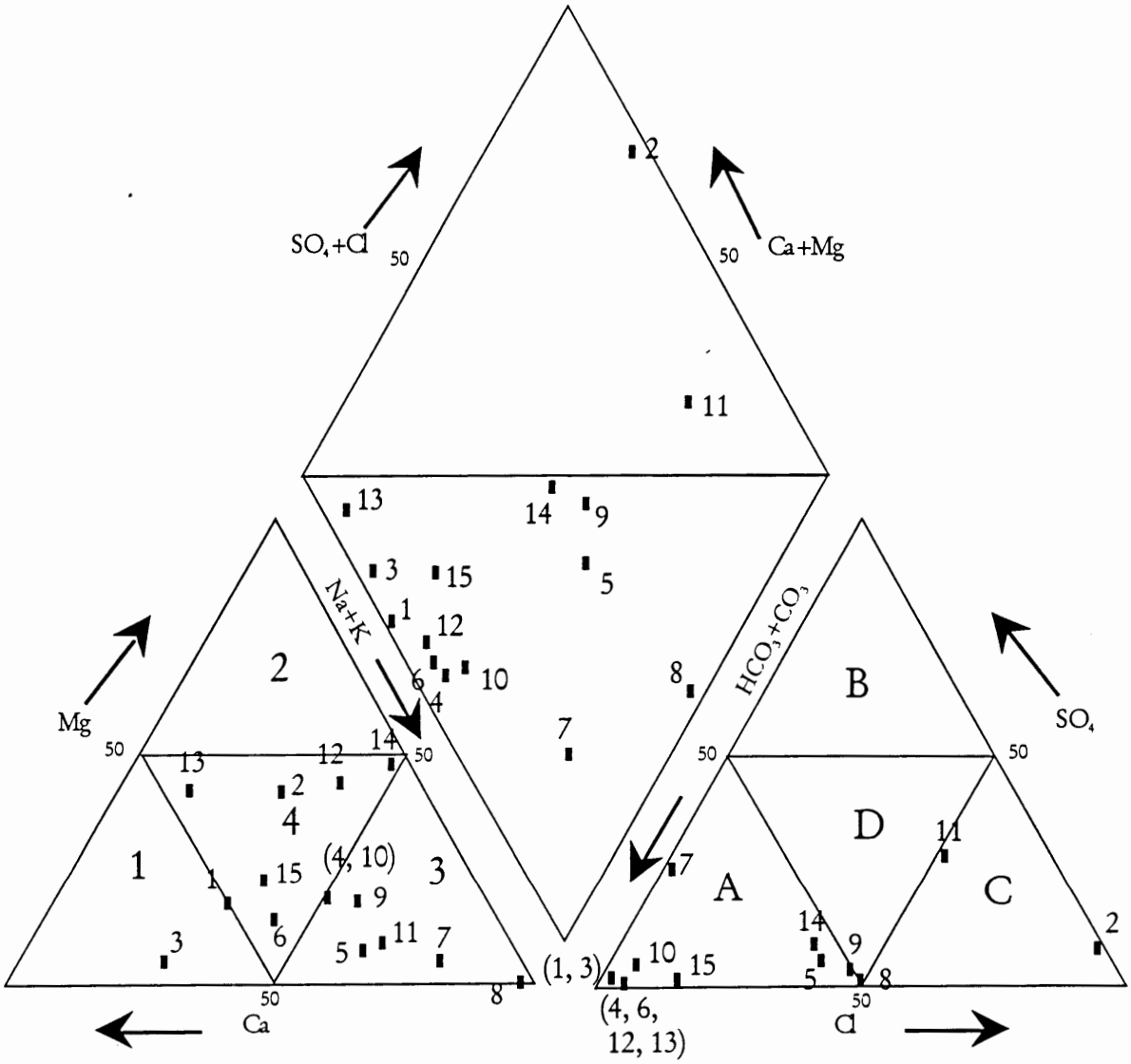

1.) O-17 i-1
2.) K-2 e-4
3.) L-13 i-2
4.) Hyde Plant
5.) Columbia
6.) Belhaven
7.) Plant Yorktown
8.) Waves
9.) CA-2
10.) BO-190
11.) HA-133
12.) HY-23
13.) HY-75
14.) TY-16
15.) WS-17

1. Ca-rich
2. Mg-rich
3. Alkali-rich
4. Mixed cations

A. Bicarbonate-rich
B. Sulfate-rich
C. Chloride rich
D. Mixed anions

Figure 65. Piper diagram of wells in the Yorktown aquifer.

Minor Elements

Silica concentrations (6-48 ppm)(Figure 66) first increase and then decrease from the northwest towards Pamlico Sound. Fe and pH changes are erratic (Figures 67 and 68). Phosphate (0.01-0.7 ppm) and nitrate (0-4.5 ppm) (Figures 69 and 70) are generally low and don't show a clear pattern of geographic variation. Fluoride (0-1.47 ppm) (Figure 71) varies irregularly but seems to be highest in the region between Albemarle Sound and the Pamlico River.

Strontium Content and Isotopic Signature

Strontium concentrations and $^{87}Sr/^{86}Sr$ ratios for three samples of Yorktown groundwater vary from 0.427-6.84 ppm and 0.70907-0.70920, respectively (Table 5). The $^{87}Sr/^{86}Sr$ ratios are in keeping with those of materials from these Yorktown Formation analyzed by Denison et al. 1993, but are somewhat higher than predicted by mixing calculations described below. Calculations were pursued to compare the observed groundwater ratios to those that should theoretically result from progressive addition of aquifer strontium to groundwater moving downgradient.

Carbon and Oxygen Isotopes and Organic Carbon

Yorktown $\delta^{13}C$ values range from -15.28 $^{\circ}/_{oo}$ to -4.38 $^{\circ}/_{oo}$, becoming more positive from southwest to northeast (Figure 72). Except at the extreme northern and southern well sites, $\delta^{13}C$ in the Yorktown is more negative than in the U-CHAS (Figure 52) at the same site. North of the Pamlico River, $\delta^{18}O$ values for the Yorktown become more positive southeast and northwest of New Lake (Figure 73). The three samples south of the Pamlico River suggest that the $\delta^{18}O$ becomes more negative southward toward the Neuse River. At the same site the $\delta^{18}O$ for Yorktown groundwater is more negative than that of the U-CHAS (Figure 54). Total organic carbon (TOC) values for Yorktown groundwater north of the Pamlico River are fairly consistent (1.73 to 1.88 $^{mgC}/_{L}$); south of the river, however, values are much more variable (0.32 to 1.87 $^{mgC}/_{L}$) (Figure 74). No consistent relationship between TOC values from samples of the Yorktown and U-CHAS at the same site was observed.

PEEDEE WATER CHEMISTRY AND ISOTOPES

Major elements

The same problem that exists for the high-salinity Yorktown well at site K2e4 affects the analysis of the high-salinity Peedee well (Table 7). The electrical neutrality balance for well J13d4

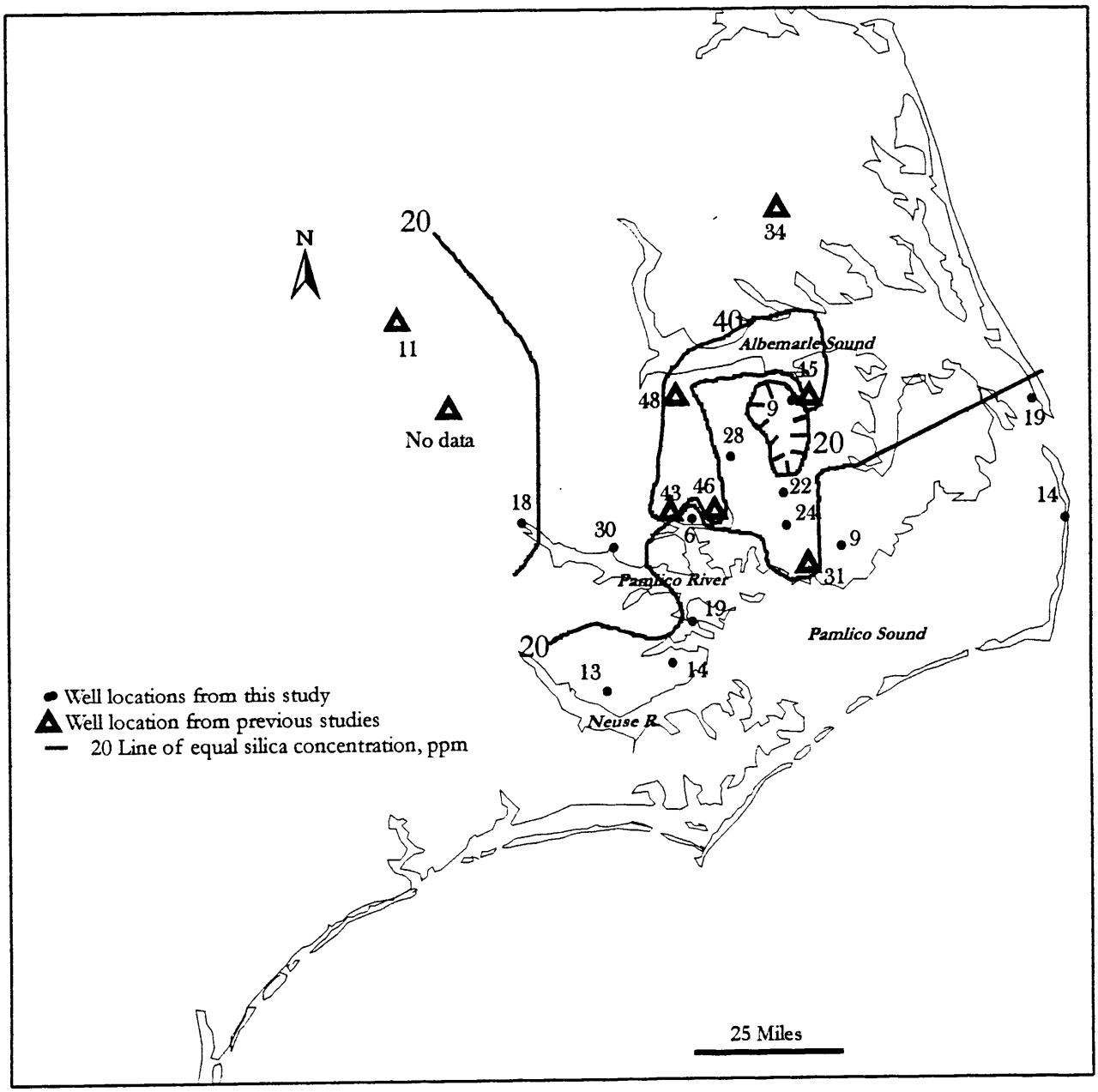

Figure 66. Silica concentrations in the Yorktown Aquifer.

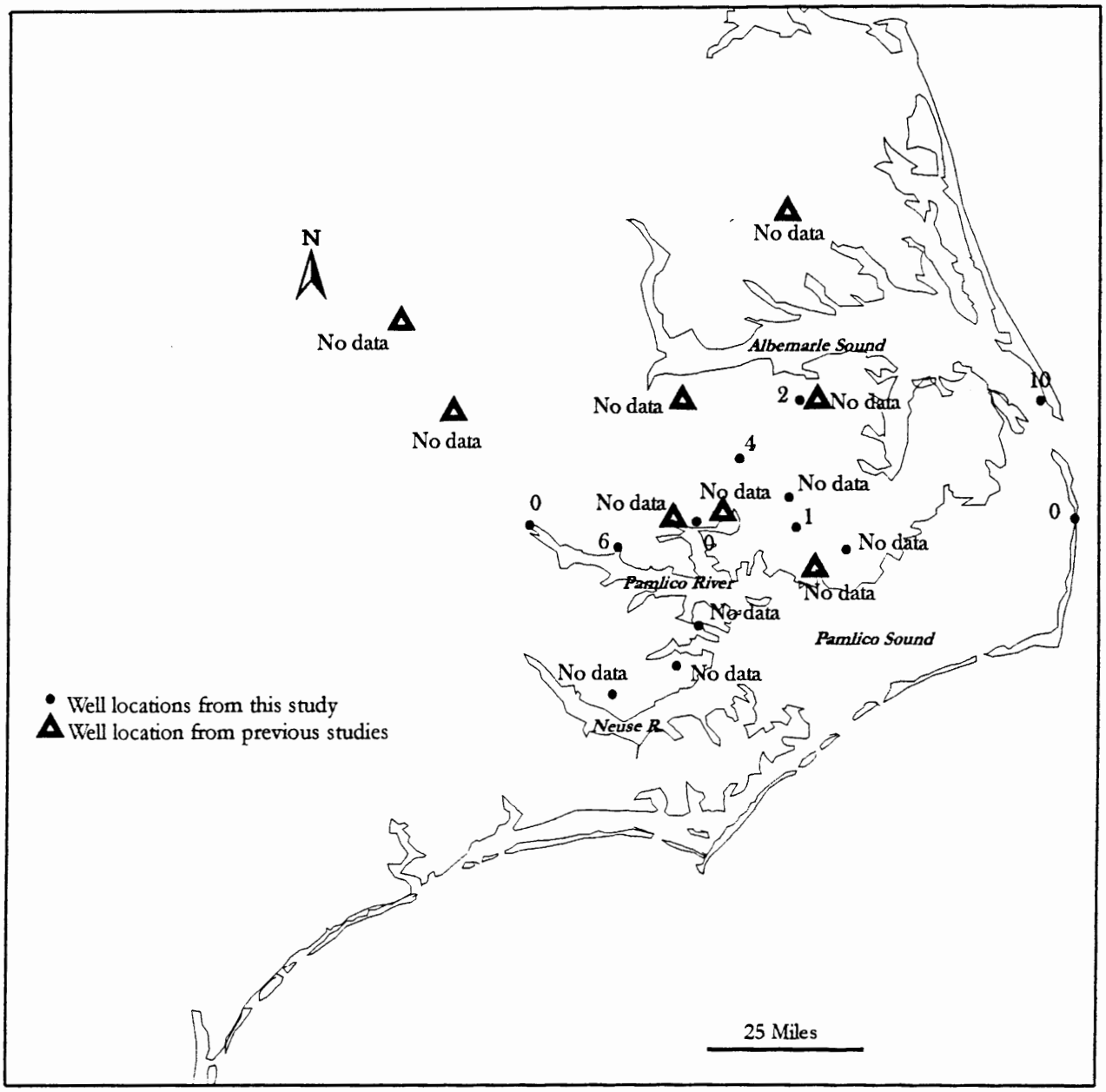

Figure 67. Iron concentrations in the Yorktown Aquifer.

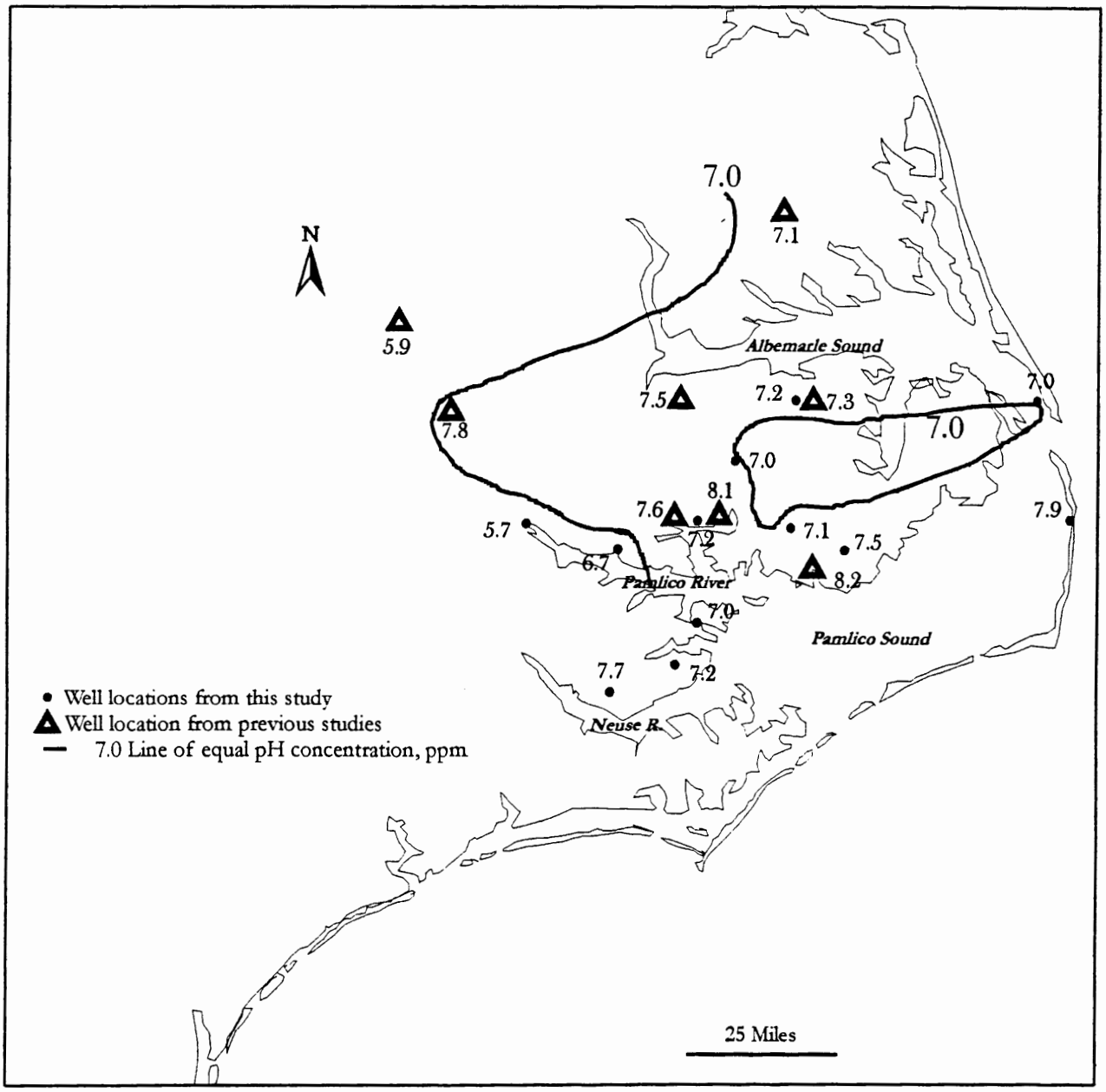

Figure 68. pH in the Yorktown Aquifer.

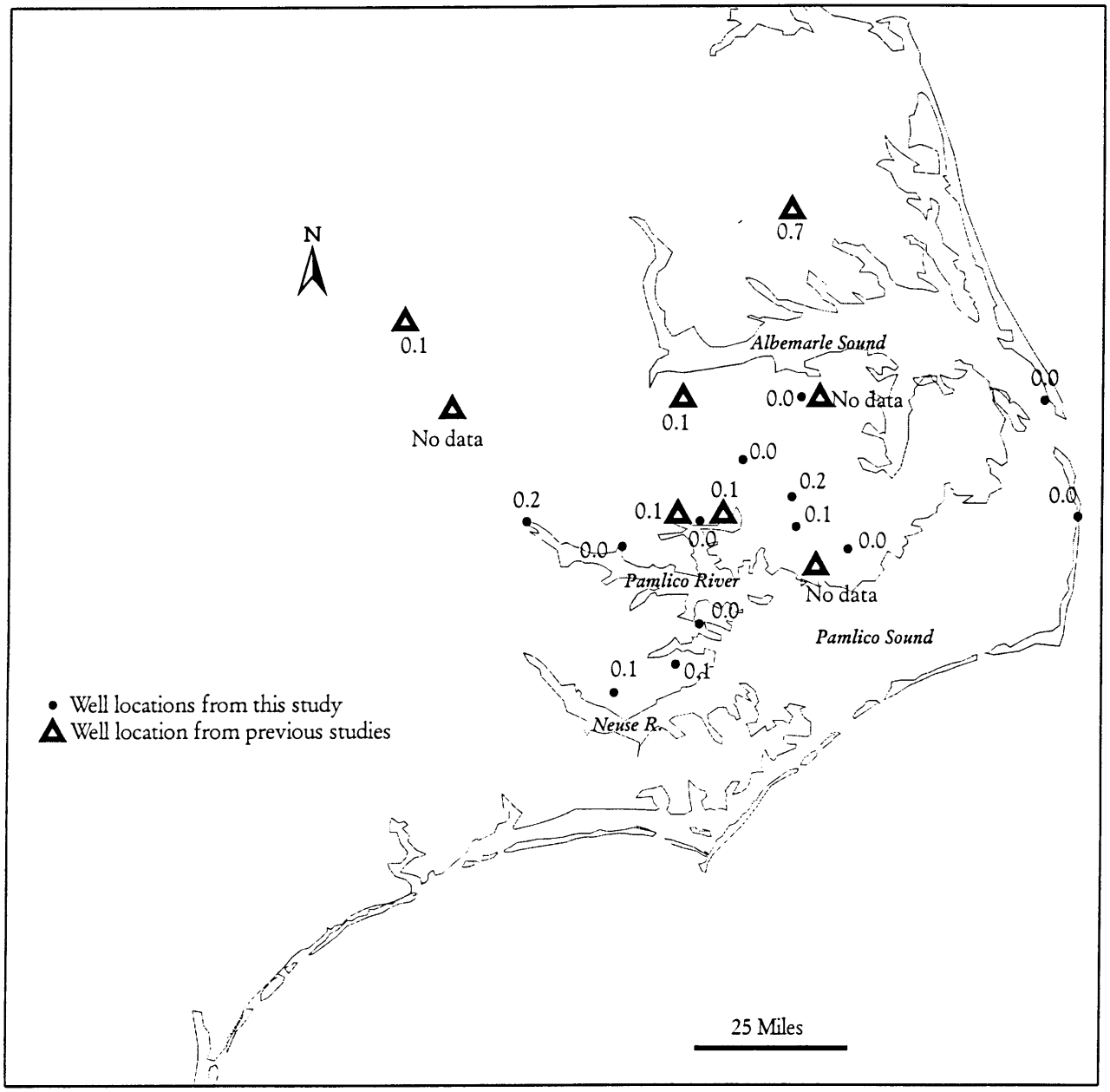

Figure 69. Phosphate concentrations in the Yorktown Aquifer.

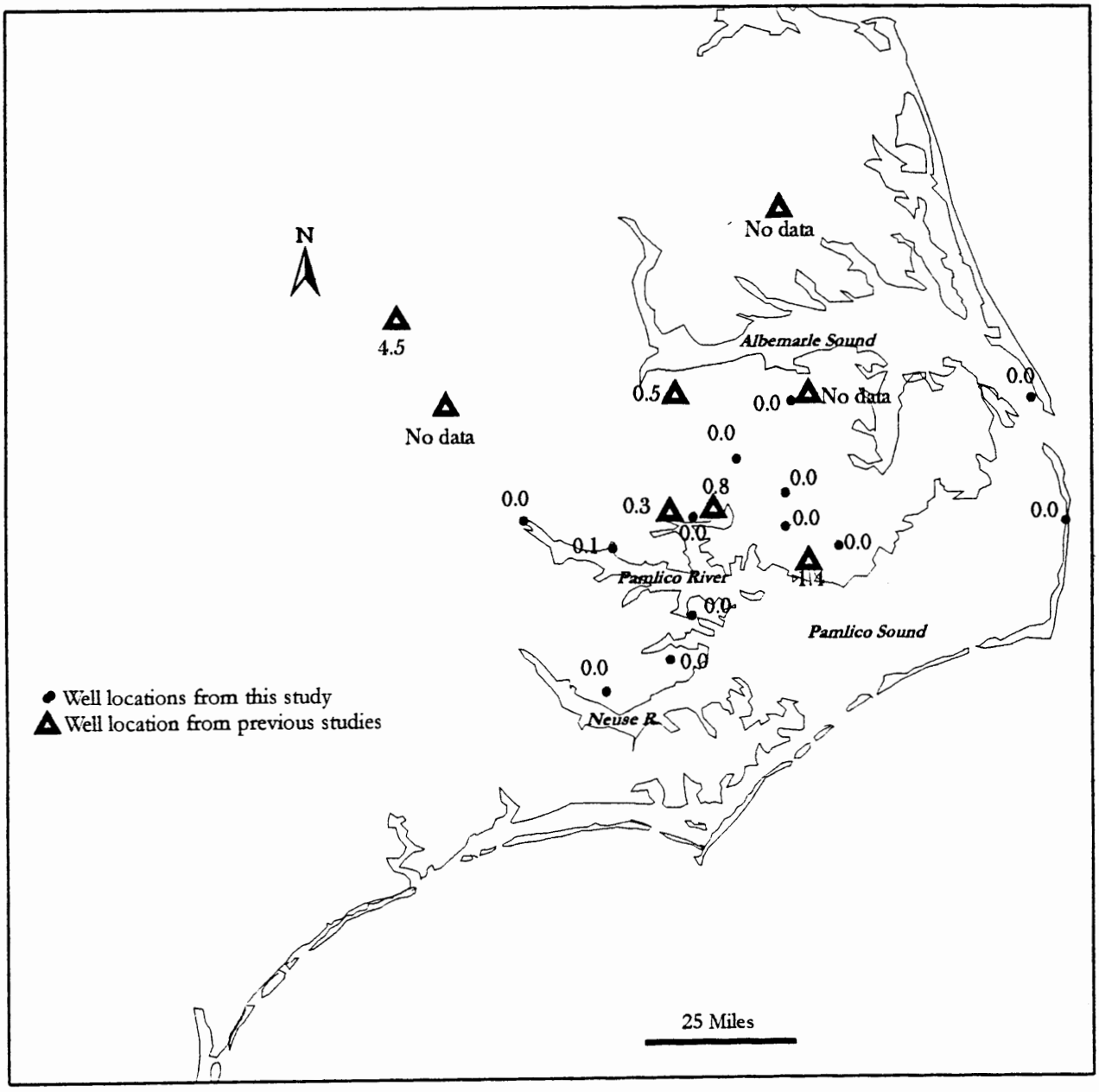

Figure 70. Nitrate concentrations in the Yorktown Aquifer.

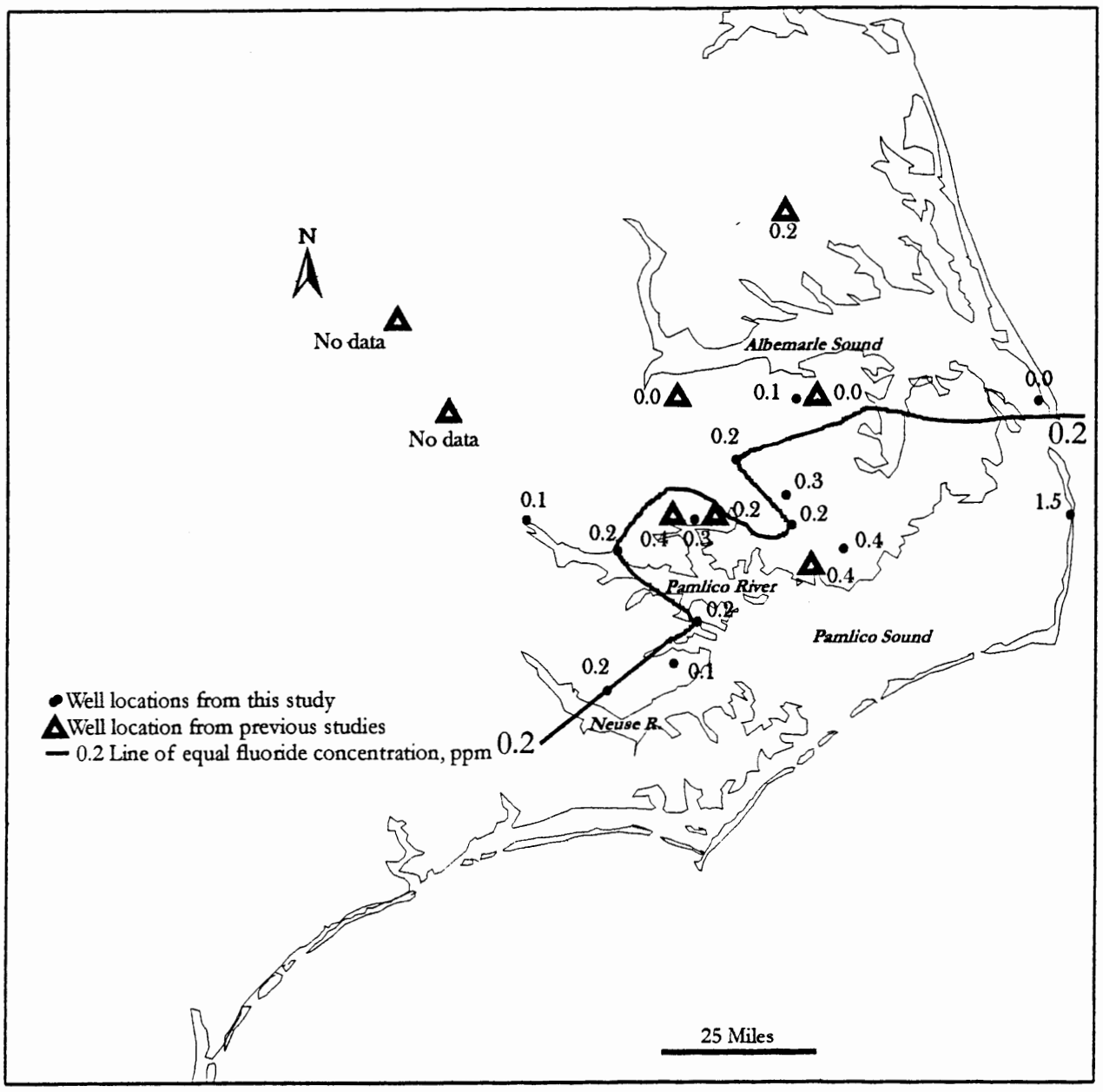

Figure 71. Fluoride concentrations in the Yorktown Aquifer.

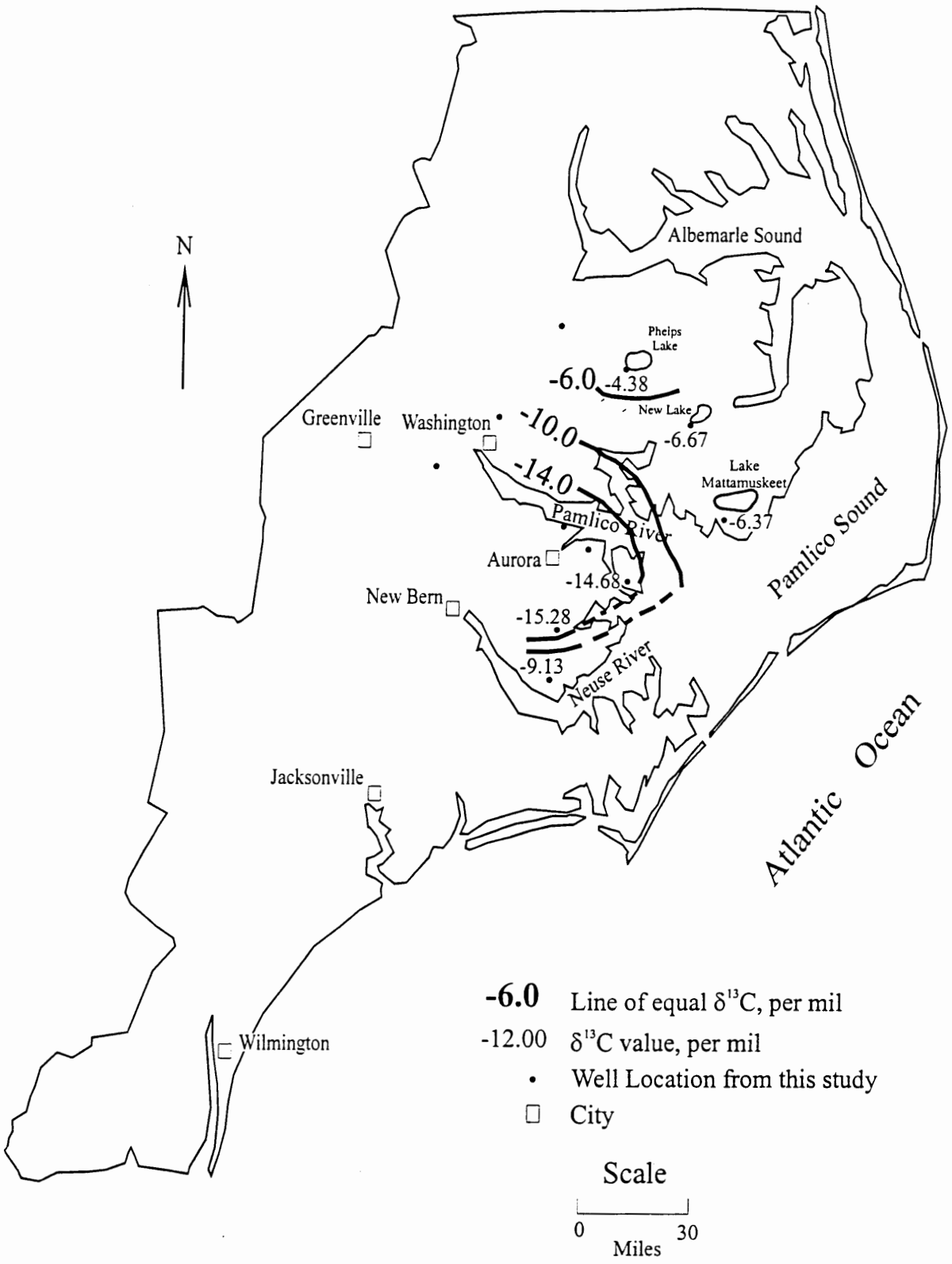

Figure 72. $\delta^{13}C$ of dissolved inorganic carbon in the Yorktown Aquifer

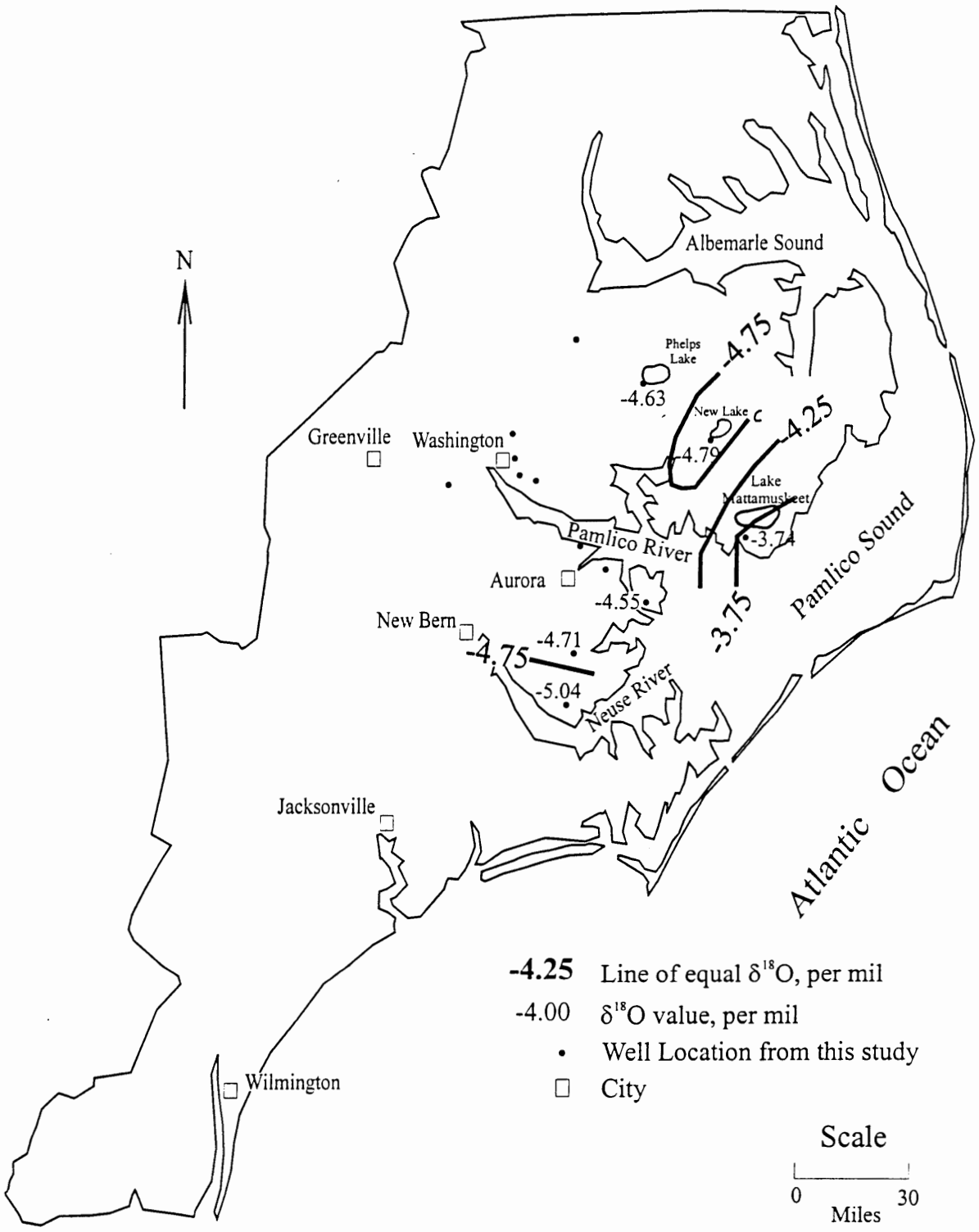

Figure 73. $\delta^{18}O$ in the Yorktown Aquifer

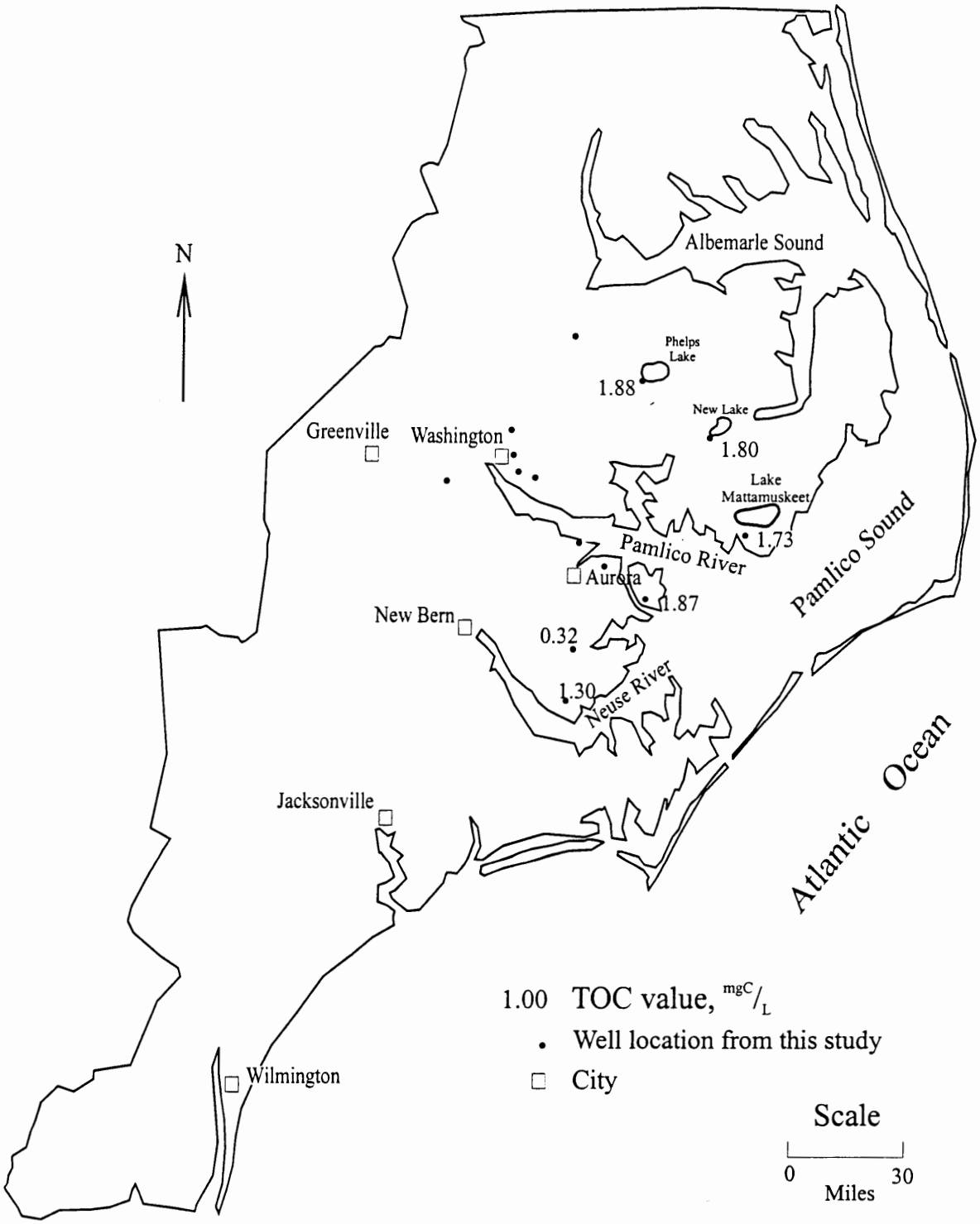

Figure 74. Total organic carbon concentrations in the Yorktown Aquifer ($^{mg\ C}/_{L}$)

Table 7. Chemical analyses of Peedee groundwater.(Knobel 1985 data *)

Well Identifer	Temp (°C)	pH	Eh mv	TDS ppm	HCO_3 ppm	Cl^- ppm	SO_4^{2-} ppm	Na^+ ppm	K^+ ppm	Ca^{2+} ppm	SiO_2 ppm	Mg^{2+} ppm
P-26 n-1	19	7.1	182	330	210	0	7	9	27	64	8	5
J-13 d-4	19	7.1	179	14456	340	8800	1120	3590	220	91	5	290
Chinquapin 1	o dat	8.3	567	255	190	0	0	45	5	5	6	4
Rose Hill	o dat	7.6	188	266	190	0	2	9	22	33	8	2
Pink Hill	o dat	8.3	367	229	150	0	2	13	11	45	5	3
Wallace (Ann St.	o dat	7.8	434	261	180	0	2	38	14	16	7	4
B0-29*	o dat	7.7	o dat	2128	479	765	142	612	40	25	39	26
PI-298*	o dat	7.7	o dat	465	303	9	7	93	19	13	16	6
CR-258*	o dat	8.1	o dat	1915	762	445	112	545	19	12	10	11
JO-21*	o dat	7.6	o dat	330	217	6	2	3	5	68	26	3
PI-375*	o dat	7.9	o dat	289	191	5	3	21	6	37	20	6
DD33Y1	o dat	7.3	92	332	215	21	13	8	4	66	3	2
FF32Y1	o dat	6.9	117	563	371	29	22	20	8	94	16	3
Relative Error %					4	8	2	2	8	4	3	4

Relative errors [as percent (%)] were calculated for each pair of duplicate analyses by 1) determining the average of the two concentrations, 2) determining the differences from the average of the pair of analyses, 3) dividing that difference by the average concentration, and 4) multiplying by 100. These percentages were then averaged over all pairs of duplicate anaylses to yield an estimate of relative error.

Table 7.(cont,d)Chemical analyses of Peedee groundwater.(Knobel 1985 data *)

Well Identifer	F^- ppm	S^{2-} ppm	NH_4^+ ppm	NO_3^- ppm	PO_4^{3-} ppm	Fe^{3+} ppm
P-26 n-1	0.1	0.0	0.200	0.000	0.020	0.00
J-13 d-4	0	0.0	4.000	0.001	0.020	5.25
Chinquapin 1	0.1	0.0	0.200	0.001	0.050	0.00
Rose Hill	0.1	0.0	0.160	0.013	0.180	0.00
Pink Hill	0	0.0	0.140	0.000	0.040	0.00
Wallace (Ann St.)	0.1	0.0	0.250	0.012	0.040	0.00
B0-29*	1.6	No data	No data	No data	No data	No data
PI-298*	2	No data	No data	No data	No data	No data
CR-258*	1.7	No data	No data	No data	No data	No data
JO-21*	0.2	No data	No data	No data	No data	No data
PI-375*	0.3	No data	No data	No data	No data	No data
DD33Y1	0	0.0	0.04	0.002	0.013	1.00
FF32Y1	0.1	0.0	0.22	0.001	0.02	4.00
Relative Error %	4		31		9	0

Relative errors [as percent (%)] were calculated for each pair of duplicate anaylses by 1) determining the average of the two concentrations, 2) detemining the differences from the average of the pair of analyses, 3) dividing that difference by the average concenrations, and 4) multiplying by 100. These percentages were then average over all pairs of duplicate anaylses to yield an estimate of relative error.

was not within acceptable limits so some of the values reported for this sample could be appreciably in error. As with K2e4, almost all concentrations at J13d4 are significantly higher than in other wells, so the numbers for J13d4 were recorded on the maps and considered in the contouring. Concentrations of Ca, Mg, Na, and K range from 5-94, 2-290, 3-3590, and 4-220 ppm, respectively (Table 7). Concentrations of Ca show the most complex pattern of geographic variation, with a region of high values near Kinston, between two regions of lower Ca content (Figure 75). Magnesium, Na, and K increase from southwest to northeast (Figures 76-78) and the easternmost well contains very salty water. Alkalinity and other major anion concentrations generally increase from southwest to northeast (Figures 79-81), although Cl (0-8850 ppm) and sulfate (0-1120 ppm) seem to increase abruptly just east of Kinston. Peedee waters are either Ca and HCO_3 rich (1A), alkali and HCO_3 rich (3A), or alkali and Cl rich (3C) with the latter occurring farther to the east (Figure 82).

Minor Elements

Silica concentrations (Figure 83) are higher in the central region around the Pamlico and Neuse Rivers east of Kinston, decreasing to the northeast and southwest. Iron was only detected in a few Peedee wells, so no contour map was drawn. pH (Figure 84) appears to increase from northwest to southeast, but phosphate (Figure 85) concentrations delineate no clear trend. Nitrate concentrations increase east of Kinston (Figure 86) and fluoride is low except for the region around the Pamlico and Neuse Rivers where it increase to 1.6-2.0 (Figure 87). The North Carolina groundwater standard for fluoride is 2.0 ppm (15A NCAC 2L Classifications and Water Quality Standards 1993).

Strontium Content and Isotopic Signature

Strontium concentrations and $^{87}Sr/^{86}Sr$ ratios for groundwater from 11 wells penetrating the Peedee vary from 0.129-6.157 ppm and 0.70806-0.70944, respectively (Table 5). These results are described and discussed in a recent thesis completed at UNC-W (Sirtariotis 1998), but no maps are included here.

WATER CHEMISTRY OF OTHER AQUIFERS

A few samples were collected from other aquifers (Surficial, Pungo River, Beaufort, Black Creek, and Cape Fear) (Table 8), but these data are not plotted on maps or discussed. Some results are described and discussed in a recent thesis completed at UNC-W (Sirtariotis 1998). Analyses from the WATSTORE database (Knobel 1985) compiled for the Yorktown, Peedee, Black Creek, and Cape Fear and are available from the first author.

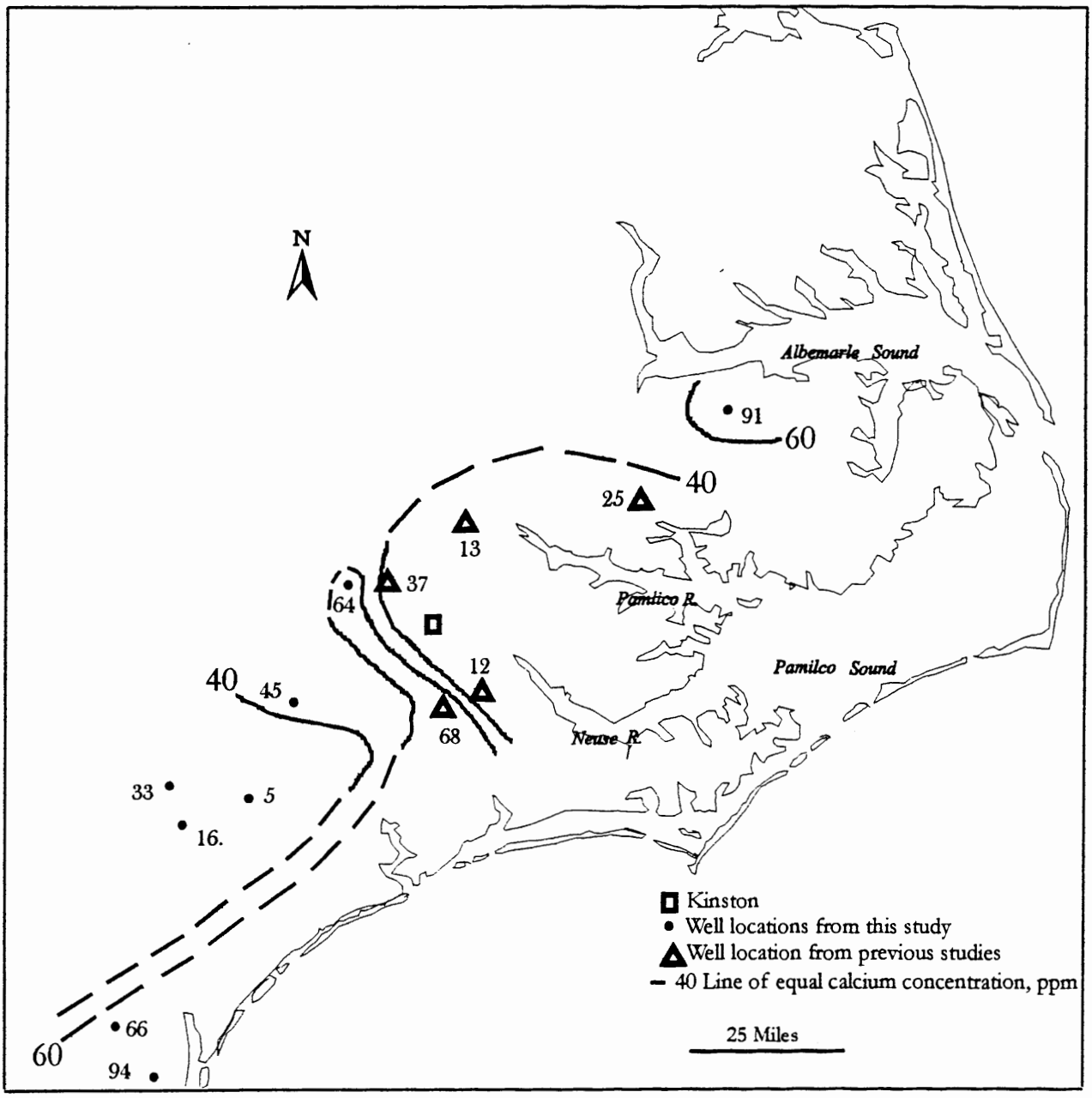

Figure 75. Calcium concentrations in the Peedee Aquifer.

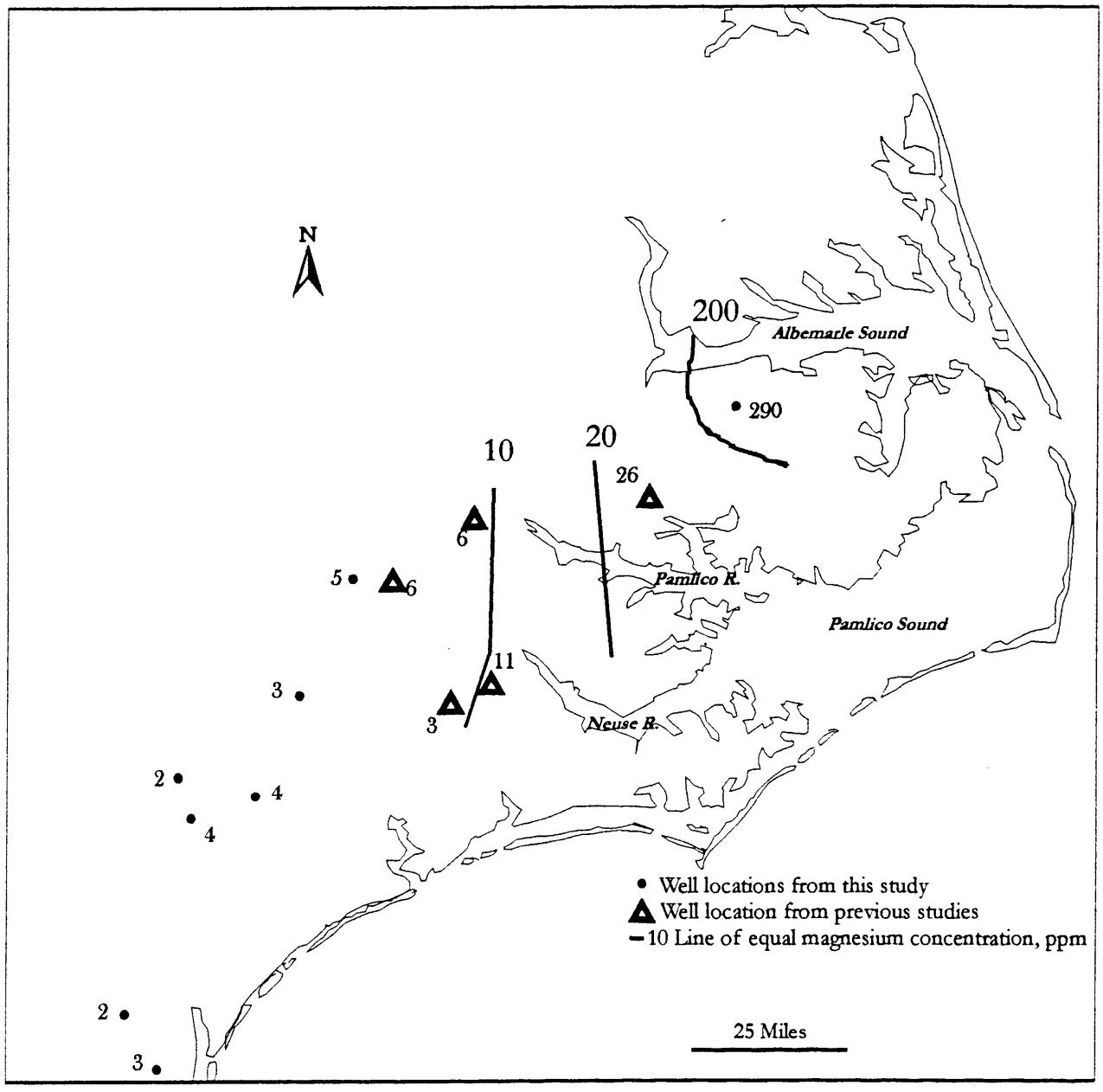

Figure 76. Magnesium concentrations in the Peedee Aquifer.

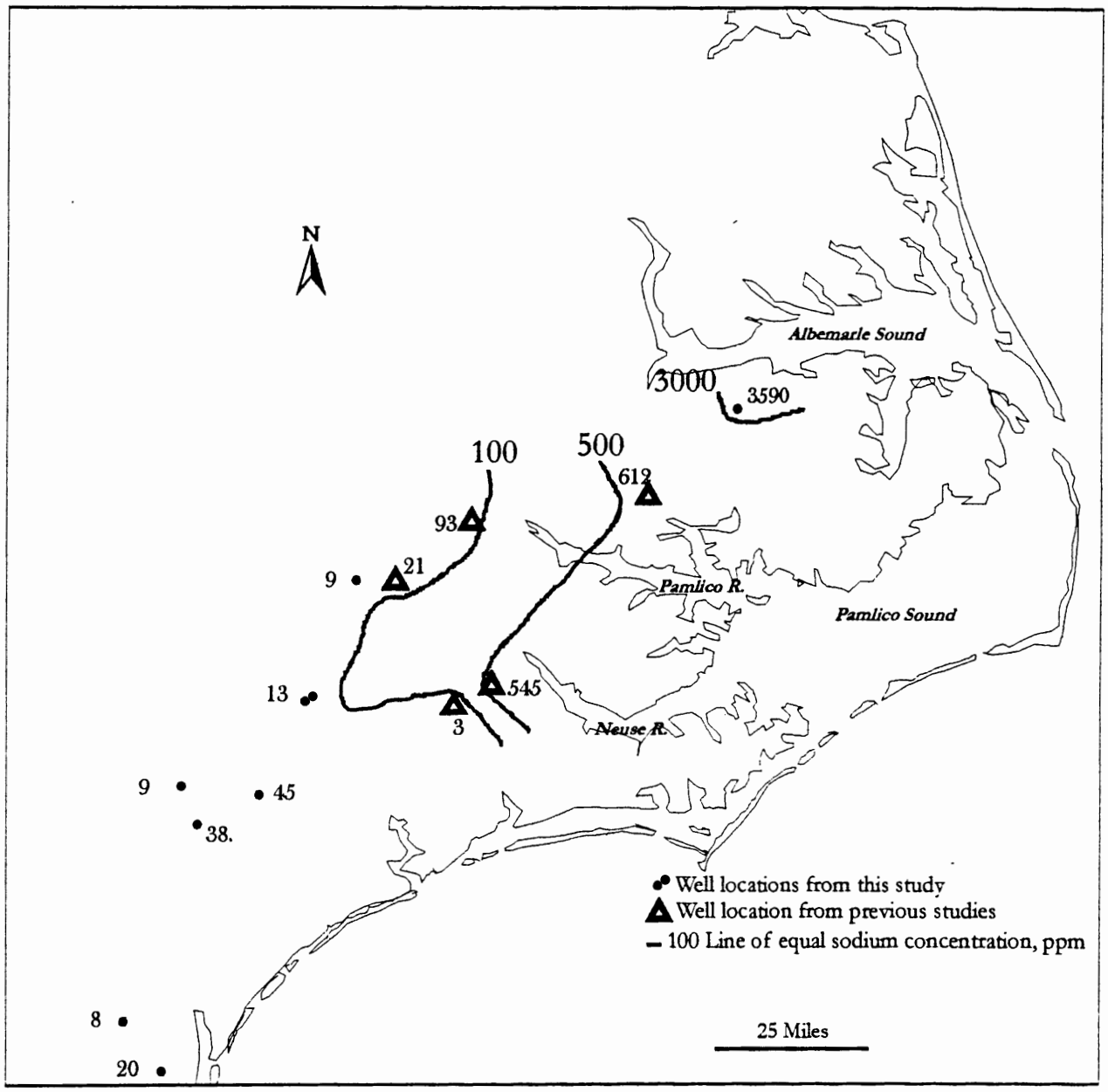

Figure 77. Sodium concentrations in the Peedee Aquifer.

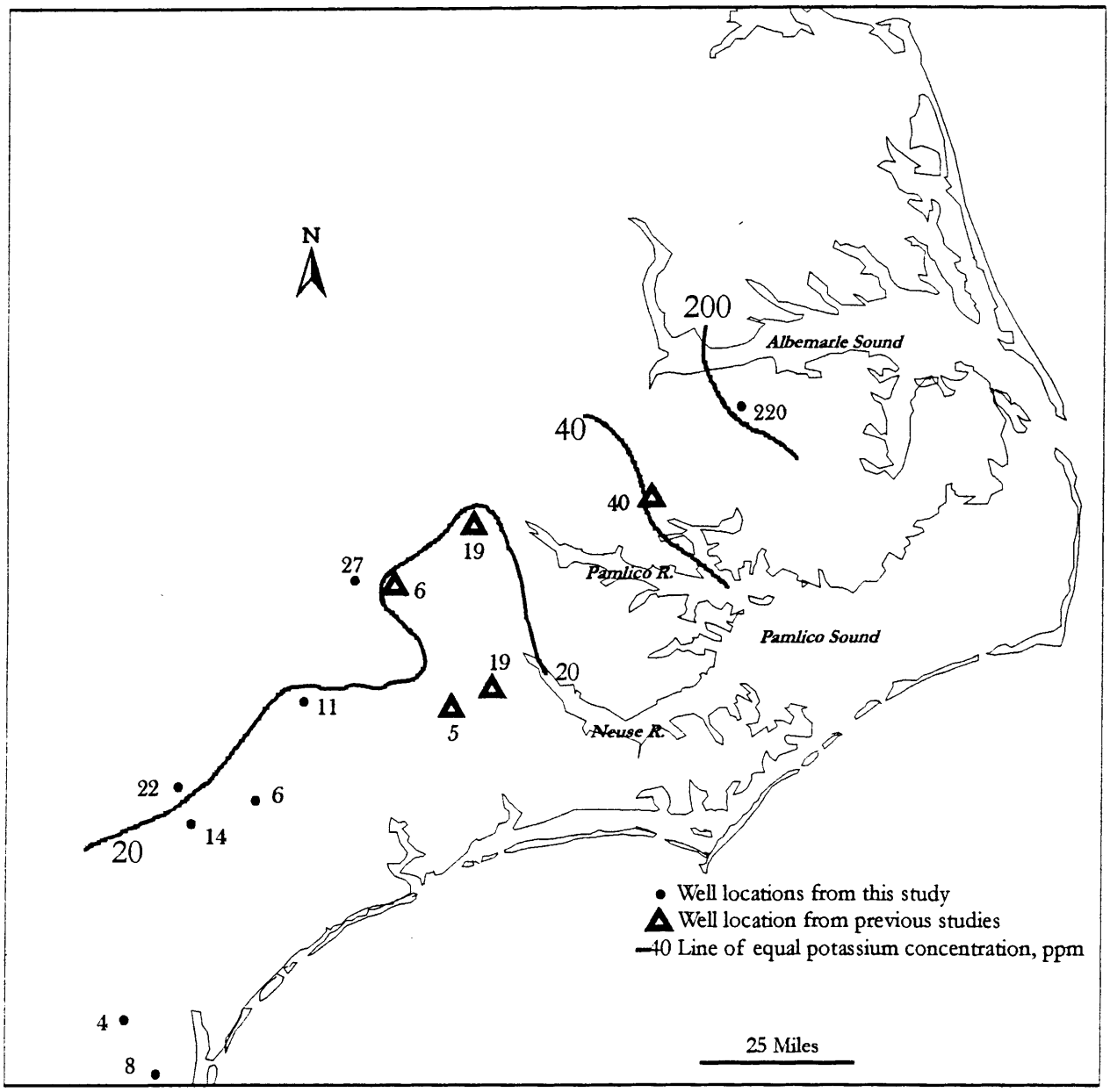

Figure 78. Potassium concentrations in the Peedee Aquifer.

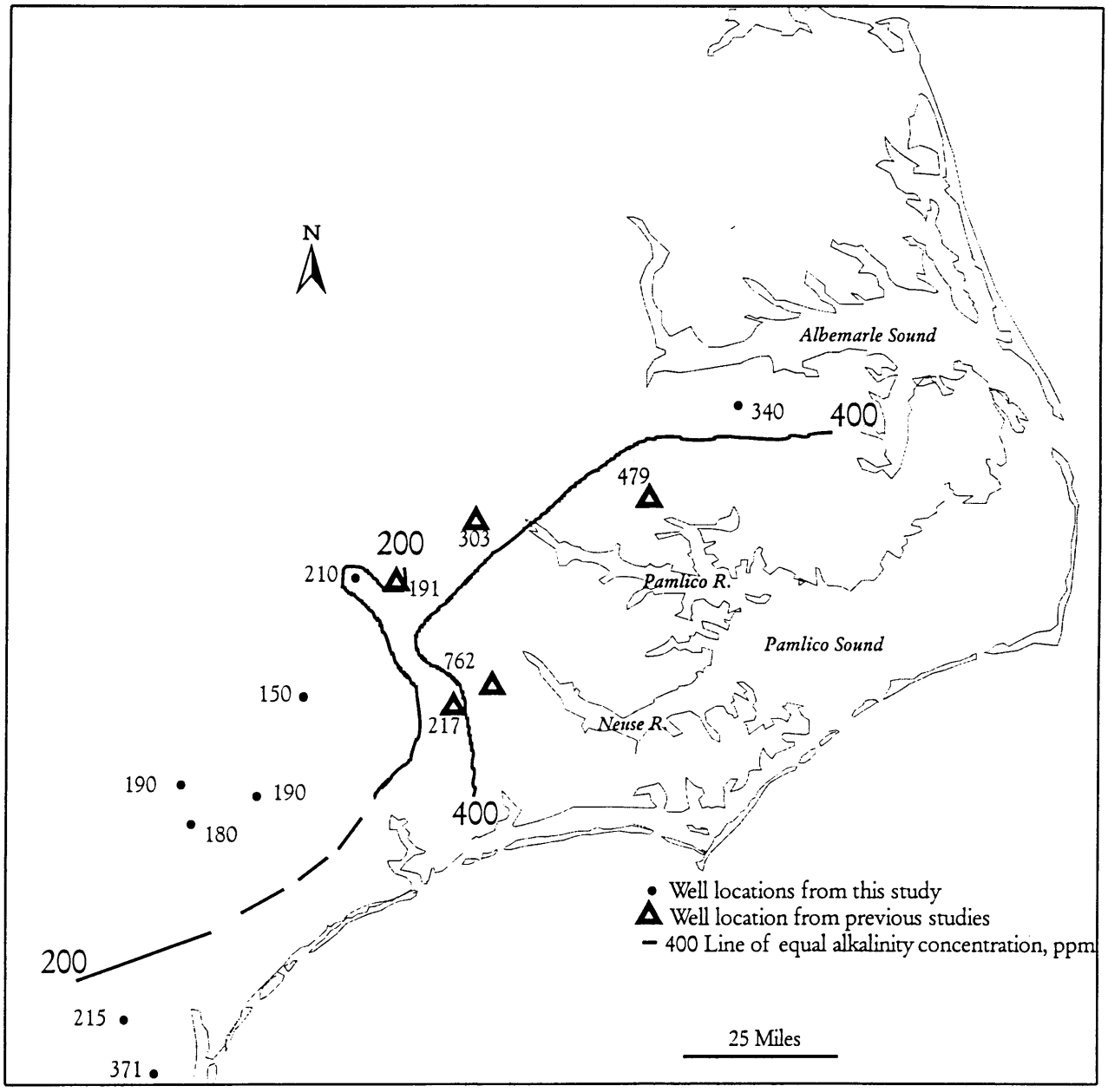

Figure 79. Alkalinity in the Peedee Aquifer(as ppm of HCO_3).

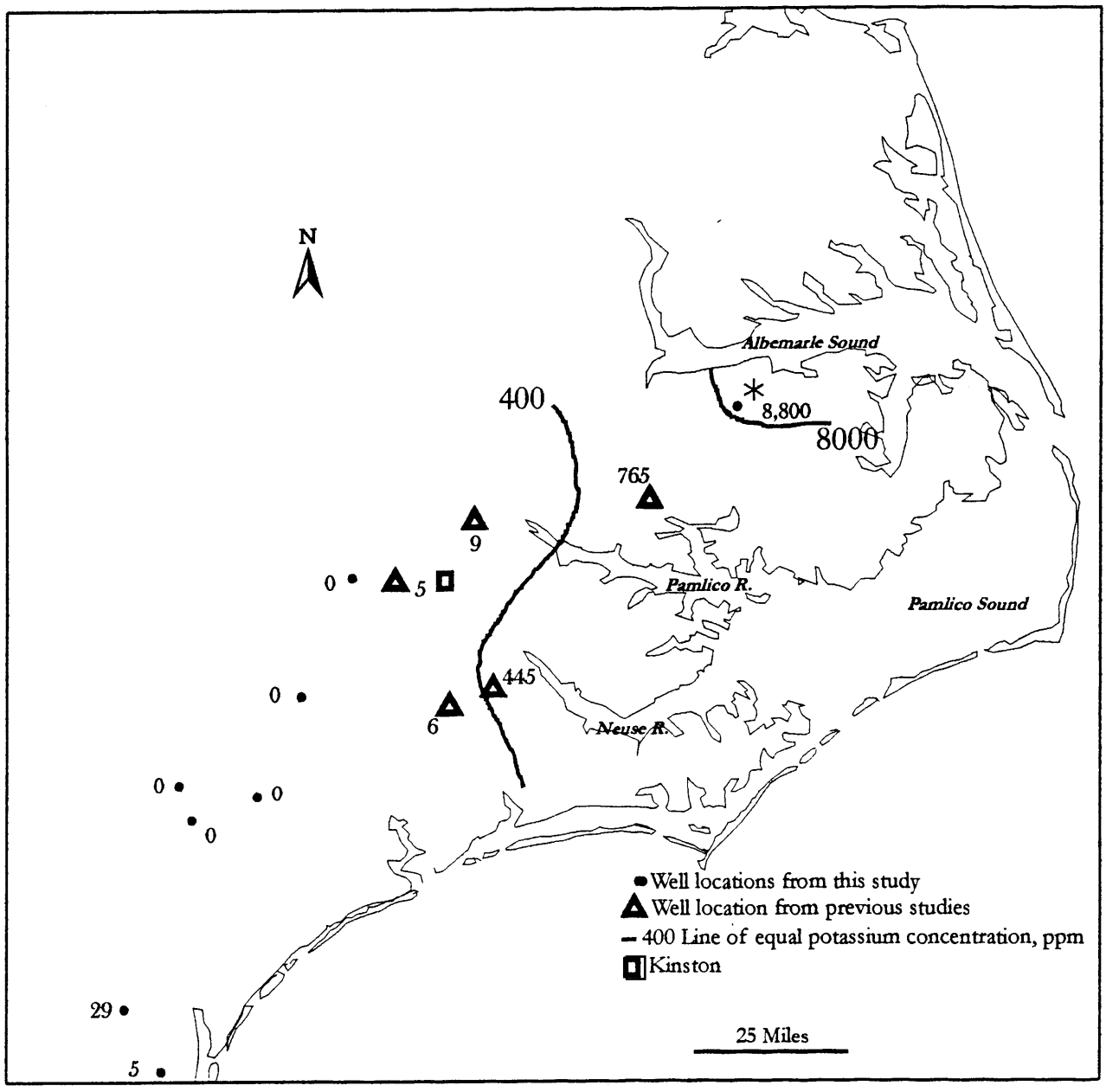

Figure 80. Chloride concentrations in the Peedee Aquifer. (* See text: Probably significantly lower than this, but still much higher than any of the wells farther west.)

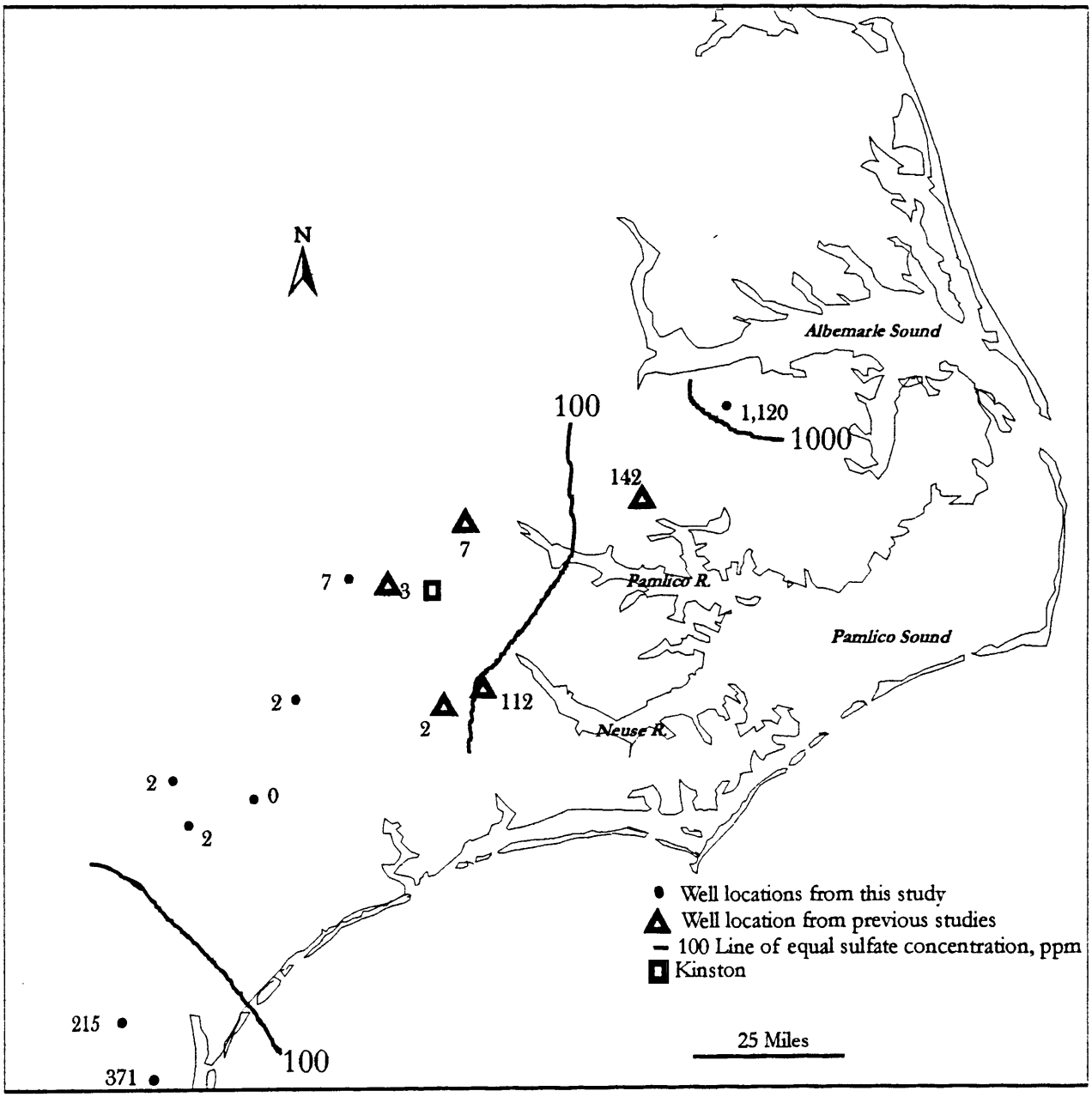

Figure 81. Sulfate concentrations in the Peedee Aquifer.

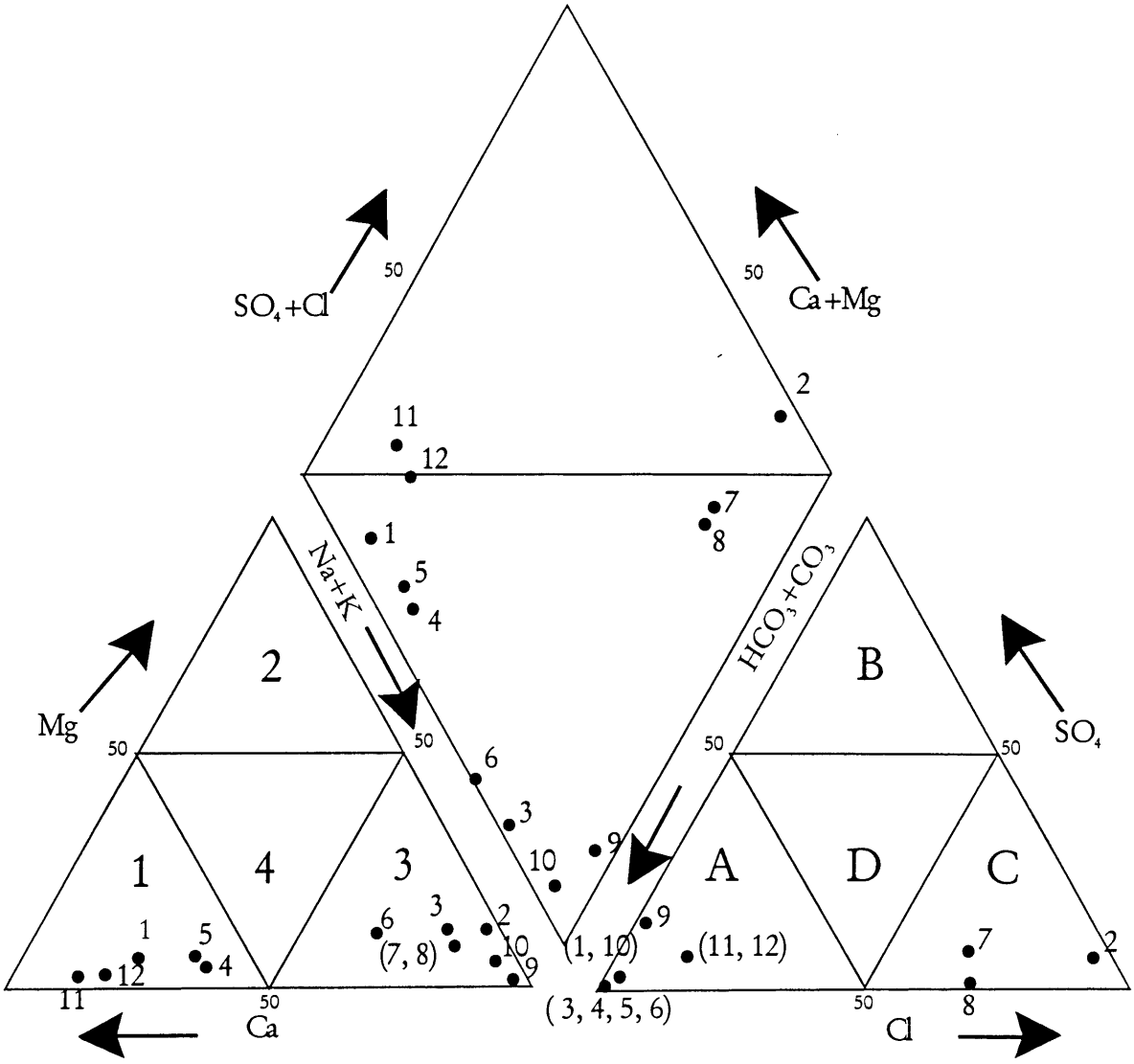

1.) P-26 n-1
2.) J-13 d-4
3.) Chinquapin 1
4.) Rose Hill
5.) Pink Hill
6.) Wallace (Ann St.)
7.) BO-29
8.) PI-298
9.) CR-258
10.) JO-21
11.) DD33Y1
12.) FF32Y1

1. Ca-rich
2. Mg-rich
3. Alkali-rich
4. Mixed cations

A. Bicarbonate-rich
B. Sulfate-rich
C. Chloride rich
D. Mixed anions

Figure 82. Piper diagram of wells in the Peedee aquifer.

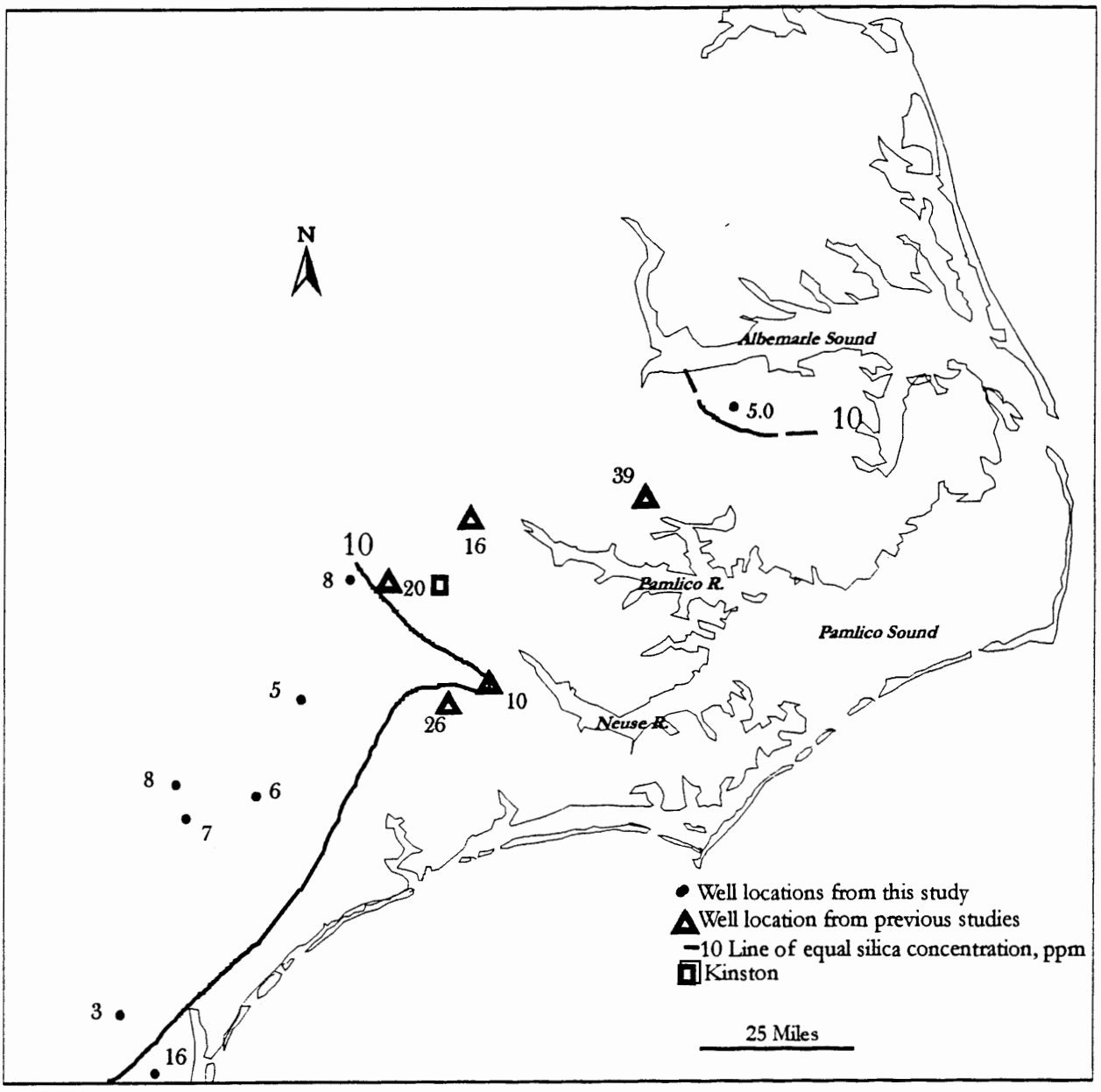

Figure 83. Silica concentrations in the Peedee Aquifer.

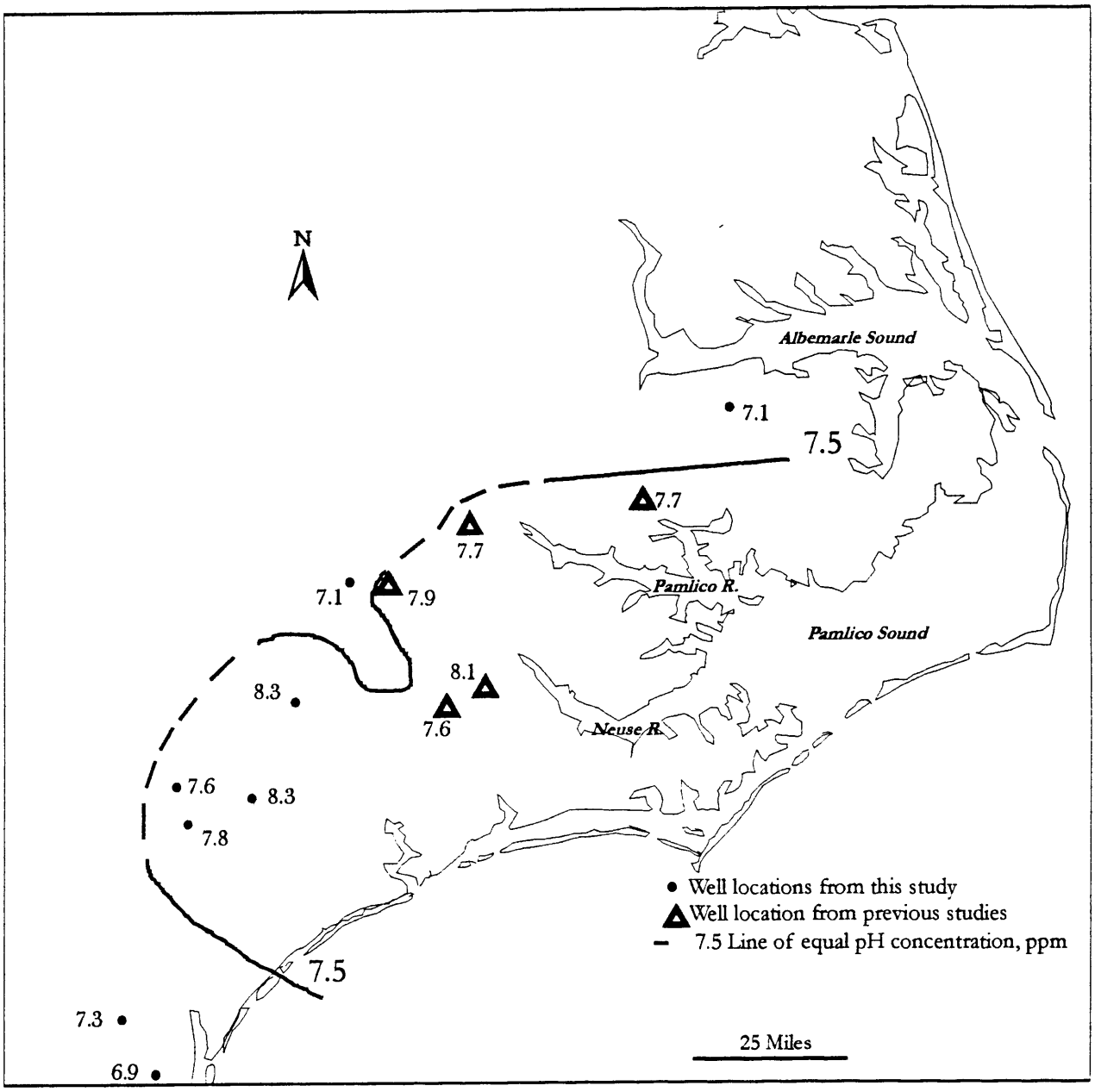

Figure 84. pH in the Peedee Aquifer.

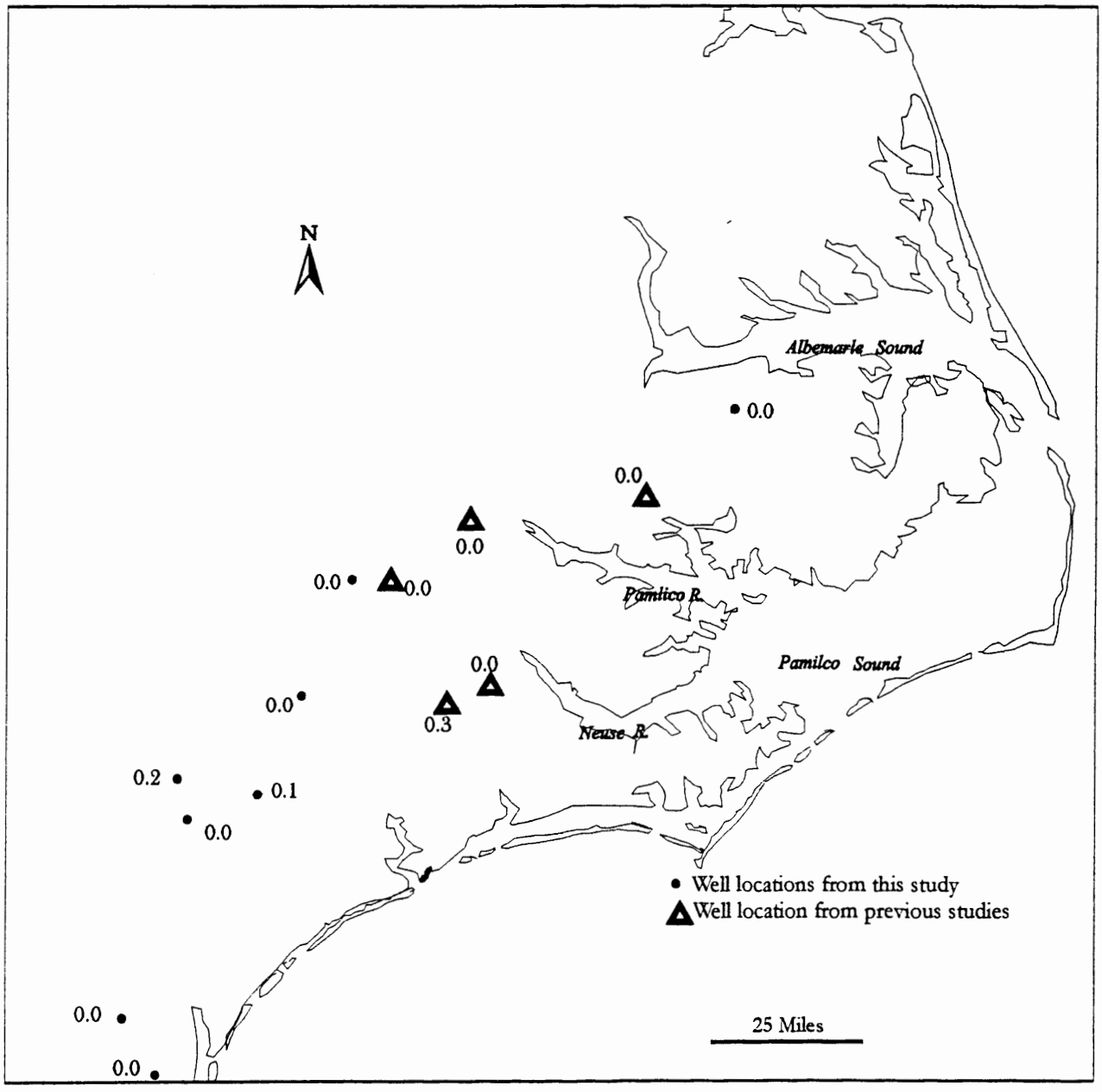

Figure 85. Phosphate concentrations in the Peedee Aquifer.

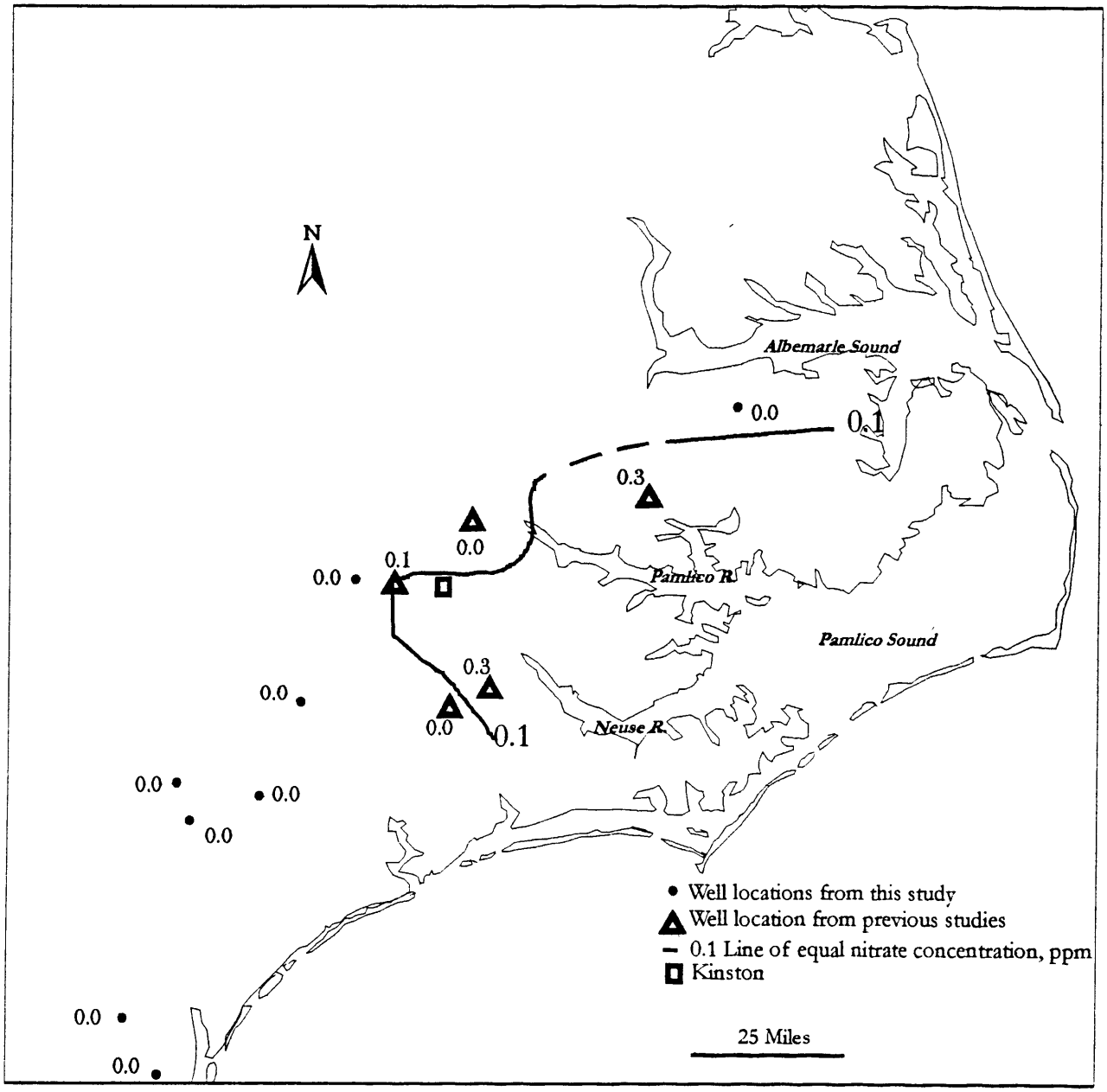

Figure 86. Nitrate concentrations in the Peedee Aquifer.

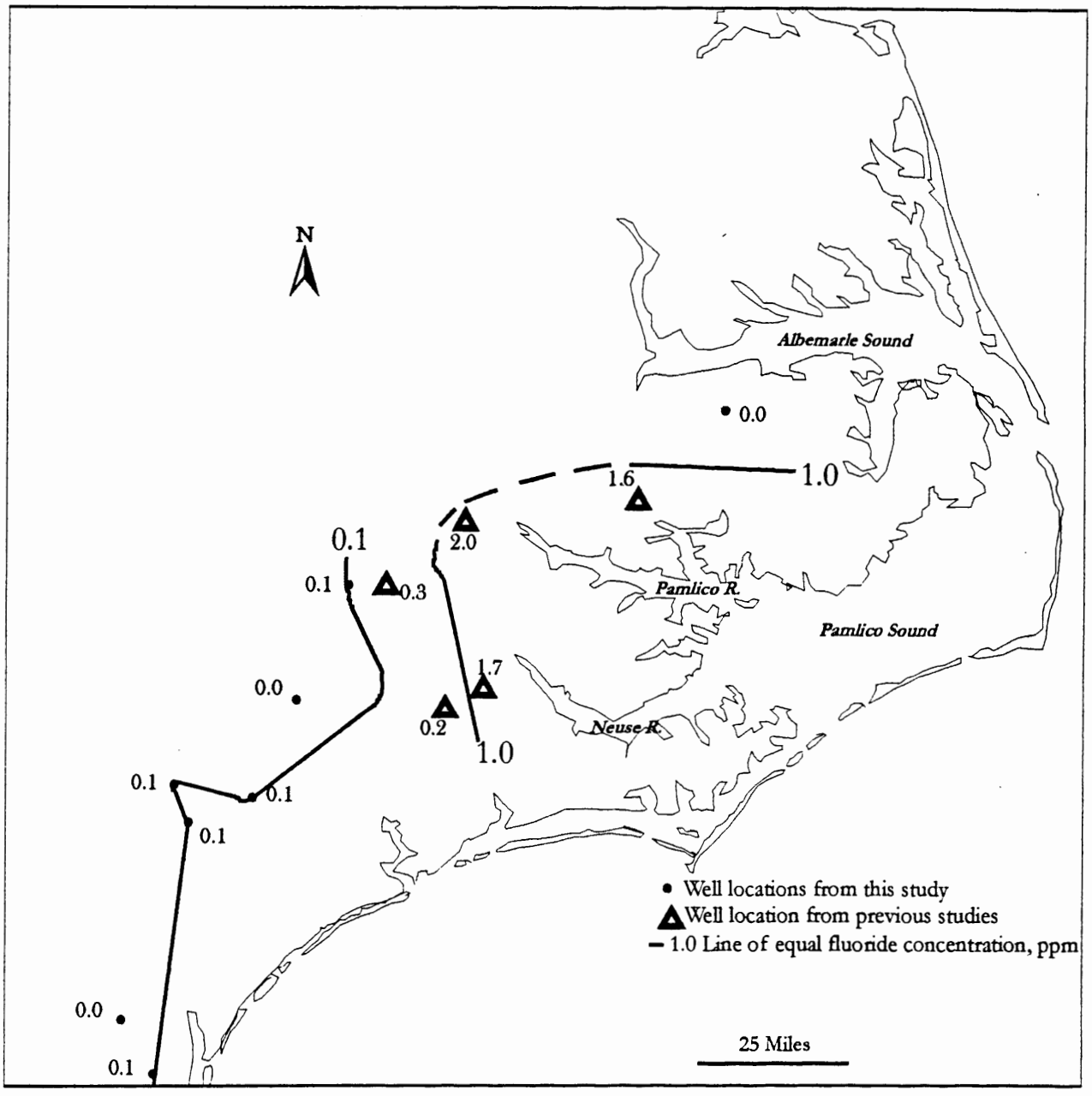

Figure 87. Fluoride concentrations in the Peedee Aquifer

Table 8. Groundwater analyses for other aquifers in ppm

Well	Identifier	Aquifer	County	Temp.	pH	DO	Sulfide	HCO3	Si	Sulfate	Phosphate	Nitrite
CC 38	b 5	Surficial	Columbus	18	6.97	0.296	0	292	9.6	7	0.113	0.018
CC 38	b 5 (d)	Surficial	Columbus	18	6.97	0.296	0	292	9.5	7	0.115	0.016
EE 36	k 4	BC	Brunswick	19.5	8.07	0.286	0	7	10	10	35	0
EE 36	k 5	BC	Brunswick	21	7.77	0	0	10	8.9	8	0.019	0
FF 33	d 1	UCH	Brunswick	18.5	7.34	0	0	299	10.5	7	0.11	0.002
F-22	b 3	Surficial	Bertie	17	5.7	0	0	20	10.8	0	0.01	0
S-18	u 7	PR	Pamlico	16	7.1	0	0	276	24.3	8	0.063	0
WWF		PR	Beaufort	19	6.5	0	0	251	16.9	16	0.065	0.002
G-19	b 3	Beaufort	Bertie	17	7.8	0	0	427	8	1	0.033	0
C-15	s 5	BC	Gates	18	8.5	0	0	708	5.3	26	0.245	0
P-21	k 5	UCF	Beaufort	21	8.1	0	0	498	5.1	63	0.408	0

Table 8. (cont'd.)

Well	Identifier	$NO_3 + NO_2$	Nitrate	NH3	Cl	F	Fe	Ca	K	Mg	Na
CC 38	b 5	0.114	0.096	0.04	46	0.09	2	90	5	3	21
CC 38	b 5 (d)	0.1	0.083	0.04	49	0.09	2	94	5	3	21
EE 36	k 4	0.003	0.003	0.7	3200	0.34	0.3	832	50	10	773
EE 36	k 5	0.003	0.003	1.12	3240	0.31	0.3	71	84	16	1673
FF 33	d 1	0	0.002	102	25	0.11	4	111	4	2	12
F-22	b 3		2.027	0.01	0	0.03	0.2	2	3	0	6
S-18	u 7		0	1.84	0	0.12	0.1	20	19	14	14
WWF			0.013	0.09	0	0.15	7	59	24	1	21
G-19	b 3		0.001	1.17	2	0.64	0	11	18	8	108
C-15	s 5		0.01	1.47	65	3.08	0	0	16	1	277
P-21	k 5		0.018	0.22	741	3.84	0	1	18	30	398

CASTLE HAYNE MINERALOGY AND MINERAL CHEMISTRY

Core samples from wells BF-T6-67, BF-T1-69, and PA-T2-XX (Figure 13) were examined petrographically, point-counted (Tables 9-11), and analyzed by EDX. Two samples from well BF-T1-69 were analyzed by X-ray diffraction (XRD) because they contain abundant peloids. Initially, the drill cuttings from wells BF-T5-67, TY-T1-76, and WH-T2-78 (Figure 13) were analyzed by XRD to distinguish areas within the CHAS containing minerals other than calcite and quartz. Samples representing mineralogically distinct zones were chosen for EDX analysis. Drill cuttings were not analyzed by point counting, but were examined under a binocular microscope.

Petrography

Within the study area, the CHAS is a sandy, fossiliferous and occasionally dolomitic limestone. It is dominated by a micrite matrix with quartz, bioclasts, and very high percent secondary moldic porosity due to the dissolution of bioclasts (Tables 9-11). There are also minor amounts of glauconite, phosphate, feldspar, and iron sulfide present in the aquifer. Two morphologic types of glauconite are observed in the CHAS within the study area -- internal molds of bioclasts and granular peloids. Occasionally the micrite is aggrading to microsparite due to burial and diagenesis. Carbonate grains in samples from wells BF-T1-69, PA-T2-XX, and BF-T6-67 (Figure 13) were stained with a mixture of Alizarin Red-S and potassium ferricyanide in 0.2% hydrochloric acid, which revealed the presence of calcite only with no dolomite or ferroan calcite. The paucity of dolomite and ferroan calcite in these samples is also indicated by EDX analysis. Sample TY-T1-76 contains rhombohedra of dolomite, some of which have been replaced with SiO_2; however, XRD and EDX data support the existence of dolomite in this sample. Based on the Folk (1962) classification scheme, which emphasizes composition over texture, the CHAS is a quartz glauconitic biomicrite. Using the Dunham (1962) classification, which emphasizes texture, the CHAS is a wackestone.

Matrix and Cement. The CHAS is a matrix-supported limestone with minor amounts of calcite cement, which is secondary replacement in origin. The micrite is frequently aggrading to microsparite due to burial and diagenesis. Occasionally, the cement is dolomitic (based on EDX data) partially replacing several bioclasts and glauconite grains.

Allochems. Bioclasts account for up to 35% of the volume of the CHAS (Tables 9-11). Mollusks and echinoderm fragments are dominant, but brachiopods, bryozoans, and foraminifera are also present. The total number of bioclasts increases from east to

Table 9. Point count data for well BF-T1-69.

DEPTH OF SAMPLE	24-30	30-32	23.25-32.33	32.52	52-62
	PERCENT OF TOTAL ROCK				
matrix	58.50	58.00	65.50	54.50	42.96
cement			1.00	2.00	7.04
quartz sand	9.00	14.50	4.00	5.50	12.68
feldspar				0.50	2.11
peloids	3.00	10.50	2.50	2.00	18.31
lithic fragments				0.50	
bioclasts	29.50	17.00	27.00	35.00	16.90
TOTAL	100	100	100	100	100
	% BIOCLASTS (based on # present in each sample)				
mollusk	27.12	20.60	55.56	14.29	100
brachiopod	15.25	8.82	7.41	10.00	
bryozoan	1.70	8.82	3.70	48.57	
foraminifera		5.88	11.11		
echinoderm	55.93	55.88	22.22	27.14	
TOTAL	100	100	100	100	100

Table 10. Point count data for well PA-T2-XX.

DEPTH OF SAMPLE	200-220	220-231	231-240	240-270
	PERCENT OF TOTAL ROCK			
matrix	56.00	57.50	53.50	33.33
cement		0.50	3.50	7.33
quartz sand	13.00	18.50	14.50	30.33
feldspar			0.50	
peloids		0.50	0.50	0.33
lithic fragments			0.50	
biotite	0.50	0.50	0.50	
opaque	1.50			
intraclasts	7.00	4.50		
bioclasts	21.50	18.00	26.00	5.68
pore space			0.50	23.00
TOTAL	100	100	100	100
	% BIOCLASTS (based on # present in each sample)			
mollusk	79.06	77.78	53.84	63.64
brachiopod	2.33	8.33	34.62	
bryozoan	11.63	2.78		18.18
foraminifera	6.98	2.78	3.85	18.18
echinoderm		8.33	7.69	
TOTAL	100	100	100	100

Table 11. Point count data for well BF-T6-67.

DEPTH OF SAMPLE	135-178 feet	78-198 fee	198-203 feet	203-238 feet	238-243 feet
	PERCENT OF TOTAL ROCK				
matrix	42.25	55.50	50.50	54.50	59.00
cement	7.50	6.50	15.00	1.50	5.50
quartz sand	33.50	2.50	9.50	19.50	12.50
peloids		1.50		1.00	1.50
bioclasts	13.00	18.50	16.00	12.50	8.50
pore space	3.75	15.50	9.00	11.00	13.00
TOTAL	100	100	100	100	100
	% BIOCLASTS BASED ON # PRESENT IN EACH SAMPLE				
mollusk	86.53	64	75	52	64.71
brachiopod	9.62	8	12.5	8	
bryozoan		21.33	6.25	36	26.47
foraminifera		4	3.12		
echinoderm	3.85	2.67	3.13	4	8.82
TOTAL	100	100	100	100	100

west in the upper CHAS lead by increasing percentages of echinoderms, whereas mollusks and bryozoans decrease. Bioclast percentage increases slightly from north to south in the study area but decreases with depth in the limestone. Echinoderms increase in abundance from north to south, but there is no apparent north-south trend for mollusks and bryozoans.

Accessories. Non-carbonate peloids account for a smaller percentage (0.33-18%) of the CHAS. Chemical data revealed that the peloids are either glauconite or phosphate. They range from 0.03 to 0.22 mm in diameter and vary in color from light olive green to dark, almost-blackish green. Peloids are present in all six of the wells at various depths and abundances. They make-up 2-18% of the limestone in well BF-T1-69 (Table 9). In this well there are two zones in which peloids are locally abundant, the first from 30-32 feet below sea level where peloids account for 10.5% of the rock, and the second from 52 to 62 feet below sea level where peloids comprise over 18% of the rock sample. Well PA-T2-XX, the southernmost well in the study area, contains the lowest percentage of peloids (0.3% of the total rock) (Table 10). Well BF-T6-67 also contains few peloids, which make up 1.0-1.5% of the rock (Table 11). In general, the overall percentage of peloids increases from east to west and from south to north in the study area, but they are concentrated in localized vertical intervals.

Extraclasts. The extraclasts are dominated by sand-size, well-rounded to angular quartz grains (0.03 to 1.88 mm) that account for up to 33% of the rock (Tables 9-11). Other extraclasts present in minor amounts are feldspar and lithic fragments found in wells BF-T1-69 (Table 9) and PA-T2-XX (Table 10), and biotite flakes found only in well PA-T2-XX (Table 10).

Lithology

Cross-sections B-B′ and C-C′ were constructed from the six sampled wells penetrating the CHAS (Figures 13, 88 and 89). All depths are given in feet with respect to sea level and the occurrence of accessory minerals is indicated. The position of the U-CHAS/L-CHAS boundary was chosen based on significant lithologic, mineralogical, and chemical changes observed during this investigation. Along section B-B′, samples from the three northeastern wells include continuous drill cuttings of the entire CHAS, but the two southwestern wells are samples from cored intervals containing parts of the Upper and Lower CHAS. Along section C-C′, the samples also represent cored intervals of parts of the Upper and Lower CHAS.

The CHAS is a biomicrite with quartz sand, glauconite, dolomite, apatite, other clay minerals, and lesser amounts of iron

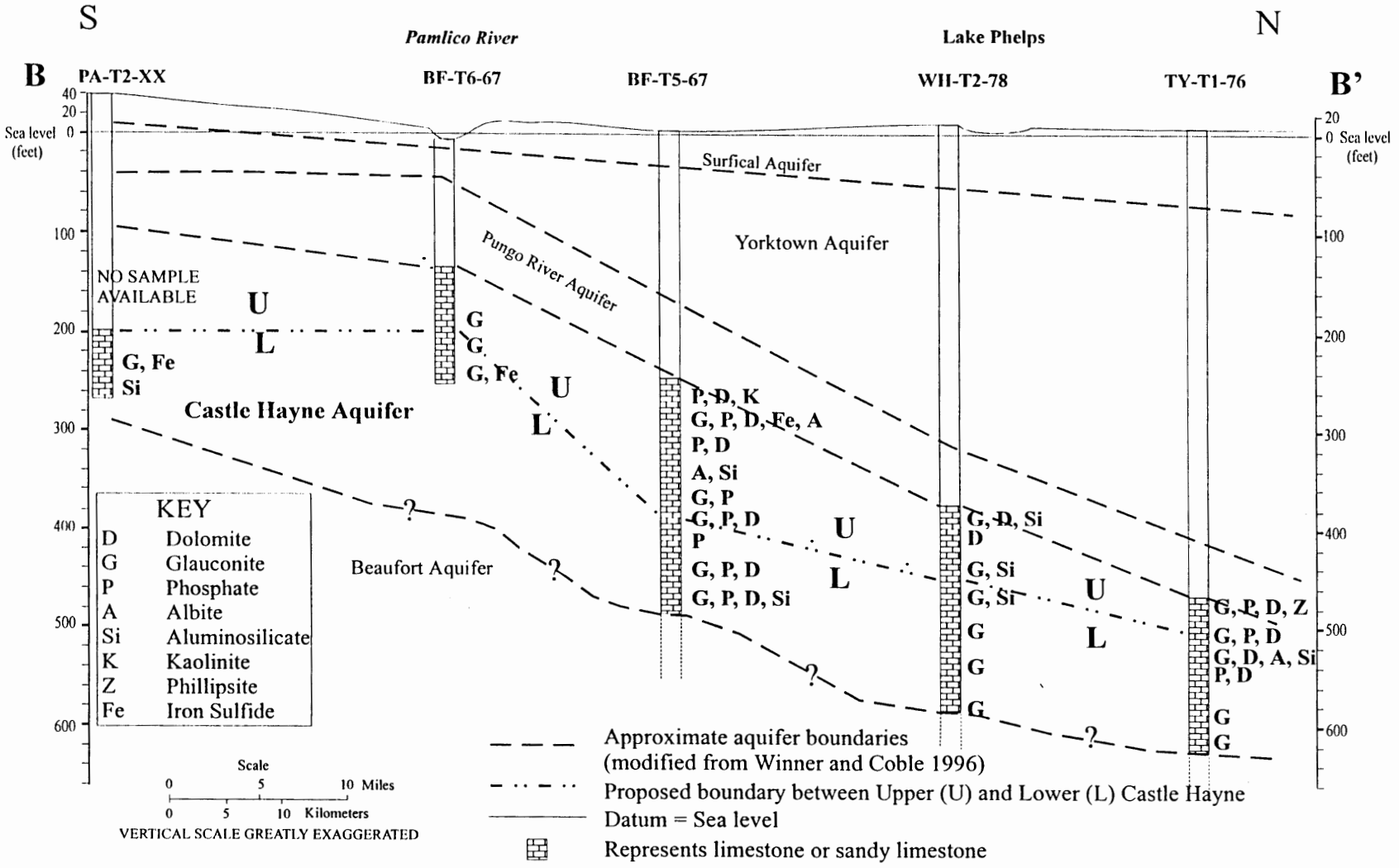

Figure 88. North/south cross-section showing sample locations within the Castle Hayne Limestone. Mineral assemblages indicated were determined from all types of analyses.Pure calcite and quartz are abundant in all wells. (Location of B - B′ shown in Figure 13).

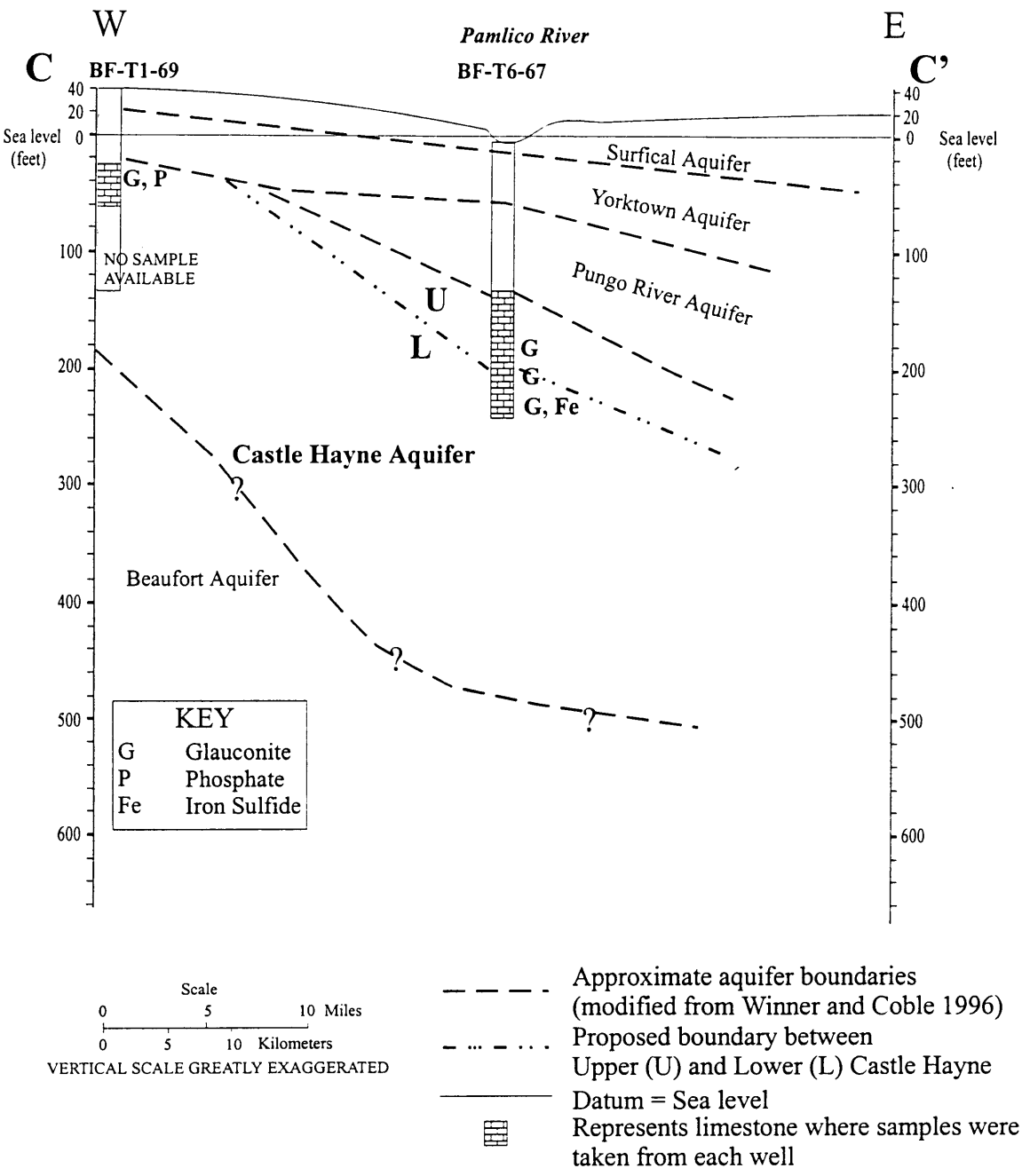

Figure 89. East/west cross-section showing sample locations within the Castle Hayne Limestone. Mineral assemblages indicated were determined from all types of analyses. Pure calcite and quartz are abundant in each well. (Location of C - C' shown in Figure 13).

sulfide, and aluminosilicates (Figures 90-95). The upper part of the CHAS is characterized by sandy, fossiliferous limestone containing glauconite, phosphate, dolomite and minor iron sulfide. The Lower CHAS is also a fossiliferous limestone with accessory phosphate and iron sulfide, but generally contains more abundant glauconite and less dolomite than the Upper CHAS. The lower part of the aquifer is also sandier than the upper part in the eastern section of the study area. Lower CHAS samples were not available for the western part of the study area.

In well BF-T5-67 the aquifer becomes distinctively arenaceous between 380 - 400 feet below sea level, possibly representing the transition between the upper and lower units of the CHAS (Figures 88 and 90). A distinct transition to a sandier lithology is also present in well BF-T6-67 at 200 feet below sea level (Figures 88, 89, and 91) and in well TY-T1-76, the northernmost well, at 500 feet below sea level (Figures 88 and 92). Wells PA-T2-XX (Figures 88 and 93), and WH-T2-78 (Figures 88 and 94) are sandy, in parts, throughout the entire sampled zone. Because the entire sample section of well PA-T2-XX is sandy, it is placed in the Lower CHAS. The transition between the Upper and Lower CHAS in WH-T2-78 is placed at 450 feet below sea level based on the abundance of dolomite in the uppermost section. Samples from well BF-T1-69 are placed in the lower unit based on the abundance of glauconite (Figures 89 and 95).

Dolomite is present at three localities and is most pervasive north of the Pamlico River. Well BF-T5-67 (Figures 88 and 90) has zones of dolomite throughout the CHAS. Wells TY-T1-76 (Figures 88 and 92) and WH-T2-78 (Figures 88 and 94) contain dolomite in the upper part of the aquifer. Glauconite is dispersed throughout the CHAS, but is most abundant in wells WH-T2-78 and BF-T1-69 (Figures 94 and 95). Phosphate is also present in the CHAS and is most abundant in well BF-T5-67 (Figure 90). Two northernmost wells (TY-T1-76 and WH-T2-78) contain the majority of the aluminosilicate minerals in the upper portion of the aquifer (Figures 88, 92, and 94). Aluminosilicate minerals are associated with glauconite, phosphate and dolomite.

X-ray Diffraction

Peak intensities and 2θ angles on XRD patterns were used to identify accessory minerals (e.g., Figure 96). Accessory mineral absence on the XRD pattern does not, however, indicate absence from the sample because of the XRD detection limit. In well WH-T2-78, the CHAS is present from 375-585 feet below sea level (Table 12, Figure 94). XRD analysis detected glauconite only at the base of the aquifer (565-585 feet below sea level).

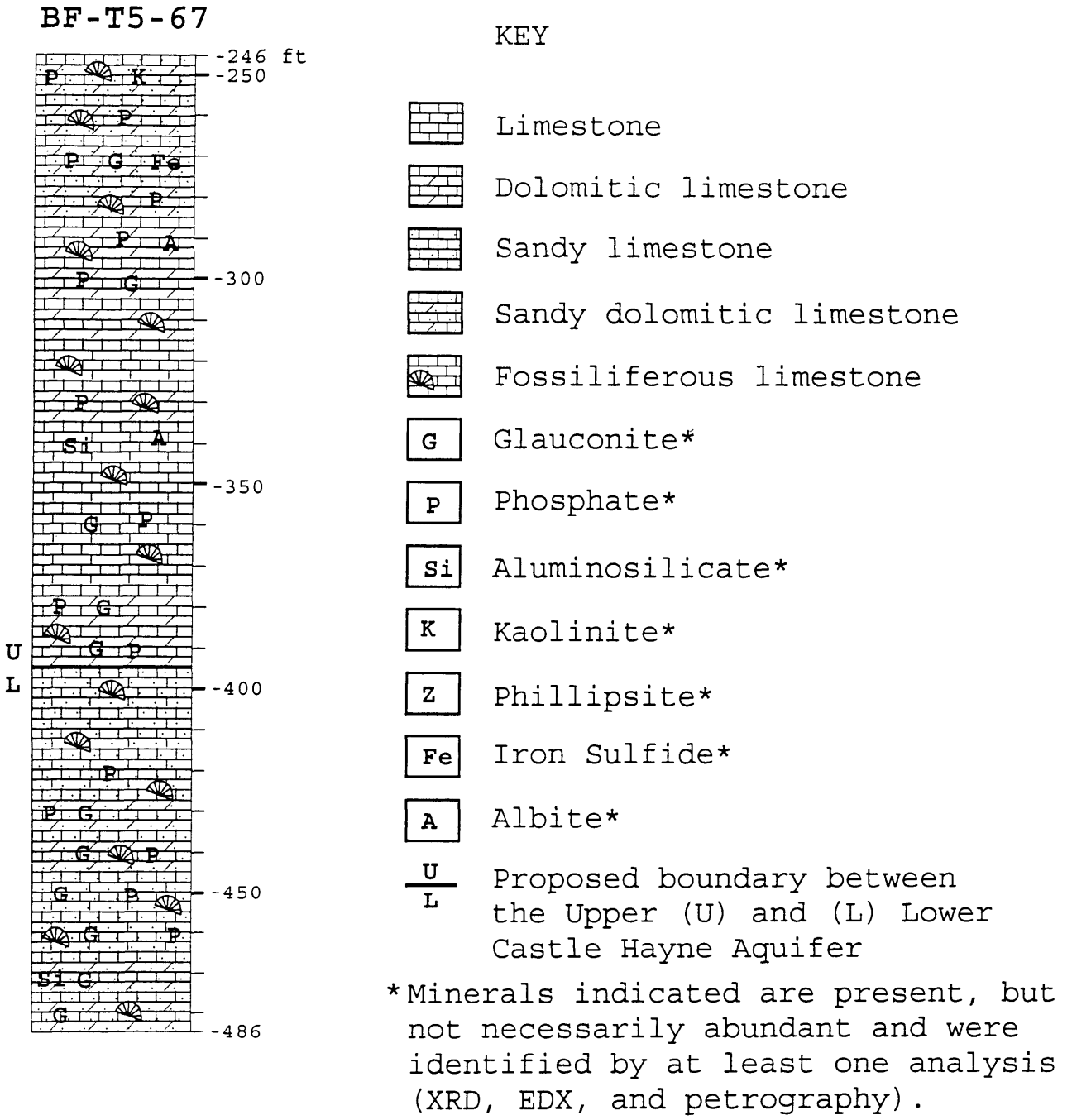

Figure 90. Stratigraphic column for well BF-T5-67. Depths with respect to sea level.

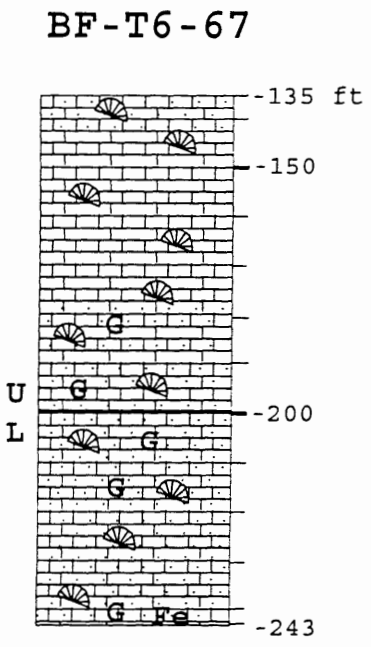

KEY

- Limestone
- Dolomitic limestone
- Sandy limestone
- Sandy dolomitic limestone
- Fossiliferous limestone
- G — Glauconite*
- P — Phosphate*
- Si — Aluminosilicate*
- K — Kaolinite*
- Z — Phillipsite*
- Fe — Iron Sulfide*
- A — Albite*
- U / L — Proposed boundary between the Upper (U) and (L) Lower Castle Hayne Aquifer

*Minerals indicated are present, but not necessarily abundant and were identified by at least one analysis (XRD, EDX, and petrography).

Figure 91. Stratigraphic column for well BF-T6-67. Depths with respect to sea level.

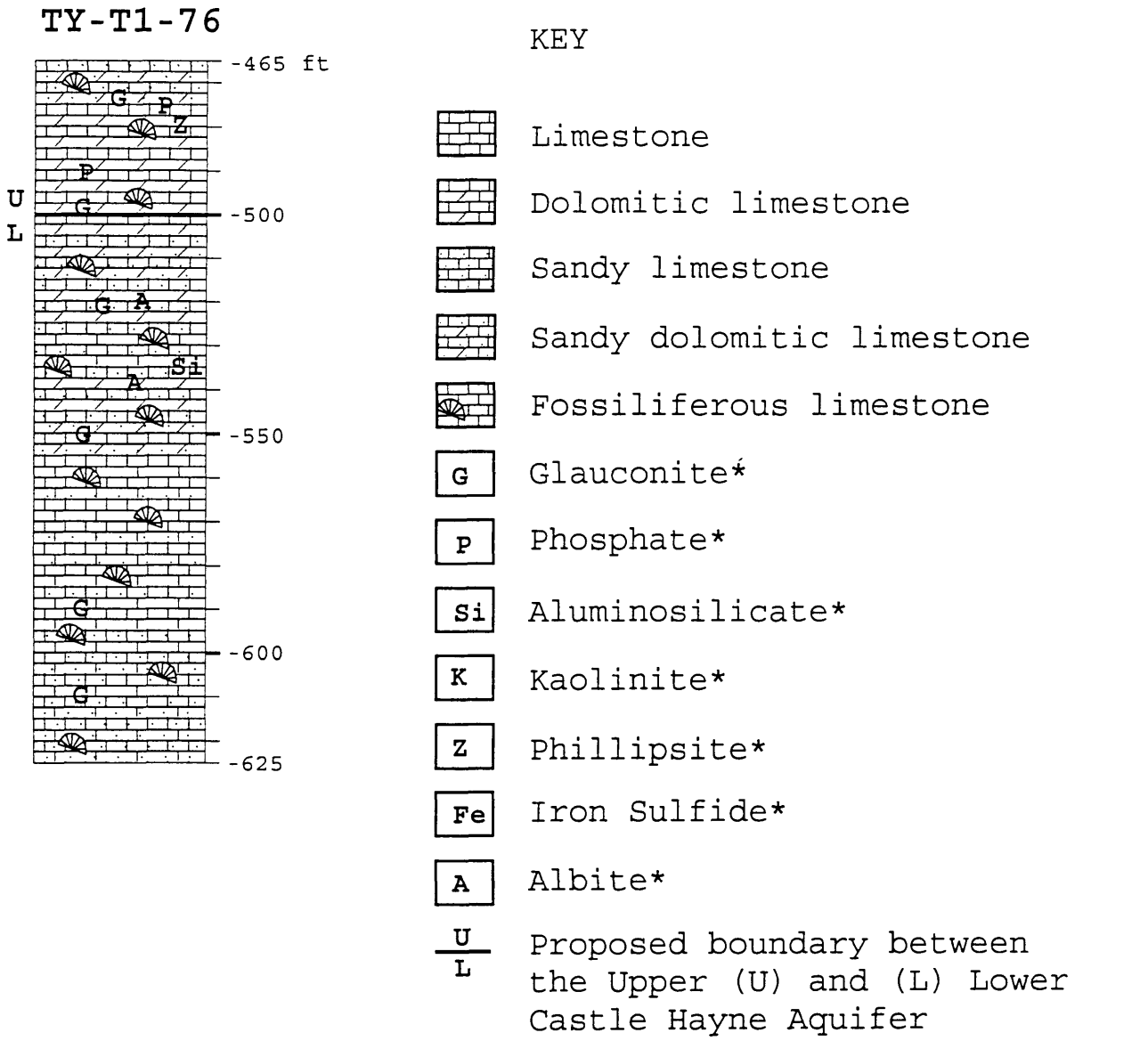

Figure 92. Stratigraphic column for well TY-T1-76. Depths with respect to sea level.

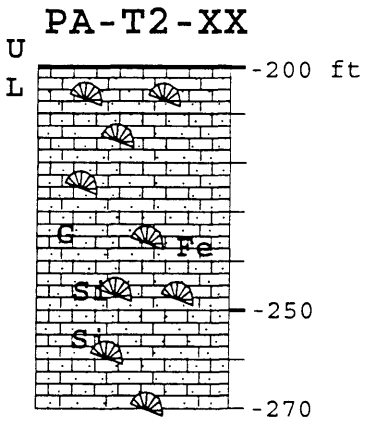

KEY

- Limestone
- Dolomitic limestone
- Sandy limestone
- Sandy dolomitic limestone
- Fossiliferous limestone
- G — Glauconite*
- P — Phosphate*
- Si — Aluminosilicate*
- K — Kaolinite*
- Z — Phillipsite*
- Fe — Iron Sulfide*
- A — Albite*
- U / L — Proposed boundary between the Upper (U) and (L) Lower Castle Hayne Aquifer

*Minerals indicated are present, but not necessarily abundant and were identified by at least one analysis (XRD, EDX, and petrography).

Figure 93. Stratigraphic column for well PA-T2-XX. Depths with respect to sea level.

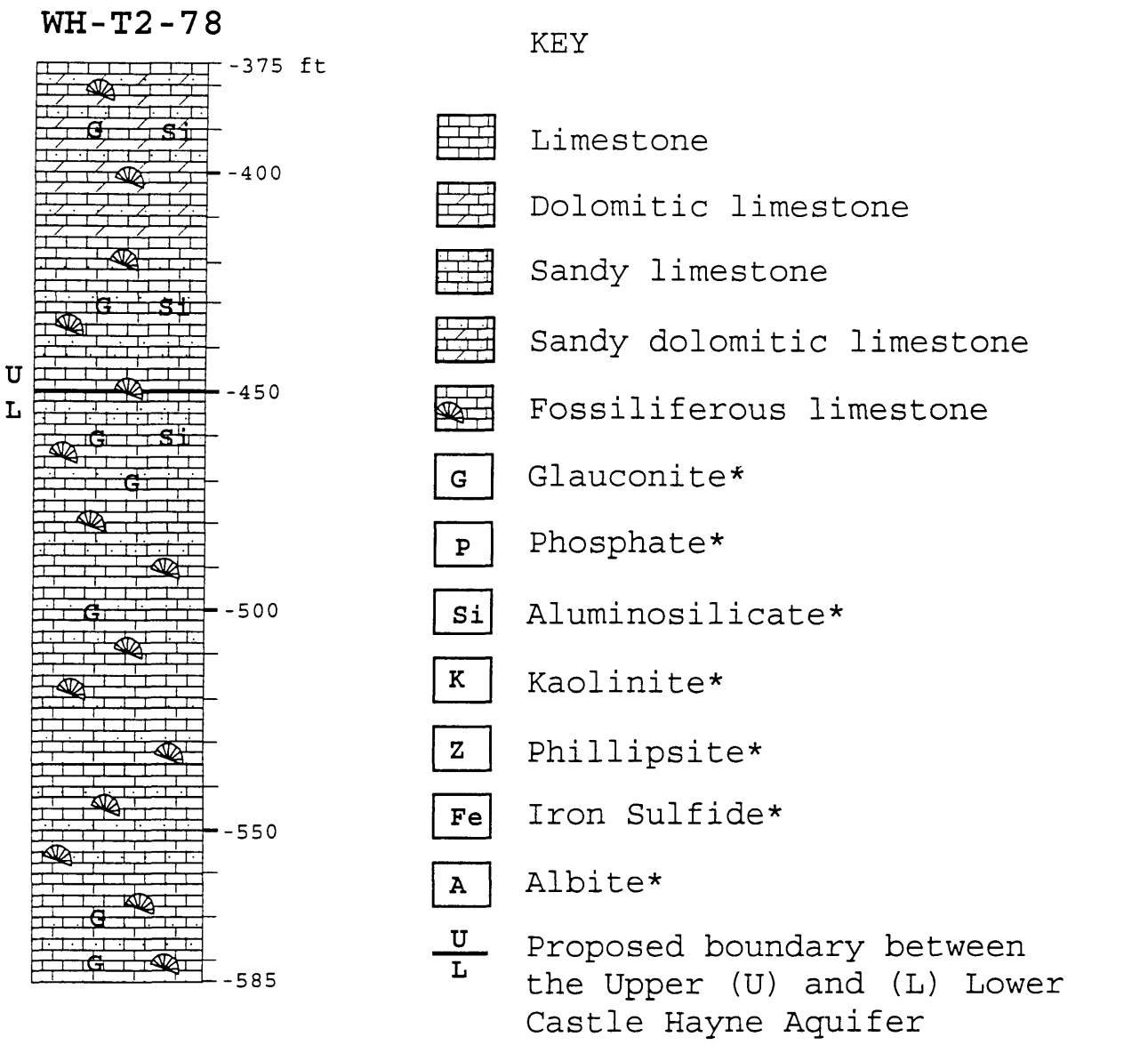

Figure 94. Stratigraphic column for well WH-T2-78. Depths with respect to sea level.

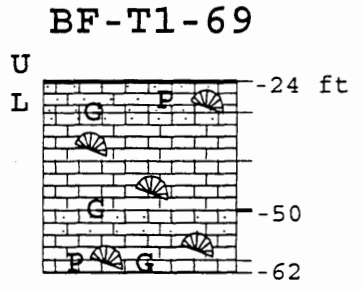

KEY

- Limestone
- Dolomitic limestone
- Sandy limestone
- Sandy dolomitic limestone
- Fossiliferous limestone
- G — Glauconite*
- P — Phosphate*
- Si — Aluminosilicate*
- K — Kaolinite*
- Z — Phillipsite*
- Fe — Iron Sulfide*
- A — Albite*
- U / L — Proposed boundary between the Upper (U) and (L) Lower Castle Hayne Aquifer

*Minerals indicated are present, but not necessarily abundant and were identified by at least one analysis (XRD, EDX, and petrography).

Figure 95. Stratigraphic column for well BF-T1-69. Depths with respect to sea level.

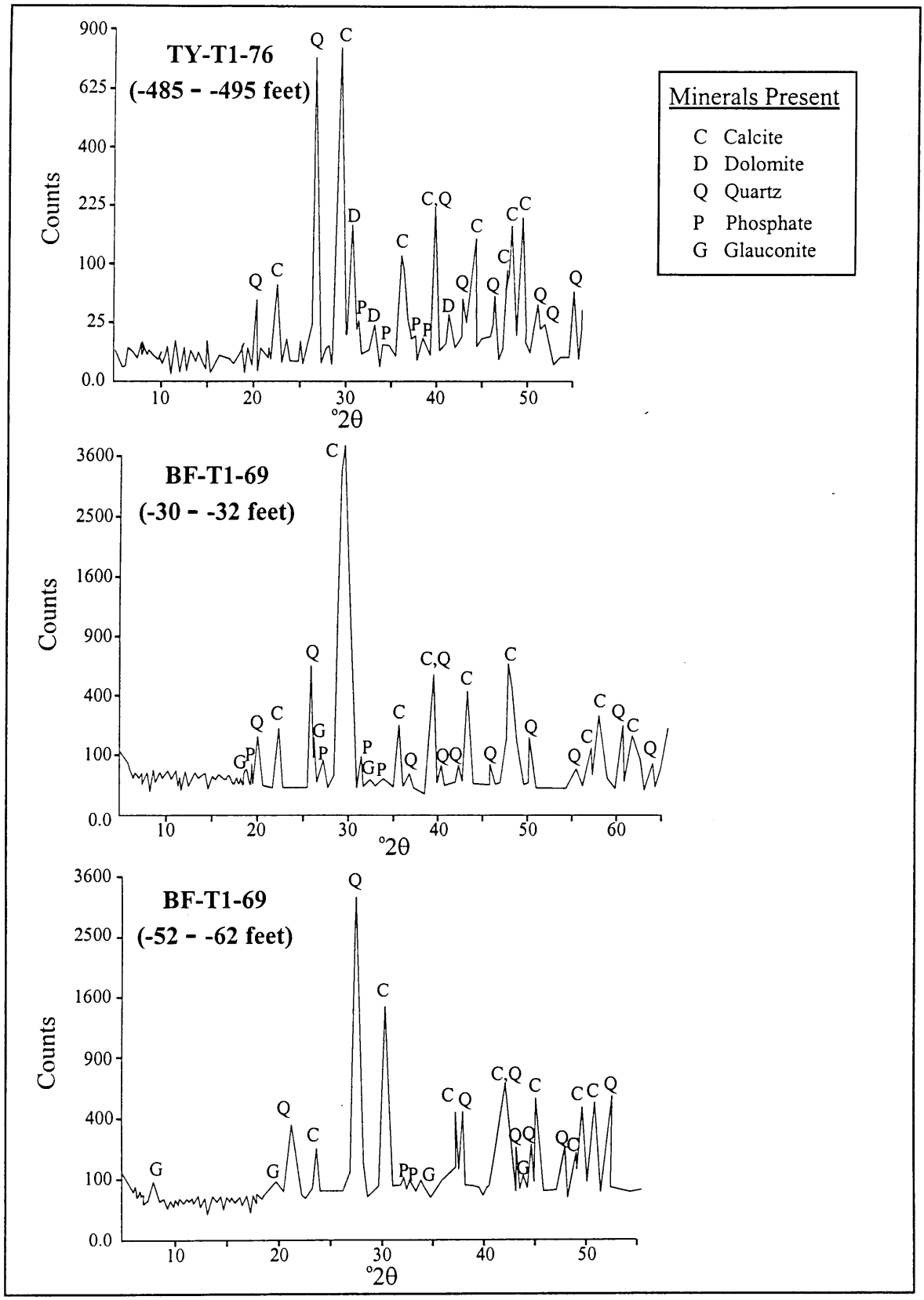

Figure 96. XRD patterns from wells TY-T1-76 and BF-T1-69.

Table 12. XRD Data for Well WH-T2-78.

MINERALS IDENTIFIED				
Depth (feet)	Calcite	Dolomite	Quartz	Glauconite
375-385	X	X	X	
385-395	X	X	X	
395-405	X	X	X	
405-415	X	X	X	
415-425	X		X	
425-435	X		X	
435-445	X		X	
445-455	X		X	
455-465	Lo Mg		X	
465-475	X		X	
475-485	X		X	
485-495	X		X	
495-505	X		X	
505-515	X		X	
515-525	X		X	
525-535	X		X	
535-545	X		X	
545-555	X		X	
555-565	X		X	
565-575	X		X	X
575-585	X		X	X

Table 13. XRD Data for Well TY-T1-76.

MINERALS IDENTIFIED						
Depth (feet)	Calcite	Dolomite	Quartz	Phosphate minerals	Albite	Phillipsite
465-475	X	X	X	X		
475-485	X	X	X	X		X
485-495	X	X	X	X		
495-505	X	X	X	X		
505-515	X	X	X			
515-525	X	X	X		X	
525-535	X		X			
535-545	X		X		X	
545-555	X		X			
555-565	X		X			
565-575	X		X			
575-585	X		X			
585-595	X		X			
595-605	X		X			
605-615	X		X			
615-625	X		X			

Dolomite is present in relatively high abundance from 375-415 feet below sea level. In several additional intervals from this well, peaks that may correspond to either glauconite, dolomite, phosphate, phillipsite (zeolite), or albite were observed. Due to the low intensities of additional distinguishing peaks, these minerals could not be listed in Table 12 with confidence.

The CHAS occurs between 465-625 feet below sea level in well TY-T1-76 (Table 13, Figure 92) and dolomite is pervasive in the upper part (465-555 feet below sea level) of the aquifer. Phosphate minerals are present throughout many intervals of the aquifer, but are most abundant between 465-505 feet below sea level (Figure 92). Albite is present at 515-545 feet below sea level and phillipsite is present at 475-485 feet below sea level.

In well BF-T5-67, the CHAS occurs from 246-486 feet below sea level (Table 14). Dolomite is present in both the upper and lower portions of the aquifer (between 246-336, 376-396, and 426-486 feet below sea level) and phosphate minerals are pervasive throughout. Glauconite is detectable only in the lower portion of the aquifer (between 436-486 feet below sea level) and in the 466-476 interval, there is one peak that could correspond to either dolomite or phosphate. Due to the low intensities of additional distinguishing peaks these minerals could not be listed in Table 14 with confidence. Well BF-T1-69 contains a portion of the lower CHAS between 24-62 feet below sea level (Figure 89). Glauconite and phosphate were detected between 30-62 feet below sea level (Table 15, Figure 95).

Mineral Chemistry

Mineral chemistry was studied using an HNU Systems EDX unit attached to a Phillips SEM. No semi-quantitative analysis was performed on the 250 to 300 pure calcium carbonate or quartz grains for which spectra were collected. Semi-quantitative analysis of 147 glauconite, 48 phosphate, 23 Mg carbonate, 9 aluminosilicate, and 5 iron sulfide grains was conducted and total Fe is reported as Fe_2O_3 for glauconite. The EDX system is unable to distinguish between Fe^{3+} and Fe^{2+}. In order for this EDX system to detect a particular oxide, the oxide must be present in amounts of at least 0.1 wt.%. The EDX system cannot detect or identify elements lighter than Na.

Statistical Analysis of EDX Standards. The ZAP standardless analysis program was used for all standards and samples, which were analyzed from 0 to 10KeV for 200 seconds of Live Time. Each standard was analyzed ten times to evaluate the accuracy and precision of the system (Table 16). Based on the standard

Table 14. XRD Data for Well BF-T5-67.

MINERALS IDENTIFIED							
Depth (feet)	Calcite	Dolomite	Quartz	Phosphate minerals	Kaolinite	Albite	Glauconite
246-256	X	X	X	X	X		
256-266	X	X	X	X			
266-276	X	X	X	X			
276-286	X	X	X	X			
286-296	X	X	X	X			
296-306	X	X	X	X		X	
306-316	X	X	X				
316-326	X		X				
326-336	X	X	X				
336-346	X		X			X	
346-356	X		X				
356-366	X		X	X			
366-376	X		X	X			
376-386	X	X	X	X			
386-396	X	X	X	X			
396-406	X		X				
406-416	NO	SAMPLE		NO SAMPLE			
416-426	X		X	X			
426-436	X	X	X	X			
436-446	X	X	X	X			X
446-456	X		X	X			
456-466	X	X	X	X			X
466-476	X		X				X
476-486	X	X	X				X

Table 15. XRD Data for Well BF-T1-69.

MINERALS IDENTIFIED				
Depth (feet)	Calcite	Glauconite	Quartz	Phosphate minerals
30-32	X	X	X	X
52-62	X	X	X	X

Table 16. Statistical analysis of EDX standards.

Mineral	Oxide/Carbonate	Accepted Value[1]	Mean[2]	Standard Deviation[3]	Accuracy %[4]
Albite	Na_2O	11.59	7.97	1.35	-31
	Al_2O_3	19.54	19.88	0.61	2
	SiO_2	68.52	72.11	1.85	5
	K_2O	0.22	0.04	0.03	-82
	CaO	0.13	0.14	0.13	8
Apatite	CaO	55.81	61.11	2.11	9
	P_2O_5	42.39	40.62	6.61	-4
Biotite	Al_2O_3	15.13	17.60	1.37	16
	SiO_2	38.72	45.82	2.78	18
	K_2O	9.91	9.26	0.48	-7
	CaO	0.10	0.44	0.31	340
	MgO	19.52	18.62	1.24	-5
	TiO_2	1.77	1.16	0.52	-34
	MnO	0.04	1.46	0.90	3550
	FeO	10.72	6.92	1.34	-35
	H_2O	4.11	0.0	0.0	-100
Chlorite	Al_2O_3	18.08	23.33	0.55	29
	SiO_2	30.04	39.81	0.74	33
	CaO	0.03	0.0	0.0	-100
	MgO	33.51	33.65	0.57	0
	FeO	3.31	1.94	0.83	-41
	NiO	0.24	0.0	0.0	-100
	Cr_2O_3	0.98	1.28	0.61	31
	H_2O	13.76	0.0	0.0	-100
	CO_2	0.07	0.0	0.0	-100
	F	0.02	0.0	0.0	-100
Dolomite	$CaCO_3$	54.00	51.25	0.59	-5
	$MgCO_3$	46.00	48.75	0.59	6
Plagioclase	Na_2O	4.35	2.65	1.09	-39
	Al_2O_3	28.53	29.17	0.39	2
	SiO_2	54.21	57.35	1.28	6
	K_2O	0.41	0.25	0.16	-39
	CaO	11.80	9.45	0.63	-20
	MgO	0.13	0.94	0.55	623
	TiO_2	0.07	0.0	0.0	-100
	FeO	0.37	0.8	0.32	116

1. Values given in weight percent oxide
2. Average of 10 analyses of each standard analysis
3. Standard deviation of 10 standard analyses
4. Accuracy = [(Mean - Accepted Value)/Mean] x 100

deviation of these analyses, the HNU Systems unit is quite precise, although analyses of sheet silicates, such as clays and micas, are not as good as those of feldspars. In addition, the quality of EDX analyses of sheet silicates is degraded because the edges of mica and clay books are difficult to polish. The system underestimates Fe and overestimates Al and Si in the biotite and chlorite standards (Table 16), which partially explains why some clay analyses did not appear to meet the chemical criteria for glauconite (Fe^{3+}>>Al). Glauconite analyses may be as much as 3-9 wt.% high for SiO_2 and Al_2O_3 and 1.5-4 wt.% low for Fe_2O_3 (APPENDIX E is available from the first author and WRRI). The values determined for mol% of the $CaCO_3$ and $MgCO_3$ end-members could be as much as 3 mol% low for $CaCO_3$ and 2 mol% high for $MgCO_3$. In summary, these EDX analyses give only a semi-quantitative indication of mineral chemistry, but are useful for indicating compositional variation from well to well and from top to bottom of each well. Such analyses also provide adequate chemical information for constructing future geochemical models of the interactions between groundwater and aquifer materials.

Glauconite Chemistry. In 1978, the Association Internationale Pour l'Etude des Argiles (AIPEA) Nomenclature Committee recommended the following definition of glauconite: "Glauconite is defined as an Fe-rich dioctahedral mica with tetrahedral Al (or Fe^{3+}) usually greater than 0.4 atoms per formula unit and octahedral R^{3+} correspondingly greater than 2.4 atoms (Buckley et al. 1978, Bailey 1980). A generalized formula is:

(octahedral) (tetrahedral)

$$K_2 \ (R^{+3}_{2.66} \ R^{+2}_{1.34}) \ (Si_{7.34} \ Al_{0.66}) \ O_{20} \ (OH)_2$$

with $R^{+3} = Fe^{3+} >> Al$ and $R^{+2} = Mg >> Fe^{2+}$ ..." (Odom 1984, p.546). Many of the green peloids and internal molds analyzed meet these criteria. Glauconite is present in all six of the wells at various depths and abundance and 147 grains were analyzed (APPENDIX E). Future statistical evaluation of these 147 glauconite analyses will assess the significance of chemical trends suggested below.

At this point in the study, evaluation of glauconite chemistry in the CHAS focuses on the changing proportions of Al, Fe, and Mg in the octahedral site. Glauconite samples analyzed range from 10-75 mol% Al, 10-65 mol% Fe, and 0-50 mol% Mg in the octahedral site (Figure 97). Potassium was the only large, univalent cation detected. In general, octahedral Mg shows less variability than Al or Fe; however, peloids have a wider variability than the internal mold glauconite. The low-Mg outliers are all peloids.

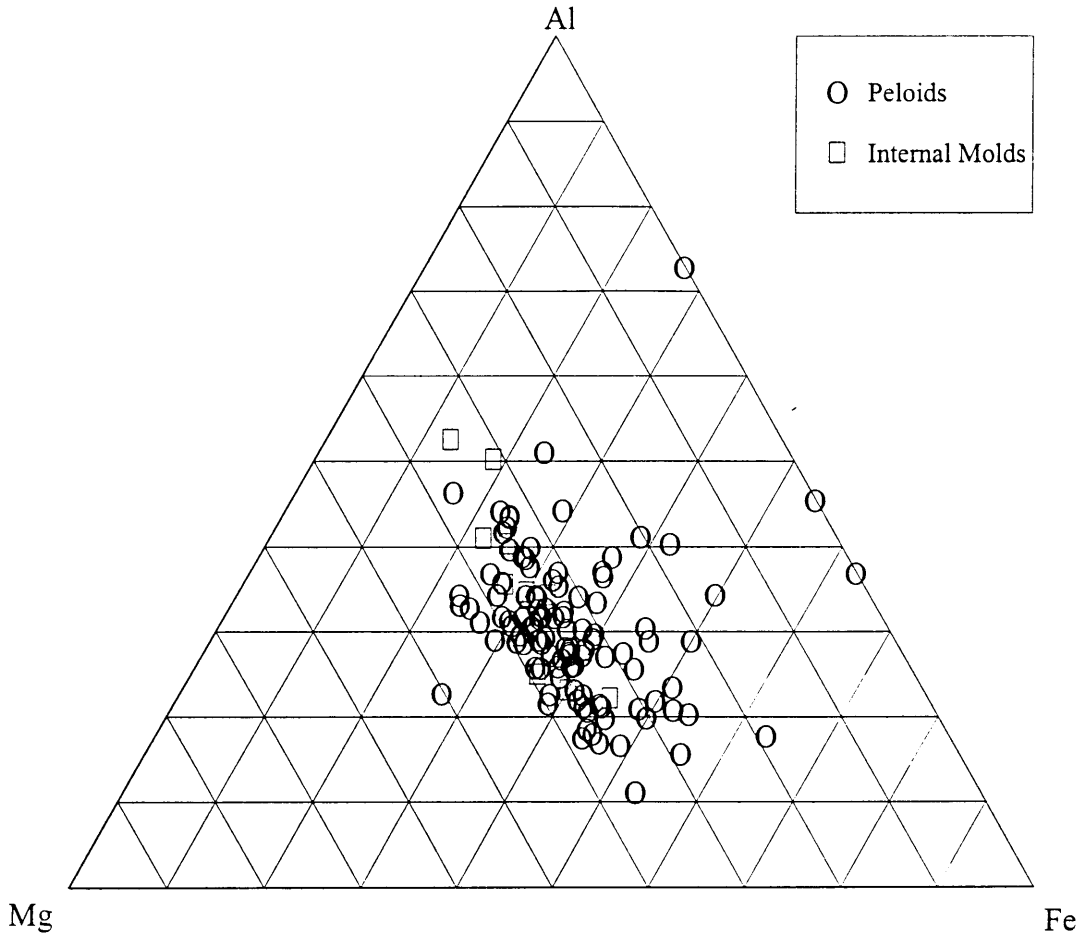

Figure 97. Ternary diagram for glauconite analyses.

Figure 98 illustrates variations in glauconite chemistry throughout the study area by portraying data for each well on a separate ternary diagram. The glauconite chemistry of PA-T2-XX is not discussed because only one glauconite grain was analyzed. This grain occurred at 231 feet below sea level and had 24, 43, and 44 mol% of octahedral Fe, Al, and Mg, respectively. In the other wells average Fe appears to decrease from southwest to northeast as the maximum and minimum mole percents of Fe decrease. Average Al seems to increase from southwest to northeast and the mol% Mg is less variable ranging from 30-40 mol%. Wells BF-T1-69 and BF-T6-67 along the west-east cross-section (Figure 89) mainly contain core from the Upper CHAS. Iron contents of glauconite grains are significantly higher in the western well (BF-T6-67). Magnesium contents are very similar throughout both cores. The statistical significance of these geographic variations will be evaluated by a future study.

Carbonate Chemistry. Hundreds of carbonate spectra revealed pure calcium carbonate and only 21 dolomite and two low-Mg calcite grains (Table 17). In wells TY-T1-76 and BF-T5-67 dolomite is found with low-Mg calcite. In the northernmost well, TY-T1-76 (Figure 88), dolomite occurs with glauconite in the upper part of the core (Figure 92).

Phosphate Chemistry. Phosphate minerals are present as peloids in three wells within the study area (Table 18). Phosphate is most abundant in well BF-T5-67 where it is found with glauconite and iron sulfide (Figure 90). Well TY-T1-76 has intervals containing both phosphate and dolomite (Figure 92). In well BF-T1-69, the westernmost and shallowest (Figure 98), phosphate occurs with glauconite (Figure 95).

Iron Sulfide Chemistry. An iron sulfide mineral was found at three locations (Table 19). It occurs with glauconite in well BF-T6-67 and in the presence of phosphate and glauconite in well BF-T5-67 (Figure 98).

Aluminosilicate Chemistry. Aluminosilicate minerals, most likely zeolites (phillipsite) and/or feldspar were found in four of the wells sampled (Table 20). In well WH-T2-78, two aluminosilicates are present in a vein, as replacement surrounding the vein, and as sub-rounded clasts. They are present with glauconite in the upper portion of the CHAS in well WH-T2-78 (Figure 94). In well TY-T1-76, an aluminosilicate mineral (well-rounded clasts) is present with dolomite and phosphate (Figure 92). Aluminosilicate clasts are found with either phosphate or glauconite in well BF-T5-67 (Figure 90). Well PA-T2-XX contains aluminosilicate clasts with only quartz and calcite (Figure 93).

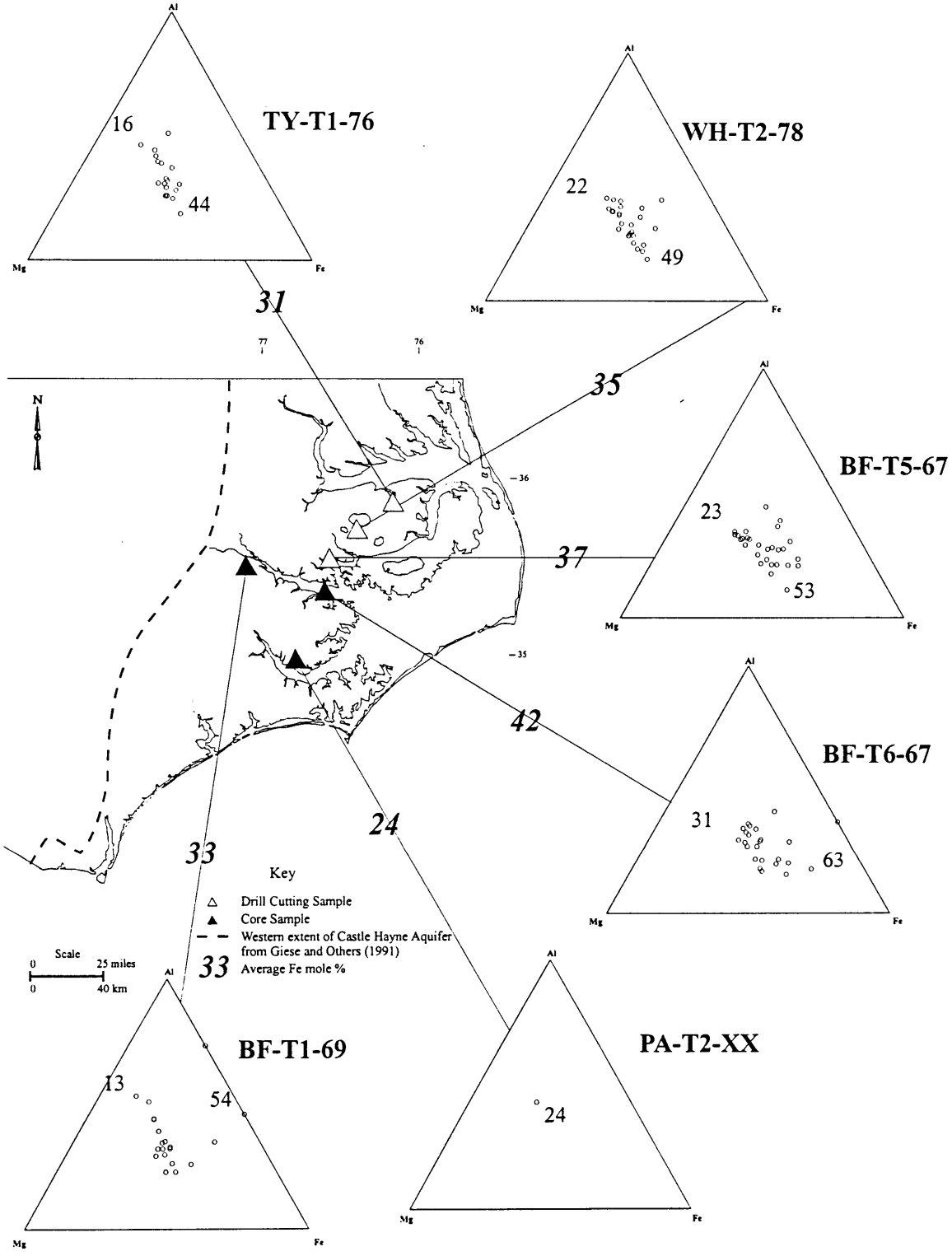

Figure 98. Geographic variation of Fe in glauconite. (Small numbers in triangles represent high and low mole percent values for Fe).

Table 17. EDX analyses of carbonate minerals.

		Mole %	
Sample	Depth (feet)	$CaCO_3$	$MgCO_3$
B1-unkn5	465-475	53	47
B1-unkn7		54	46
B1-unkn8		56	44
B2-unkn6	485-495	57	43
B2-unkn7		54	46
B2-unkn8		53	47
B2-unkn9		53	47
B2-unkn10		50	50
B2-unkn11		52	48
B3-unkn11	495-505	53	47
B3-unkn12		53	47
B4-unkn5	515-525	51	49
B4-unkn6		51	49
B4-unkn7		53	47
B6-unkn2	545-555	93	7
C10-unkn9	246-256	54	46
C10-unkn10		55	45
C11-unkn9	296-306	51	49
C3-unkn1	306-316	48	52
C3-unkn2		52	49
C3-unkn7		51	49
C6-unkn1	376-386	99	1
C6-unkn2		56	44

B = Well TY-T1-76
C = Well BF-T5-67

Table 18. EDX analyses of phosphate minerals.

Sample	Depth (feet)	P_2O_5	CaO
B1-unkn1	465-475	36	64
B1-unkn2		35	65
B1-unkn3		35	65
B1-unkn4		35	65
B2-unkn1	485-495	32	68
B2-unkn2		30	70
B2-unkn3		34	66
B2-unkn4		35	66
B2-unkn5		31	69
B3-unkn1	495-505	36	64
B3-unkn2		34	66
B3-unkn8		35	65
B3-unkn9		34	66
B3-unkn10		35	65
C10-unkn1	246-256	35	65
C10-unkn2		33	67
C10-unkn3		35	65
C10-unkn4		37	63
C10-unkn5		35	65
C10-unkn6		35	65
C10-unkn7		34	66
C10-unkn8		33	67
C2-unkn1	266-276	35	65
C11-unkn4	296-306	34	66
C11-unkn6		33	67
C11-unkn8		35	65
C11-unkn4		34	66
C11-unkn6		33	67
C11-unkn8		35	65
C3-unkn3	306-316	34	66
C3-unkn4		34	66
C3-unkn5		34	66
C3-unkn6		35	65
C4-unkn2	326-336	34	66
C5-unkn1	336-346	35	65
C5-unkn2		31	69
C5-unkn3		36	64
C12-unkn1	356-366	32	63
C7-unkn1	386-396	33	67
C7-unkn2		34	66
C7-unkn3		33	67
C7-unkn4		30	70
C7-unkn6		31	62
C7-unkn7		32	64
C9-unkn2	446-456	33	67
D1-unkn5	24-30	38	62
D5-unkn5	52-62	37	63

Note: Values given in weight percent oxide

B = TY-T1-76

C = BF-T5-67

D = BF-T1-69

Table 19. EDX analyses of iron sulfide.

Sample	Depth (feet)	Fe	S
C2-unkn8	266-276	48	52
C2-unkn9		52	48
C2-unkn10		53	47
E3-unkn1	231-240	52	48
F6-unkn10	238-243	44	56

Note: Values given in weight percent element

C = Well BF-T5-67 F = Well BF-T6-69

E = Well PA-T2-XX

Table 20. EDX analyses of aluminosilicates.

	A1-unkn1	A3-unkn4	A3-unkn5	A2-unkn1	A2-unkn2	A2-unkn3	A2-unkn4	A2-unkn5	C1-unkn3	B5-unkn1	C5-unkn4	B5-unkn2	B5-unkn3	B5-unkn4	B5-unkn5	E4-unkn1
SiO_2	50	49	48	56	61	58	62	62	65	72	71	75	74	73	72	74
Al_2O_3	39	33	33	23	18	21	19	18	18	12	13	4	7	6	9	8
MgO		6	6	5	5	5	5	5	5			5	5	5	5	5
CaO	5	3	4	3	5	4	4	4	4	5	5	5	5	5	4	3
Na_2O	7	8	8	10	10	10	9	10	9	11	11	11	10	11	10	11
K_2O		1	1	1	1	1	1	1	0					1	1	
Cl_2O				2	0	1										
Total	100	100	100	100	100	100	100	100	100	100	100	100	100	100	100	100
	# of ions on the basis of 32 O equivalents, ignoring H_2O															
Si	9	9	9	10	11	11	11	11	11	13	13	13	13	13	13	13
Al	8	7	7	5	4	4	4	4	4	2	3	1	1	1	2	2
Mg		2	2	1	1	1	1	1	1			1	1	1	2	
Na	2	3	3	3	3	3	3	3	3	4	4	4	3	4	3	4
Ca	1	1	1	1	1	1	1	1	1	1	1	1	1	1	1	1
K		0	0	0	0	0	0	0	0					0	0	
Cl				0	0	0										

Note: Values given in weight percent oxide

A = Well WH-T2-78 C = Well BF-T5-67

B = Well TY-T1-76 E = Well PA-T2-XX

DISCUSSION

The discussion that follows focuses on groundwater geochemistry of the U-CHAS because data for this aquifer are most abundant. The study of the groundwater chemistry of the Yorktown and Peedee Aquifers is in its early stages so the results presented earlier will not be discussed, but will be mentioned where they impact on analysis of the groundwater geochemistry of the U-CHAS. The discussion section begins with a preliminary evaluation of the mineralogical and lithological data collected on the Castle Hayne Formation because its mineral chemistry significantly affects its water chemistry.

CASTLE HAYNE MINERAL CHEMISTRY AND LITHOLOGY

Glauconite Chemistry

Granular peloids and internal molds of bioclasts are the two morphologic types of glauconite observed in the CHAS within the study area. According to Odin and Fullagar (1988), fecal pellets are the predominate substrate on which glauconitization occurs. The verdissment (greening as a sign of maturity) seems to occur by infilling of the diffuse pores of the pellet with green clays. The origin of internal molds is unclear and it is not known whether green clays directly fill the voids of bioclast tests or if glauconite replaces the previous clay-size material that filled the chambers (Odin and Fullagar, 1988).

Glauconite analyses show a negative linear relationship between octahedral Al and Fe (Figure 99a) in agreement with the observations of Weaver and Pollard (1975), who explained that the major substitution in the octahedral site is between Fe and Al. Octahedral Fe and Al show no obvious correlation with octahedral Mg (Figures 99b and 99c). There is a weak positive correlation between octahedral and tetrahedral Al and between K and Si (Figures 99d and 99e). Octahedral Mg shows a weak inverse correlation with K, which may reflect cation exchange between clays and groundwater (Figure 99f).

For wells TY-T1-76, BF-T5-67, BF-T1-69, and BF-T6-67 (Figure 98), Al increases initially with depth in the uppermost part of the Upper CHAS as Fe decreases (Figures 100-103). Well WH-T2-78 is the only well where Al initially decreases with depth as Fe increases (Figure 104). Below this interval in well WH-T2-78, there is less variability of Al and Fe with depth than in the other wells. Wells BF-T1-69 and BF-T6-67 are along an east-west line through the study area and are approximately twenty miles apart (Figures 89, 102 and 103). Both of these wells sample mainly the upper portions of the CHAS and data indicate that the magnesium content changes very little with depth in the two

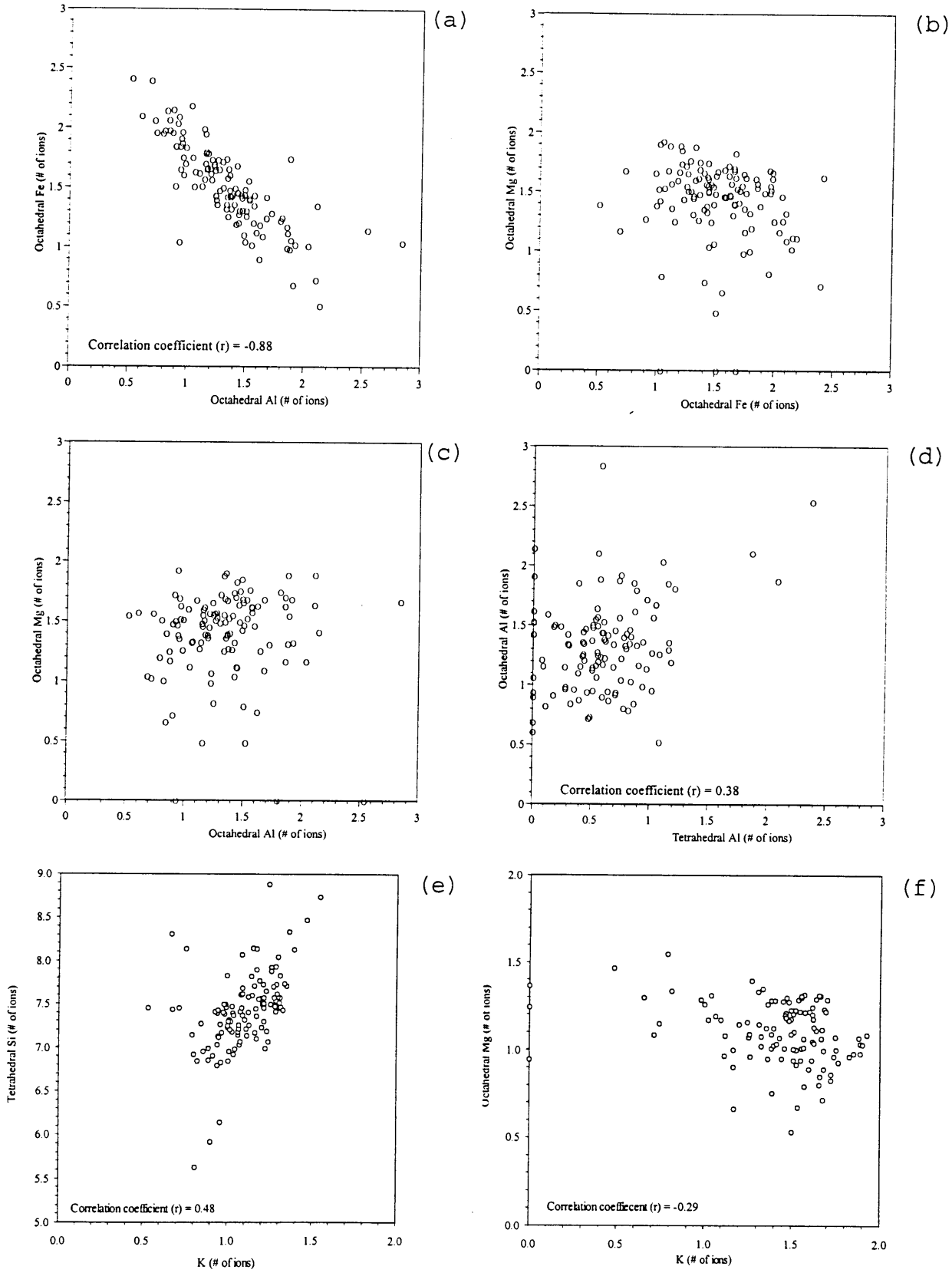

Figure 99. Comparative distribution of ions in glauconite.

TY-T1-76

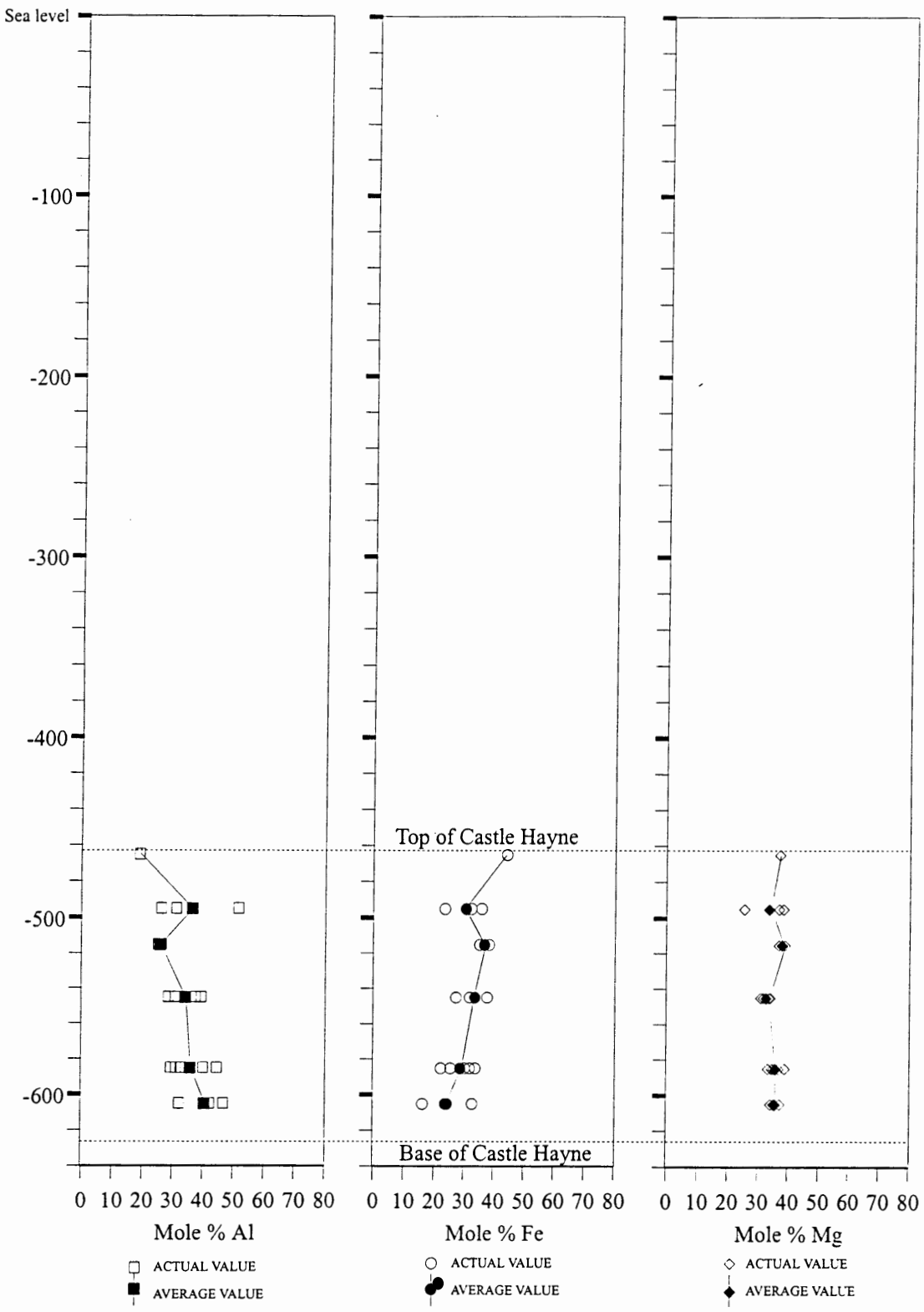

Figure 100. Mole % of octahedral Al, Fe, and Mg vs. depth in well TY-T1-76.

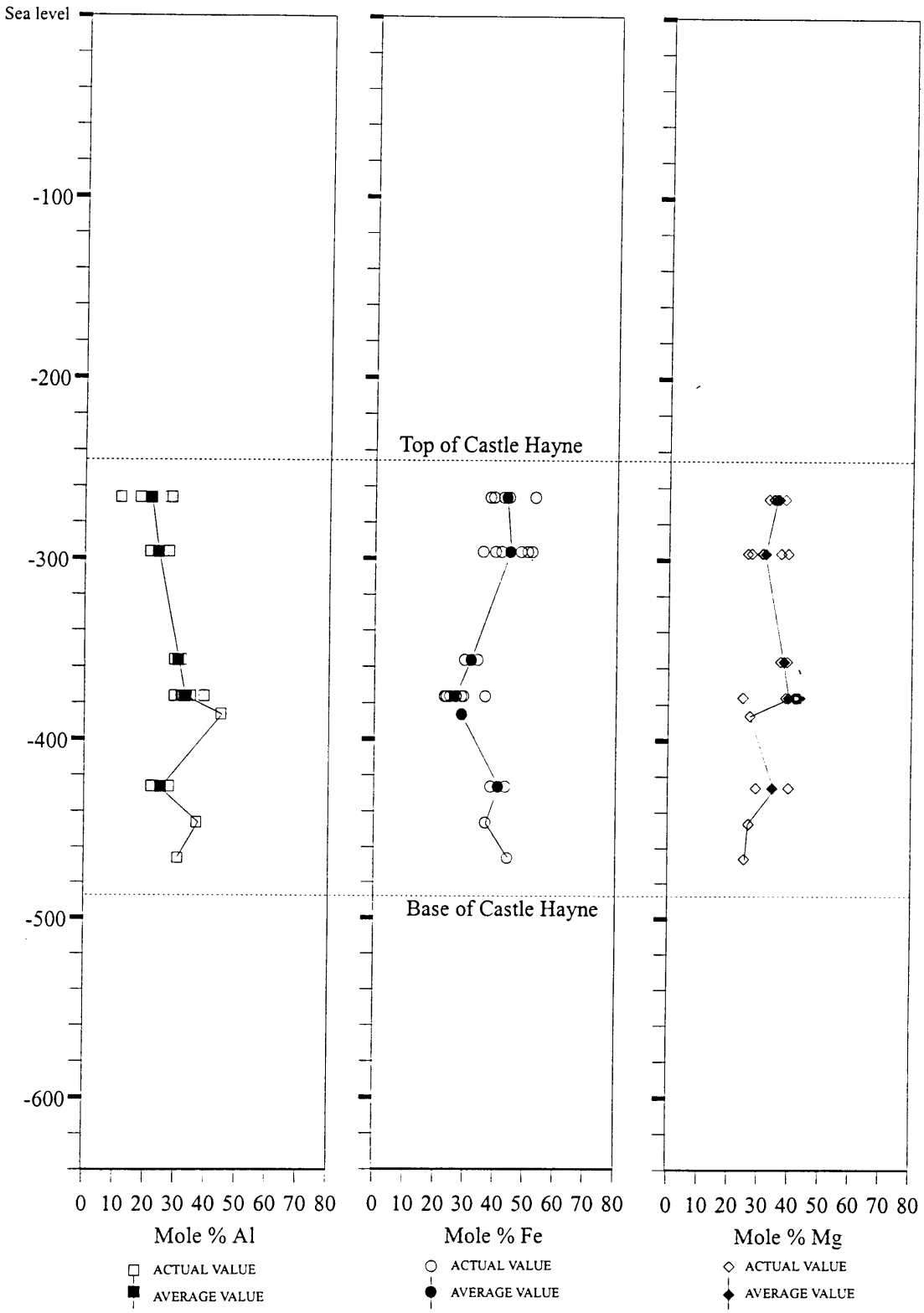

Figure 101. Mole % of octahedral Al, Fe, and Mg vs. depth in well BF-T5-67.

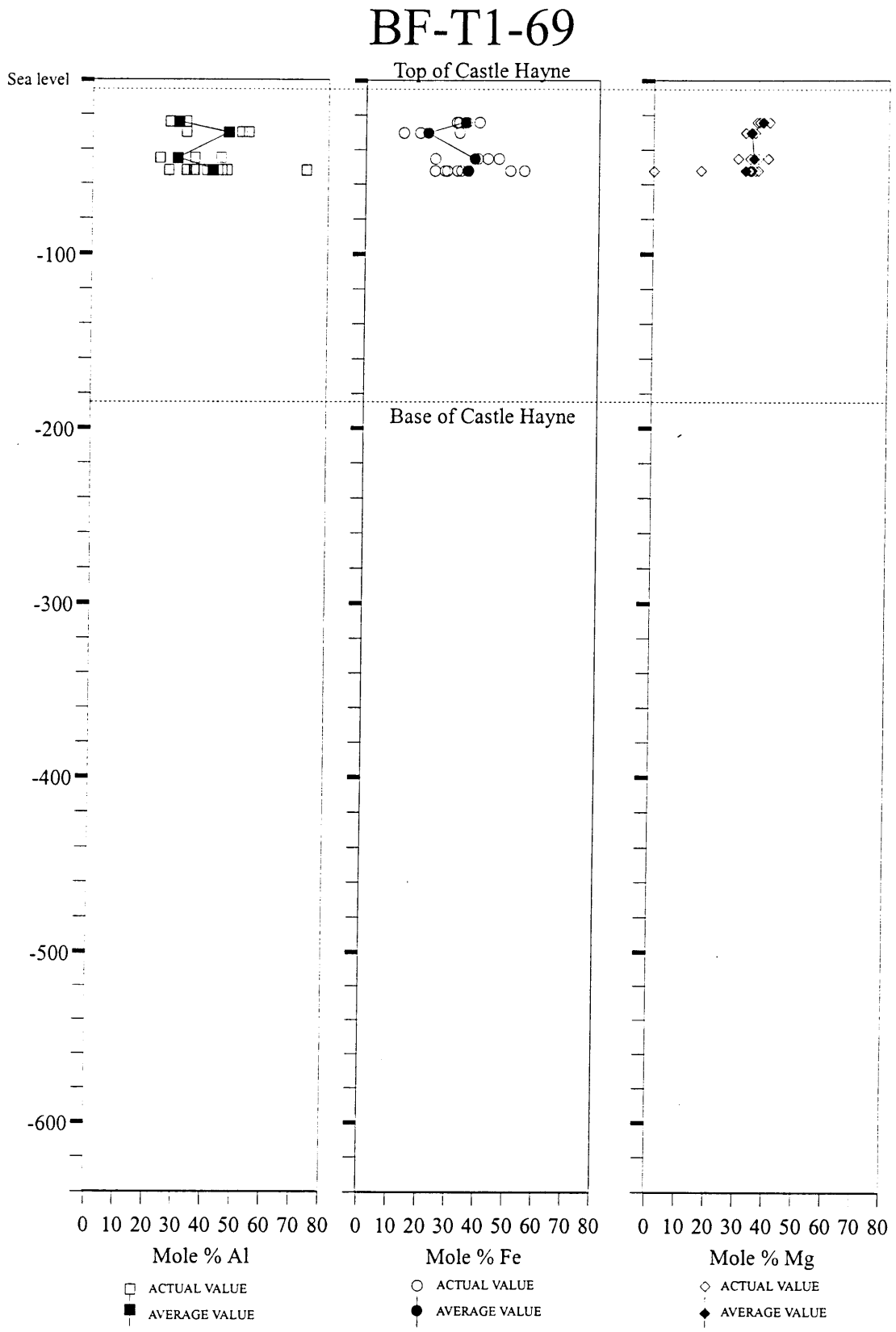

Figure 102. Mole % of octahedral Al, Fe, and Mg vs. depth in well BF-T1-69.

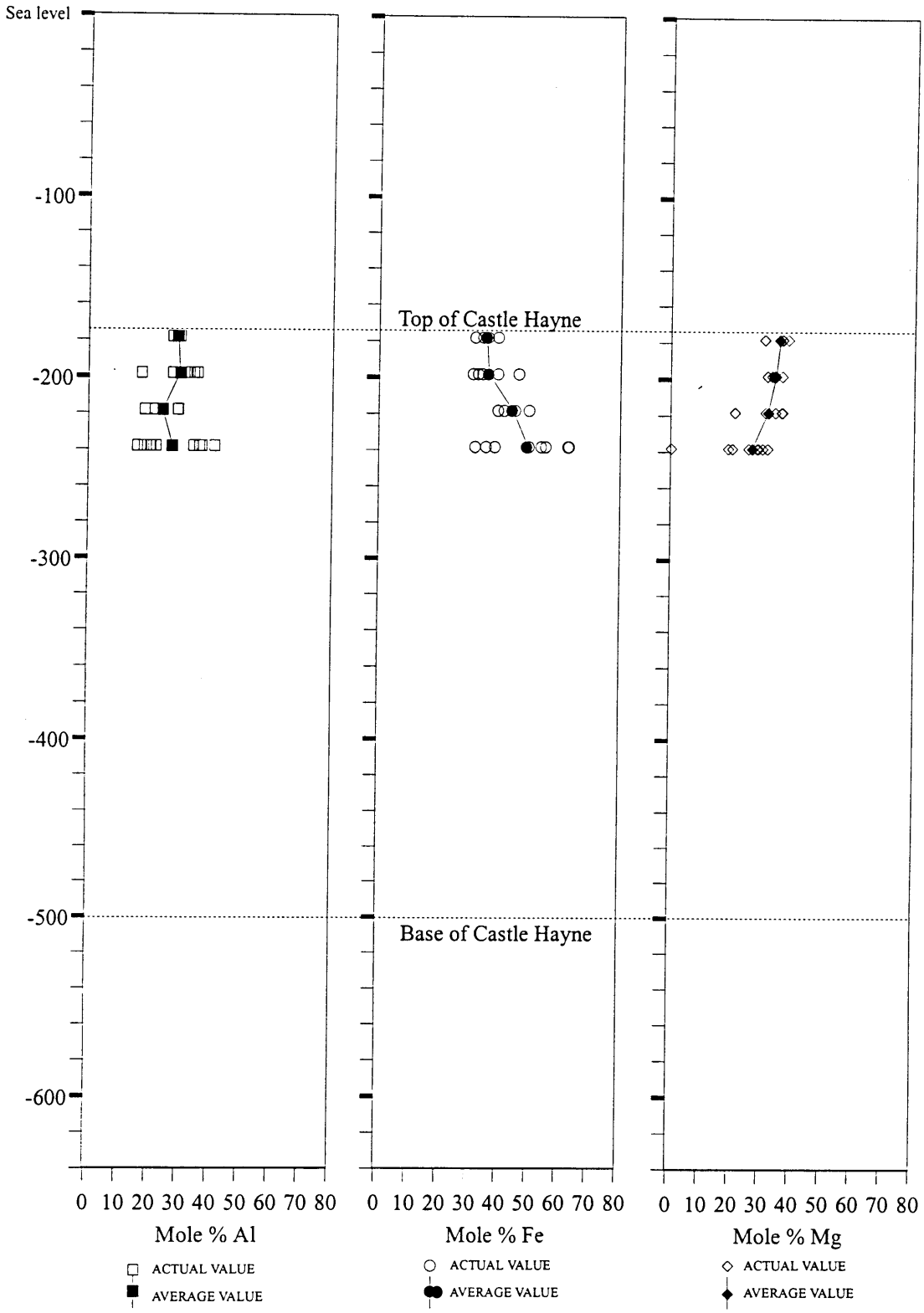

Figure 103. Mole % of octahedral Al, Fe, and Mg vs. depth in well BF-T6-67.

WH-T2-78

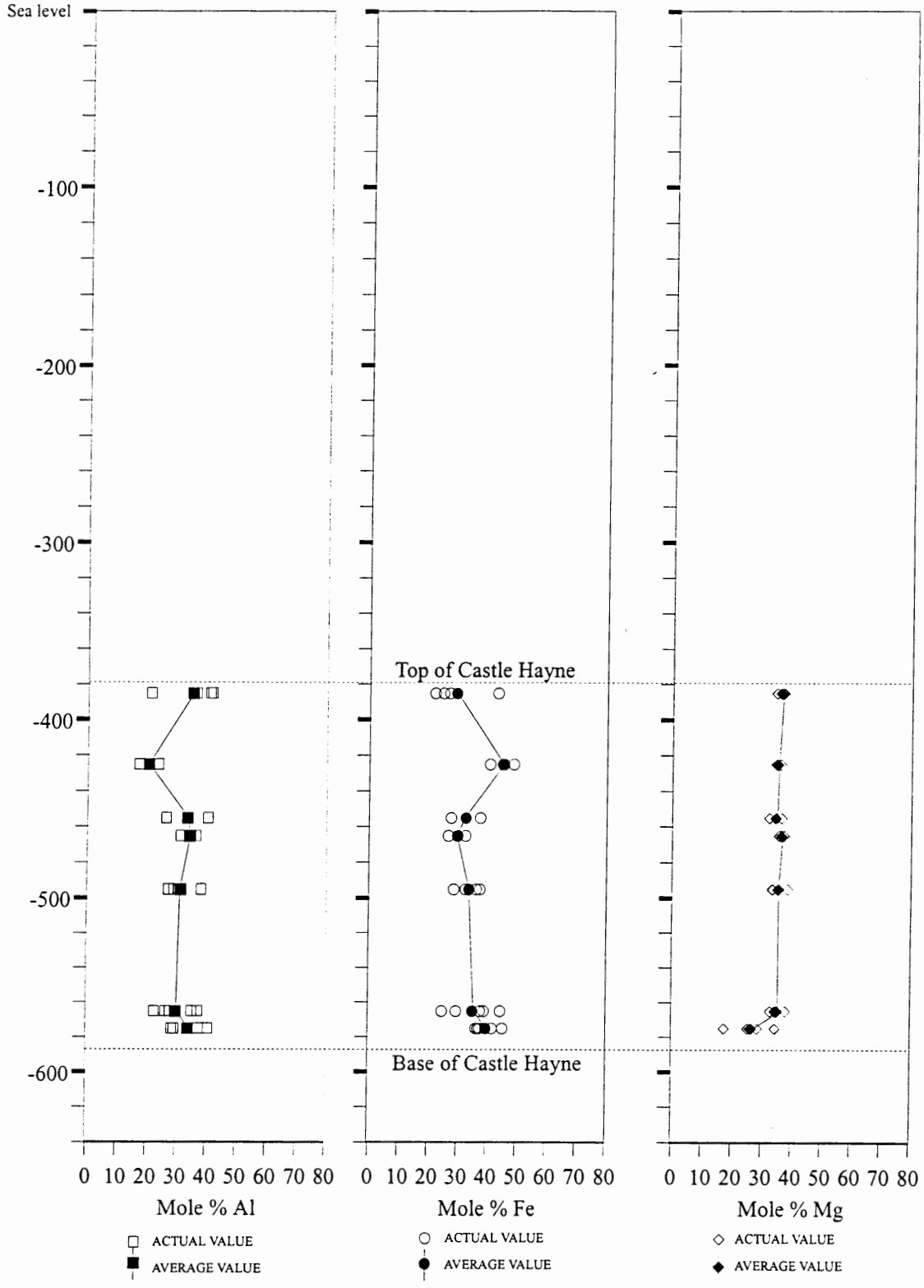

Figure 104. Mole % of octahedral Al, Fe, and Mg vs. depth in well WH-T2-78.

wells. Glauconite in well BF-T1-69 was observed to have higher Fe content when phosphate is present and in well BF-T6-67, Fe is at its highest where iron sulfide is present.

Figures 105 and 106 show a proposed correlation of changes in the concentrations of octahedral Al and Fe in glauconite with depth below sea level (wells BF-T5-67, WH-T2-78, and TY-T1-76). These wells represent a complete vertical sequence through the CHAS on a transect from southwest to northeast in the northern part of the study area (Figure 98). The shaded patterns represent zones in which changes in concentrations of octahedral Al and Fe with depth are similar. The proposed position of the boundary between the Upper and Lower Castle Hayne Aquifers was originally based on lithology and mineralogy (Figure 88), but also appears to be marked by changes in glauconite chemistry (Figures 105-106).

Carbonate Chemistry

Pure calcite, minor dolomite, and 2 low-magnesium calcite grains were detected during EDX analysis. Neither EDX analysis nor staining revealed any trace elements, such as iron or manganese, in the pure calcium carbonates. However, in order for the EDX system used to detect a particular element, it must occur in amounts of at least 0.1 wt%.

The dolomite (stoichiometric or non-stoichiometric) in this study appears to be secondary, replacing the matrix material. Stoichiometric dolomite contains 49 to 51 mol% $MgCO_3$ and non-stoichiometric dolomite contains 44 to 48 mol% $MgCO_3$ (Randazzo and Hickey, 1978). The values for the mole percent of $CaCO_3$ and $MgCO_3$ end-members in Table 17 could be as much as 3 mol% low for $CaCO_3$ and 2 mol% high for $MgCO_3$. If these percentages are corrected by these amounts, only the C3-unkn1 grain in well BF-T5-67 appears to be stoichiometric dolomite. Stoichiometric dolomite crystals are frequently found where the original texture of the rock is preserved, whereas, non-stoichiometric dolomite is associated with obscured or obliterated original depositional texture (Dunham 1962). Because of the limited accuracy of the semi-quantitative EDX analyses and the paucity of dolomite grains identified during petrographic analysis, it was impossible to distinguish between stoichiometric and non-stoichiometric dolomite during this study.

Phosphate Chemistry

Phosphate samples are hydroxy-, fluor-, or carbonate- apatites, and do not contain any chloride (Cl^-) (Table 18).

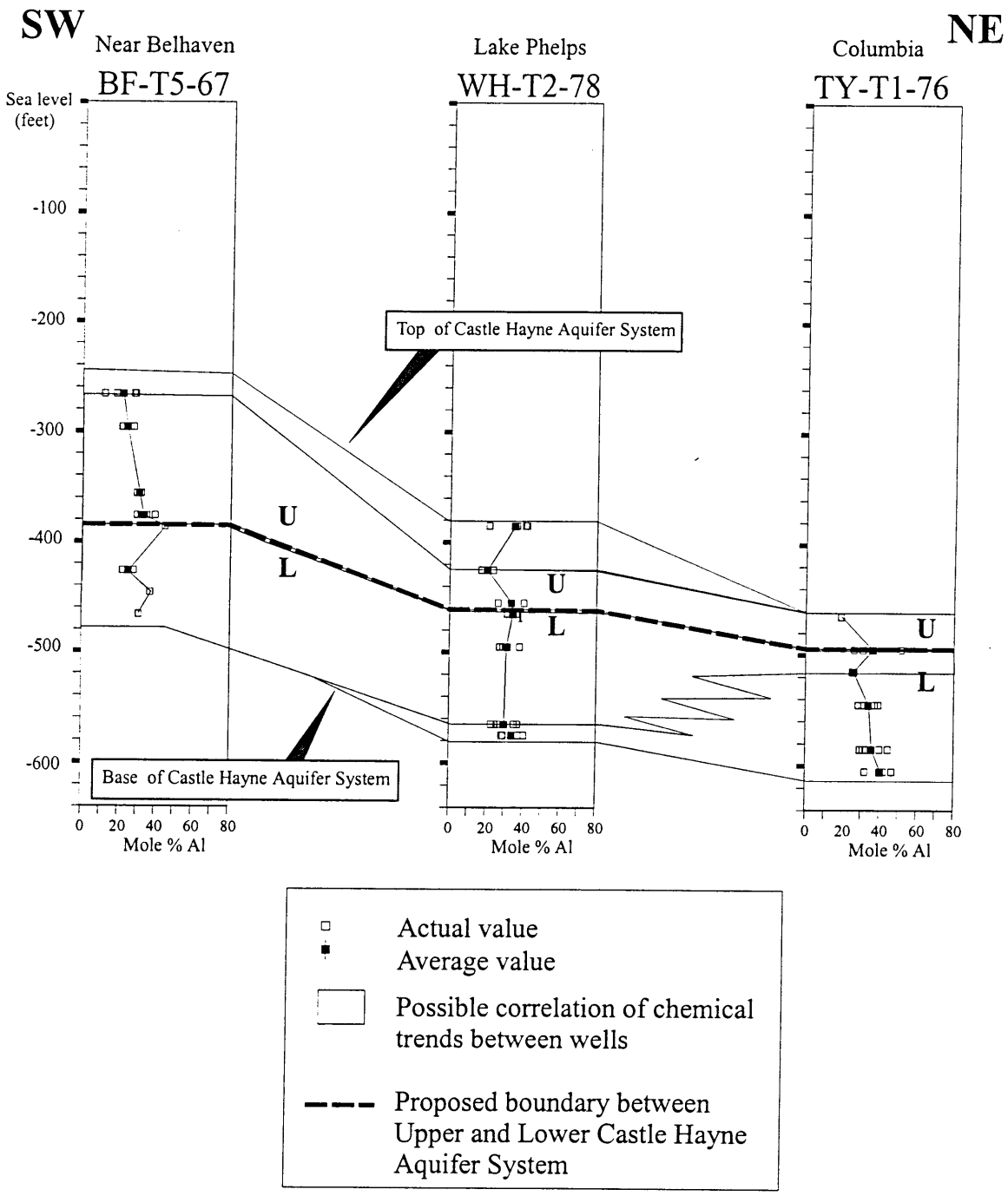

Figure 105. Proposed correlation of trends in octahedral Al for glauconite in wells BF-T5-67, WH-T2-78, and TY-T1-76.

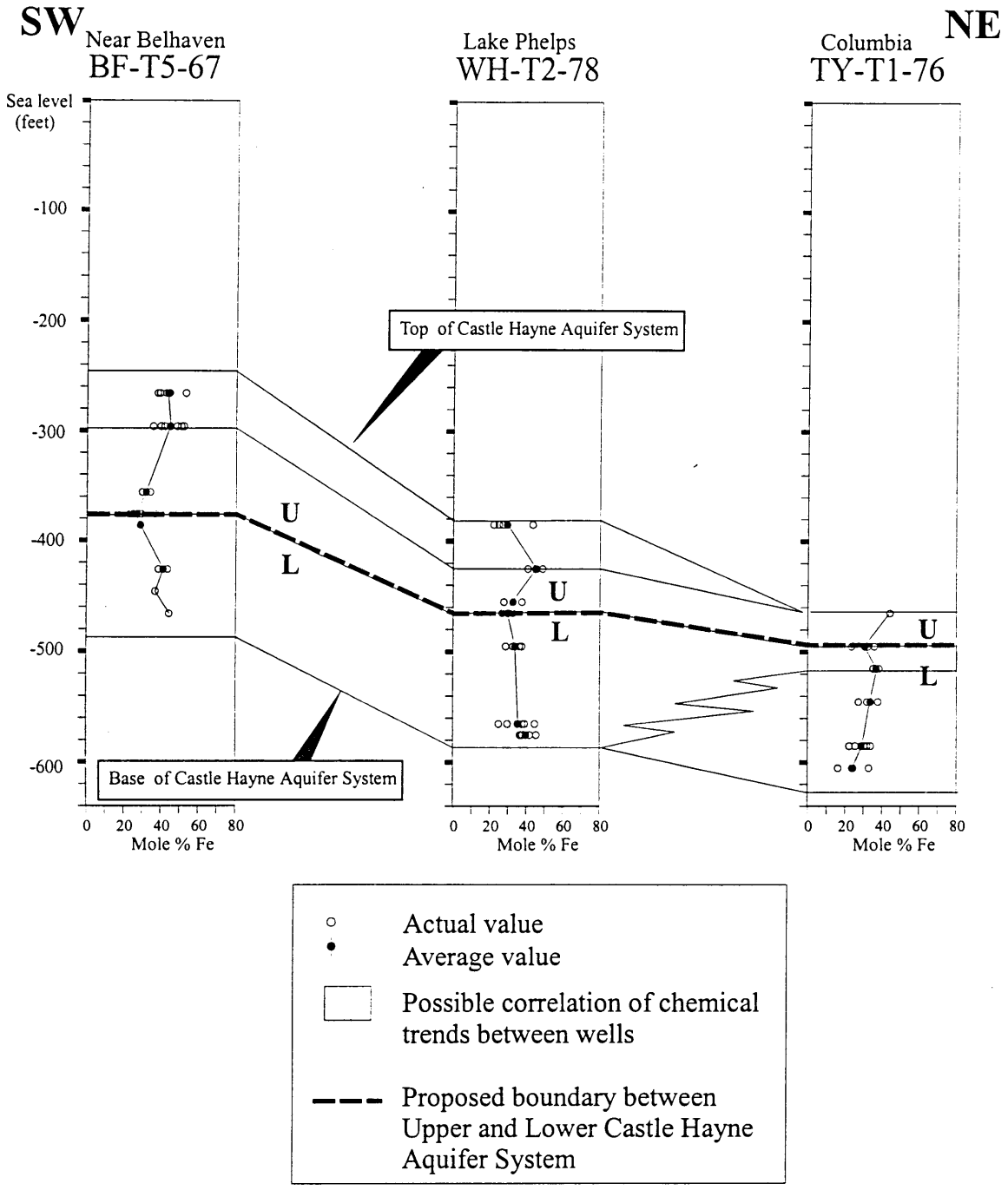

Figure 106. Proposed correlation of trends in octahedral Fe for glauconite in wells BF-T5-67, WH-T2-78, and TY-T1-76.

Iron Sulfide Chemistry

Based on a limited amount of reflected-light microscope work, the iron sulfide described in Table 19 is tentatively identified as pyrite (Fe 46.6 and S 53.4 wt.%). For wells BF-T5-67 and PA-T2-XX, the calculated formula is $Fe_{1.2}$ S_2, but in well BF-T6-69 the formula is slightly different ($Fe_{0.9}$ S_2).

Aluminosilicate Chemistry

The aluminosilicates found in this study are most likely Na-rich feldspars, zeolites, (phillipsite) or clay minerals (Table 20). Feldspars and zeolites are very similar in structure and chemistry and both are built of AlO_4 and SiO_4 tetrahedral frameworks. Zeolites, however, have highly variable amounts of water in the voids of their framework (Klein and Hurlbut, 1985). Unfortunately, the EDX detector used for this study is unable to evaluate the amount of water or other light constituents present, making it impossible to conclusively identify these minerals.

The greatest variability in the aluminosilicate minerals is in the concentration of Al_2O_3 (2-39 wt.%) and SiO_2 (48-79 wt.%) (Table 20). Well WH-T2-78 contains two types of aluminosilicates. Na-rich feldspar occurs in veins and as replacements surrounding the veins. The other type, present as sub-rounded clasts, seems to be phillipsite (zeolite), although the Al values are high. Data from XRD also suggest that phillipsite may be present in this well. In well TY-T1-76, the well-rounded clasts are possibly Na-rich feldspars with high Si and low Al values, although X-ray diffraction data also identified phillipsite in this well (Table 13). The samples analyzed from wells BF-T5-67 and PA-T2-XX are also possibly Na-rich feldspars (Table 20). Albite was identified in well BF-T5-67 by XRD analysis (Table 14), and petrographic analysis of well PA-T2-XX revealed the presence of minor amounts of feldspar.

Environment of Deposition

The aquifer is comprised of sediments deposited on the middle to outer shelf during sea level high- and low-stands as indicated by the bioclast assemblage (mollusks, echinoderms, bryozoans, brachipods, and foraminifera). The presence of glauconite and phosphate peloids indicates low energy and low sedimentation rates in temperate latitudes during sea level high-stands. Conversely, the occurrence of abundant bioclasts (shell hash) and sand in certain intervals suggests higher sedimentation rates during sea level low-stands. This is especially evident in the lower CHAS, which is more arenaceous than the upper CHAS. The boundary between the Upper and Lower CHAS can apparently be

deduced from geochemical trends, as well as from lithology. The similarity of geochemical facies observed from well to well in Figures 105 and 106 suggests that present-day rock chemistry is strongly related to lithofacies and their regional trends in the subsurface. These chemical facies trends are most likely reflecting original responses to sea level changes and their impact on the depositional environment. Furthermore, these data suggest not only changing lithofacies in response to a change in environment of deposition, but also changing geochemical facies in response to changing chemistries in the marine waters on the continental shelf during the Tertiary.

GEOCHEMISTRY OF CASTLE HAYNE GROUNDWATER

Methodology

The computer program PHREEQE (Parkhurst et al. 1980) was used to determine the chemical speciation of solutes and the saturation state of various phases. Another program, PHRQINPT, was used to create input files for PHREEQE. Any initial charge imbalance was maintained during the calculations. For each solution the solute concentrations, temperatures, pH, and Eh measured at each well were entered into the data base. The extended Debye-Huckel equation was used to calculate activity coefficients for all species with an ion size parameter, and the Davies equation was used for all species with no ion size parameter.

The geochemical modeling program, NETPATH (Plummer et al. 1991), was used to study geochemical processes occurring between CHAS aquifer materials, CHAS groundwater, and waters leaking into the CHAS. The program is useful for interpreting net geochemical mass-balance reactions between an initial and final water along a hydrologic flow path. Alternatively, NETPATH computes the mixing proportion of two initial waters and net geochemical reactions that can account for the observed composition of a final water. The program uses chemical and isotopic data for groundwater and plausible phases present in the environment to investigate every possible geochemical mass balance reaction model that could explain the changes from the initial to final water.

Major Elements

Calcium and Mg dominate the cations in the dilute Ca-HCO_3 waters from the U-CHAS in the western part of the study area (Figures 26 and 28). Rainfall (Table 21) does not contribute significant Ca and Mg to the groundwater. Trends in alkalinity, Ca, and Mg suggest that dissolution/precipitation of carbonate minerals exerts the major control on water chemistry to the west. Indices

of saturation for calcite (Figures 107 and 108) and dolomite (Figures 109 and 110) were calculated for the analyzed waters

Table 21. Average chemical composition of rainfall in the recharge area of the CHAS.

Ion	Conc. ppm	Ion	Conc. ppm
Na^+	0.27[3]-1[2]	Cl^-	2[2,4]
K^+	0.1[1]-0.2[2]	SO_4^{2-}	1.6-2[5]
Mg^{2+}	0.15 [1]	NO_3^-	0.4-4[3,5,6]
Ca^{2+}	0.08[3]-0.65[1]	NH_4^+	0.21-0.61[3,6]

1 Gambell and Fisher 1966
2 Junge and Werby 1958
3 Willey and Kiefer 1993
4 Willey and Kiefer 1990
5 Willey et al. 1988
6 D. Daniels, pers. com., 1996

using field measurements of temperature, pH, and alkalinity and laboratory analyses of the concentrations of Ca and Mg. The saturation index of a mineral is defined as

$$\text{saturation index} = \log (IAP/K_T)$$

where IAP is the ion activity product of the dissolved components and K_T is the solubility product at the specified temperature. A saturation index = zero indicates saturation or oversaturation. However, because of the possibility of CO_2 outgassing and errors in determination of pH and alkalinity, Sprinkle (1989) considered that a saturation index of -0.2 to +0.2 is indicative of calcite saturation in the Floridan aquifer of Central Florida. The calcite saturation index ranged from -0.20 to 0.13 in the U-CHAS aquifer and from -0.25 to 0.14 in the L-CHAS. According to the criterion used by Sprinkle (1989), only S15y3 in the L-CHAS (Figure 9) is not saturated with calcite, thus, Ca concentrations are controlled in most of the aquifer by calcite saturation. Locally, however, cation exchange undoubtedly affects Ca concentrations (Chapelle and Knobel 1983; Sprinkle 1989). For example, Ca reaches a maximum near Washington in the Northwestern Coastal Plain, and then decreases eastward. One possible explanation is the precipitation of calcite cements by groundwater as it moves away from the recharge area, becomes depleted in CO_2 gas, and saturates with respect to calcite (Plummer et al. 1983). However, cation exchange between clays and groundwater is also possible and could take the following form:

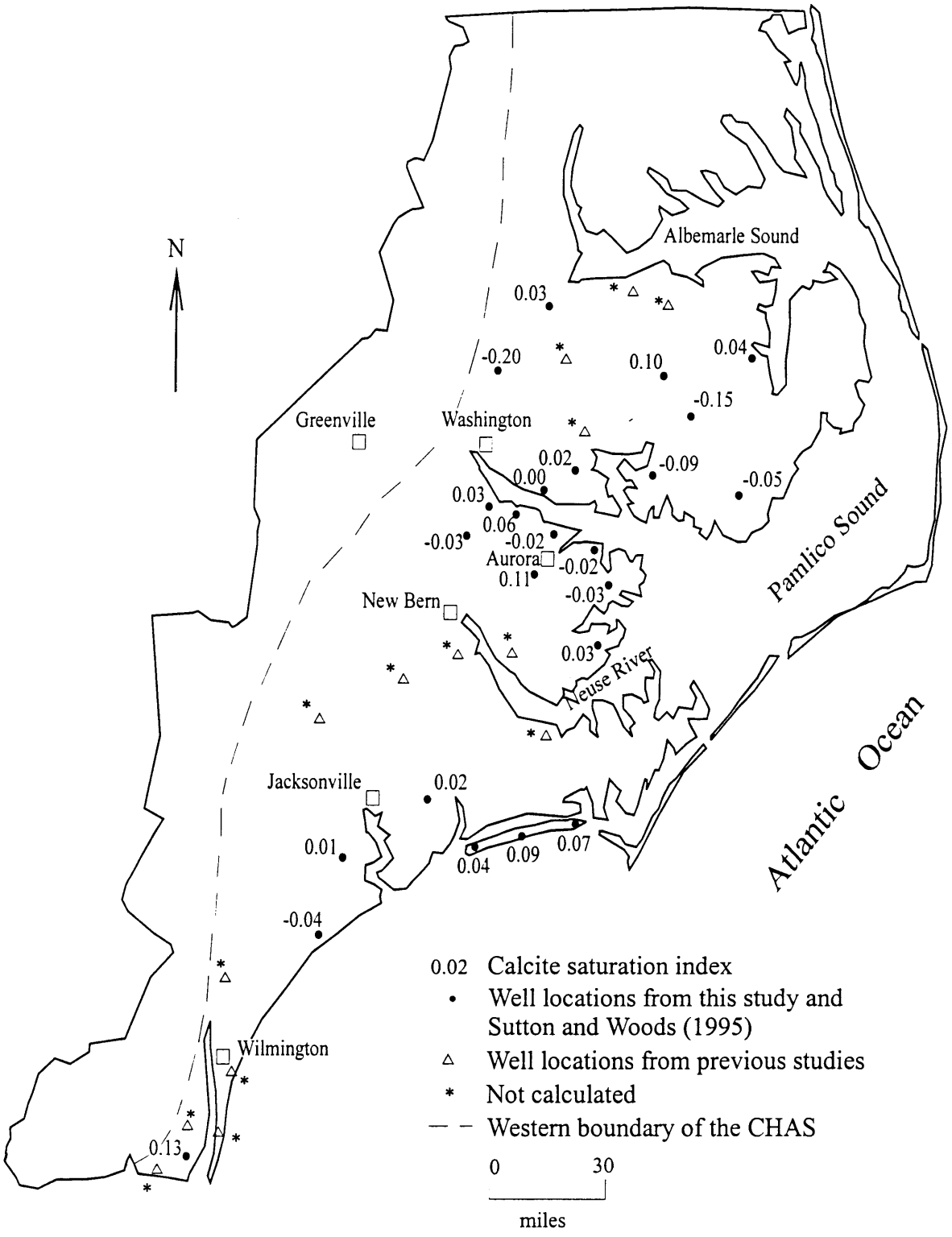

Figure 107. Calcite saturation index of the U-CHAS * Indicates that because of insufficient data the SI could not be determined. This was the case for most of the data from previous studies.

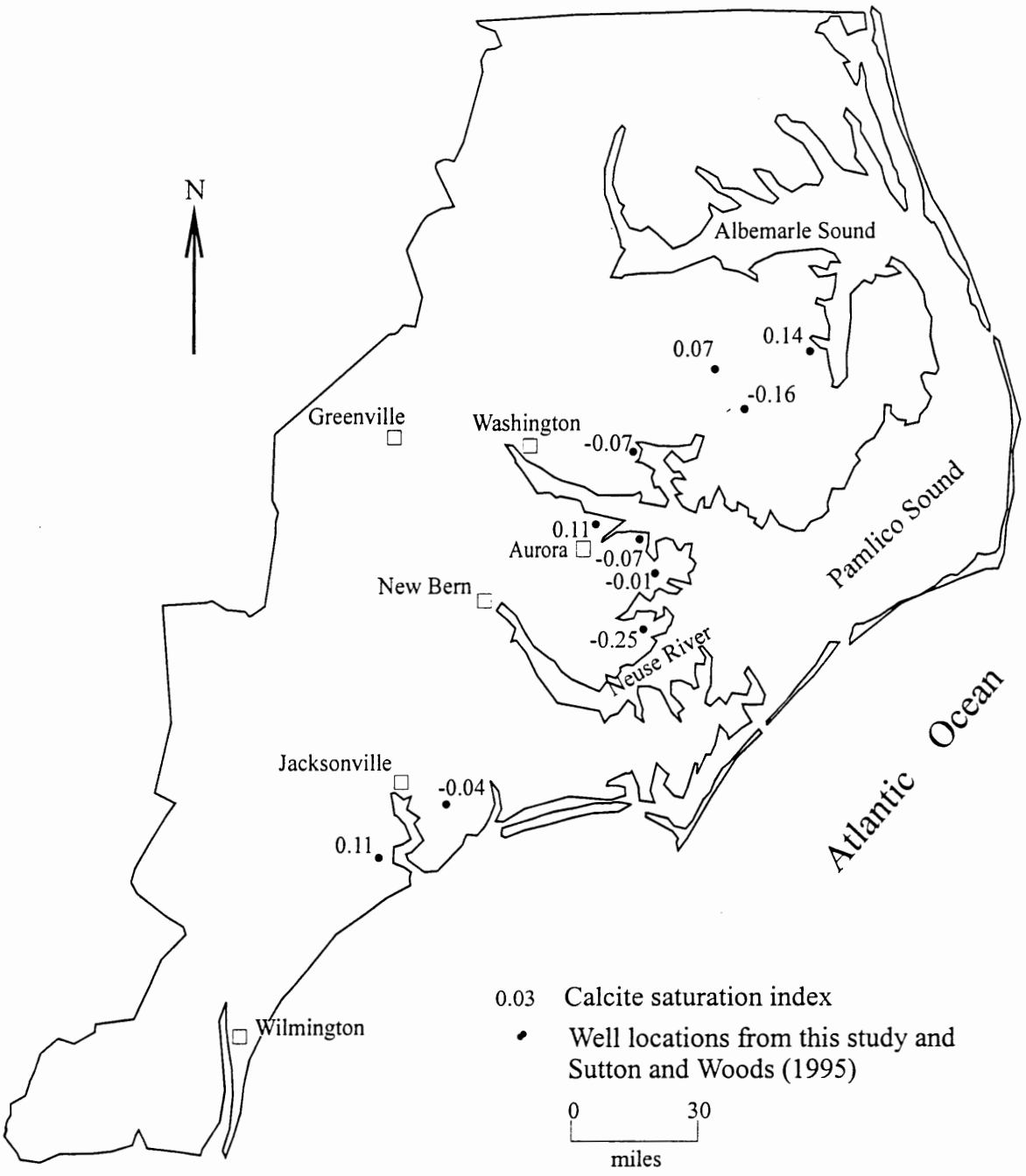

Figure 108. Calcite saturation index of the L-CHAS

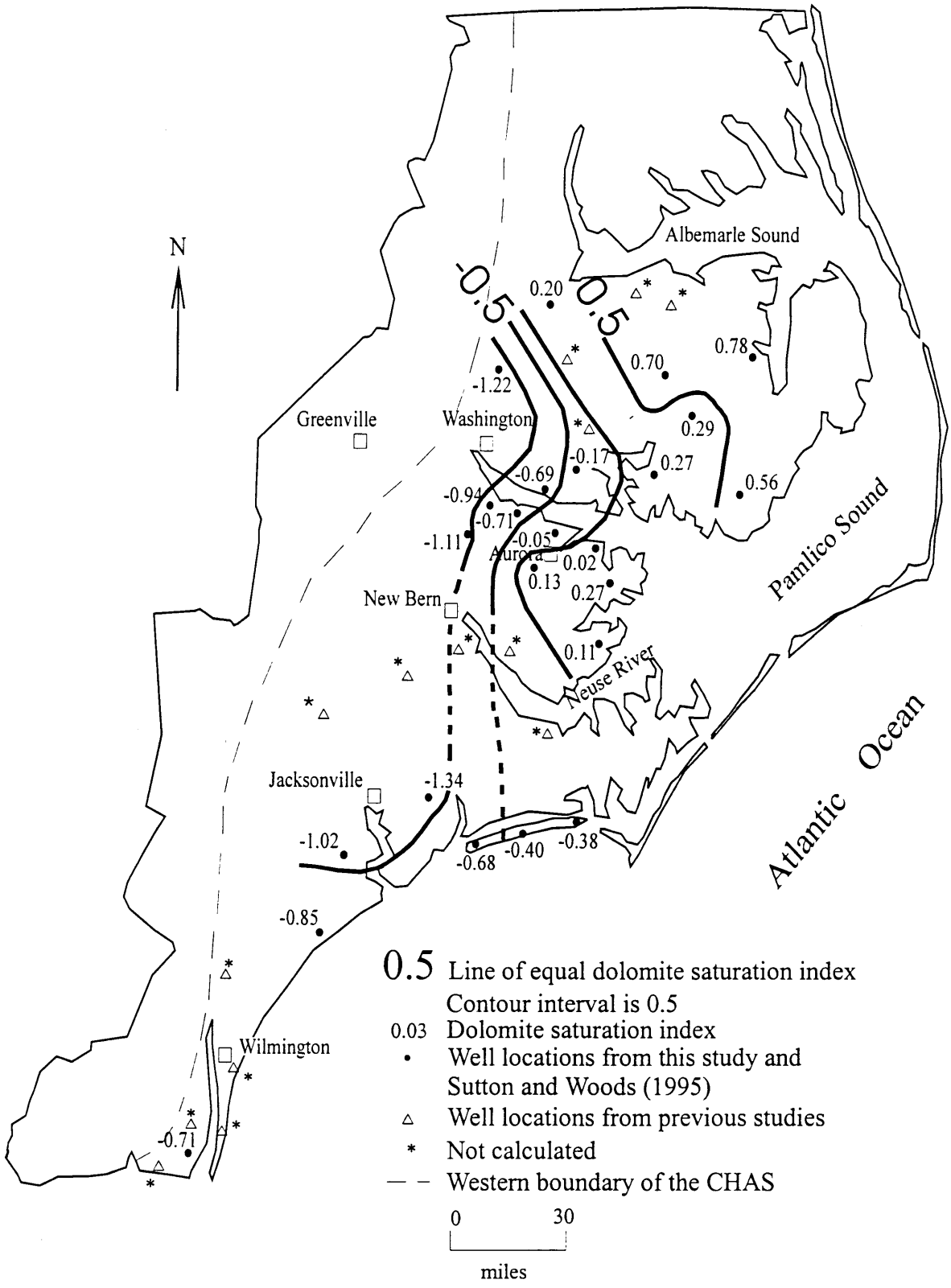

Figure 109. Dolomite saturation index of the U-CHAS
* Indicates that because of insufficient data the SI could not be determined.

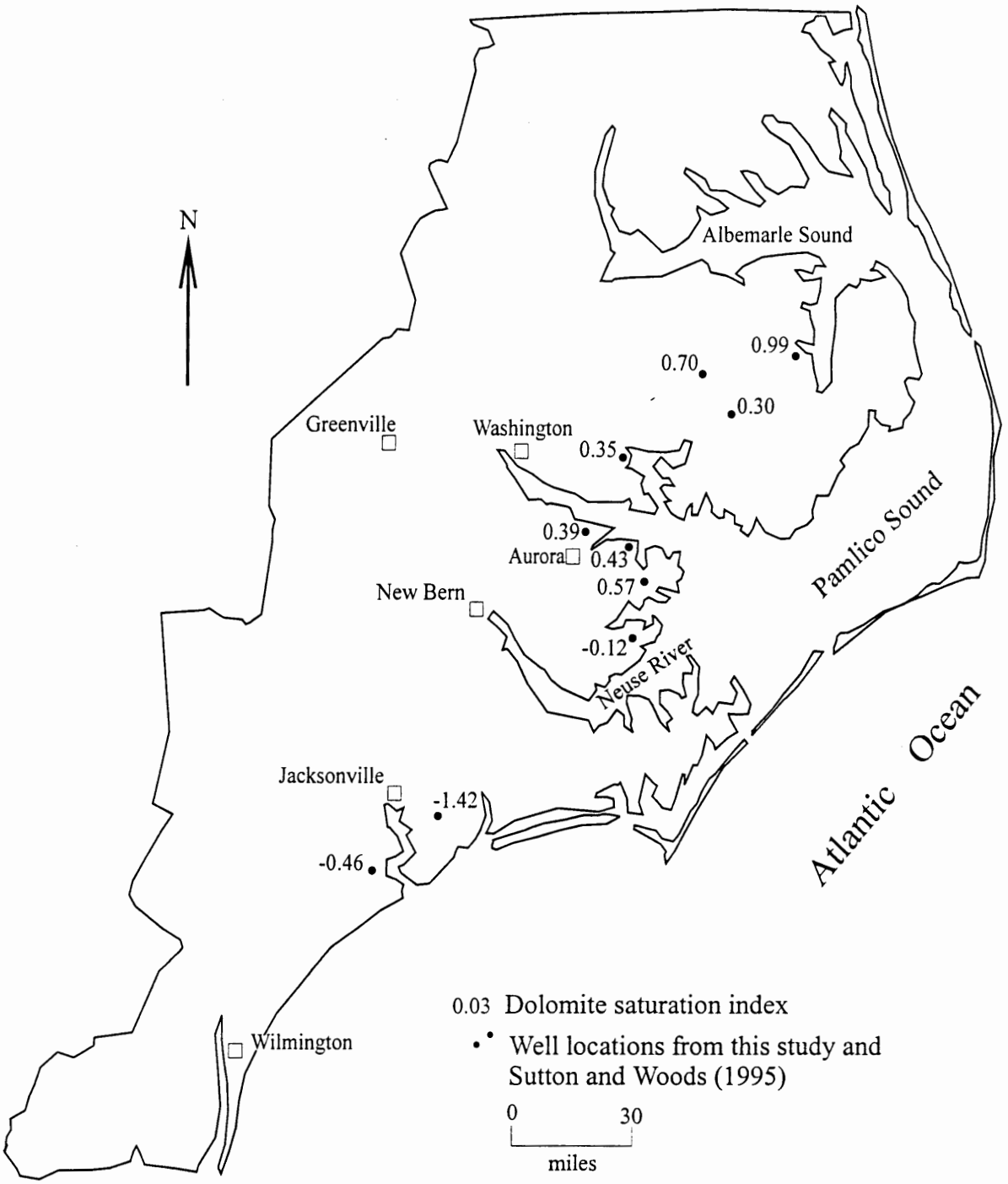

Figure 110. Dolomite saturation index of the L-CHAS

$$Ca^{2+}\ (aq) + 2Na^{+} - EX\ (s) \Leftrightarrow 2Na^{+}\ (aq) + Ca^{2+} - EX\ (s)$$

which describes the process whereby Ca from groundwater replaces Na on the solid exchanger and releases Na to the water (Sprinkle 1989). Negative saturation indices to the east may be related to intrusion of SFW.

Dolomite saturation index ranges from -1.60 to 0.78 and increases from west to east (Figures 109-110). Sprinkle (1989) considered that values from -0.4 to +0.4 indicate saturation, thus, dolomite is oversaturated (>0.4) in the northeastern part of the study area and undersaturated to the west. Dolomite dissolution is a potential Mg source to the west, although mineralogical data discussed above suggest the presence of insufficient dolomite to provide the required Mg. Hundreds of EDX analyses of carbonates yielded only twenty-one dolomites and 2 low-Mg calcites (Table 17) -- the rest were 100% $CaCO_3$. Preliminary geochemical computer modeling with NETPATH (Plummer et al. 1991) also suggests dissolution of an unreasonably large amount of dolomite would be required to provide the necessary Mg. Porosity of the moldic limestone results mainly from dissolution of fossil bioclasts, many of which were originally composed of Mg-calcite (Veizer 1983). In the aquifer today, however, very little Mg-carbonate remains.

Another source of Mg is cation exchange between groundwater and clays such as glauconite, which are present in most Castle Hayne core samples in amounts of 0.5% to 3%, but sometimes make up as much as 30% (Tolen-Mehlhop 1998). The weak inverse correlation between K and octahedral Mg observed for CHAS glauconite in the Northern Coastal Plain (Figure 99f) is further evidence that this may be occurring. Chapelle and Knobel (1983) in their study of glauconite and groundwater chemistry in the Aquia Aquifer of southern Maryland suggested that incongruent dissolution of glauconite in the recharge area may also release Mg to groundwater, along with K and SiO_2.

Ratios of Ca to Mg (by weight) are higher in the west and decrease to the east (Figures 111-112). Aquifer mineralogy is dominated by calcite but dolomite dissolution could lower the ratio to 1.65. The decrease to values as low as 0.41 in the eastern portion of the study area is probably due to influx of saline formation waters. The Ca/Mg ratio in seawater is 0.32.

Bicarbonate is a principal anion in U-CHAS waters; potential sources include (1) dissolution of CO_2 in recharge water, (2) dissolution of carbonate minerals, and (3) oxidation of organic materials. The close relationship between concentrations of Ca and HCO_3 ions in wells from the western part of the study area

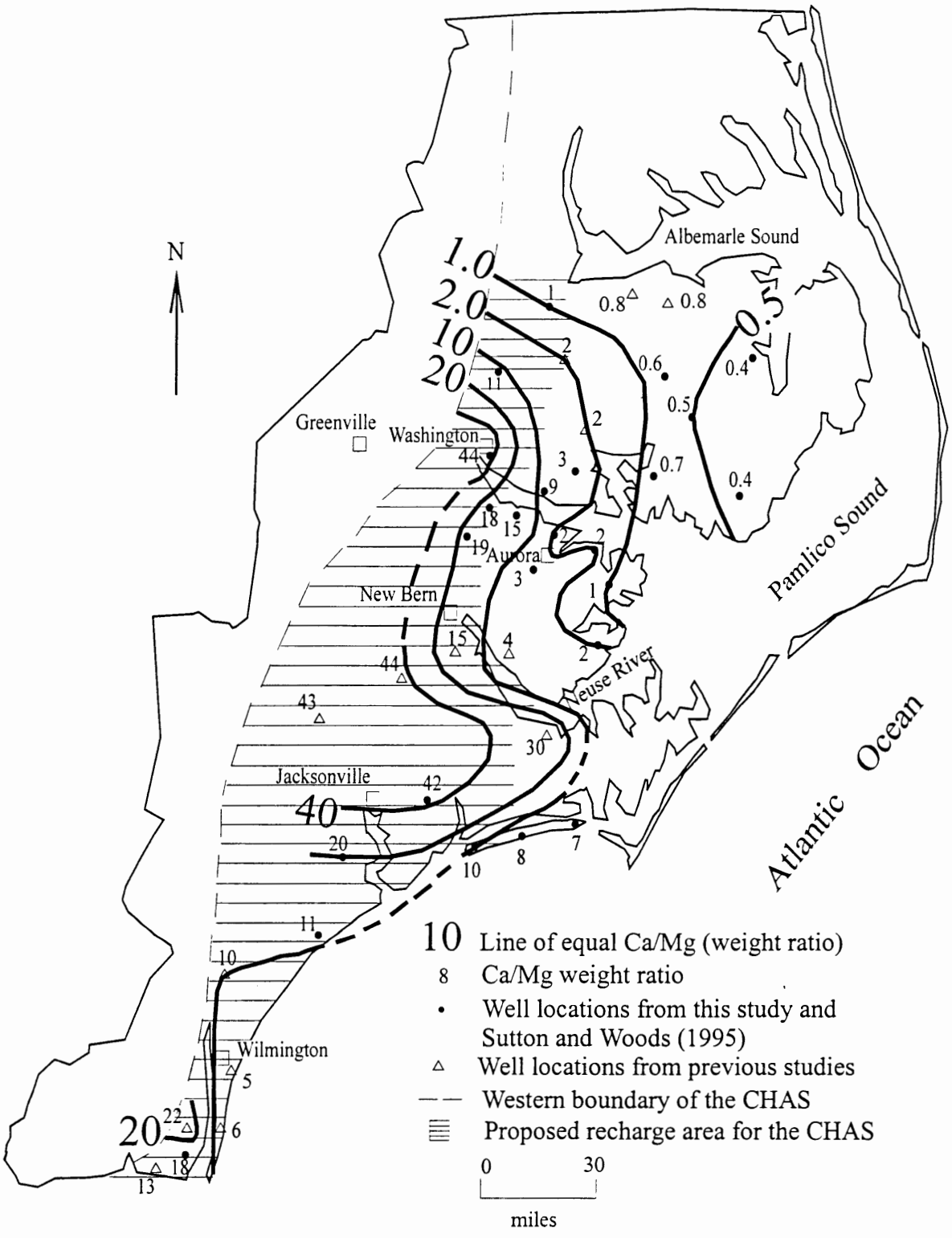

Figure 111. Weight ratio of Ca/Mg in the U-CHAS with proposed recharge area. (Ca/Mg weight ratio of seawater is 0.32.)

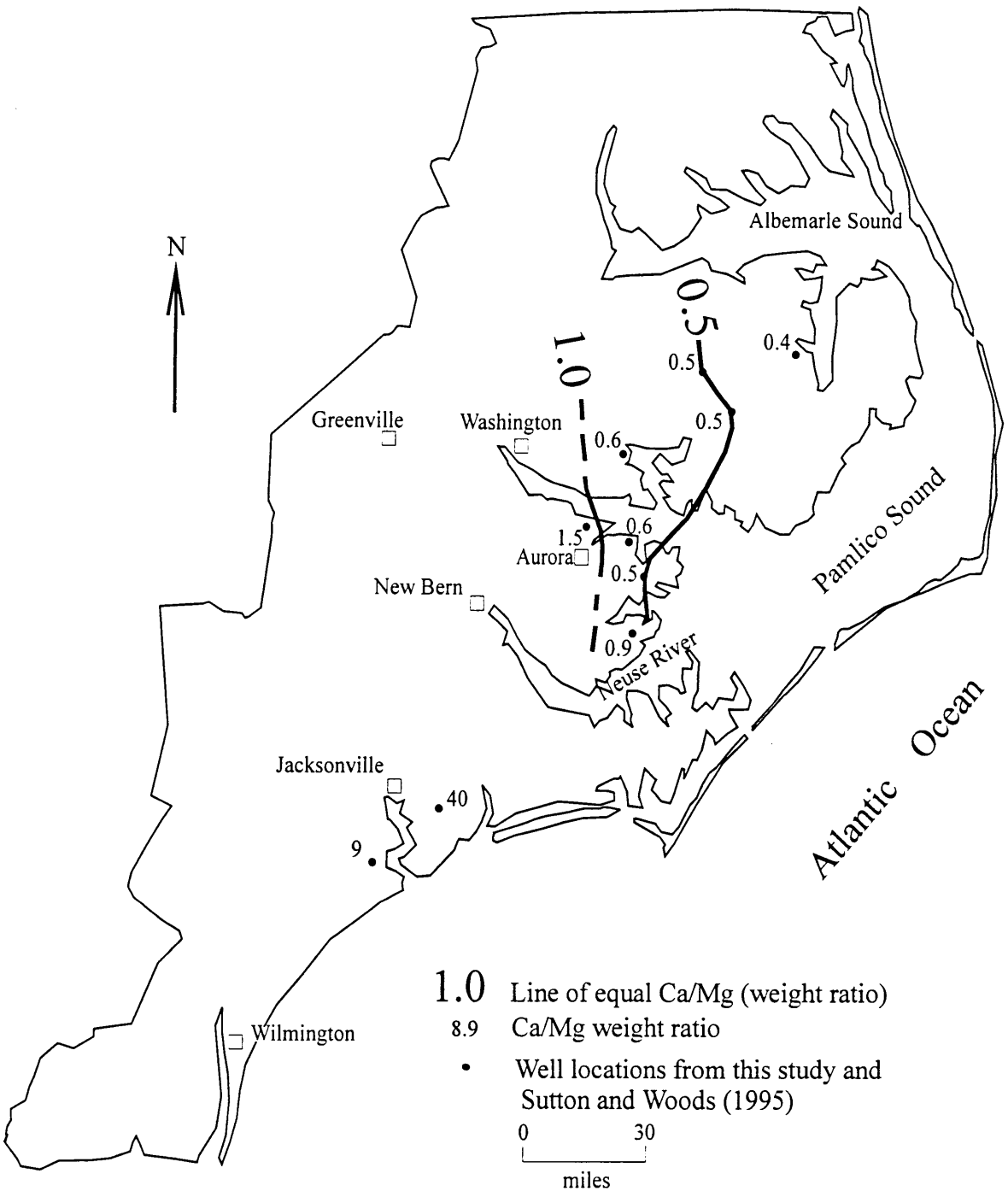

Figure 112. Weight ratio of Ca/Mg in the L-CHAS (Ca/Mg weight ratio for seawater is 0.32.)

suggests that these constituents are largely derived from carbonate dissolution. This process is enhanced by dissolved CO_2 in recharge water. Alkalinities in this area are typical of waters whose solute composition is dominated by calcite dissolution (Sprinkle 1989; Trainer and Heath 1976). Carbonate buffering maintains the pH between 6.9 and 8.1 (Figure 42) and HCO_3 is the predominant carbonate species. Alkalinity generally increases from west to east (Figure 20). The HCO_3 concentration in 90% of the Floridan Aquifer does not exceed 244 ppm, except in a coastal region along the Gulf of Mexico and in a few small upland areas. The much higher alkalinities observed in the eastern half of the CHAS must have a source other than limestone dissolution.

Water from well L13i1 (Figure 8) has very high alkalinity (783 ppm) and low Ca and Mg concentrations. High HCO_3 concentrations are balanced by Na. Similar high HCO_3-low Ca water was found in the Floridan Aquifer where it is overgrown by hardwood and pine forests (Sprinkle 1989). Assuming that the source of the bicarbonate is oxidation of organic matter (Chapelle 1983), Sprinkle (1989) suggested that decaying forest litter produces waters high in soluble organic acid anions. He theorized that these organic acid anions would be titrated in addition to inorganic carbon species, thus giving higher alkalinity. Trainer and Heath (1976) also found that high concentrations of organic matter in soils resulted in a relatively high bicarbonate concentration in the soil water. The high alkalinity in this area may be due to a very thin confining layer, which permits local recharge from lakes, swamps, and pocosins (perched swamps).

North of the Neuse River, sulfate concentrations increase from west to east in both the U-CHAS and L-CHAS (Figures 18 and 19). No sulfate was found in water in the northwestern recharge area, so rainfall concentrations (2 ppm of SO_4) are being removed from the groundwater. South of the Neuse River all concentrations are below 10 ppm, except BBPW5 and NH-262 (Figure 8), which suggests that rain could be the source of sulfate to groundwater in the southwestern recharge area.

No sulfate minerals have been reported in the CHAS. Figure 113 (modified from Rightmire et al. 1974) shows a gypsum trend and a seawater trend on a graph of sulfate concentrations versus SO_4/Cl ratio. These trends may be used to identify the sources of SO_4 in a groundwater sample. Points A and C represent the SO_4 and Cl concentrations found in dilute groundwater, with point C representing a more mineralized starting point. Analyses that plot near line A-B or C-D indicate that gypsum is the primary source of SO_4, and analyses that plot along line A-E or C-E represent a mixing trend with seawater (E). All samples

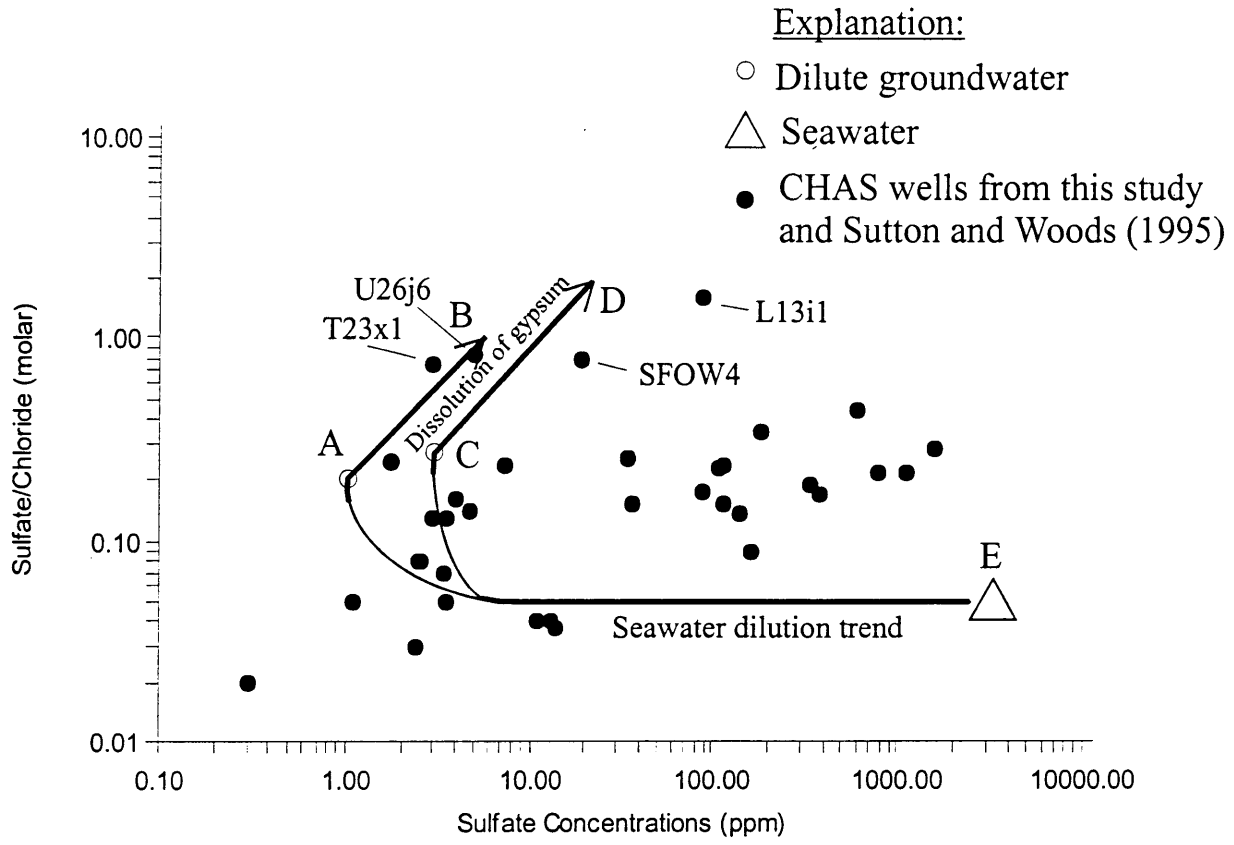

Figure 113. Graph of sulfate-to-chloride ratios versus sulfate concentrations.

fall along the seawater trend, except T23x1, U26j6, SFOW4, and L13i1 (Figure 8) indicating that seawater is the primary source of SO_4. Gypsum is undersaturated over the entire study area (Figures 114 and 115). T23x1 and U26j6 lie within the recharge area, which has dilute, acidic, oxygenated water, and the source of SO_4 could be rainfall or oxidation of sulfide minerals. The high SO_4 /Cl ratio at L13i1 may be due to a very thin confining layer, which could permit local recharge from lakes, swamps, and pocosins (perched swamps). The high ratio in SFOW4 may be influenced by the upward movement of waters from the Cretaceous aquifer system.

The Cl and Na in some western waters were acquired in the subsurface because the concentrations greatly exceed those in local rainfall (Table 21). Nesbitt and Cramer (1993) suggest that dissolution of soil salts precipitated by evaporation in capillary fringes above the water table and exchange of cations and anions with organic materials and soil minerals can explain these high concentrations in groundwater.

Sprinkle (1989) noted that, in general, dissolved-solids concentrations in the Upper Floridan Aquifer are = 500 mg/l and are held at or below that level by calcite and dolomite saturation. He reported that higher concentrations are generally due to mixing with seawater. U-CHAS waters with TDS > 640 ppm show Na/Cl and K/Cl ratios similar to seawater (Figures 116-119). For these waters, a gradual eastward increase in the proportion of SFW explains the increasing concentrations of SO_4 and Cl. No sulfate minerals have been identified in the aquifer and gypsum is undersaturated everywhere in the study area so increasing amounts of SFW undoubtedly accounts for increasing sulfate. Increasing Ca and Mg concentrations are related to this SFW influx, although other processes are required to explain minor changes.

Trapp and Meisler (1992) studied the regional aquifer system underlying the Northern Atlantic Coastal Plain and found that the hydrochemical facies of each aquifer follows a general down-dip sequence from (1) water of variable composition, to (2) Ca and Mg bicarbonate water, to (3) Na bicarbonate water, to (4) Na chloride water. In the U-CHAS of the Northern Coastal Plain this sequence is observed (Figure 36) and the following hydrochemical facies are seen from west to east:

1) Ca and bicarbonate waters,
2) mixed cations and bicarbonate waters
3) alkali and bicarbonate waters, and
4) alkali and Cl waters.

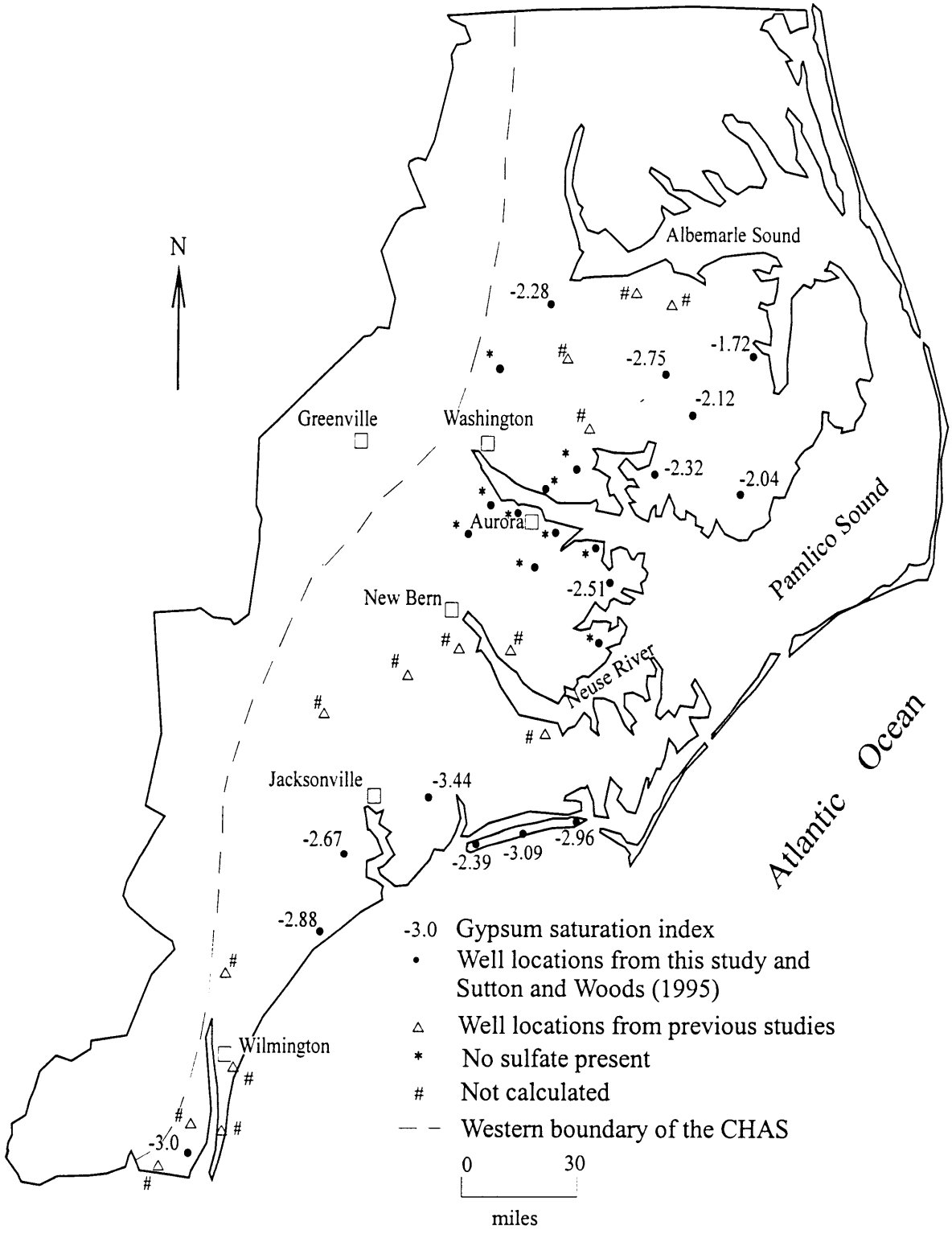

Figure 114. Gypsum saturation index of the U-CHAS
* Indicates that sulfate is absent or below the detection limit.
# Indicates that because of insufficient data the SI could not be determined.

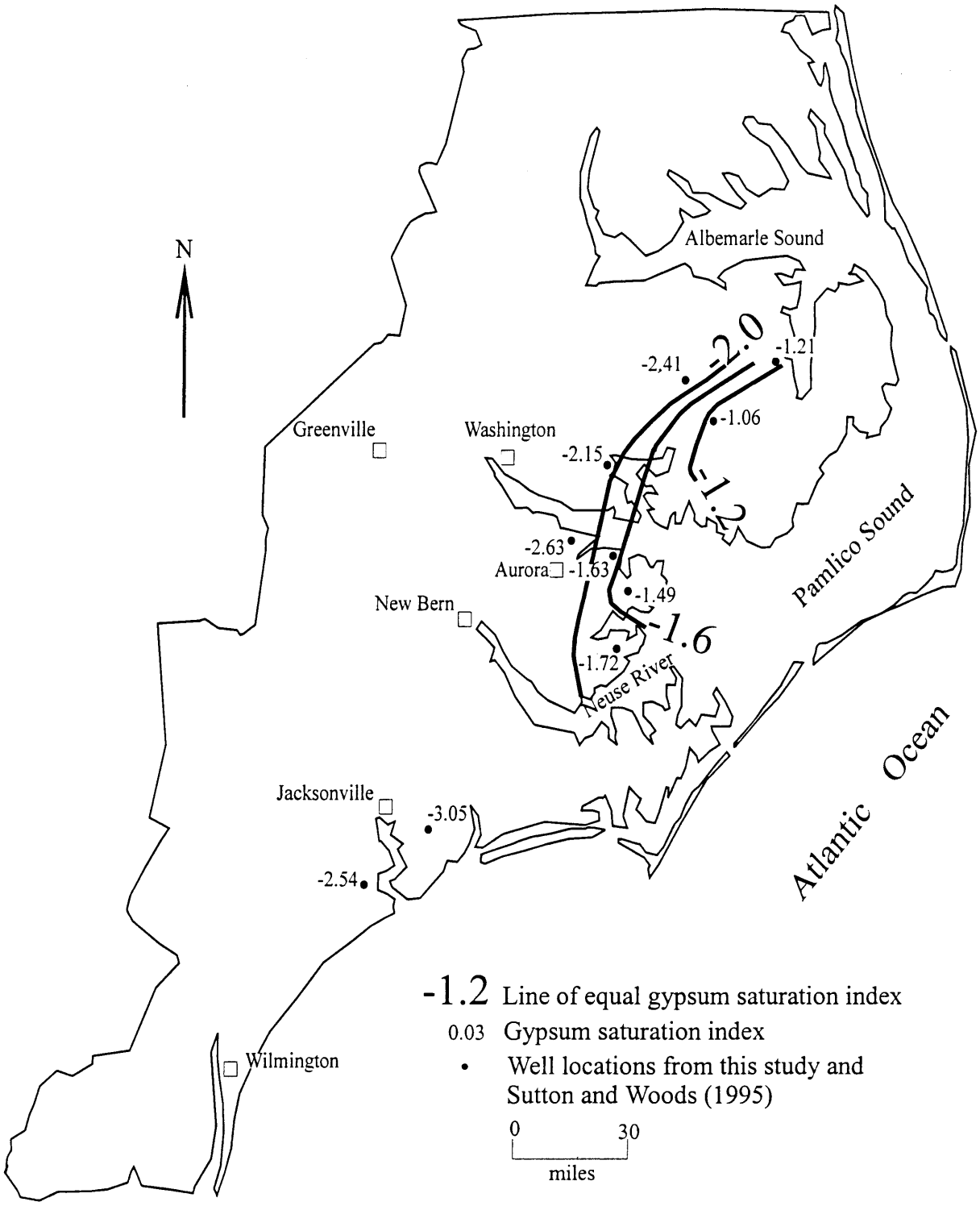

Figure 115. Gypsum saturation index of the L-CHAS

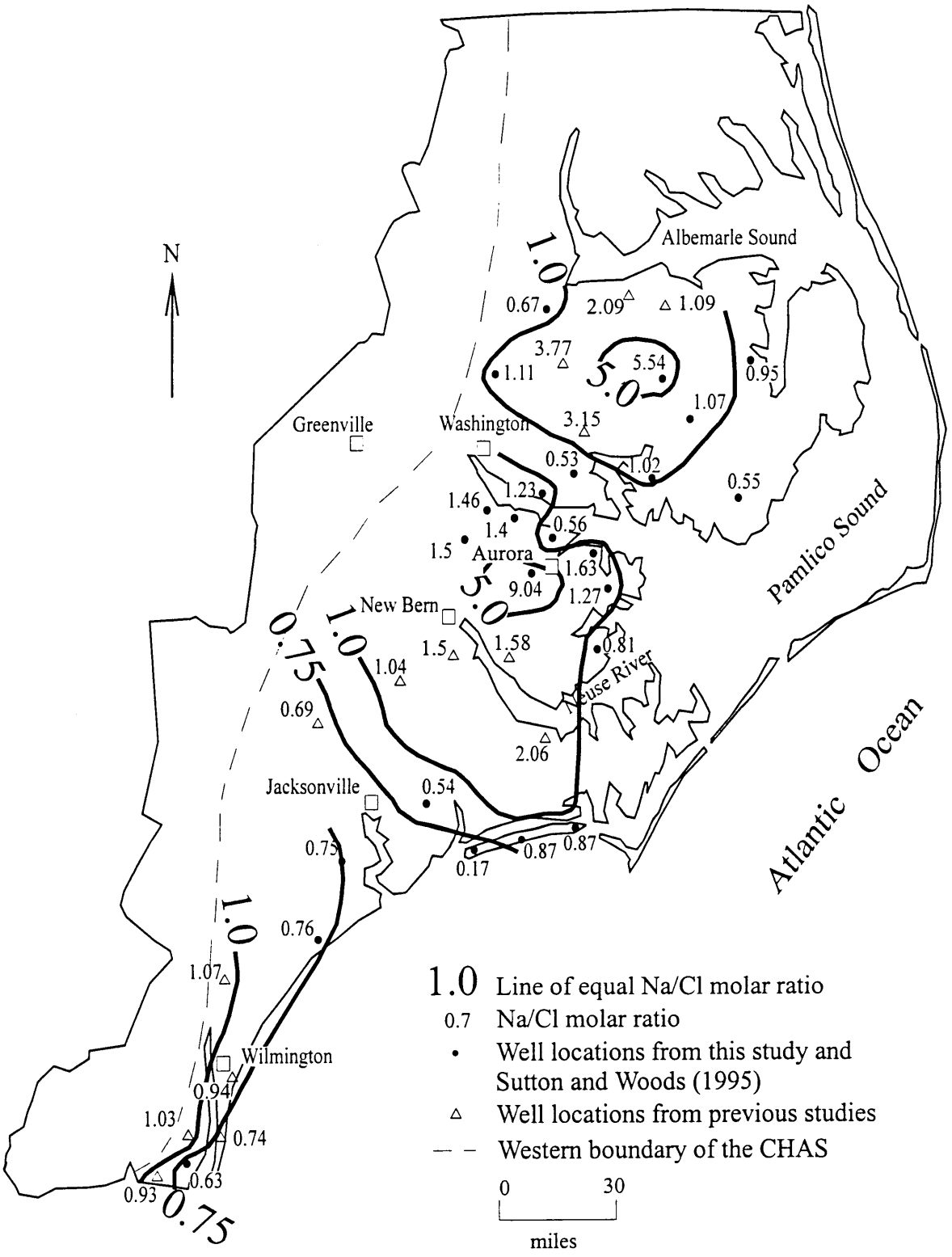

Figure 116. Molar ratio of Na/Cl in the U-CHAS The molar ratio for seawater is 0.86.

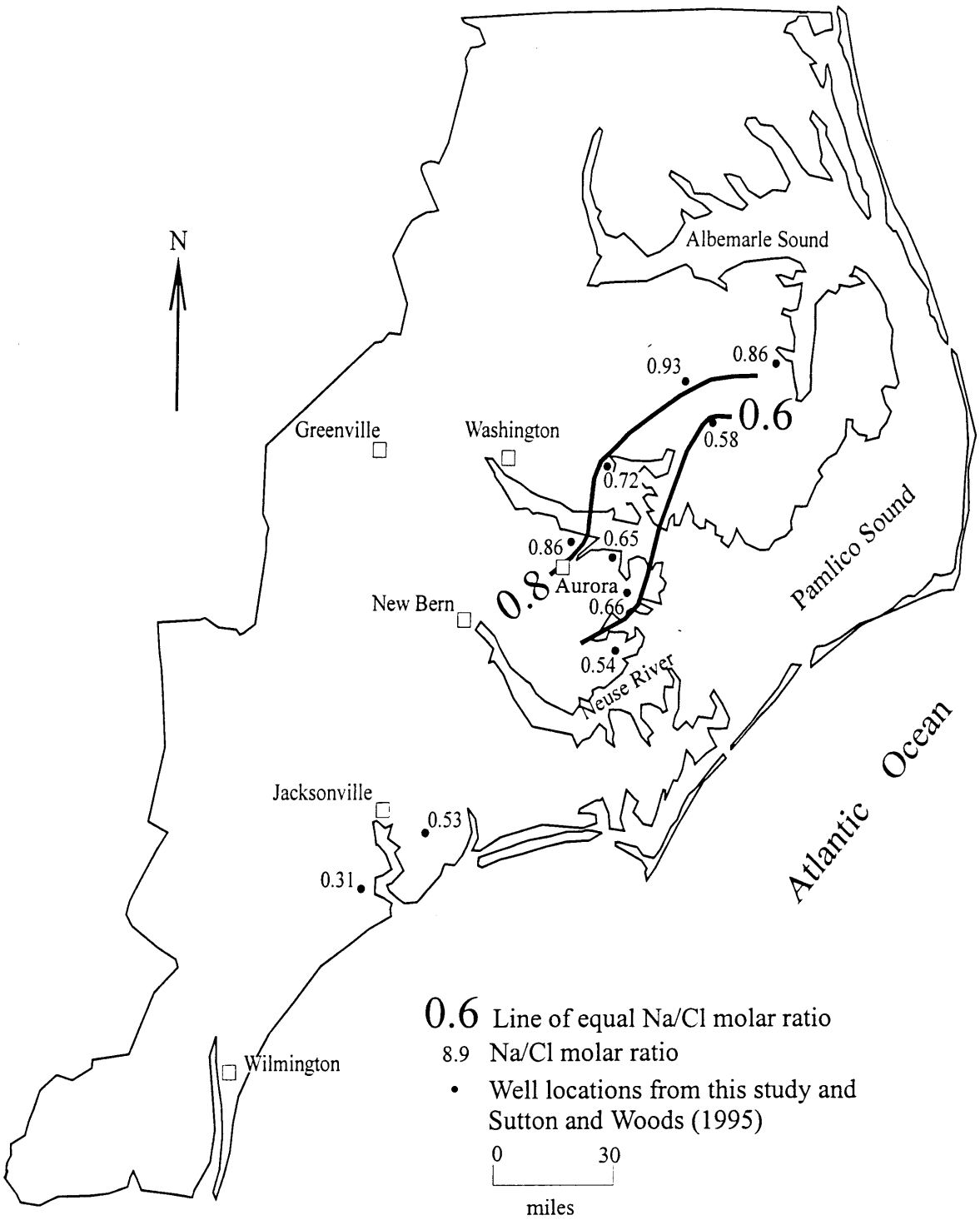

Figure 117. Molar ratio of Na/Cl in the L-CHAS The molar ratio for seawater is 0.86.

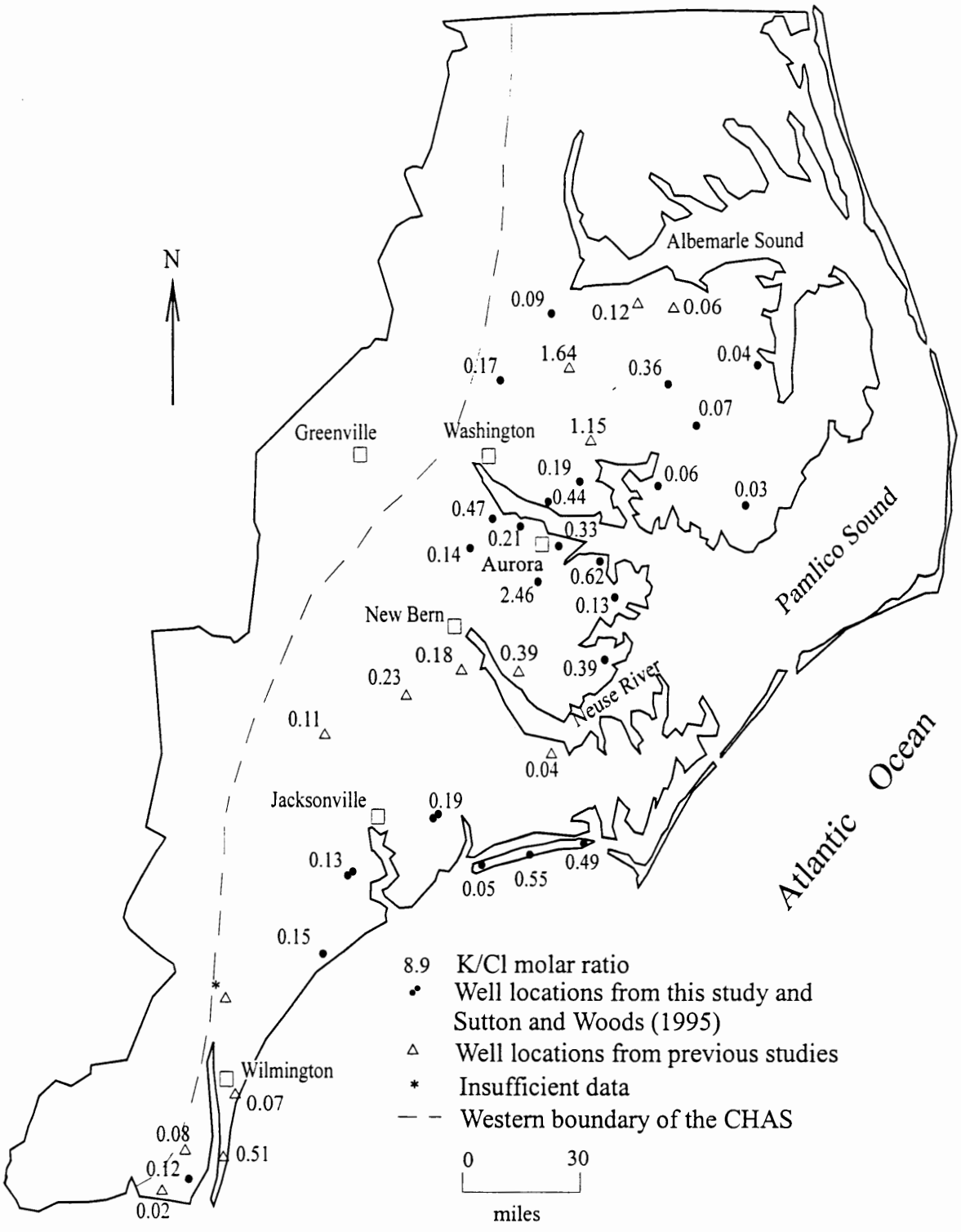

Figure 118. Molar ratio of K/Cl in the U-CHAS
* Indicates that potassium data were not available.
The molar ratio for seawater is 0.02.

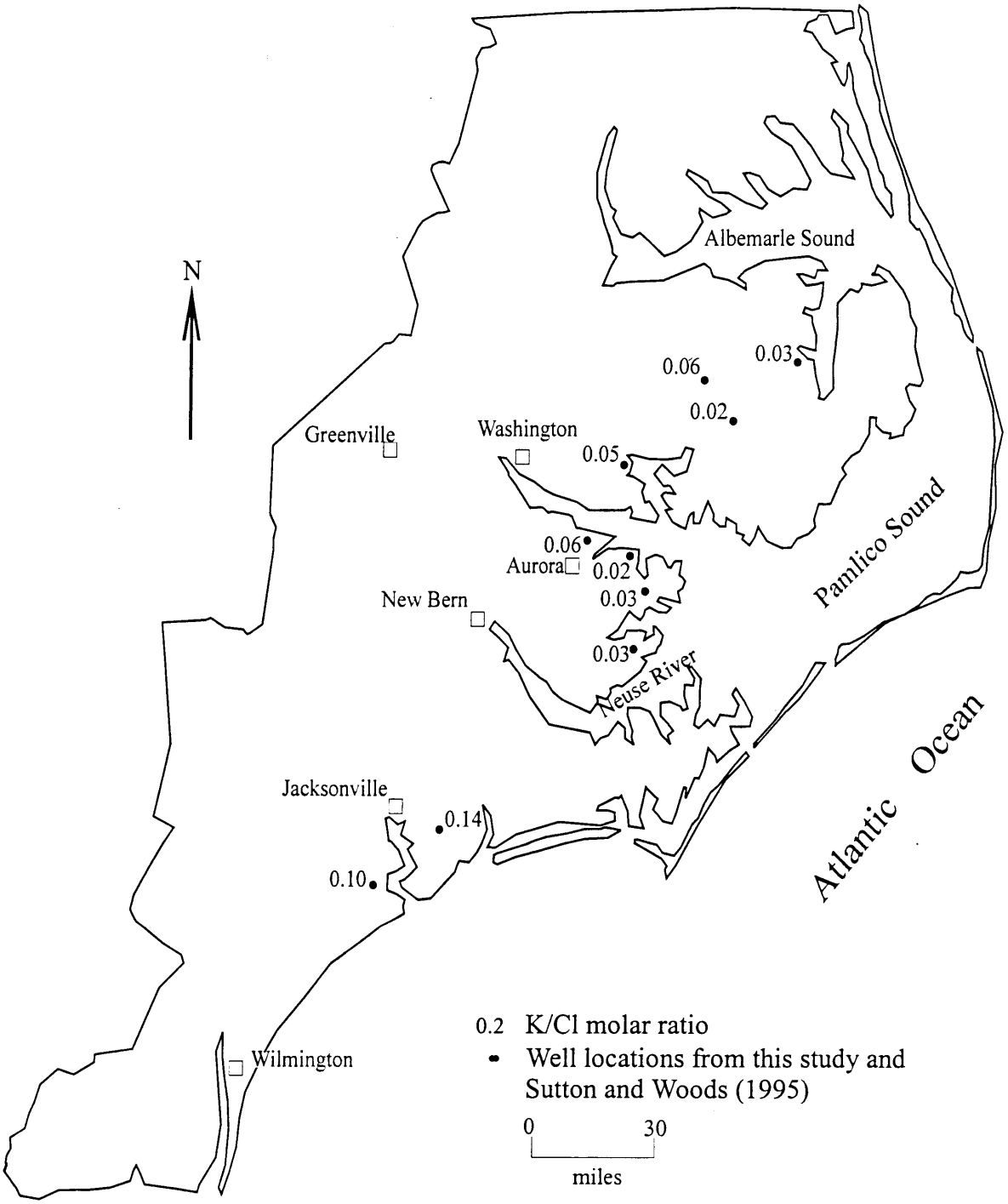

Figure 119. Molar ratio of K/Cl in the L-CHAS (The molar ratio for seawater is 0.02.)

In the Southern Coastal Plain, however, the Ca and bicarbonate water is the only hydrochemical facies seen in both the U-CHAS (Figure 36) and the L-CHAS (Figure 37), except for NH262 and BBPW5 (Figure 8). This is due to the fact that the downdip portions of the CHAS are encountered only offshore, beneath the Atlantic Ocean. NH262 is a municipal production well for Wrightsville Beach (Knobel 1985) that has probably been heavily pumped so the alkali-rich conditions here could have been induced by pumping. Well BBPW5 is probably Cl rich because of the landward migration of Cl through the White Oak River paleochannel located beneath the southwestern end of Bogue Banks. This paleochannel ranges in depth from 20 m on the landward side of the island to over 40 m on the inner continental shelf and cuts through Quaternary sediments into Tertiary units (Hine and Snyder, 1985).

Minor Elements

Fluoride concentrations generally increase from west to east in the U-CHAS (Figure 46); U-CHAS wells in the northeast corner generally have higher concentrations than L-CHAS wells (Figure 47). In wells L13i1 and M12l1 (Figure 8), F concentrations are higher than in surrounding wells. Upper and Lower CHAS wells north of the Neuse River have higher concentrations than wells south of the Neuse River. This could be due to carbonate fluorapatite in the CHAS or Pungo River Formation (Riggs 1979, 1984). The Pungo River is not present south of the Neuse River except in eastern Craven and Carteret Counties (Giese et al. 1991). As discussed earlier, leakage from overlying aquifers around L13i1 and M12l1 may explain these high F concentrations via anion exchange of OH in groundwater for F in fossils of the Pungo River Formation. With laboratory experiments and field sampling, Zack (1980) verified the potential for such ion exchange between fossil sharks teeth and groundwater in the Black Creek aquifer of South Carolina, especially in the presence of carbonate minerals and high alkalinity waters.

Fe enters groundwater due to the action of acidic, recharge waters which dissolve Fe compounds contained in soil (Wilder et al. 1978) or through the biologically mediated reduction and dissolution of Fe oxide coatings on soil minerals (Chapelle 1993). Dissolved Fe in groundwater can occur as either the ferrous (Fe^{2+}) or ferric (Fe^{3+}) ion. Ferric is highly insoluble and mobile only in strongly acidic environments, while ferrous is much more soluble and mobile over a wide range of pH (Chapelle 1993).

Two possible explanations suggest why Fe concentrations are highest in the western wells of the U-CHAS (Figure 48). First, groundwater may acquire high concentrations of Fe via the two

mechanisms discussed above, but may rapidly lose this Fe as downdip reactions with aquifer carbonates raise pH and decrease Fe solubility (Wilder et al. 1978). On the other hand, because Fe concentrations are highly dependent on the nature and thickness of the overlying units through which recharge waters pass, Fe content may be related to the lithology and thickness of surficial material and not to distance traveled down gradient (Richard Spruill, professor of geology, ECU, pers.com., 1997). Incomplete data prevent our choosing between these two alternatives at this time, but a study in progress should shed some light on this important problem. Fe in groundwater is one of the most expensive water quality issues facing suppliers of public water. Limited data inhibit description of the trend in Fe concentrations in the L-CHAS (Figure 49).

The ferrihydrite ($Fe(OH)_3$) saturation index ranges from -3.90 to +1.77 and -5.11 to +1.48 in the U-CHAS and L-CHAS, respectively (Figures 120 and 121). Ferrihydrite was chosen as the likely phase controlling Fe concentration because it is abundant in natural environments (Matsunaga et al. 1993) and has higher solubility than goethite and hematite (Langmuir 1997). Ferrihydrite also dissolves significantly faster than other Fe-oxides (e.g., goethite and hematite) (Postma 1993). The oxidation of ferrous Fe and the precipitation of ferrihydrite is shown by the following reactions:

$$Fe^{2+} + H^+ + \tfrac{1}{4}\, O_2 \rightarrow Fe^{3+} + \tfrac{1}{2}\, H_2O$$
$$Fe^{3+} + 3H_2O \rightarrow Fe(OH)_3 + 3H^+$$

(Chapelle 1993). Wells in the U-CHAS north of the Neuse River are undersaturated with ferrihydrite, while several wells south of the Neuse are oversaturated. This situation is probably because of the decreased degree of confinement in the Southwestern Coastal Plain permitting the higher O_2 concentrations to oxidize the Fe, thereby oversaturating the groundwater with ferrihydrite. Ion-exchange that involves K released into solution and Fe^{2+} adsorbed on clays is another possible explanation for the decrease in Fe concentrations from west to east (Plummer et al. 1991):

$$Fe^{2+}\ (aq) + 2K^+ - EX\ (s) \Leftrightarrow 2K^+\ (aq) + Fe^{2+} - EX\ (s).$$

Ammonia concentrations show a general increase from west to east in both CHAS units (Figures 38 and 39). At locations where wells penetrated both units, concentrations in the L-CHAS exceeded those in the U-CHAS. Concentrations in average seawater do not exceed 0.04 ppm, so intermixing of SFW is not a likely source of the ammonia unless the saline water contains significant amounts of organic matter. A possible explanation

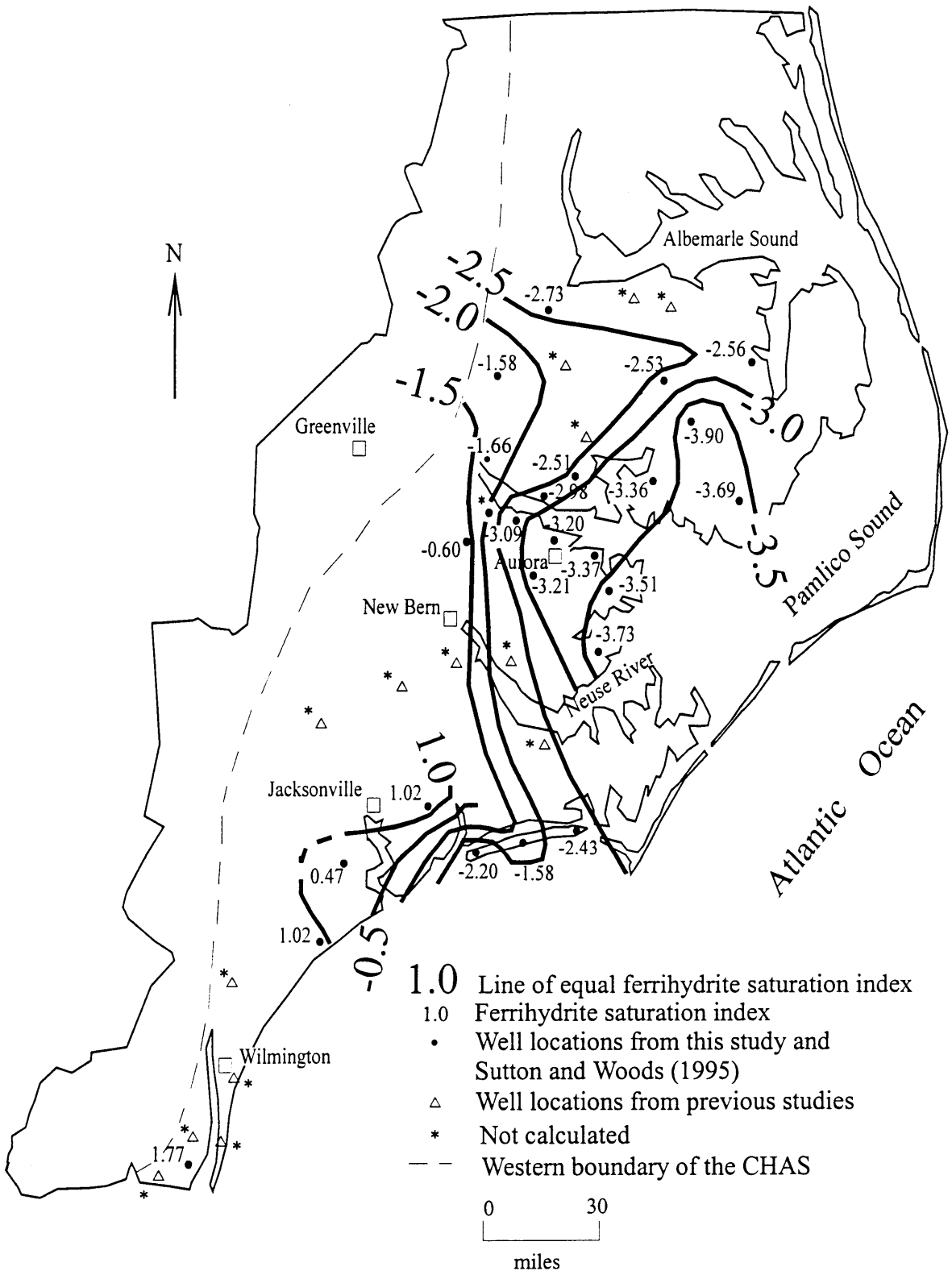

Figure 120. Ferrihydrite saturation index of the U-CHAS
* Indicates that because of insufficient data the SI could not be determined.

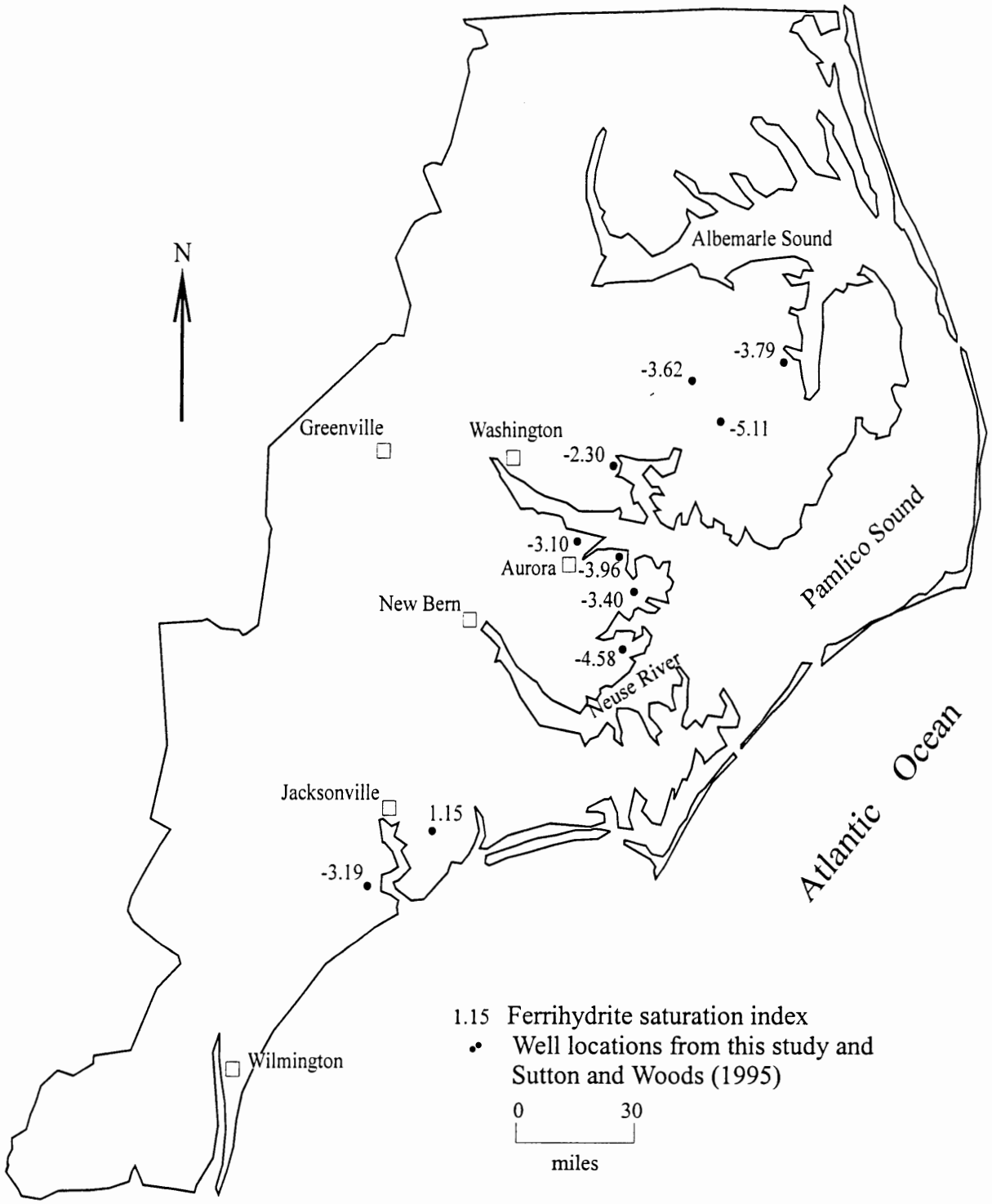

Figure 121. Ferrihydrite saturation index of the L-CHAS

for the high levels of ammonia is decomposition of amino acids in organic matter in the aquifer or in the SFW that intrudes into the aquifer. Under certain anaerobic conditions (present in the downdip portion of the CHAS), this process may release ammonia into groundwater (Drever 1997).

As pointed out by Stumm and Morgan (1981) and Drever (1997) measurements of Eh in natural waters using platinum electrodes represent mixed potentials not appropriate for quantitative interpretation. Such measurements can, however, be useful for identifying reducing and oxidizing (redox) zones. Eh values in the Upper and Lower CHAS, north of the Neuse River, generally become more negative from west to east (Figures 44 and 45) indicating that aquifer waters are becoming less oxidizing. Gradual O_2 depletion as groundwater flows down gradient away from an atmospheric source also causes a decrease in Eh. Except for BBPW5 (-6 mV), all values in the U-CHAS south of the Neuse are positive, indicating that aquifer waters are oxidizing. The anomalous Eh at BBPW5 can probably be attributed to its unconfined condition permitting recharge of lower Eh waters from overlying organic-rich soils or reactions with lithologies in the paleo-White Oak River channel.

Isotopic, Major Element, and TDS Relationships in the U-CHAS of the Northern Coastal Plain

Carbon and Oxygen Isotopes. Because most recharge waters initially contain little dissolved inorganic carbon, the carbon isotopic signature of groundwater is strongly influenced by the solids through which it flows. The $\delta^{13}C$ of dissolved inorganic carbon in recharge water percolating through soil becomes strongly depleted due to the dissolution of biogenic carbon from oxidizing organic matter. Fractionation of carbon isotopes during photosynthesis results in biogenic carbon compounds that are strongly depleted in ^{13}C and, therefore, have negative $\delta^{13}C$ values. Recharge water that has acquired it's $\delta^{13}C$ through equilibration with atmospheric CO_2 ($\delta^{13}C$ = - 7$^{o}/_{oo}$) will become even more negative as it percolates through organic-rich sediments, so $\delta^{13}C$ values in the CHAS are most negative in the recharge area (Figures 52-53). Groundwater retains the $\delta^{13}C$ acquired during percolation until it is changed by mixing with waters having different $\delta^{13}C$ values, or until it interacts with aquifer materials. Groundwater in the CHAS interacts with marine carbonate rocks of Phanerozoic age, which have $\delta^{13}C$ values near 0$^{o}/_{oo}$ wrt PDB (Keith and Weber, 1964).

As CHAS groundwater flows downgradient $\delta^{13}C$ values progressively become more positive and approach those of Castle Hayne Limestone (0$^{o}/_{oo}$) (Figures 52 and 53). In other words, incorporation of aquifer carbonate enriches groundwater in the

heavier isotope as residence times increase. Using hydraulic gradients for the U-CHAS three potential flowpaths for groundwater have been postulated (Figure 122). Flow distances from a postulated recharge boundary have been calculated for wells along these flowpaths and have been plotted versus $\delta^{13}C$ values (Figure 123). $\delta^{13}C$ values of groundwater approach those of the aquifer rock much more rapidly along flowpath 1 than they do along the two southern flowpaths. Yorktown $\delta^{13}C$ values (Figure 72) are depleted compared to those of the U-CHAS (Figure 52). Along flow paths 2 and 3 leakage from the Yorktown into the U-CHAS may be contributing to the more negative carbon isotopic signatures observed to the south. Water from some wells sampled along flowpaths 2 and 3 may also be influenced by pumping at the PCS Phosphate mine near Aurora or influx of surface water from Pamlico Sound.

In a productive aquifer with high flow rates, such as the U-CHAS, water/rock ratios are relatively high so that groundwater contains a virtually infinite reservoir of oxygen, whose composition is not readily affected by exchange reactions with minerals in the aquifer (Faure 1998). Therefore, it is commonly assumed that the oxygen isotopic content of groundwater is a conservative property, which is assumed to be equivalent to that of the precipitation in the recharge area at the time the water entered the aquifer. Studies of the Floridan Aquifer in Florida and Georgia have, in fact, shown that oxygen isotope values are largely characteristic of the recharge water that initially entered the aquifer (Plummer 1993, Clark et al. 1997). Oxygen isotopic characteristics of this recharge water were determined by the temperature and patterns of local precipitation at the time of recharge. The Floridan Aquifer is similar in age, lithology, and hydrogeologic framework to the Castle Hayne.

Adjusted radiocarbon ages in the Upper Floridan Aquifer exceed 20,000 years, which is in agreement with calculations using Darcy's Law and representative hydraulic parameters (Plummer (1993). Groundwater recharged during the last glacial maximum shows depletion in $\delta^{18}O$ and D compared to Holocene groundwater worldwide. However, oxygen isotopic data for the Floridan show a downgradient enrichment in $\delta^{18}O$ of 0.7 $^{o}/_{oo}$ to 2.3 $^{o}/_{oo}$. Eocene rocks in the Floridan range from +29 to +26 $^{o}/_{oo}$ (Sprinkle 1989) and, therefore, reaction with aquifer materials could have been responsible for the observed enrichment. However, because these paleowaters plot along the Global Meteoric Water Line with a d_{excess} similar to regional Holocene waters, Plummer (1993) concluded that the enrichment in $\delta^{18}O$ could not be attributed to isotopic exchange with the rock matrix or evaporation. Plummer (1993) attributed the enriched $\delta^{18}O$ signature of older Floridan groundwater to changes in recharge season and precipitation transport mechanism in the southeastern United States during the last glacial maximum.

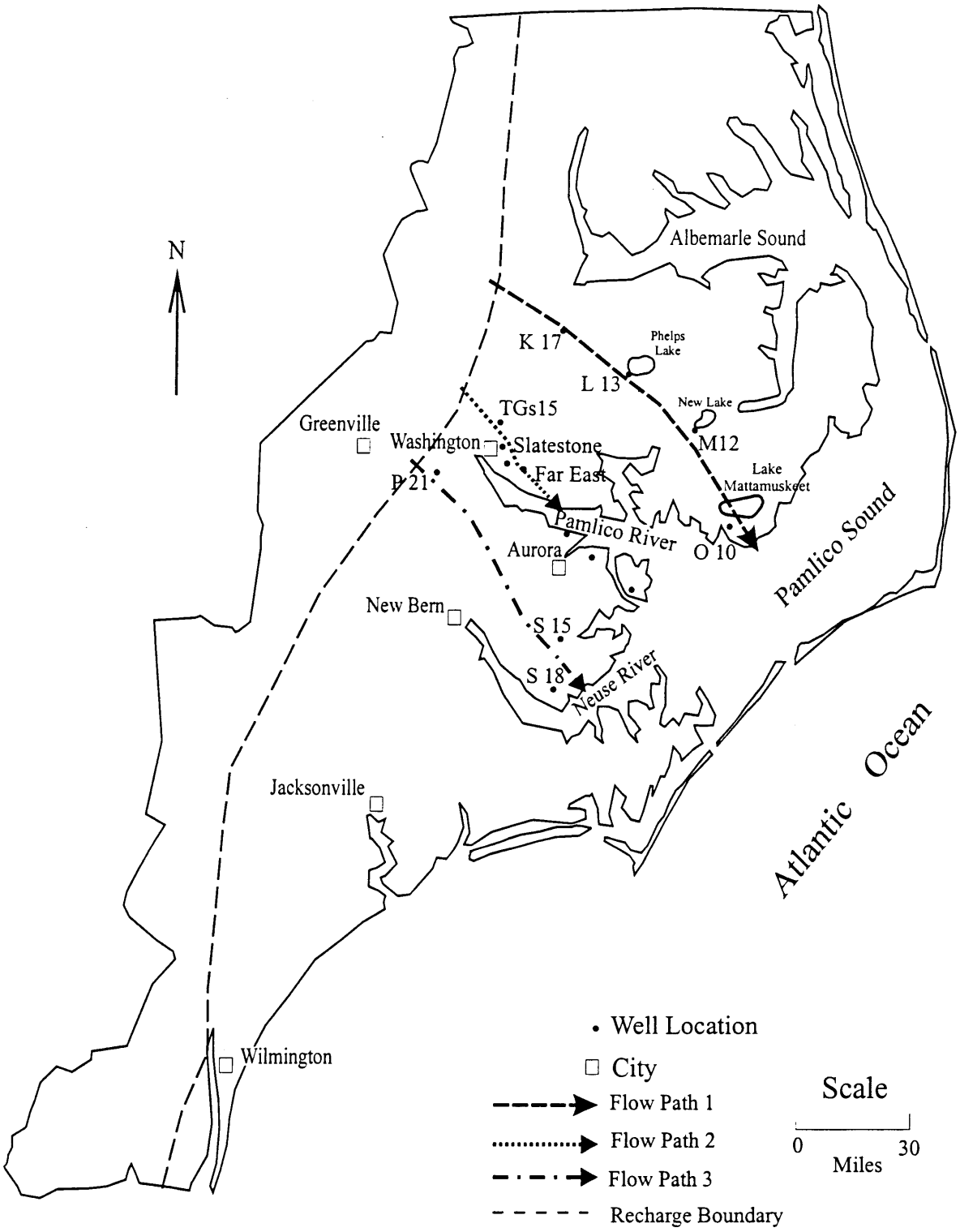

Figure 122. Three flowpaths for the U-CHA

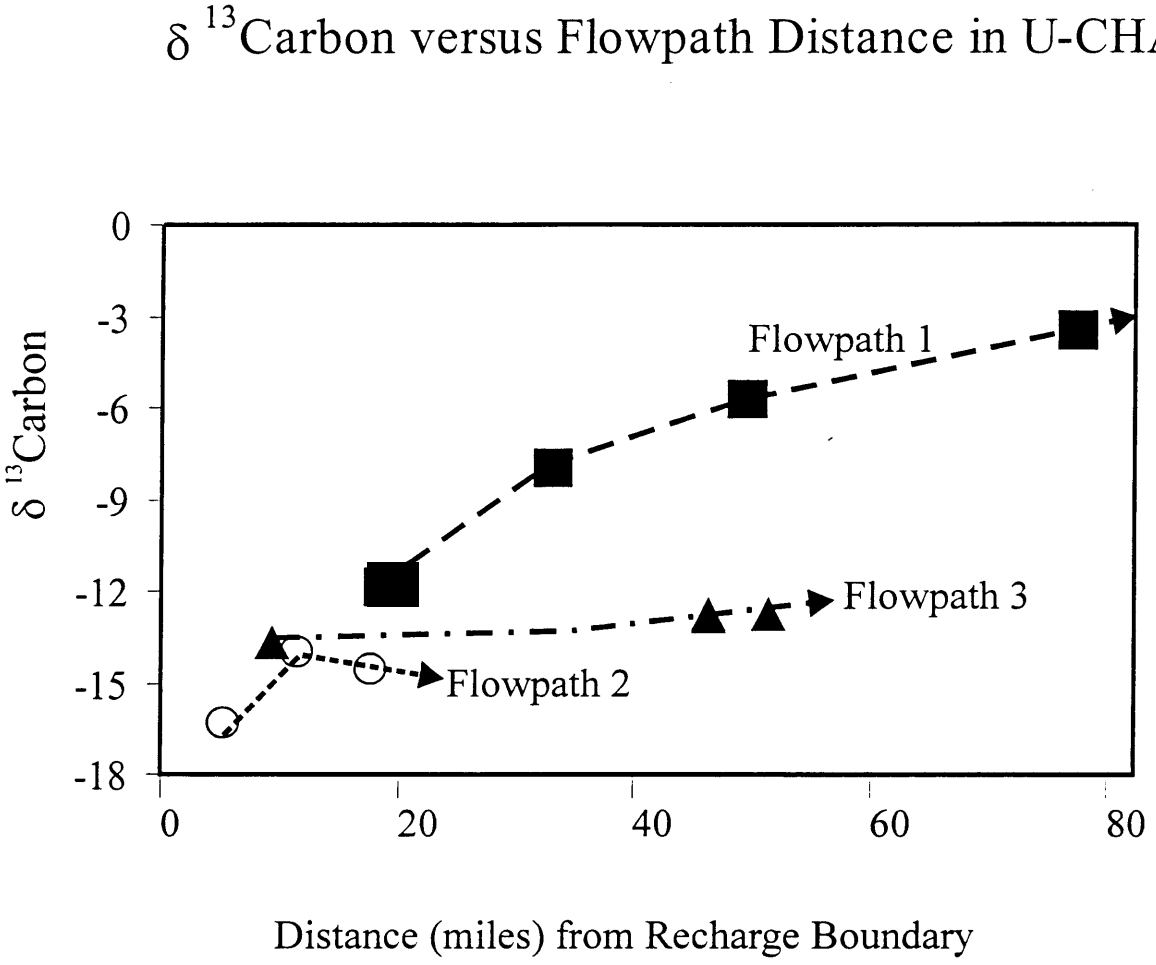

Figure 123: Graph of $\delta^{13}C$ values vs. Distance from the recharge area. Groundwater approaches $\delta^{13}C$ of Phanerozoic carbonates ($0^{\circ}/_{00}$)

Similarly to Plummer (1993), in a study of the $\delta^{18}O$ signature of U-CHAS groundwater from the Southwestern Coastal Plain of North Carolina, Sirtariotis (1998) concluded that mixing with seawater, rock-water interaction, and evaporation could not explain the observed enrichments in $\delta^{18}O$. Unlike Plummer (1993), however, he found no evidence to corroborate a change in recharge season. Instead, Sirtariotis (1998) believes that the U-CHAS groundwater preserves a paleoclimate signature inherited as a result of the ice volume effect (Faure 1998).

In the U-CHAS of the Northern Coastal Plain, wells near the recharge area show $\delta^{18}O$ values similar to average, local Holocene meteoric water (4.5 $^{\circ}/_{oo}$, Plummer 1993). Downgradient, an enrichment of 2.16 $^{\circ}/_{oo}$is observed, in comparison to a downgradient enrichment of 0.7 $^{\circ}/_{oo}$ to 2.3 $^{\circ}/_{oo}$ for different flowpaths in the Floridan Aquifer (Plummer 1993). Preliminary calculations of residence times for U-CHAS groundwater using Darcy's Law and representative hydraulic properties suggest that the oldest U-CHAS groundwater sampled so far has been in the aquifer for no more than 14,000 years. U-CHAS water from the eastern third of the study area under Pamlico Sound has not been sampled. Adjusted radiocarbon ages for Floridan groundwater are similar to estimated ages for the oldest U-CHAS, so this groundwater may preserve the $\delta^{18}O$ of water recharged during the last glacial maximum.

A reversal in the $\delta^{18}O$ enrichment trend in U-CHAS water occurs south of the Pamlico River along the western edge of Pamlico Sound (Figure 54). Leakage of surface water from Pamlico Sound is a potential cause of local depletions in $\delta^{18}O$. At the same well site, the $\delta^{18}O$ of Yorktown groundwater (Figure 73) is always depleted with respect to that from the U-CHAS suggesting that younger groundwater may also be leaking down into the U-CHAS. However, because upconing of SFW from deeper aquifers has been postulated for this region, conclusions with regards to the cause of observed isotopic patterns in U-CHAS groundwater of the Northern Coastal Plain must await further analysis of the data.

Strontium Concentrations and Isotopes. $^{87}Sr/^{86}Sr$ ratios and Sr concentrations for local surface waters and groundwater are listed in Table 5. Isotopic values for local river waters serve as a proxy for the composition of water recharging the aquifers. Rocks and fossils from Coastal Plain aquifers are characterized by strontium concentrations greater than 200 ppm (Denison et al. 1993) and groundwater and surface waters display strontium concentrations less than 10 ppm (Figure 124).

As predicted by the change in $^{87}Sr/^{86}Sr$ ratio of seawater through time (Figure 7), the ratios of rocks and fossils precipitated

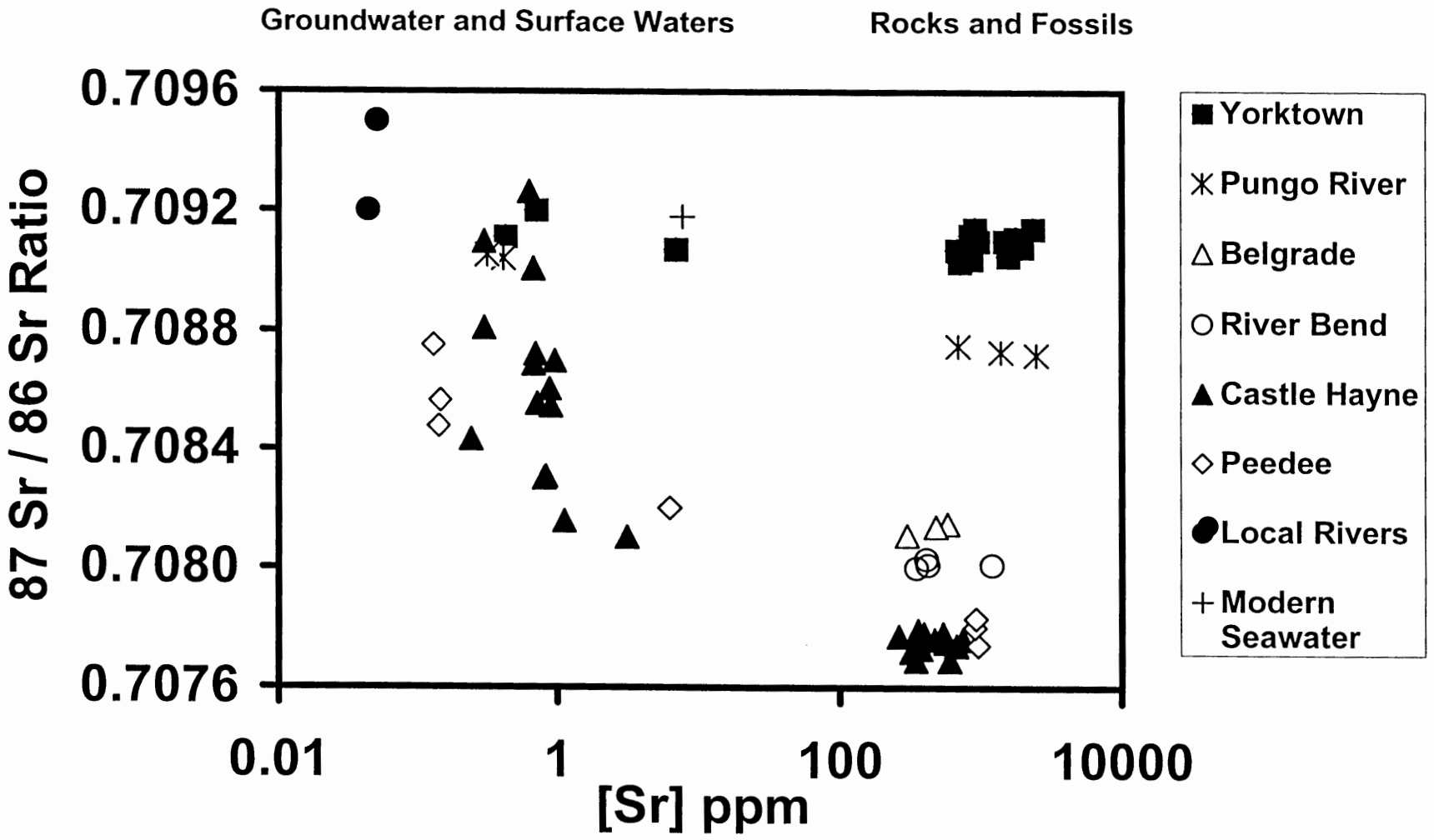

Figure 124. $^{87}Sr/^{86}Sr$ ratios plotted against strontium concentrations [Sr] for surface water, groundwater, and rocks/fossils from the Northern Coastal Plain Formations. Data for rocks/fossils are from Denison et al. 1993.

from seawater have increased with decreasing age since Eocene time (e.g., Burke et al. 1982, DePaolo and Ingram 1985, Hess et al. 1986). Paleo-seawaters and coeval rocks from marine formations have the same $^{87}Sr/^{86}Sr$ ratios because no significant fractionation of strontium isotopes occurs during formation of Sr-bearing marine precipitates. Therefore, the $^{87}Sr/^{86}Sr$ ratio of a marine precipitate records the $^{87}Sr/^{86}Sr$ ratio of the seawater from which it formed.

The relative constancy of the $^{87}Sr/^{86}Sr$ ratio in Eocene seas makes the Upper Castle Hayne a good aquifer in which to study evolution of strontium chemistry of groundwater along a flow path. Because the strontium isotopic ratio of seawater remained essentially constant throughout the time of Upper Castle Hayne deposition, this aquifer can be treated as a large reservoir of strontium with a fixed isotopic ratio (≈ 0.7077). When reaction with limestone controls strontium chemistry in groundwater, a predictable correlation between $^{87}Sr/^{86}Sr$ ratios and strontium concentrations should result. Incorporation of increasing amounts of aquifer strontium into groundwater should progressively shift the $^{87}Sr/^{86}Sr$ ratio of the groundwater towards that of the aquifer material. Poor correlations of $^{87}Sr/^{86}Sr$ ratio to Sr concentration suggest the importance of other processes such as influx of fresh or salt water from other aquifers, influx of modern sea water in estuarine environments, or influx of fresh surface waters.

To investigate this hypothesis, theoretical mixing lines were calculated describing the change in the strontium isotopic signature of groundwater as it acquires strontium from aquifer materials along a flow path. Equation 1 describes the variation in the $^{87}Sr/^{86}Sr$ ratio to be expected in a mixture generated by combining various proportions of strontium from two different end-members with different $^{87}Sr/^{86}Sr$ ratios (Faure 1998):

$$\left(^{87}Sr / ^{86}Sr\right)_{mix} = \frac{a}{[Sr]_{mix}} + b \,. \qquad (1)$$

The slope of the mixing line is calculated from Equation 2:

$$a = \frac{[Sr]_A[Sr]_B\{(^{87}Sr/^{86}Sr)_B - (^{87}Sr/^{86}Sr)_A\}}{[Sr]_A - [Sr]_B} \qquad (2)$$

and the y-intercept from Equation 3:

$$b = \frac{[Sr]_A(^{87}Sr/^{86}Sr)_A - [Sr]_B(^{87}Sr/^{86}Sr)_B}{[Sr]_A - [Sr]_B}. \qquad (3)$$

These equations require input of the $^{87}Sr/^{86}Sr$ ratios and strontium concentrations ([Sr]) of the end-members (Table 22). In this case, the first of the two end-members (A) is recharge water represented by central Coastal Plain rivers. The second end-member (B) is the aquifer material, and the average $^{87}Sr/^{86}Sr$ ratios and strontium concentrations determined by Denison et al. (1993) for appropriate rock units were used.

Table 22. Strontium chemistry of mixing end-members

End-member	87Sr/86Sr	[Sr] ppm
Local Rivers	0.70935	0.0475
Yorktown Fossils	0.70908	1376
Pungo River Fossils	0.70874	1305
Castle Hayne LS	0.70775	470

Theoretical mixing lines calculated for Yorktown, Pungo River, and Castle Hayne groundwater (Figure 125) show rapid initial decreases in $^{87}Sr/^{86}Sr$ ratio as strontium from aquifer materials is added to strontium-poor recharge water. The $^{87}Sr/^{86}Sr$ ratio of the groundwater is predicted to asymptotically approach the isotopic ratio for the aquifer materials. Replotting these data on a graph of $^{87}Sr/^{86}Sr$ ratio versus 1/Sr using an arithmetic scale yields straight lines and reverses the position of the aquifer materials and recharge waters (Figure 126). Groundwater analyses plot on or above the theoretical mixing line calculated for the source aquifer. Castle Hayne samples have much higher $^{87}Sr/^{86}Sr$ ratios than predicted by the mixing calculations and there is significant scatter.

Processes other than incorporation of aquifer strontium into groundwater are indicated by the U-CHAS isotopic data. Strontium with a higher $^{87}Sr/^{86}Sr$ ratio is being added, and groundwater in aquifers above the U-CHAS is characterized by higher $^{87}Sr/^{86}Sr$ ratios. In western parts of the U-CHAS aquifer, leakance of groundwater from overlying aquifers may account for the observed variability in strontium isotope geochemistry. Other studies have indicated that a significant hydraulic connection exists between the Castle Hayne and overlying aquifers (Warner 1993, Amsbaugh 1996, Consolvo 1998) and that significant vertical head differences generated in these aquifers since the onset of heavy pumping have initiated downward leakance (Winner and Coble 1996, Giese et al. 1991).

Variations in major elements and isotopic ratios with TDS. Graphs of major element concentrations (in ppm) versus TDS were constructed to compare samples and help identify regions affected by different hydrologic and geochemical processes

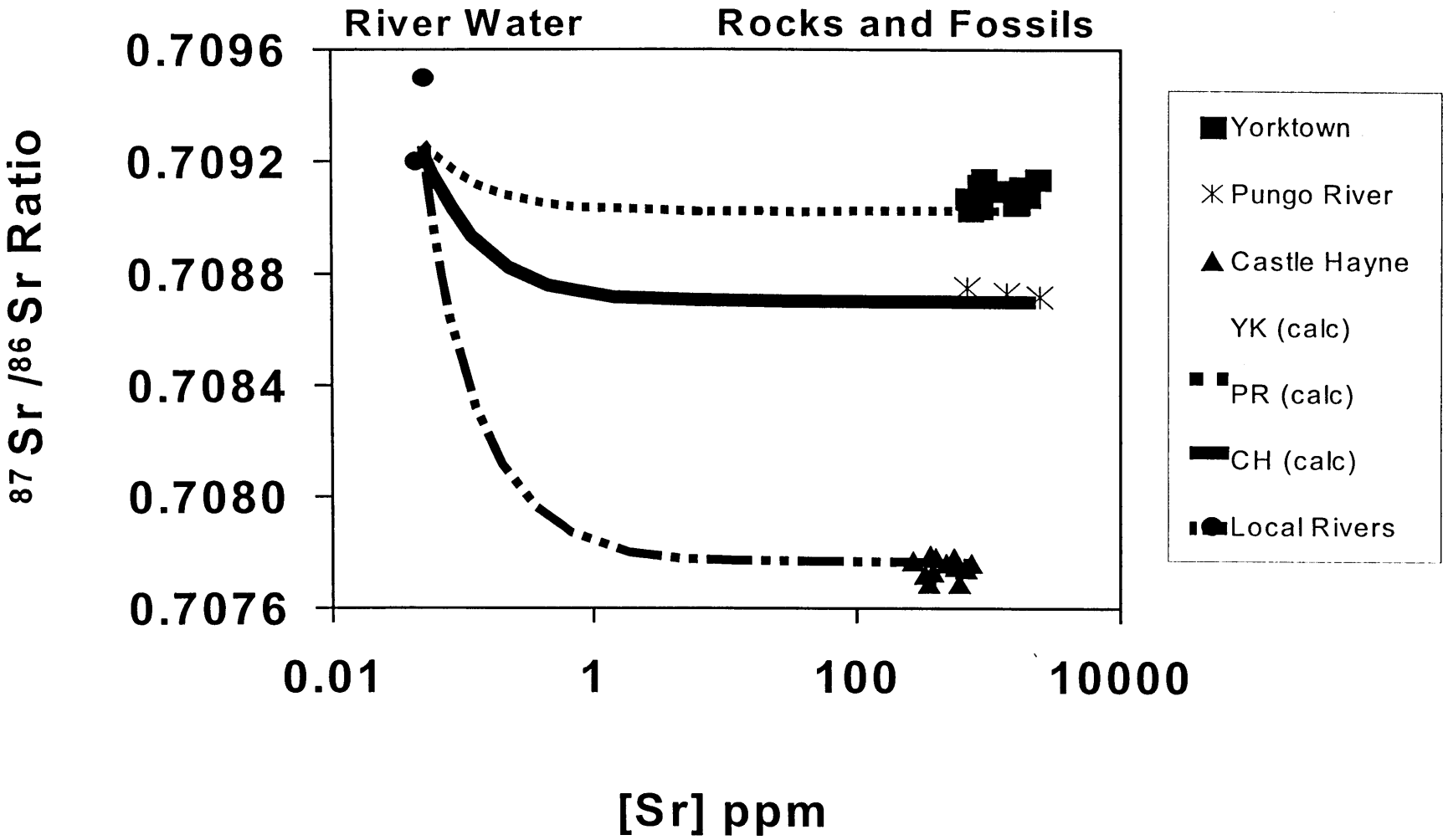

Figure 125. Calculated strontium concentrations [Sr] and $^{87}Sr/^{86}Sr$ ratios for mixtures containing various proportions of aquifer strontium. Data for rocks/fossils are from Denison et al. 1993.

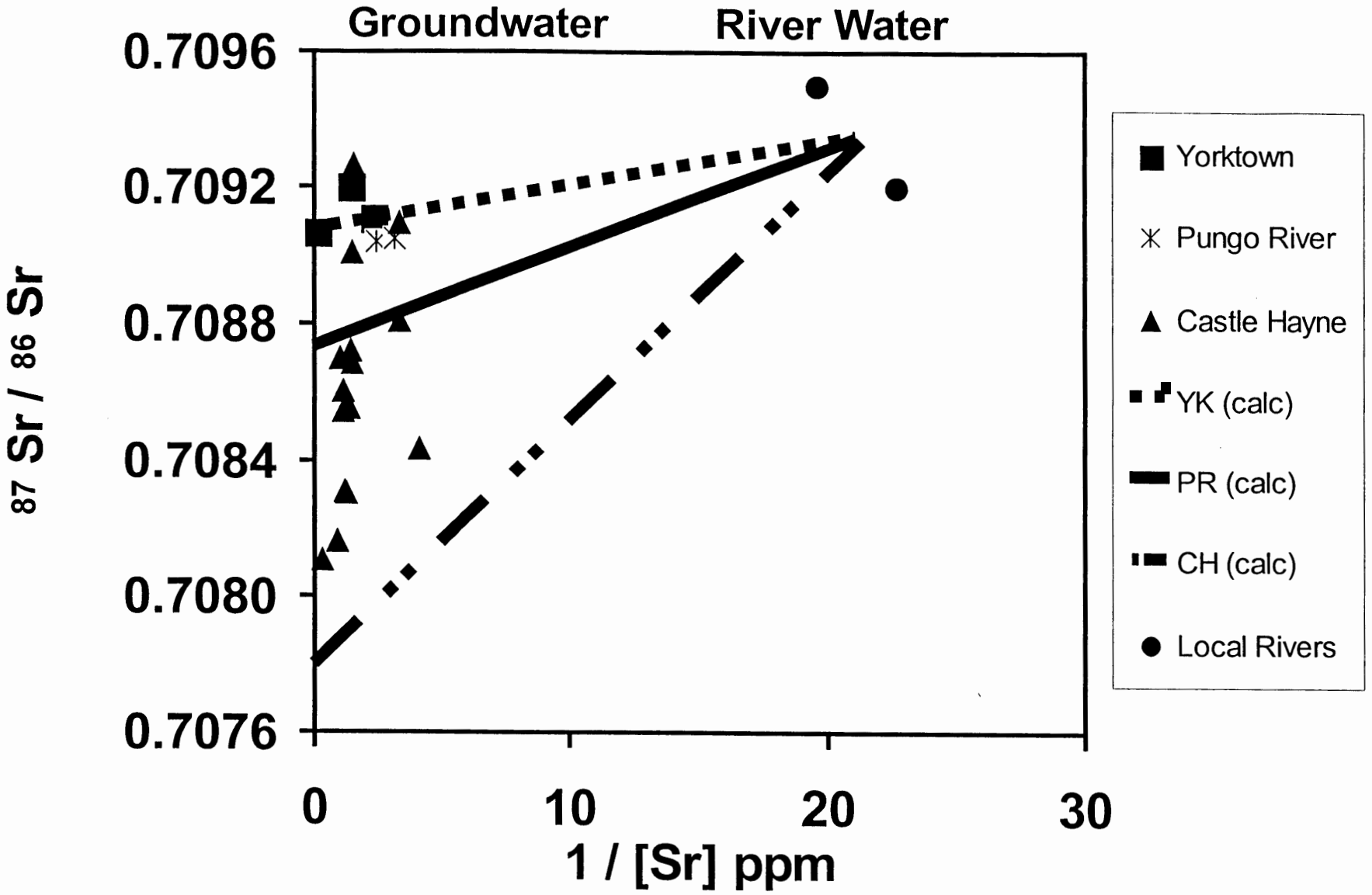

Figure 126. Strontium chemistry of groundwater from the Yorktown, Pungo River and U-CHAS compared to calculated mixing lines.

(Figure 127). These relationships consistently reveal three groups with TDS ranges of 310-640 ppm, 950-970 ppm, and 1290-4690 ppm, respectively. Low-TDS groundwater from the western part of the study area shows a linear increase in alkalinity as TDS increases (Figure 127). Data points identified by sample site plot off this trend and do not show a close correlation between alkalinity and TDS. On the alkalinity, calcium, and magnesium graphs (Figures 127a, b, and d) the low- and high-TDS samples define different trends of concentration versus TDS. On the sulfate, chloride, and sodium graphs (Figures 127c, e, and f) low-TDS samples are virtually devoid of the constituent ion and high-TDS water shows an increasing concentration of the ion with increasing TDS. Water analyses from wells K17a5 and Q15u3 (Figure 8) generally plot between the two trends. These different groupings or trends delineate waters that may have been subjected to different geochemical and hydrologic processes.

$^{87}Sr/^{86}Sr$ ratios and strontium concentrations for U-CHAS groundwater (Figure 128) fall into similar high-, low-, and intermediate-TDS groupings. The low-TDS groundwater has higher $^{87}Sr/^{86}Sr$ ratios and the more saline samples have low $^{87}Sr/^{86}Sr$ ratios. These relationships indicate that groundwater from the U-CHAS displays a decrease in $^{87}Sr/^{86}Sr$ ratio with increasing TDS.

Regional Groundwater System Controls on Groundwater Chemistry. Chemical evolution of U-CHAS groundwater is influenced by large scale hydrologic processes and the aquifer system can be subdivided into two distinct hydrologic environments (Figure 129). At the same time, however, chemical reaction and exchange with aquifer minerals significantly affect groundwater chemistry throughout the system. The western up-dip area is characterized by a low degree of aquifer confinement and by significant interaction with shallow aquifers and surface water recharge. The eastern down-dip area of the U-CHAS is characterized by significant aquifer confinement and is influenced by proximity to the fresh water/salt water interface. Near the boundary between these two areas, long-term (1965 to present), depressurization pumping (average rate of 50 mgd; Leggette et al. 1991) at the phosphate mine at Aurora (Figure 1) has resulted in significant upconing of saline water directly beneath the mine. Processes within these distinct hydrologic environments significantly affect groundwater chemistry, as evidenced by the strontium isotopic relationships (Figure 129). Near the western recharge areas, low-TDS groundwater with variable $^{87}Sr/^{86}Sr$ ratios is the result of mixing of surface water with U-CHAS groundwater and other shallow groundwater derived from younger aquifers. Farther down-dip, high-TDS groundwater with $^{87}Sr/^{86}Sr$ ratios of 0.7084 (or less) is apparently influenced by

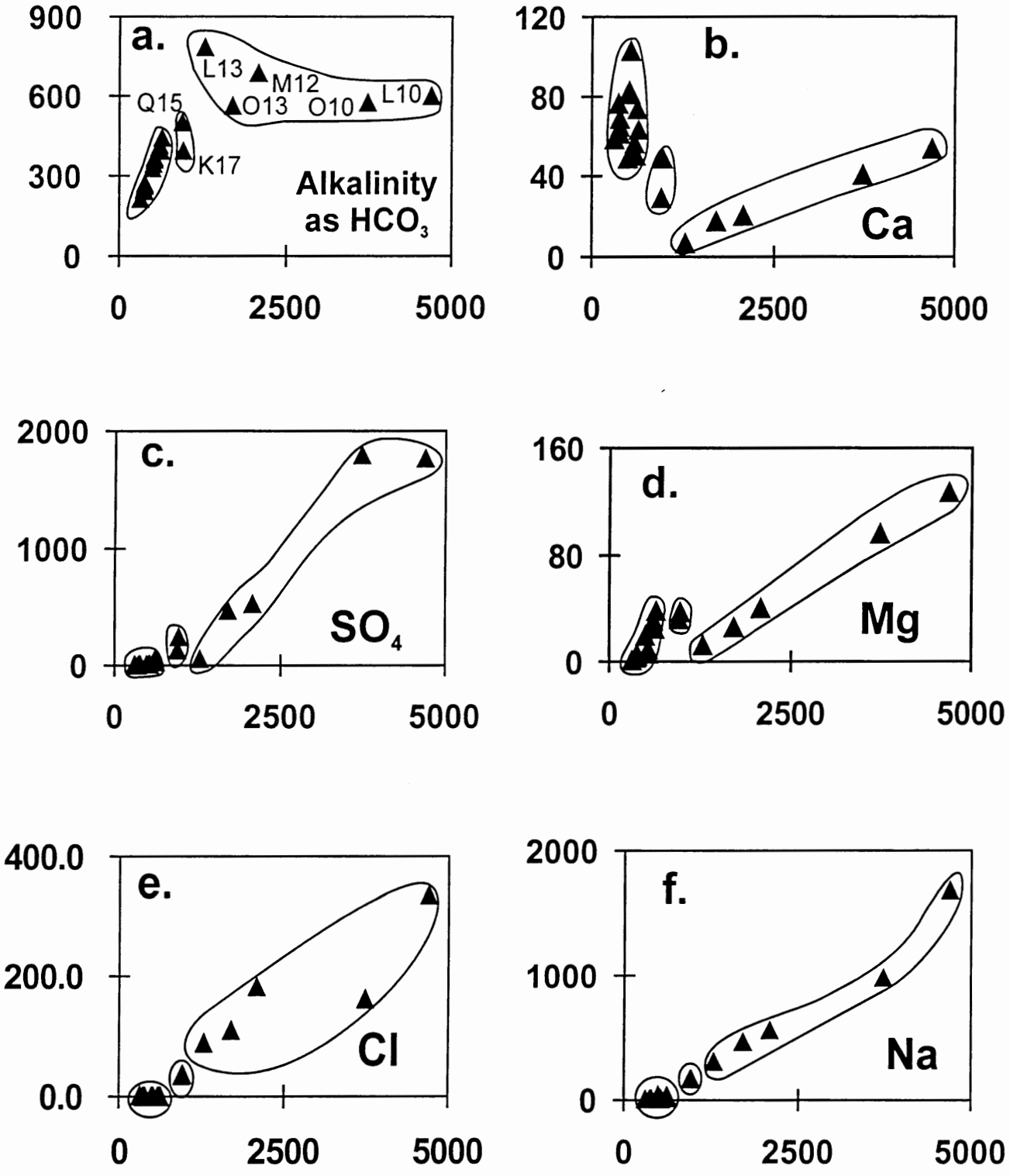

Figure 127. Major element concentrations plotted against TDS for U-CHAS groundwater from the Northern Coastal Plain

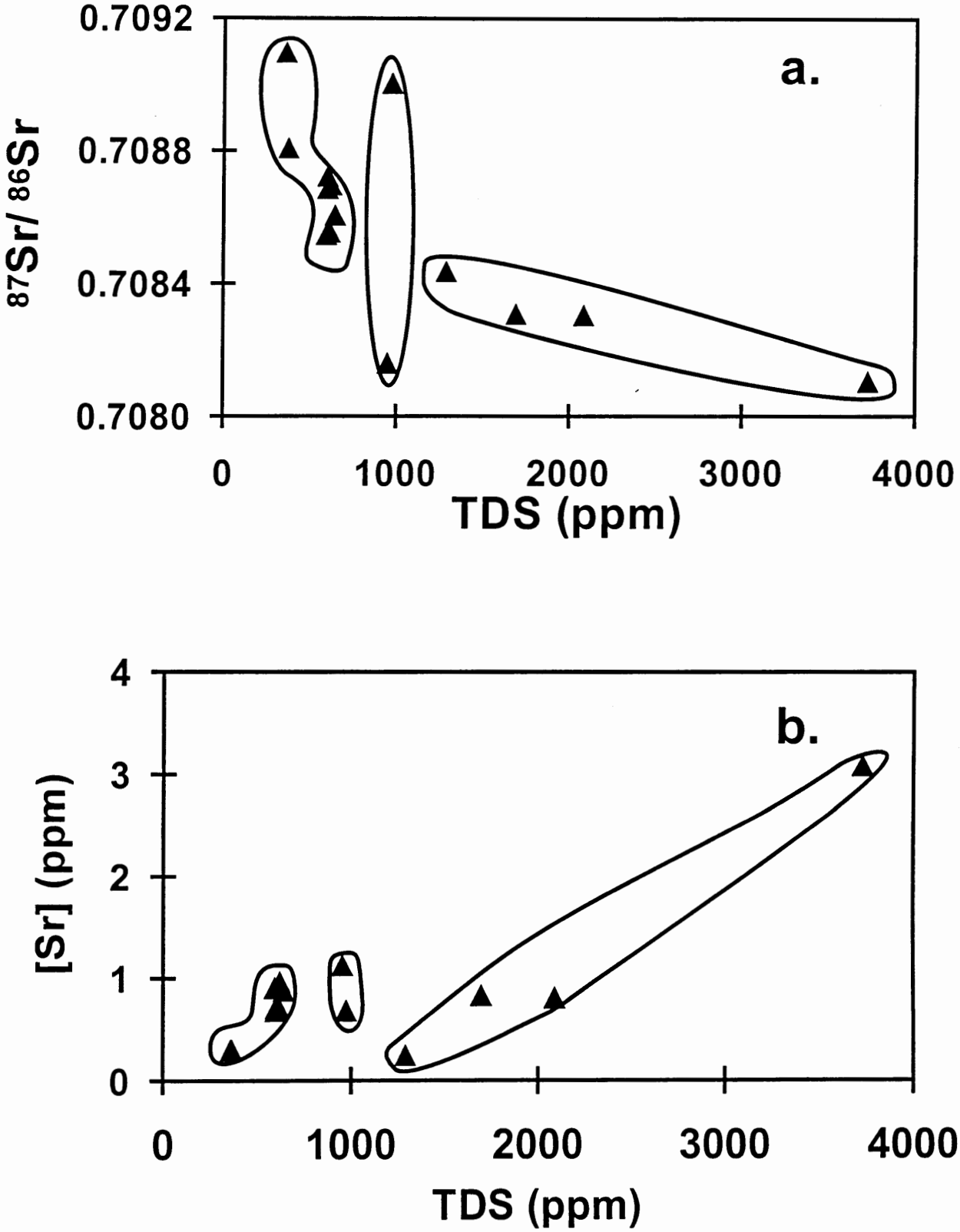

Figure 128. $^{87}Sr/^{86}Sr$ ratios and strontium concentrations plotted against TDS for U-CHAS groundwater from the Northern Coastal Plain

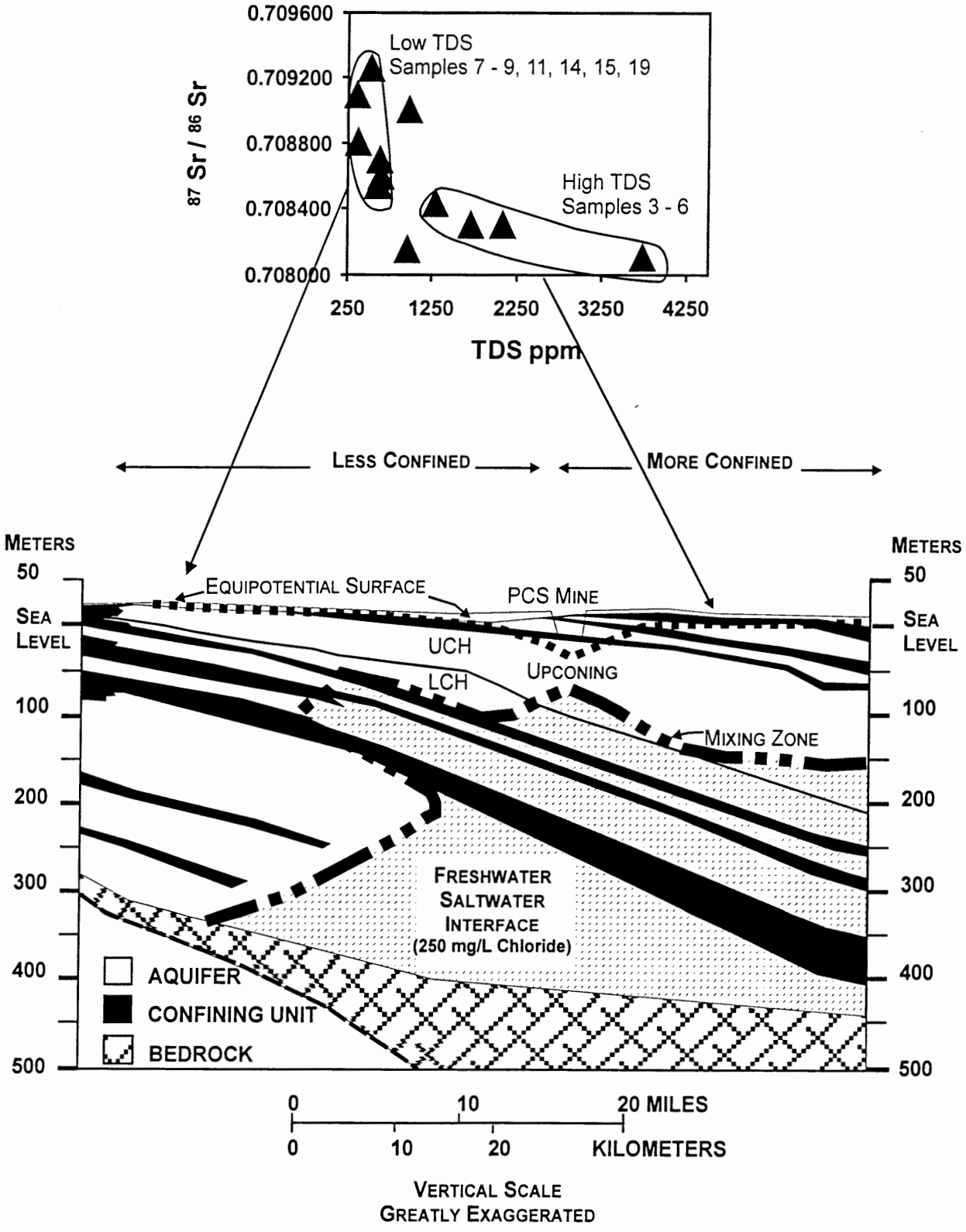

Figure 129. Conceptual view of hydrologic processes in the Northern Coastal Plain

interaction between progressively older eastward flowing groundwater in the U-CHAS and mixing at the fresh water/salt water interface.

Plots of ion concentrations versus TDS (Figures 127-128) delineate waters with chemistries that are apparently determined by different geochemical and hydrologic processes. Two obvious processes influencing the water chemistry of carbonate aquifers in coastal plain settings are dissolution/precipitation reactions involving limestone and intermixing of saline formation waters. In the U-CHAS system these two distinct processes appear to dominate water chemistry in the up-dip and down-dip regions, respectively. However, as indicated most clearly by strontium data described here, leakance of water from overlying aquifers can also be very important in areas where an aquifer is poorly confined.

Calcium and magnesium dominate the cations in the dilute Ca-HCO_3 waters from the U-CHAS in the western part of the study area (Figures 26 and 28). Observed trends in alkalinity, calcium, and magnesium (Figure 127) suggest the importance of dissolution and precipitation reactions involving carbonate minerals. Within analytical error, all waters in the study are saturated with calcite, which may control the concentration of Ca^{2+} throughout the aquifer. Water to the west is less saturated where influx of CO_2-rich recharge occurs, and undersaturated groundwater to the east may be related to the position of the salt water/fresh water interface. However, as observed by Chapelle and Knobel (1983) and Sprinkle (1989), local cation exchange reactions with clay minerals undoubtedly affect concentrations of calcium and other cations. As pointed out by Katz et al. (1996), cation exchange may also be a major mechanism for changing the $^{87}Sr/^{86}Sr$ ratio of groundwater. They discovered significant variation in the $^{87}Sr/^{86}Sr$ ratio of groundwater from the Floridan Aquifer where calcite was saturated and should not have been dissolving. In these regions they found no evidence that salt water intrusion or leakance from other aquifers was significantly influencing groundwater chemistry.

U-CHAS groundwater with high TDS (>1290) is characterized by the lowest $^{87}Sr/^{86}Sr$ ratios (L13i1, M12l1, O10w3, and O13f1 on Figure 126), and was collected farthest east in the aquifer from greater depths below the land surface. These wells are outside the cone of depression generated by pumping at the mine and have, therefore, not been disturbed by downward leakance generated by this pumping. The data points plot on a trend of decreasing $^{87}Sr/^{86}Sr$ ratio with increasing strontium concentration that generally parallels the theoretical mixing line, suggesting that strontium chemistry has been determined by progressive exchange with the U-CHAS limestone. The increasing

salinity may be due to the westward migration of the salt water/fresh water interface within the aquifer, which could bring older U-CHAS water westward. This water has been reacting with the limestone for a longer period of time and has evolved farther toward the low $^{87}Sr/^{86}Sr$ ratio of U-CHAS rock (0.70775). Influx of modern seawater or water from Pamlico Sound is an unlikely source of saline water because these surface waters would have much higher $^{87}Sr/^{86}Sr$ ratios ($\cong$0.7092) than the limestone and would tend to raise the ratio in groundwater.

Samples with higher $^{87}Sr/^{86}Sr$ ratios (0.7085 or higher) are from farther west in the recharge area where the aquifer is semi-confined to unconfined and where relatively young waters have not had much time to acquire aquifer strontium. Some of these samples may also have been affected by downward leakance of higher $^{87}Sr/^{86}Sr$ water due to the head reversals generated by extensive pumping at the PCS Phosphate Mine.

LIST OF REFERENCES

Ames, D.v.d.P. 1994. Petrology and stratigraphy of the Miocence Pungo River and Pliocene Yorktown Formations in the Aurora area, North Carolina. M.S. thesis, East Carolina Univ., Department of Geology, Greenville, NC.

Amsbaugh, M.B. 1996. Ground-water geology of the Castle Hayne aquifer system in the vicinity of Hubert and Sneads Ferry, North Carolina: for the Onslow County well field. M.S. thesis, East Carolina Univ., Department of Geology, Greenville, NC.

American Public Health Association. 1992. Standard methods for the examination of water and waste water. 18th ed., Washington, D.C.

American Public Health Association. 1995. Standard methods for the examination of water and waste water. 19th ed., Washington, D.C.

Bailey, S.W. 1980. Summary of recommendation of AIPEA Nomenclature Committee. Clay Minerals 23:85-93.

Baker, P.A., and M. Kastner. 1981. Constraints on the formation of sedimentary dolomite. Science 213:214-16.

Banner, J.L. 1995. Application of the trace element and isotope geochemistry of strontium to studies of carbonate diagenesis. Sedimentology 42:805-24.

Banner, J.L., G.N. Hanson, and W.J. Meyers. 1988. Determination of initial Sr isotopic compositions of dolostones from the Burlington-Keokuk Formation (Mississippian): Constraints from cathodoluminescence, glauconite paragenesis and analytical methods. Journal of Sedimentary Petrology 58:673-87.

Banner, J.L., G.J. Wasserburg, P.F. Dobson, A.B. Carpenter, and C.H. Moore. 1989. Isotopic and trace element constraints on the origin and evolution of saline groundwaters from central Missouri. Geochim. Cosmochim. Acta 53:383-98.

Banner, J.L., M. Musgrove, and R.C. Capo. 1994. Sr isotopes: Effects of multiple sources of dissolved ions and mineral-solution reactions. Geology 22:687-90.

Baum, G.R. 1977. Stratigraphic framework of the Middle Eocene to Lower Miocene Formations of North Carolina. Ph.D. diss., University of North Carolina, 139p.

Baum, G.R., W.B. Harris, and V.A. Zullo. 1978. Stratigraphic revision of the exposed Middle Eocene to Lower Miocene Formations of North Carolina. Southeastern Geol. 20:1-19.

Baum, G.R., J.S. Collins, R.M. Jones, B.A. Madlinger, and R.J. Powell. 1979a. Tectonic history and correlation of the Eocene strata of the Carolinas, Preliminary report *in* Baum, G.R. et al. (eds.), Structural and Stratigraphic Framework for the Coastal Plain of North Carolina: Carolina Geological Society Field Trip Guidebook, American Coastal Plain Geological Association Guidebook for the Annual Field Conference, p. 87-94.

Baum, G.R., H.B. Harris, and V.A. Zullo. 1979b, Historical review of Eocene to Early Miocene stratigraphy, North Carolina, *in* Baum, G.R. et al. (eds.), Structural and Stratigraphic Framework for the Coastal Plain of North Carolina: Carolina Geological Society Field Trip Guidebook, American Coastal Plain Geological Association Guidebook for the Annual Field Conference, p. 2-15.

Beck, E.G. 1997. Groundwater geochemistry of the Castle Hayne Aquifer System in the North Carolina Coastal Plain. M.S. thesis, East Carolina Univ., Department of Geology, Greenville, NC.

Birch, G.F., J.P. Willis, and R.S. Rickard. 1976. An electron microscope study of glauconites from the continental margin off the west coast of South Africa. Marine Geol. 22:271-83.

Bohlke, J.K., and J.M. Denver. 1995. Combined use of groundwater dating, chemical, and isotopic analyses to resolve the history and fate of nitrate contamination in two agricultural watersheds, Atlantic coastal plain, Maryland, Water Resources Research 31:2319-39.

Bohn, H.L., B.L. McNeal, and G.A. O'Conner. 1985. Soil Chemistry, 2nd ed. New York: Wiley and Sons.

Boichard, R., P.F. Burollet, B. Lambert, and J.M. Villain. 1985. La plateforme carbonatee du Pater Noster (Indonesie). Total C^{ie} Franc. Petroles Publ., Mem. 20, 130p.

Brown, P.M., J.A. Miller, and F.M. Swain. 1972. Structural and Stratigraphic Framework and Spatial Distribution of the

Permeability of the Atlantic Coastal Plain, New York to North Carolina. U.S. Geol. Surv. Prof. Paper 796, 79 p.

Buchler Instruments, Inc. 1981. Buchler digital Choridometer Instruction Manual, Model 4-2500, Fort Lee, N.J.: Buchler Instruments, Inc. 10 p.

Buckley, H.A., J.C. Bevan, K.M. Brown, L.R. Johnson, and V.C. Farmer. 1978. Glauconite and celadonite: Two separate mineral species. Mineralogical Magazine 42:373-382.

Burst, J.F. 1958a. "Glauconite" pellets: Their mineral nature and application to stratigraphic interpretation. Amer. Assoc. of Petroleum Geologists Bull. 42:310-327.

Burst, J.F. 1958b. Mineral heterogeneity in "glauconite" pellets. Amer. Mineralogist 43:481-497.

Caldeira, K. 1992. Enhanced Cenozoic chemical weathering and the subduction of pelagic carbonate. Nature 357:578-81.

Cander, H.S. 1994. An example of mixing-zone dolomite, Middle Eocene Avon Park Formation, Floridan aquifer system. Jour. of Sed. Research A64:615-29.

Carpenter, J.S., and K.C. Lohmann. 1992. Sr/Mg ratios of modern marine calcite: Empirical indicators of ocean chemistry and precipitation rate. Geochim. Cosmochim. Acta 56:1837-49.

Chapelle, F.H. 1983. Ground-water geochemistry and calcite cementation of the Aquia aquifer in southern Maryland. Water Resource Research 19:545-58.

Chapelle, F.H. 1993. Ground-water microbiology and geochemistry. New York: John Wiley & Sons, Inc.

Chapelle, F.H., and L.L. Knobel. 1983. Aqueous geochemistry and the exchangeable cation composition of glauconite in the Aquia Aqifer, Maryland. Ground Water 21:343-52.

Chapelle, F.H., and D.R. Lovley. 1990. Rates of microbial metabolism in deep Coastal Plain aquifers. Applied and Environmental Microbiology 56:1865-74.

Chapelle, F.H., and P.B. McMahon. 1991. Geochemistry of dissolved inorganic carbon in Coastal Plain aquifer: Sulfate from confining beds as an oxidant in microbial CO_2 production. Journal of Hydrology 127:85-108.

Chapelle, F.H., J.T. Morris, P.B. McMahon, and J.L. Zelibor, Jr. 1988. Bacterial metabolism and the delta-13C composition of ground water, Floridan aquifer system, South Carolina. Geology 16:117-121.

Chaudhuri, S., V. Broedel, and N. Clauer. 1987. Strontium isotopic evolution of oilfield waters from carbonate reservoir rocks in Bindley field, central Kansas, USA. Geochim. Cosmochim. Acta 51:45-53.

CHEMetrics Inc. 1995. CHEMetrics Sulfide Instruction Manual, Model K-9510. Calverton, VA. CHEMetrics Inc. 4 p.

Clark, W.B. 1909. Results of a recent investigation of the Coastal Plain Formation in the area between Massachusetts and North Carolina. Geol. Soc. of Amer. Bull. 20:646-654.

Clark, J.F., M. Stute, P. Schlosser, and S. Drenkard. 1997. A tracer study of the Floridan aquifer in southeastern Georgia: Implications for groundwater flow and paleoclimate. Water Resources Research 33:281-289.

Collerson, K.D., W.J. Ullman, and T. Torgersen. 1988. Ground waters with unradiogenic $^{87}Sr/^{86}Sr$ ratios in the Great Artesian Basin, Australia. Geology 16:59-63.

Consolvo, C. 1998. Hydrogeologic investigation and wellhead protection planning for the Castle Hayne Aquifer near Washington, North Carolina. M.S. thesis, East Carolina Univ., Department of Geology, Greenville, NC.

Cunliffe, J.E. 1968. Petrology of the Cretaceous Peedee Formation and Eocene Castle Hayne Limestone in northern New Hanover County, North Carolina. M.S. thesis, University of North Carolina, Department of Geology, Chapel Hill, NC.

Cunliffe, J.E. and D.A. Textoris. 1969. Petrology of the Cretaceous Peedee Formation and Eocene Castle Hayne Limestone in northern New Hanover County, North Carolina. Geol. Soc. of Amer. Special Paper 121, 178 p.

Denison, R.E., E.A. Hetherington, B.A. Bishop, D.A. Dahl, and R.B. Koepnick. 1993. The use of strontium isotopes in stratigraphic studies: An example from North Carolina. Southeastern Geol. 33:53-69.

DePaolo, D.J., and B.L. Ingram. 1985. High-resolution stratigraphy with strontium isotopes. Science 227:938-41.

DeWiest, R.J.M. 1969. Hydrologic relationship between the Pamlico River and the Castle Hayne Aquifer in Eastern North Carolina. Preprint 830, American Society of Civil Engineers, Annual Meeting on Water Resources Engineering, Feb. 1969.

Drever, J.I. 1997. The geochemistry of natural waters 3rd ed. Upper Saddle River, N.J.: Prentice Hall.

Driscoll, F.G. 1986. Groundwater and wells. 2nd ed. St. Paul MN: Johnson Infiltration Systems, Inc.

Dunham, R.J. 1962. Classification of carbonate rocks according to depositional texture *in* Ham, W.E. (ed.), Classification of Carbonate Rocks. Amer. Assoc. of Petroleum Geologist, Memoir, 1, p. 108-121.

Edmond, J.M. 1992. Himalayan tectonics, weathering processes, and the strontium isotope record in marine limestones. Science 258:1594-97.

Ehlmann, A.J., N.C. Hulings, and E.D. Glover. 1963. Stages of glauconite formation in modern foraminiferal sediments. Jour. of Sed. Pet. 33:87-96.

Environmental Protection Agency. 1979. Methods for chemical analysis of water and wastes, EPA-600/4-79-020.

Faure, G. 1998. Principles and applications of inorganic geochemistry. New York: Macmillan Publ. Co.

Faure, G., P.M. Hurley, and J.L. Powell. 1965. The isotopic composition of strontium in surface water from the North Atlantic Ocean. Geochim. Cosmochim. Acta 29:209-20.

Faure, G., R. Assereto, and E.L. Tremba. 1978. Strontium isotope composition of marine carbonates of the Middle Triassic to Early Jurassic age, Lombardic Alps, Italy. Sedimentology 25:523-43.

Folk, R.L. 1962. Spectral subdivision of limestone types *in* Ham, W.E., (ed.), Classification of Carbonate Rocks. Amer. Assoc. of Petroleum Geologists, Memoir 1:62-84.

Francois, L.M., and J.C.G. Walker. 1992. Modelling the Phanerozoic carbon cycle and climate: constraints from the 87Sr/86Sr isotopic ratio of sea water. American Jour. Science 292:81-135.

Gambell, A.W., and D.W. Fisher. 1966. Chemical composition of rainfall, western North Carolina and southeastern Virginia: U.S. Geol. Surv. Water Supply Paper 1535-K.

Gamus, W.J. 1972. Analysis of factors controlling groundwater flow for prediction of rates for groundwater movement and changes in quality, Atlantic Coastal Plain. Ph.D. diss., University of Arizona, Department of Hydrology, Tucson, Arizona.

Geophex, Ltd. 1994. Final report on groundwater resource evaluation at Marine Corps Air station, New River Engineering Study 93-09. Submitted to Department of the Navy Officer in Charge of Construction Naval Engineering Facilities Command Environmental Management Division, Camp Lejeune, NC, Job No. 365.

Giese, G.L., J.L. Eimers, and R.W. Coble. 1991. Simulation of ground-water flow in the coastal plain aquifer system of North Carolina. U.S. Geol. Surv. Open-File Report 90-372.

Giese, G.L., R.R. Mason, and A.G. Strickland. 1987. North Carolina ground-water quality. U.S. Geol. Surv. Open-File Report 87-0743.

Grasshoff, K., M. Erhardt, and K. Kremling (eds). 1983. Methods of seawater analysis, 2nd ed. Weinheim, West Germany: Verlag Chemie.

Hardy, M.A., P.P. Leahy, and W.M. Alley. 1989. Well installation and documentation, and ground-water sampling protocols fro the pilot national water-quality assessment program. U.S. Geol. Surv. Open-File Report 89-396.

Harned, D.A., and M.S. Davenport. 1990. Water-quality trends and basin activities and characteristics of the Albemarle-Pamlico Estuarine System, North Carolina and Virginia. U.S. Geol. Surv. Open File Report 90-398.

Harned, D.A., O.B. Lloyd, Jr., and M.W. Treece, Jr. 1989. Assessment of hydrologic and hydrogeologic data at Camp Lejeune Marine Corps base, North Carolina. U.S. Geol. Surv. Water-Resource Investigation Report 89-4096.

Harris, W.B., and V.A. Zullo. 1980. Rb-Sr glauconite isochron of the Eocene Castle Hayne Limestone, North Carolina. Geol. Soc. of Amer. Bull., Part I 91:587-92.

Heald-Wetlaufer, N.K. Foley, and D.O. Hayba. 1982. Process mineralogy II: Application in metallurgy, ceramics, and

geology, *in* Hagni, R.D. (ed.), Proceedings of a Symposium Sponsored by the Process Mineralogy Committee of the Metallurgical Society of AIME: Dallas, TX, p. 451-68.

Hess, J., M.L. Bender, and J.G. Schilling. 1986. Evolution of the ratio of Strontium-87 to Strontium-86 in seawater from Cretaceous to present. Science 231:979-984.

Hine, A.C., and S.W. Snyder. 1985. Coastal lithosome preservation: Evidence from the shoreface and inner continental shelf off Bogue Banks, NC. Marine Geology 63:307-30.

Instrumentation Laboratory, Inc. 1981. Operator's manual for models IL357 and 457 AA/AE spectrophotometers. Wilm., MA.

Jackson, M.L. 1979. Soil Chemical Analysis Advanced Course. Department of Soil Science, University of Wisconsin, Madison, 895 p.

Joint Study, 1971. (North Carolina Board of Water and Air Resources, Texasgulf Sulfur, NC Phosphate Corp.) Hydrogeology and effects of pumping from Castle Hayne aquifer system. 146 p.

Johnson, J.J. 1992. Evaluation of potential recharge of the Castle Hayne aquifer system in the vicinity of Tranters Creek, Beaufort County, North Carolina. M.S. thesis, East Carolina Univ., Department of Geology, Greenville, NC.

Jones, M. 1984. Nitrate reduction by shaking with cadmium: alternative to cadmium columns. Water Research 18:643-46.

Junge, C.E., and R.T. Werby. 1958. The concentration of chloride, sodium, potassium, calcium, and sulfate in rainwater over the United States. Journal of Meteorology 15:417-25.

Katz, B.G. 1992. Hydrochemistry of the Upper Floridan Aquifer, Florida. U.S. Geol. Surv. Water-Resources Investigations Report 91-4196.

Katz, B.G. and T.D. Bullen. 1996. The combined use of $^{87}Sr/^{86}Sr$ and carbon and water isotopes to study the hydrochemical interaction between groundwater and lake water in mantled karst. Geochim. Cosmochim. Acta 60:5075-5087

Katz, B.G., L.N. Plummer, E. Busenberg, K.M. Revesz, B.F Jones, and T.M. Lee. 1995. Chemical evolution of groundwater near a sinkhole lake, northern Florida: Chemical patterns, mass

transfer modeling, and rates of mass transfer reactions. Water Resources Research 31:1565-84.

Keith, M.L., and J.N. Weber. 1964. Carbon and oxygen isotopic composition of selected limestones and fossils. Geochim. Cosmochim. Acta 28: 1787-1816.

Klein, C., and C.S. Hurlbut, Jr. 1993. Manual of mineralogy. New York: John Wiley & Sons, Inc.

Knobel, L.L. 1985. Ground-water quality data for the Atlantic Coastal Plain: New Jersey, Delaware, Maryland, Virginia, and North Carolina. U.S. Geol. Surv. Open-File Report 85-154, 84 p.

Koroleff, F. 1976. Deterimination of ammonia, *in* Grasshoff, K. (ed.), Methods of seawater analysis. Weinheim, West Germany: Verlag Chemie. p. 126-33.

Langmuir, D. 1997. Aqueous environmental geochemisty. New York: Prentice Hall, Inc.

Lautier, J.C. 1994. Wilmington Harbor Ground Water Study: Interim Report: North Carolina Department of Environment, Health, and Natural Resources Division of Water Resources.

Lawrence, F.W., and S.B. Upchurch. 1982. Identification of recharge areas using geochemical factor analysis. Ground Water 20:680-87.

Leggette, Brashears, and Graham, Inc. 1991. Texasgulf, Inc. Aurora Phosphate Mine-Technical report in support of renewal and modification of water use permit no. 3. Tampa, Florida.

LeGrand, H.E. 1960. Geology and ground-water resource of Wilmington-New Bern area. U.S. Geol. Surv. Ground-water Bulletin Number 1.

Lindholm, R.C., and R.B. Finkelman. 1972. Calcite staining: Semiquantitative determination of ferrous iron. Jour. of Sed. Pet. 42:239-42.

Lloyd, O.B., Jr., and C.C. Daniel. 1988. Hydrogeologic setting, water levels, and quality of water from supply wells at the U.S. Marine Corps Air Station, Cherry Point, North Carolina. U.S. Geol. Surv. Water-Resources Investigations Report 88-4034.

Lovley, D.R., J.P. Phillips, and D.J. Lonergan. 1991. Enzymatic versus nonenzymatic mechanisms for Fe(III) reduction in aquatic sediments. Environmental Sciences and Technology 26:1062-1067.

Lovley, D.R., and F.H. Chapelle. 1995. Deep Subsurface Microbial Processes. Reviews of Geophys. 33:365-81.

Lyke, W.L., and A.R. Brockman. 1990. Ground-water pumpage and water-level declines in the Peedee and Black Creek aquifers in Onslow and Jones Counties, North Carolina, 1900-86. U.S. Geol. Surv. Water-Resources Investigation Report 89-4197.

Lyke, W.L., and M.W. Treece, Jr. 1988. Hydrogeology and effects of ground-water withdrawals in the Castle Hayne aquifer in coastal North Carolina, *in* Lyke, W.L. and T.G. Hoban (eds.), Proceedings of the Symposium on Coastal Water Resources, Wilmington, NC.

Matsunaga, T., G. Karametaxas, H.R. von Gunten, and P.C. Lichtner. 1993. Redox chemistry of iron and manganese minerals in river-recharged aquifers: A model of interpretation of a column experiment. Geochim. Cosmochim. Acta 57:1691-1704.

McMahon, P.B., and F.H. Chapelle. 1991. Geochemistry of dissolved inorganic carbon in a Coastal Plain aquifer: 2. Modeling carbon sources, sinks, and delta-13 C evolution. Jour. of Hydrology 127:109-35.

McNutt, R.H., S.K. Frape, and P. Fritz. 1984. Strontium isotopic composition of some brines from the Precambrian Shield of Canada. Isotope Geosci. 2:205-15.

McNutt, R.H., S.K. Frape, P. Fritz, M.G. Jones, and I.M. MacDonald. 1990. The 87Sr/86Sr values of Canadian Shield brines and fracture minerals with applications to groundwater mixing, fracture history, and geochronology. Geochim. Cosmochim. Acta 54:205-15.

Meisler, H. 1989. The occurrence and geochemistry of salty ground water in the northern Atlantic Coastal Plain. U.S. Geol. Surv. Prof. Paper 1404-D.

Moran, L.K. 1989. Petrography of unconformable surfaces and associated stratigraphic units of the Eocene Castle Hayne Formation, southeastern North Carolina coastal plain. M.S. Thesis, East Carolina University, Department of Geology, Greenville, NC.

Morton, A.C., R.J. Merriman, and J.G. Mitchell. 1984. Genesis and significance of glauconite sediments of the Southwest Rockall Plateau, *in* Roberts, D.G. et al. (eds.), Initial Reports of the Deep Sea Drilling Project, 81, U.S. Government Printing Office, Washington, D.C., p. 645-652.

Murphy, E.N., S.N. Davis, A. Long, D. Donahue, and A.J.T Jull. 1989. Characterization and isotopic composition of organic and inorganic carbon in the Milk River Aquifer. Water Resources Research 25:1893-1905.

Nesbitt, H.W., and J.J. Cramer. 1993. Genesis and evolution of HCO_3-rich and SO_4-rich ground waters of Quaternary sediments, Pinawa, Canada. Geochim. Cosmochim. Acta 57:4933-46.

North Carolina Department of Natural and Economic Resources (NCDNER). 1974. Status report on ground-water conditions in Capacity Use Area No. 1, central coastal plain: North Carolina Ground-water Bulletin No. 21.

North Carolina Department of Natural and Economic Resources (NCDNER). 1976. Interim report on groundwater conditions in Capacity Use Area No. 1, central coastal plain, North Carolina, 1974-1975, Washington, NC.

North Carolina Department of Environment, Health, and Natural Resources (NCDEHNR). 1987. Unpublished water chemistry data for the Castle Hayne Aquifer System, Wilmington, NC.

O'Brien, G.W., A.R. Milnes, H.H. Veeh, D.T. Heggie, S.R. Riggs, D.J. Cullen, J.F. Marshall, and P.J. Cook. 1990. Sedimentation dynamics and redox iron-cycling: Controlling factors for the apatite-glauconite association on the East Australian Continental Margin, *in* A.J.G. Notholt and I. Jarvis (eds.), Phosphorite Research and Development, Geological Society Special Publication 52:61-86.

Oceanography International Corporation Model 524C Instruction Manual. 1976.

Odin G.S., and A. Matter. 1981. De glauconiaurm origine. Sedimentology 28:611-641.

Odin, G.S. and Stephan, J.F. 1981. The occurrence of deep water glaucony from the Eastern Pacific: The result of *in situ* genesis or subsidence? *in* J.S. Watkins et al. (eds.), Initial Reports of Deep Sea Drilling Project, vol. 66, p. 419-428.

Odin, G.S., and P.D. Fullagar. 1988. Geological significance of the glaucony facies, *in* Odin, G.S. (ed.), Green Marine Clays, Developments in Sedimentology No. 45. New York: Elsevier.

Odom, I.E. 1984. Glauconite and celadonite Minerals, *in* Bailey, S.W. (ed.), Reviews in Mineralogy, vol. 13, Mineralogical Society of America, Washington, D.C., p. 545-572.

Orion Scientific Instruments Corporation. No date. Nitrite or nitrate and nitrite in water or seawater, Product Information Pamphlet for Modular Continuous Flow Analyzer (M/CFA).

Orion Scientific Instruments Corporation. No date. Orthophosphate in water and seawater, Product Information Pamphlet for Modular Continous Flow Analyzer (M/CFA).

Orion Research, Inc. 1989. Model 94-16 silver/sulfide electrode manual. Part No. 502700-033 Form IM9416/9860 Rev. B.

Otte, L.J. 1981. Petrology of the exposed Eocene Castle Hayne Limestone of North Carolina: Ph.D. diss., University of North Carolina, Chapel Hill, NC.

Otte, L.J. 1986. Regional perspective on the Castle Hayne Limestone, *in* Textoris, D.A. (ed.), SEPM Field Guidebook: Southeastern United States, Third Annual Midyear Meeting, Raleigh, NC.

Palmer, M.R., and J.M. Edmond. 1989. The strontium isotope budget of the modern ocean. Earth and Planetary Science Letters 29:11-26.

Palmer, M.R., and J.M. Edmond. 1992. Controls over the strontium isotope composition of river water. Geochim. Cosmochim. Acta 56:2099-2111.

Parkhurst, D.L., D.C. Thorstenson, and L.N. Plummer. 1980. PHREEQE - A computer program for geochemical calculations. U.S. Geol. Surv. Water-Resources Investigations Report 80-96.

Piper, A.M. 1944. A graphic procedure in the geochemical interpretation of water analyses. Trans. Amer. Geophys. Union 25:914-23.

Pitman, W.C., III. 1978. Relationship between eustacy and stratigraphic sequences of passive margins. Geol. Soc. Amer. Bull. 89:1389-1403.

Plummer, L.N., E.C. Prestemon, and D.L. Parkhurst. 1991. An interactive code (NETPATH) for modeling NET geochemical reactions along a flow PATH. U.S. Geol. Surv. Water-Resources Investigations Report 91-4078.

Plummer, L.N., J.F. Busby, R.W. Lee, and B.B. Hanshaw. 1990. Geochemical modeling of the Madison Aquifer in parts of Montana, Wyoming, and South Dakota. Water Resources Research 26:1981-2014.

Plummer, L.N., D.L. Parkhurst, and D.C. Thorstenson. 1983. Development of reaction models for ground-water systems. Geochim. Cosmochim. Acta 47:665-86.

Postma, D. 1993. The reactivity of iron oxides in sediments: A kinetic approach. Geochim. Cosmochim Acta 57:5027-34.

Randazzo, A.F. and E.W. Hickey. 1978. Dolomitization in the Floridan Aquifer. Amer. Jour. of Sci. 278:1177-84.

Raymo, M.E., and W.F. Ruddiman. 1992. Tectonic forcing of late Cenozoic climate. Nature 359:117-22.

Reynolds, J.W. 1992. Aquifer depressurization for mining at Texasgulf, Inc.: evaluation and modeling of hydrogeologic impacts and potential mitigative strategies: M.S. Thesis, East Carolina Univ., Department of Geology, Greenville, NC.

Reynolds, J.W., and R.K. Spruill. 1995. Ground-water flow simulation for management of a regulated aquifer system: A case study in the North Carolina Coastal Plain. Ground Water 33:741-748.

Riggs, S.R. 1979. Phosphorite sedimentation in Florida--A model phosphogenic system. Economic Geol. 74:285-314.

Riggs, S.R. 1984. Paleoceanographic model of Neogene phosphorite deposition, US Atlantic continental margin. Science 223:123-31.

Riggs, S.R., D.W. Lewis, A.K. Scarborough, and Scott W. Snyder. 1982. Cyclic deposition of Neogene phosphorites in the Aurora area, North Carolina, and its possible relationship to global sea-level fluctuations. Southeastern Geol. 23:189-204.

Rightmire, C.T., F.J. Pearson, Jr., W. Back, R.O. Rye, and B.B. Hanshaw. 1974. Distribution of sulphur isotopes of sulphates in ground waters from the principal artesian

aquifer of Florida and the Edwards aquifer in Texas, U.S.A., *in* Isotope techniques in ground-water hydrology 2:191:207, International Atomic Energy Agency, Vienna, Austria.

Rossum, J.R., and P. Villarruz. 1961. Suggested methods for turbidimetric determination of sulfate in water. Jour. Amer. Water Works Assoc. 53:873.

San Juan, F.C., Jr., and R.P. Sinha. 1994. Preliminary investigation of the uranium isotope disequilibrium in the ground and surface waters of northeastern North Carolina and southeastern Virginia. Report SRS-13 of The Univ. of North Carolina Water Resources Research Institute, Raleigh, NC.

Sheen, R.T., H.L. Kahler, and E.M. Ross. 1935. Turbidimetric determination of sulfate in water. Ind. Eng. Chem., Anal. Ed. 7:262.

Sherwani, J.K. 1980. Public policy for the management of groundwater in the Coastal Plain of North Carolina. Report No. 129 of The Univ. of North Carolina Water Resources Research Institute, Raleigh, NC.

Siegal, M.D., and S. Anderholm. 1994. Geochemical evolution of groundwater in the Culebra Dolomite near the Waste Isolation Pilot Plant, southeastern New Mexico, USA. Geochim. Cosmochim. Acta 58:2299-2323.

Sirtariotis, Nikolaos. 1998. Application of isotopes to the study of regional groundwaters in the Southern Coastal Plain of North Carolina. M.S. thesis, Univ. of North Carolina, Department of Geology, Wilmington, NC.

Smith, D.G., E.D. George, and P.L. Breton. 1996. Water Resources Data North Carolina Water Year 1995, Volume 2. Ground-Water Records. US Geol. Surv. Water-Data Report NC-95-2.

Sohl, N.F., and J.P. Owens. 1991. Cretaceous stratigraphy of the Carolina Coastal Plain, *in* Horton J.W., Jr. and V.A. Zullo (eds.), The Geology of the Carolinas. Carolina Geol. Soc. 50th Anniv. Vol. Knoxville: Univ. of Tenn. Press., p. 191-220.

Solorzano, L. 1969. Determination of ammonia in natural waters by the phenol hypochlorite method. Limnol. Oceanogr. 14:799-801.

Sotera, J.J., and R.L. Stux. 1979. Instrumentation Laboratory, Inc. Atomic Absorption Methods Manual. vol. 1, Wilmington, MA.

Sprinkle, C.L. 1989. Geochemistry of the Floridan aquifer system in Florida and in parts of Georgia, South Carolina, and Alabama. U.S. Geol. Surv. Prof. Paper 1403-I.

Stainton, M.P., M.J. Capel, and F.A.J. Armstrong. 1974. The chemical analysis of fresh water. Environment Canada Miscellaneous Publ. No. 25, Research and Development Directorate, Freshwater Institute, Winnipeg, Canada, 119 p.

Stanley, D.W. 1987. Water quality in the Pamlico River Estuary. Institute for Coastal and Marine Resources Technical Report 87-01. East Carolina Univ., Greenville, NC.

Starinsky, A., M. Bielski, B. Lazar, G. Steinizt, and M. Raab. 1983. Strontium isotope evidence on the history of oilfield brines, Mediterranean Coastal Plain, Israel. Geochim. Cosmochim. Acta 47:687-95.

Strickland, J.D.H., and T.R. Parsons. 1968. A practical handbook of sea water analysis. Fisheries Research Board of Canada Bull. 167.

Stueber, A.M., L.M. Walter, T.J. Huston, and P. Pushkar. 1993a. Origin and chemical evolution of formation waters from Silurian-Devonian strata in the Illinois basin, USA. Geochim. Cosmochim Acta 55:309-25.

Stueber, A.M., L.M. Walter, T.J. Huston, and P. Pushkar. 1993b. Formation waters from Mississippian-Pennsylvanian reservoirs, Illinois basin, USA: Chemical and isotopic constraints on evolution and migration. Geochim. Cosmochim Acta 57:763-84.

Stueber, A.M., P. Pushkar, and E.A. Hetherington. 1987. A strontium isotopic study of formation waters from the Illinois basin, USA. Appl. Geochem. 2:477-94.

Stueber, A.M., P. Pushkar, and E.A. Hetherington. 1984. A strontium isotopic study of Smackover brines and associated solids, southern Arkansas. Geochim. Cosmochim. Acta 48:1637-49.

Stumm, W., and J.J. Morgan. 1981. Aquatic Chemistry. New York: John Wiley & Sons, Inc.

Sunwall, M.T., and P. Pushkar. 1979. The isotopic composition of strontium in brines from petroleum fields of southeastern Ohio. Chem. Geol. 24:189-97.

Sutton, L.C., and T.L. Woods. 1995. Geochemistry of ground water from the Castle Hayne aquifer in northeastern North Carolina. Southeastern Geol. 35:93-119.

Sutton, L.C., and T.L. Woods. 1994. Groundwater geochemistry of the Castle Hayne aquifer in the region of Capacity Use Area No. 1, northeastern North Carolina. Report SRS-15 of The Univ. of North Carolina Water Resources Research Institute, Raleigh, NC.

Textoris, D.A. 1967. Preliminary investigation of the petrology of the Castle Hayne Limestone: Proceedings of symposium on hydrology of the coastal waters of North Carolina. Report No. 5 of The Univ. of North Carolina Water Resources Research Institute, Raleigh, NC.

Textoris, D.A. 1969. Porosity control by original skeletal mineralogy in Mesozoic and Tertiary carbonates. Geol. Soc. of Amer. Special Paper 121, 295 p.

Textoris, D.A., A.F. Randazzo, and P.A. Thayer. 1972. Diagenesis of carbonate sediments as important non-cavern porosity controls. Proceedings of 24th International Geological Congress, Montreal, Canada, p. 190-197.

Thayer, P.A. and D.A. Textoris. 1972. Petrology and Diagenesis of Tertiary Aquifer Carbonates, North Carolina. Transactions of the Gulf Coast Association of Geol. Societies 22:257-266.

Thomas, J.F., and J.E. Cotton. 1954. A turbidimetric sulfate determination. Water Sewage Works 101:462.

Tolen-Mehlhop, D.L. 1998. Mineralogical and chemical analysis of the Castle Hayne Aquifer in East-Central North Carolina. M.S. thesis, East Carolina Univ., Department of Geology, Greenville, NC.

Trainer, F.W., and R.C. Heath. 1976. Bicarbonate content of ground water in carbonate rock in eastern North America. Jour. of Hydrology 31:37-55.

Trapp, H., Jr., and H. Meisler. 1992. The regional aquifer system underlying the Northern Atlantic Coastal Plain in parts of North Carolina, Virginian, Maryland, Delaware, New

Jersey, and New York - Summary, U.S. Geol. Surv. Prof. Paper 1404-A.

Upchurch, M.L. 1973. Petrology of the Eocene Castle Hayne Limestone at Ideal Cement Quarry, New Hanover County, NC. M.S. thesis, University of North Carolina, Department of Geology, Chapel Hill, NC.

Vaughan, T.W. 1918. Correlations of the Tertiary geologic formations of the Southeastern United States, Central America, and the West Indies. Washington Academy of Sciences Journal 8:268-276.

Veizer, J. 1983. Trace elements and isotopes in sedimentary carbonates, *in* Ribbe, P.H. (ed.), Reviews in Mineralogy, v. 11, Mineralogical Society of America, Washington, D.C.

Veizer, J., and W. Compston. 1974. $^{87}Sr/^{86}Sr$ composition of sea water during the Phanerozoic. Geochim. Cosmochim. Acta 38:1461-84.

Ward, L.W. 1977. Stratigraphic revision of the Middle Eocene, Oligocene, and Lower Miocene - Atlantic Coastal Plain of North America. M.S. thesis, University of South Carolina, Department of Geology, Columbia, SC.

Ward, L.W., D.R. Lawrence, and B.W. Blackwelder. 1978. Stratigraphic revision of the Middle Eocene, Oligocene, and Lower Miocene Atlantic Coastal Plain of North Carolina. U.S. Geol. Surv. Bull. 1457F.

Ward, L.W., R.H. Bailey, and J.G. Carter. 1991. Pliocene and Early Pleistocene stratigraphy, depositional history, and Molluscan paleobiogeography of the coastal plain, *in* Horton J.W., Jr. and V.A. Zullo (eds.), The Geology of the Carolinas. Carolina Geol. Soc. 50th Anniv. Vol. Knoxville: Univ. of Tenn. Press, p. 274-89.

Warner, D. 1993. Hydrogeologic study of the Castle Hayne aquifer system in northern Beaufort County, North Carolina: Verification of well field design. M.S. thesis, East Carolina Univ., Department of Geology, Greenville, NC.

Weaver, C.E. 1989. Clays, muds, and shales: Developments in sedimentology no. 44. New York: Elsevier.

Wickman, F.W. 1948. Isotope ratios: A clue to the age of certain marine sediments. Jour. of Geol. 56:61-6.

Wilder, H.B., and C.E. Simons. 1982. Program for evaluating stream quality in North Carolina, *in* Water Quality of North Carolina Streams. U.S. Geol. Surv. Water-Supply Paper 2185-A.

Wilder, H.B., T.M. Robinson, and K.L. Lindskov. 1978. Water resources of northeast North Carolina. U.S. Geol. Surv. Water-Resources Investigations Report 77-81.

Willey, J.D., and R.H. Kiefer. 1990. A contrast in winter rainwater composition: Maritime versus continental rain in eastern North Carolina. Monthly Weather Review 118:488-94.

Willey, J.D., and R.H. Kiefer. 1993. Atmospheric deposition in southeastern North Carolina: Composition and quantity. The Journal of the Elisha Mitchell Scientific Soc. 109:1-19.

Willey, J.D., R.I. Bennett, J.M. Williams, R.K. Denne, C.R. Kornegay, M.S. Perlotto, and B.M. Moore. 1988. Effect of storm type on rainwater composition in southeastern North Carolina. Environmental Science and Technology 22:41-6.

Williams, P.J. 1975. Biological and chemical aspects of dissolved organic material in sea water, *in* Riley, J.P., and G. Skirrow (eds.), Chemical Oceanography, 2nd ed. v. 2. London: Academic Press, p. 301-63.

Wilson, T.R.S. 1975. Salinity and the major elements of sea water, *in* Riley, J.P., and G. Skirrow (eds.), Chemical Oceanography, 2nd ed. v. 2. London: Academic Press, p. 365-413.

Winner, M.D., Jr., and R.W. Coble. 1996. Hydrogeologic framework of the North Carolina Coastal Plain. U.S. Geol. Surv. Professional Paper 1404-I.

Winner, M.D., Jr., and W.L. Lyke. 1989. Aquifers in Cretaceous rocks of the central Coastal Plain of North Carolina. U.S. Geol. Surv. Water-Resources Investigations Report No. 87-7178.

Winner, M.D., Jr., and W.L. Lyke. 1986. History of ground-water pumpage and water-level decline in the Black Creek and Upper Cape Fear aquifers of the central Coastal Plain of North Carolina. U.S. Geol. Surv. Water-Resources Investigations Report No. 86-4168, 21 p.

Wood, W. W. 1976. Guidelines for collection and field analysis of ground-water samples for selected unstable constituents: Techniques of Water-Resources Investigations of the United

States Geological Survey, Book 1, Chapter D2, Washington, D.C.

Woods, T.L., L.C. Sutton, and P.D. Fullagar. 1994. Chemical and strontium isotope composition of ground water from the Eocene Castle Hayne Limestone of North Carolina [abs.]. American Geophysical Union - Spring Meeting Abstracts, Baltimore, MD, April 1994.

Zack, A.L. 1980. Geochemistry of fluoride in the Black Creek aquifer system of Horry and Georgetown Counties, South Carolina -- and its physiological implications. U.S. Geol. Surv. Water-Supply Paper 2067.

Zullo, V.A. and W.B. Harris. 1986. Introduçtion: Sequence stratigraphy, lithostratigraphy, and biostratigraphy of the North Carolina Eocene carbonates, *in* Textoris, D.A. (ed.), Society of Economic Paleontologists and Mineralogist Field Guidebook, Southeastern United States: Third Annual Midyear Meeting, Raleigh, North Carolina, p. 257-263.

GLOSSARY AND LIST OF ABBREVIATIONS

AA — atomic absorption spectrometry

CHAS — Castle Hayne Aquifer

$\delta^{13}C$ — del ^{13}C value is the unit in which carbon isotopic values ($\delta^{13}C$) are reported relative to a standard (PDB)

$$\delta^{13}C = \frac{R_{spl} - R_{std}}{R_{std}}$$

spl = sample
std = standard
R = the ratio of the heavy to the light isotope of an element = $^{13}C/^{12}C$ for carbon

$\delta^{18}O$ — del ^{18}O value is the unit in which oxygen isotopic values are reported relative to a standard (VSMOW)

$$\delta^{13}C = \frac{R_{spl} - R_{std}}{R_{std}}$$

spl = sample
std = standard
R = the ratio of the heavy to the light isotope of an element = $^{18}O/^{16}O$ for carbon

DOC — dissolved organic carbon

EDX — energy dispersive X-ray analysis

L-CHAS — Lower Castle Hayne Aquifer

meq/L — milliequivalents per liter

mgd — millions of gallons per day

mL — milliter

mol% — mol percent

mV — millivolts

NCDEHNR — North Carolina Department of Environment, Health, and Natural Resources

o/oo — parts per thousand

PCS	Potash Corporation of Saskatchewan - operates the phosphate mine at Aurora that was originally owned by the TexasGulf Corporation
PDB	standard to which carbon isotopic values ($\delta^{13}C$) are reported. Refers to the fossil, Peedee Belemnite, found in the Peedee Formation of South Carolina
POC	particulate organic carbon
sd	standard deviation
SEM	scanning electron microscope or microscopy
SFW	saline formation water of various origins found in aquifers
[Sr]	dissolved strontium concentration
TDS	total dissolved solids
U-CHAS	Upper Castle Hayne Aquifer
USGS	United States Geologic Survey
VSMOW	Vienna Standard Mean Ocean Water = the standard to which oxygen isotopic values ($\delta^{18}O$) are compared
wt.%	weight percent
XRD	X-ray diffraction

Appendix A: Chemical analyses of CHAS from previous studies

LOCATION NAME	WELL IDENTIFIER	COUNTY	DATE SAMPLED
SOUTHPORT MUNICIPAL	BR-16*	BRUNSWICK	6/8/58
US ARMY TERMINAL	BR-19*	BRUNSWICK	12/12/69
OLIVERS CROSS ROADS	T23x1#	JONES	3/30/87
COMFORT RESEARCH STATION	U26j5#	JONES	3/30/87
CAROLINA BEACH MUNICIPAL	NH-399*	NEW HANOVER	12/4/58
WILMINGTION PACKING CO.	NH-23*	NEW HANOVER	5/20/52
USMC CHERRY POINT	USMC 30%	CRAVEN	10/20/86
USGS WELL	CR-258*	CRAVEN	6/19/63
GG BRINSON (PRIVATE)	PA-75*	PAMLICO	8/24/61
WRIGHTSVILLE BEACH	NH-262*	NEW HANOVER	4/21/65
JW ALLEN (PRIVATE)	WS-82*	WASHINGTON	8/20/63
C FURLOUGH (PRIVATE)	WS-13*	WASHINGTON	9/1/63
CRESWELL MUNICIPAL	WS-27*	WASHINGTON	8/20/63
O JONES (PRIVATE)	BO-207*	BEAUFORT	3/18/55
SULLIVAN FISH FARM	FF 1^	BEAUFORT	4/30/91
NEW BERN	CR-479*	CRAVEN	11/19/52
C. J. ROBERSON	MR-347*	MARTIN	3/10/59

* = Wells from Knobel (1985)
# = Wells from NCDEHNR (1987)
% = Well from Lloyd and Daniel (1988)
^ = Richard Spruill (pers. comm.)

WELL IDENTIFIER	pH	TEMP °C	TEMP K	ALKALINITY as HCO_3^- ppm	HARDNESS mg eq $CaCO_3$/L	TDS ppm	Cl^- ppm
BR-16	7.3	ND	ND	323	267	525	142
BR-19	7.6	19	292	206	166	253	24
T23x1	8.1	ND	ND	160	124	170	4
U26j6	7.6	ND	ND	200	156	190	6
NH-399	8	16.5	289.5	203	165	236	25
NH-23	7.1	ND	ND	305	245	429	84
USMC 30	7.3	18	291	330	208	489	9
CR-258	7.4	ND	ND	203	171	290	6
PA-75	7.7	ND	ND	224	179	384	7
NH-262	7.6	15.5	288.5	222	189	502	109
WS-82	7.7	21	294	396	288	584	8
WS-13	8.2	22.5	295.5	606	149	1303	234
WS-27	8.1	ND	ND	604	306	2162	758
BO-207	7.7	ND	ND	400	238	612	19
FF 1	7.1	ND	ND	189	188	293	11
CR-479	7.3	ND	ND	249	ND	ND	7.5
MR-347	8.7	ND	ND	360	ND	ND	10

ND = Not Determined

WELL IDENTIFIER	F^- ppm	SO_4^{2-} ppm	SiO_2 ppm	NH_4^+ ppm	PO_4^{3-} ppm	Mg^{2+} ppm	Na^+ ppm	K^+ ppm
BR-16	ND	0.6	29	ND	ND	7	86	4
BR-19	0.1	3	38	ND	0.07	3	16	2
T23x1	0.2	3	11	0.11	0.07	1	3	1
U26j6	<0.1	5	7	0.09	0.17	1	3	0.7
NH-399	0.1	0.3	23	ND	ND	9	12	14
NH-23	0.1	2	41	ND	ND	9	58	ND
USMC 30	0.2	8	35	0.564	0.009	3	19	4
CR-258	ND	8	ND	ND	ND	4	6	1
PA-75	0.6	0.6	78	ND	ND	12	7	3
NH-262	0.3	10	17	ND	0.2	12	67	9
WS-82	0.5	0.6	50	ND	ND	30	19	14
WS-13	1.1	33	34	ND	0.1	24	320	30
WS-27	0.9	64	40	ND	ND	50	555	50
BO-207	0.6	0.1	52	ND	ND	28	38	24
FF 1	0.35	ND	ND	ND	ND	4.2	ND	ND
CR-479	0.1	7.7	17	ND	ND	1.8	ND	ND
MR-347	ND	3.5	10	ND	ND	29	ND	ND

WELL IDENTIFIER	Ca^{2+} ppm	LATITUDE	LONGITUDE	Na/Cl MOL RAT	K/Cl MOL RAT	Ca/Mg WEIGHT RAT
BR-16	95	33 54 41	78 07 28	0.93	0.02	13
BR-19	62	33 59 34	77 58 29	1.03	0.08	21
T23x1	48	35 00 14	77 17 43	1.04	0.23	44
U26j6	60	34 58 10	77 30 11	0.69	0.11	43
NH-399	51	34 01 47	77 53 57	0.74	0.51	6
NH-23	84	34 20 33	77 54 09	1.07	0	9
USMC 30	79	34 54 49	76 54 05	3.19	0.42	26
CR-258	62	35 05 44	77 09 08	1.5	0.18	16
PA-75	52	35 08 30	76 55 30	1.58	0.39	4
NH-262	56	34 11 18	77 48 37	0.94	0.07	5
WS-82	66	35 43 60	76 45 00	3.77	1.64	2
WS-13	20	35 55 15	76 32 15	2.09	0.12	1
WS-27	40	35 52 00	76 23 30	1.09	0.06	1
BO-207	49	35 39 22	76 41 05	3.15	1.15	2
FF 1	57	ND	ND	ND	ND	ND
CR-479	82	35 07 54	77 05 39	ND	ND	ND
MR-347	70	35 42 27	76 59 11	ND	ND	ND

Appendix B: Chemical analyses from Sutton and Woods (1995).

LOCATION NAME	WELL IDENTIFIER	COUNTY	DATE SAMPLED	pH
PLYMOUTH	K-17 a-5 (u)	Washington	5/23/93	7.39
GUM NECK	L-10 a-3 (u)	Tyrrell	5/11/93	7.37
GUM NECK	L-10 a-5 (l)	Tyrrell	5/11/93	7.31
LAKE PHELPS	L-13 i-1 (u)	Washington	5/7/93	8.05
LAKE PHELPS	L-13 i-5 (l)	Washington	5/7/93	7.67
NEW LAKE	M-12 l-1 (u)	Hyde	7/9/93	7.44
NEW LAKE	M-12 l-4 (l)	Hyde	5/5/93	7.33
NEW LAKE	M-12 l-4 (l)	Hyde	7/9/93	7.03
HUBS REC	N-15 y-5 (l)	Beaufort	5/10/93	7.46
HYDELAND	O-10 w-3 (u)	Hyde	5/6/93	7.38
SLADESVILLE	O-13 f-1 (u)	Hyde	5/10/93	7.67
SLADESVILLE	O-13 f-1 (u)	Hyde	7/8/93	7.57
RESEARCH STATION #3	O-17 i-2 (u)	Beaufort	5/17/93	7.15
FERRY LANDING	P-16 o-3 (l)	Beaufort	5/24/93	7.23
FERRY LANDING	P-16 o-4 (u)	Beaufort	5/27/93	7.18
WILMAR	P-21 k-6 (u)	Beaufort	5/17/93	7.27
HOBUCKEN	Q-15 u-3 (u)	Pamlico	5/18/93	7.41
HOBUCKEN	Q-15 u-5 (l)	Pamlico	5/27/93	7.49
TINGLEROAD	S-15 y-3 (l)	Pamlico	5/18/93	6.89
TINGLEROAD	S-15 y-4 (u)	Pamlico	5/18/93	7.17
TEXASGULF	TGCW11A (u)	Beaufort	5/20/93	7.09
TEXASGULF	TGCW14 (u)	Beaufort	6/21/93	7.27
TEXASGULF	TG S-11 (u)	Beaufort	6/21/93	7.21
TEXASGULF	TG S-11A (l)	Beaufort	6/21/93	7.29
TEXASGULF	TG S-15 (u)	Beaufort	5/20/93	6.92
TEXASGULF	TG S-18 (u)	Beaufort	6/21/93	7.41
TEXASGULF	TG S-28 (u)	Beaufort	6/22/93	7.03
WASHINGTON WELL FIELD #1	WWF #1 (b)	Beaufort	5/2/93	7.34
WASHINGTON WELL FIELD #2	WWF #2 (b)	Beaufort	5/26/93	7.64
WASHINGTON WELL FIELD #3	WWF #3 (b)	Beaufort	5/25/93	7.3
WASHINGTON WELL FIELD #4	WWF #4 (b)	Beaufort	5/22/93	7.2

(l) = L-CHA
(u) = U-CHA
(b) = Within both U- and L-CHA

WELL IDENTIFIER	TEMP °C	TDS ppm	Cl^- ppm	F^- ppm	SO_4^{2-} ppm	SiO_2 ppm	Fe^{2+} ppm
K-17 a-5 (u)	18	970	243	0.55	37	17.6	0.21
L-10 a-3 (u)	22	4690	1770	1.33	340	14.8	*7.60
L-10 a-5 (l)	21	8650	3630	1.17	790	10.6	*1.26
L-13 i-1 (u)	18	1290	55	1.96	90	16.3	0.32
L-13 i-5 (l)	20	1830	510	1.29	90	17.7	0.26
M-12 l-1 (u)	20	2090	520	3.2	180	16.8	0.19
M-12 l-4 (l)	20	10900	5500	1.31	1600	17.3	*3.12
M-12 l-4 (l)	22	10600	5100	1.35	1100	17.8	0.67
N-15 y-5 (l)	20	2090	760	1.19	120	17.4	*2.94
O-10 w-3 (u)	20	3730	1790	1.2	160	18.1	0.82
O-13 f-1 (u)	20	1700	470	1.49	110	20.2	*1.61
O-13 f-1 (u)	20	1720	470	1.52	110	19.5	0.15
O-17 i-2 (u)	18	620	54	0.6	0	32.2	0.78
P-16 o-3 (l)	21	1380	380	0.75	14	25.3	0.25
P-16 o-4 (u)	20	590	35	0.58	0	31	0.22
P-21 k-6 (u)	16	370	7	0.27	0	22.8	4.75
Q-15 u-3 (u)	20	950	134	1.11	35	26.4	0.19
Q-15 u-5 (l)	20	3660	1390	1.65	610	20.3	0.29
S-15 y-3 (l)	22	2440	1030	0.75	140	26	0.4
S-15 y-4 (u)	19	640	27	0.56	0	27.8	0.19
TGCW11A (u)	18	530	9	0.61	0	37.1	0.48
TGCW14 (u)	23	380	6	0.29	0	20.8	0.71
TG S-11 (u)	20	610	24	0.7	0	29.3	1.08
TG S-11A (l)	22	4900	2260	1.71	380	18.5	0.43
TG S-15 (u)	17	520	13	0.19	0	37.4	*9.29
TG S-18 (u)	22	490	5	1.01	0	29.1	0.23
TG S-28 (u)	18	530	7	0.23	0	32.6	3.3
WWF #1 (b)	17	310	7	0.15	1	17.3	2.93
WWF #2 (b)	17	360	4	0.19	0	27.8	2.89
WWF #3 (b)	17	380	8	0.4	0	21.2	1.2
WWF #4 (b)	17	390	5	0.27	0	32.3	1.13

* Inaccurate due to particulates

WELL IDENTIFIER	Mg^{2+} ppm	Na^{+} ppm	K^{+} ppm	Ca^{2+} ppm	HCO_3^{-} ppm	Br^{-} ppm	S^{2-} ppm
K-17 a-5 (u)	37	164	23	49	395	0	0.12
L-10 a-3 (u)	127	1690	82	54	600	3	ND
L-10 a-5 (l)	318	3130	124	129	498	8	0.06
L-13 i-1 (u)	12	305	22	7	783	0	ND
L-13 i-5 (l)	38	470	36	20	642	7	ND
M-12 l-1 (u)	41	560	39	21	688	3	1.55
M-12 l-4 (l)	251	3190	103	131	468	5	ND
M-12 l-4 (l)	273	3360	121	140	468	4	2.35
N-15 y-5 (l)	49	550	37	30	517	5	0.02
O-10 w-3 (u)	96	980	54	41	574	9	ND
O-13 f-1 (u)	25	450	27	18	570	3	0.06
O-13 f-1 (u)	28	480	29	19	556	2	0.47
O-17 i-2 (u)	25	28	11	74	393	0	0.01
P-16 o-3 (l)	52	323	26	71	478	4	7.1
P-16 o-4 (u)	28	19	13	57	407	0	0.03
P-21 k-6 (u)	4	10	1	77	242	0	0.01
Q-15 u-3 (u)	32	170	18	29	503	0	2.6
Q-15 u-5 (l)	80	920	40	41	542	16	1.1
S-15 y-3 (l)	96	560	31	84	453	0	2.6
S-15 y-4 (u)	38	22	12	63	444	0	0.57
TGCW11A (u)	9	11	4	81	371	0	5.8
TGCW14 (u)	5	8	1	69	264	0	0.02
TG S-11 (u)	30	39	16	51	415	0	0.28
TG S-11A (l)	102	1470	58	57	532	23	0.01
TG S-15 (u)	7	15	2	82	346	0	0.02
TG S-18 (u)	19	43	13	49	329	0	0.04
TG S-28 (u)	6	10	4	103	361	0	0.01
WWF #1 (b)	1	6	1	59	215	0	ND
WWF #2 (b)	3	10	1	63	249	0	0
WWF #3 (b)	4	7	2	62	273	0	0
WWF #4 (b)	4	9	2	65	273	0	0.01

ND = Not Determined

WELL IDENTIFIER	PO_4^{3-} ppm	Al^{3+} ppm	Li^{+} ppm	Mn^{2+} ppm	Zn ppm	NH_4^{+} ppm	NO_3^{-} ppm
K-17 a-5 (u)	0.009	0.03	0.03	<0.01	0.06	0.92	<0.001
L-10 a-3 (u)	0.012	0.07	0.08	0.05	0.01	6.62	0.001
L-10 a-5 (l)	0.016	0.03	0.11	0.02	0.01	7.89	<0.001
L-13 i-1 (u)	0.064	0.09	0.02	0.01	0.01	1.04	0.001
L-13 i-5 (l)	0.017	0.09	0.03	0.01	<0.01	1.49	0.001
M-12 l-1 (u)	0.0009	0.02	0.05	0.01	0.01	2.28	0.004
M-12 l-4 (l)	<0.001	0.03	0.09	0.07	<0.01	5.07	0.003
M-12 l-4 (l)	0.003	0.09	0.1	0.01	0.21	5.42	0.006
N-15 y-5 (l)	0.015	0.06	0.04	0.02	0.02	0.8	0.002
O-10 w-3 (u)	0.023	0.11	0.06	0.05	<0.01	3.99	0.002
O-13 f-1 (u)	0.039	0.09	0.03	0.03	0.02	1.03	0.002
O-13 f-1 (u)	0.012	0.01	0.03	<0.01	0.02	1.44	0.004
O-17 i-2 (u)	0.004	0.03	0.03	0.03	0.01	0.88	0.002
P-16 o-3 (l)	0.015	0.02	0.03	<0.01	0.09	1.18	0.001
P-16 o-4 (u)	0.028	<0.01	0.01	<0.01	0.03	0.93	<0.001
P-21 k-6 (u)	0.086	0.17	0.01	0.09	0.01	0.15	0.002
Q-15 u-3 (u)	0.04	0.02	0.02	0.01	<0.01	0.77	0
Q-15 u-5 (l)	0.017	0.03	0.04	0.01	0.06	0.9	0.002
S-15 y-3 (l)	0.003	0.22	0.03	<0.01	<0.01	1.12	0.004
S-15 y-4 (u)	0.006	0.02	0.01	0.01	<0.01	0.58	0
TGCW11A (u)	0.023	0.01	0.03	0.01	0.01	0.79	0.002
TGCW14 (u)	0.004	0.01	0.01	0.01	0.16	0.25	0.001
TG S-11 (u)	0.004	<0.01	0.02	0.01	<0.01	0.98	0.002
TG S-11A (l)	0.003	0.1	0.06	0.02	1.88	1.19	0.005
TG S-15 (u)	0.042	0.05	0.04	0.34	0.02	0.48	0.006
TG S-18 (u)	0.003	0.16	0.02	<0.01	1.51	0.76	0.005
TG S-28 (u)	0.004	0.06	0.03	0.15	1.04	0.38	0.002
WWF #1 (b)	0.076	0.04	0.01	0.08	0.01	0.06	<0.001
WWF #2 (b)	0.025	0.07	0.02	0.13	0.06	0.21	0.003
WWF #3 (b)	0.037	<0.01	0.02	0.06	0.09	0.34	0.001
WWF #4 (b)	0.025	0.05	0.03	0.07	0.16	0.33	<0.001

Appendix C: Results of incomplete chemical analyses from this study

Well Identifier	Aquifer	County	Latitude	Longitude
K 17a 4	Beaufort	Washington	35 54' 38"	76 51' 49"
K 17a 5	U-CHAS	Washington	35 54' 38"	76 51' 49"
K 17a 6	L-CHAS	Washington	35 54' 38"	76 51' 49"
L 13 i 1	U-CHAS	Washington	35 43' 51"	76 26' 05"
L 13 i 2	Y	Washington	35 43' 51"	76 26' 05"
L 13 i 5	L-CHAS	Washington	35 43' 51"	76 26' 05"
M 12 l 1	U-CHAS	Hyde	35 37' 20"	76 21' 18"
M 12 l 4	L-CHAS	Hyde	35 37' 20"	76 21' 18"
M 12 l 6	Y	Hyde	35 37' 20"	76 21' 18"
O 10 w1	Y	Hyde	35 25' 22"	76 12' 26"
O 10 w3	U-CHAS	Hyde	35 25' 22"	76 12' 26"
P 16 o 3	L-CHAS	Beaufort	35 22' 39"	76 44' 58"
P 16 o 4	U-CHAS	Beaufort	35 22' 39"	76 44' 58"
P 21 k 6	CHAS	Beaufort	35 22' 53"	77 05' 19"
P 21 k 7	PD	Beaufort	35 22' 53"	77 05' 19"
Q 15 u 3	U-CHAS	Pamlico	35 15' 00"	76 15' 00"
Q 15 u 5	L-CHAS	Pamlico	35 15' 00"	76 15' 00"
Q 15 u 6	Y	Pamlico	35 15' 00"	76 15' 00"
S 15 y 1	Y	Pamlico	35 05' 24"	76 38' 52"
S15 y 3	L-CHAS	Pamlico	35 05' 24"	76 38' 52"
S 15 y 4	U-CHAS	Pamlico	35 05' 24"	76 38' 52"
S 18 u 3	Y	Pamlico	35 05' 08"	76 50' 08"
S 18 u 5	CHAS	Pamlico	35 05' 08"	76 50' 08"
S 18 u 6	U-CHAS	Pamlico	35 05' 08"	76 50' 08"
S 18 u 7	PR	Pamlico	35 05' 08"	76 50' 08"
TGs15	U-CHAS	Beaufort	35 32' 57"	76 56' 25"
Plant	CHAS	Beaufort	35 30' 00"	76 56' 46"
Slatestone	CHAS	Beaufort	35 32' 9"	76 59' 44"
Far East	CHAS	Beaufort	35 29' 55"	76 52' 30"

ND = Not Determined

Y = Yorktown

PD = Peedee

PR = Pungo River

Appendix C: Results of incomplete chemical analyses from this study

Well Identifier	Sample Date	Alkalinity as HCO_3^- ppm	Temp C	pH	DO ppm	S^- ppm
K 17a 4	3/27/97	586	19.5	7.81	0.356	0.0
K 17a 5	3/27/97	403	19.0	7.37	0	0.2
K 17a 6	3/27/97	300	19.0	7.46	0	0.0
L 13 i 1	4/30/97	789	18.0	7.82	0	0.0
L 13 i 2	4/30/97	284	17.0	7.15	0	0.0
L 13 i 5	5/9/97	659	19.5	7.60	0	0.2
M 12 l 1	4/3/97	682	20.5	7.66	0	5.0
M 12 l 4	4/3/97	480	21.0	7.29	0	0.0
M 12 l 6	4/3/97	447	ND	7.15	0	0.0
O 10 w1	4/21/97	280	18.0	7.46	0	1.0
O 10 w3	4/21/97	577	21.0	7.34	0	3.0
P 16 o 3	3/20/97	478	20.0	7.20	0	0.0
P 16 o 4	3/20/97	400	19.0	7.29	0	0.0
P 21 k 6	3/19/97	254	17.0	7.18	0	0.0
P 21 k 7	5/10/97	290	18.0	7.40	0.17	0.0
Q 15 u 3	5/6/97	498	20.0	7.37	0	4.0
Q 15 u 5	5/6/97	542	21.0	7.23	0	1.0
Q 15 u 6	5/6/97	280	19.0	6.98	0	0.0
S 15 y 1	5/8/97	272	18.0	7.15	0	0.0
S15 y 3	5/8/97	446	21.0	7.09	0	4.0
S 15 y 4	5/8/97	444	19.0	7.06	0	1.0
S 18 u 3	4/25/97	150	ND	7.66	0.387	0.0
S 18 u 5	3/29/97	430	ND	7.12	0	2.0
S 18 u 6	3/22/97	359	19.0	7.25	0	0.0
S 18 u 7	3/22/97	190	18.0	7.36	0.184	0.0
TGs15	5/9/97	344	17.0	6.90	0	0.0
Plant	3/11/97	262	17.0	7.45	0	0.0
Slatestone	3/13/97	249	18.0	7.34	0	0.0
Far East	3/13/97	305	ND	7.41	0	0.2

ND = Not Determined

Y = Yorktown

PD = Peedee

PR = Pungo River

Appendix C: Results of incomplete chemical analyses from this study

Well Identifier	SiO_2 ppm	SO_4^{2-} ppm	PO_4^{3-} ppm	NO_3^{2-} ppm	NO_2^- ppm	NH^{4+} ppm	Cl^- ppm
K 17a 4	6.95	327.49	0.019	0.0002	0.0033	1.58	1927
K 17a 5	19.81	36.36	0.008	0.0005	0.0064	0.95	55.2
K 17a 6	17.04	2.01	0.008	0.0002	0.0067	0.94	56.1
L 13 i 1	6.47	83.68	0.058	0.0005	0.0064	0.91	47.3
L 13 i 2	15.91	ND	0.07	0.0031	0.0038	0.69	7.44
L 13 i 5	18.34	63.64	0.018	0.0005	0.0064	1.49	434
M 12 l 1	15.75	107.90	0.032	0.0028	0.0041	1.68	443
M 12 l 4	16.05	839.47	0.009	0.0004	0.0075	3.96	4700
M 12 l 6	22.04	1.77	0.167	0.0047	0.0000	1.35	24.4
O 10 w1	8.99	1.65	0.022	0.0013	0.0056	2.35	241
O 10 w3	10.00	97.75	0.029	0.0013	0.0056	3.28	1795
P 16 o 3	23.12	19.29	0.013	0.001	0.0059	1.18	592
P 16 o 4	26.24	1.77	0.009	0.0031	0.0027	1.03	45.7
P 21 k 6	19.73	12.25	0.257	0.0026	0.0009	0.13	13.5
P 21 k 7	18.76	8.53	0.006	0.0007	0.0037	0.37	18.7
Q 15 u 3	20.39	66.95	0.024	0.0015	0.0085	0.82	128
Q 15 u 5	16.06	153.53	0.019	0.001	0.0083	1.1	1395
Q 15 u 6	19.14	ND	0.042	0.0026	0.0021	0.19	0.906
S 15 y 1	13.76	ND	0.094	0.001	0.0037	0.09	23.7
S15 y 3	19.79	74.80	0.024	0.0013	0.0034	0.78	1020
S 15 y 4	25.37	1.53	0.009	0.0021	0.0026	0.42	21.6
S 18 u 3	13.10	1.77	0.092	0.0015	0.0032	0.82	1.17
S 18 u 5	14.00	1.89	0.016	0.001	0.0013	1.28	27
S 18 u 6	25.61	1.65	0.006	0.0013	0.0034	2.29	10.9
S 18 u 7	21.88	1.65	0.167	0.0013	0.0034	1.64	9
TGs15	34.19	ND	0.626	0.0026	0.0021	0.48	12.3
Plant	45.10	ND	0.125	0.0021	0.0049	0.19	1.17
Slatestone	17.93	10.50	0.195	0.0023	0.0047	0.08	1.45
Far East	29.05	1.53	0.013	0.0015	0.0032	1.21	0.726

ND = Not Determined

Y = Yorktown

PD = Peedee

PR = Pungo River

Appendix C: Results of incomplete chemical analyses from this study

Well Identifier	Fl^- ppm	Fe^{2+} ppm	K^+ ppm	Mg^{2+} ppm	Ca^{2+} ppm	Na^+ ppm
K 17a 4	1.37	0.23	64.18	63.91	20.76	886.59
K 17a 5	0.69	0.12	25.87	37.83	61.78	94.28
K 17a 6	0.61	0.55	23.26	33.94	54.59	25.87
L 13 i 1	2.11	0.08	24.59	12.9	7.24	150.05
L 13 i 2	0.32	4.49	0.89	4.15	65.52	7.57
L 13 i 5	1.42	0.12	55.87	38.25	21.24	250.98
M 12 l 1	1.42	0.06	42.40	38.25	19.58	199.46
M 12 l 4	1.46	0.78	142.72	232.73	124.16	1785.75
M 12 l 6	0.27	2.92	5.98	18.24	80.75	35.95
O 10 w1	0.38	0.28	58.56	66.49	49.84	130.74
O 10 w3	1.27	0.11	69.79	112.44	63.86	460.14
P 16 o 3	0.84	0.28	27.52	46.97	89.8	167.50
P 16 o 4	0.66	0.28	12.97	32.16	68.68	20.88
P 21 k 6	0.3	5.72	1.26	4.28	83.78	8.14
P 21 k 7	0.71	0.24	11.86	19.7	55.74	43.53
Q 15 u 3	1.2	0.1	31.00	33.89	41.95	65.01
Q 15 u 5	1.77	0.22	48.79	88.69	56.85	531.73
Q 15 u 6	0.24	7.71	5.48	5.32	123.15	20.02
S 15 y 1	0.12	8.75	0.84	3.3	69.25	10.52
S15 y 3	0.85	0.15	31.56	88.17	108.04	269.30
S 15 y 4	0.61	0.15	11.74	37.19	86.37	21.17
S 18 u 3	0.18	0.68	7.08	8.67	39.08	5.23
S 18 u 5	0.67	0.18	19.84	29.57	77.29	54.46
S 18 u 6	0.5	0.04	15.48	23.87	68.39	9.36
S 18 u 7	0.19	0.22	4.95	11.28	39.65	4.84
TGs15	0.22	16.4	26.35	8.57	70.98	14.07
Plant	0.24	2.4	1.98	4.44	64.08	8.00
Slatestone	0.13	3.97	1.23	1.96	64.08	6.49
Far East	0.36	0.01	5.18	13.21	65.8	8.83

ND = Not Determined

Y = Yorktown

PD = Peedee

PR = Pungo River

Appendix C: Results of incomplete chemical analyses from this study

Well Identifier	$d^{18}O$ wrt VSMOW	$d^{13}C$ wrt PDB	POC $mgC/_L$	DOC $mgC/_L$	TOC $mgC/_L$
K 17a 4	-4.14	-6.82	0.592	0.462	1.05
K 17a 5	-4.63	-11.79	1.47	1.14	2.61
K 17a 6	-4.65	-12.20	0.241	0.715	0.96
L 13 i 1	-4.49	-7.93	2.28	1.9	4.18
L 13 i 2	-4.63	-4.38	0.063	1.82	1.88
L 13 i 5	-4.06	-6.54	1.79	1.49	3.28
M 12 l 1	-3.77	-5.66	0.442	0.76	1.20
M 12 l 4	-3.59	-2.61	0.946	1.67	2.62
M 12 l 6	-4.79	-6.67	0.562	1.24	1.80
O 10 w1	-3.71	-6.37	0.322	1.41	1.73
O 10 w3	-3.12	-3.36	0.093	0.312	0.41
P 16 o 3	-3.69	-8.60	0.91	0.868	1.78
P 16 o 4	-4.04	-11.16	1.81	0.37	2.18
P 21 k 6	-4.94	-13.70	ND	0.319	ND
P 21 k 7	-4.65	-12.93	0.681	1.96	2.64
Q 15 u 3	-4.51	-9.10	0.972	0.839	1.81
Q 15 u 5	-4.15	-4.31	0.861	1.02	1.88
Q 15 u 6	-4.55	-14.68	0.719	1.15	1.87
S 15 y 1	-4.71	-15.28	0.158	0.159	0.32
S15 y 3	-3.77	-12.00	1.33	0.814	2.14
S 15 y 4	-3.72	-12.79	1.04	0.934	1.97
S 18 u 3	-5.04	-9.13	0.082	1.22	1.30
S 18 u 5	-4.4	-12.76	0.998	0.993	1.99
S 18 u 6	-4.65	-9.29	0.682	1.21	1.89
S 18 u 7	-4.75	-9.09	1.17	1.37	2.54
TGs15	-5.06	-16.29	0.601	1.64	2.24
Plant	ND	ND	ND	ND	ND
Slatestone	-5.28	-14.00	0.968	0.477	1.45
Far East	-5.12	-14.51	0.964	0.7	1.66

ND = Not Determined

Y = Yorktown

PD = Peedee

PR = Pungo River

Appendix D: Results of CHAS chemical analyses in Southern Coastal Plain

LOCATION NAME	WELL IDENTIFIER	COUNTY	DATE SAMPLED
TOWN CREEK	DD33y1(pd)	BRUNSWICK	7/17/95
BOILING SPRINGS	FF32y1(pd)	BRUNSWICK	7/18/95
SOUTHPORT	GG32t4(pd)	BRUNSWICK	7/17/95
SOUTHPORT	SPPW 002(u)	BRUNSWICK	6/17/96
SOUTHPORT	SPPW 003(u)	BRUNSWICK	6/17/96
BRUNSWICK CO. WELL FIELD	BCPW 3(b)	BRUNSWICK	6/18/96
BRUNSWICK CO. WELL FIELD	BCPW 5(b)	BRUNSWICK	6/18/96
BRUNSWICK CO. WELL FIELD	BCPW 7(b)	BRUNSWICK	6/18/96
BRUNSWICK CO. WELL FIELD	BCPW 15(b)	BRUNSWICK	6/18/96
BRUNSWICK CO. WELL FIELD	BCPW 18(b)	BRUNSWICK	6/18/96
SNEADS FERRY WELL FIELD	SFOW 1(l)	ONSLOW	2/13/96
SNEADS FERRY WELL FIELD	SFOW 2(l)	ONSLOW	2/12/96
SNEADS FERRY WELL FIELD	SFOW 3(l)	ONSLOW	1/27/96
SNEADS FERRY WELL FIELD	SFOW 4(l)	ONSLOW	2/12/96
HUBERT WELL FIELD	HPW 2(l)	ONSLOW	3/5/96
HUBERT WELL FIELD	HPW 3(l)	ONSLOW	3/5/96
HUBERT WELL FIELD	HOW 5(u)	ONSLOW	2/27/96
DIXON FIRE TOWER	Y25Q1(u)	ONSLOW	3/5/96
ATLANTIC BEACH WELL FIELD	ABPW 5(u)	CARTERET	6/20/96
ATLANTIC BEACH WELL FIELD	ABPW 6(u)	CARTERET	6/20/96
BOGUE BANKS WELL FIELD	BBPW 2(u)	CARTERET	6/21/96
BOGUE BANKS WELL FIELD	BBPW 5(u)	CARTERET	6/21/96
BOGUE BANKS WELL FIELD	BBPW 7(u)	CARTERET	6/21/96
SURF CITY	Pe 72(u)	PENDER	6/20/96

(u) = U-CHA
(l) = L-CHA
(pd) = Peedee
(b) = within both CHAS and Peedee

WELL IDENTIFIER	pH	Eh mV	Eh corrected	Eh V	pe	TEMP °C	TEMP K
DD33y1	7.3	-152	92	0.092	1.6	18	291
FF32y1	6.9	-127	117	0.117	2.03	19	292
GG32t4	7.4	-148	96	0.096	1.66	20	293
SPPW 002	7.5	-74	170	0.17	2.92	20	293
SPPW 003	7.5	-98	146	0.146	2.51	20	293
BCPW 3	7.1	-110	124	0.124	2.32	17.5	290.5
BCPW 5	7.26	-150	94	0.094	1.62	19	292
BCPW 7	7.25	-130	114	0.114	1.97	19	292
BCPW 15	7.1	-184	60	0.06	1.03	19	292
BCPW 18	7.14	-102	142	0.142	2.45	19	292
SFOW 1	7.4	-95	149	0.149	2.6	18	291
SFOW 2	7.4	-100	144	0.144	2.51	18.5	291.5
SFOW 3	7.2	-296	-52	-0.052	-0.9	19	292
SFOW 4	6.8	-169	75	0.075	1.31	18	291
HPW 2	7.2	-108	136	0.136	2.36	19	292
HPW 3	7.35	-115	129	0.129	2.25	18.5	291.5
HOW 5	7.28	-115	129	0.129	2.23	18	291
Y25Q1	7.3	-184	60	0.06	1.04	18.5	291.5
ABPW 5	7.14	-38	206	0.206	3.55	19	292
ABPW 6	7.1	-207	37	0.037	0.64	21	294
BBPW 2	7.23	-210	34	0.034	0.58	20	293
BBPW 5	7.18	-250	-6	-0.006	-0.1	19	292
BBPW 7	7.14	-167	77	0.077	1.37	21	294
Pe 72	7.36	-120	124	0.124	2.14	19	292

WELL IDENTIFIER	ALKALINITY as HCO_3^- ppm	HARDNESS mg eq $CaCO_3$/L	DO ppm	TDS ppm	Cl^- ppm
DD33y1	215	173	0.000	333	21
FF32y1	371	247	0.000	567	29
GG32t4	268	198	0.000	487	71
SPPW 002	203	194	0.412	409	76
SPPW 003	217	181	0.040	387	50
BCPW 3	325	227	0.000	484	24
BCPW 5	244	190	0.000	376	22
BCPW 7	249	188	0.000	384	25
BCPW 15	320	228	0.000	474	21
BCPW 18	337	237	0.000	501	21
SFOW 1	266	209	0.032	399	19
SFOW 2	243	206	0.350	377	20
SFOW 3	395	239	0.000	853	250
SFOW 4	290	217	0.000	467	25
HPW 2	245	208	0.000	387	31
HPW 3	210	183	0.000	340	31
HOW 5	244	203	0.000	373	24
Y25Q1	253	191	0.000	413	31
ABPW 5	317	249	0.048	487	26
ABPW 6	358	278	0.020	545	28
BBPW 2	293	233	0.154	454	28
BBPW 5	288	291	0.000	846	360
BBPW 7	343	272	0.130	536	31
Pe 72	200	192	0.024	342	33

WELL IDENTIFIER	S^- ppm	F^- ppm	SO_4^{2-} ppm	SiO_2 ppm	NH_4^+ ppm	PO_4^{3-} ppm	NO_3^- ppm
DD33y1	0.00	0.08	13	3	0.040	0.013	0.002
FF32y1	0.00	0.14	22	16	0.220	0.020	0.001
GG32t4	0.00	0.18	8	8	0.520	0.013	0.002
SPPW 002	0.00	0.13	4	9	0.242	0.043	< 0.001
SPPW 003	0.00	0.13	3	12	0.310	0.045	< 0.001
BCPW 3	0.00	0.09	5	15	0.300	0.158	< 0.001
BCPW 5	0.00	0.12	5	9	0.255	0.161	< 0.001
BCPW 7	0.00	0.12	4	10	0.229	0.134	< 0.001
BCPW 15	0.00	0.09	9	10	0.240	0.130	< 0.001
BCPW 18	0.00	0.12	4	22	0.453	0.145	< 0.001
SFOW 1	0.00	0.26	0.3	13	0.140	0.000	< 0.001
SFOW 2	0.00	0.26	0.2	13	0.170	0.002	0.001
SFOW 3	4.50	0.60	11	24	0.450	0.008	0.001
SFOW 4	0.00	0.21	20	17	0.340	0.005	< 0.001
HPW 2	0.00	0.11	3	8	0.060	0.120	0.002
HPW 3	0.14	0.08	3	7	0.030	0.110	0.001
HOW 5	0.00	0.19	1	9	0.060	0.096	0.001
Y25Q1	0.00	0.12	7	24	0.170	0.220	0.027
ABPW 5	0.00	0.26	4	17	0.697	0.009	< 0.001
ABPW 6	0.00	0.37	4	20	0.769	0.008	< 0.001
BBPW 2	0.10	0.37	4	14	0.376	0.006	< 0.001
BBPW 5	1.50	0.24	13	13	0.415	0.012	< 0.001
BBPW 7	0.05	0.19	3	20	0.564	0.009	< 0.001
Pe 72	0.00	0.17	5	8	0.036	0.108	< 0.001

WELL IDENTIFIER	NO_2^- ppm	Fe^{2+} ppm	Mg^{2+} ppm	Na^+ ppm	K^+ ppm	Ca^{2+} ppm	LATITUDE	LONGITUDE
DD33y1	0.001	1	2	8	4	66	34 10 18	78 09 56
FF32y1	0.002	4	3	20	8	94	34 00 52	78 04 58
GG32t4	0.001	0.7	8	40	17	66	33 56 37	78 00 38
SPPW 002	0.003	0.3	4	31	10	71	33 55 34	78 01 02
SPPW 003	0.003	0.4	4	26	8	66	33 55 41	78 01 42
BCPW 3	0.003	3	3	16	6	86	33 58 20	78 05 10
BCPW 5	0.003	2	3	14	5	71	33 57 10	78 05 05
BCPW 7	0.003	2	2	15	5	72	33 56 40	78 05 37
BCPW 15	0.003	2	2	16	6	88	33 59 00	78 06 09
BCPW 18	0.003	2	3	16	5	90	33 58 55	78 03 55
SFOW 1	0.001	0.6	4	12	7	77	34 34 32	77 29 05
SFOW 2	0.002	0.5	4	12	8	76	34 34 05	77 29 24
SFOW 3	0.001	0.2	9	50	27	81	34 33 34	77 29 38
SFOW 4	0.001	7	6	15	9	77	34 32 56	77 29 55
HPW 2	0.003	0.9	2	12	5	80	34 43 10	77 13 57
HPW 3	0.003	0.8	2	11	5	70	34 43 32	77 14 03
HOW 5	0.001	1	2	9	5	78	34 44 16	77 14 24
Y25Q1	0.003	4	4	15	4	70	34 36 39	77 28 59
ABPW 5	0.003	0.1	6	13	13	90	34 42 05	76 44 30
ABPW 6	0.003	0.1	13	16	15	90	34 42 05	76 42 31
BBPW 2	0.003	0.1	5	14	10	85	34 40 02	77 01 36
BBPW 5	0.003	0.3	10	40	20	100	34 39 24	77 04 09
BBPW 7	0.003	0.1	12	18	19	89	34 41 21	76 52 36
Pe 72	0.003	0.7	6	16	6	67	34 26 40	77 33 33

WELL IDENTIFIER	CALCIUM SAT. INDEX	FERRIHYDRITE SAT. INDEX	GYPSUM SAT. INDEX	DOLOMITE SAT. INDEX	Na/Cl MOL RAT
DD33y1	-0.08	0.57	-2.42	-1.49	0.61
FF32y1	-0.14	0.22	-2.14	-1.55	1.05
GG32t4	0.11	0.65	-2.69	-0.43	0.86
SPPW 002	0.13	1.77	-3	-0.71	0.63
SPPW 003	0.14	1.52	-3.03	-0.66	0.81
BCPW 3	-0.02	0.94	-2.82	-1.24	1.05
BCPW 5	-0.03	0.66	-2.87	-1.24	1.03
BCPW 7	-0.03	1.01	-2.91	-1.29	0.92
BCPW 15	0.00	-0.55	-2.53	-1.45	1.22
BCPW 18	0.07	1.14	-2.83	-1.09	1.16
SFOW 1	0.16	1.48	-4.03	-0.67	0.99
SFOW 2	0.13	1.27	-4.23	-0.76	0.91
SFOW 3	0.11	-3.19	-2.54	-0.46	0.31
SFOW 4	-0.42	-0.53	-2.24	-1.66	0.91
HPW 2	-0.04	0.84	-3.09	-1.42	0.59
HPW 3	-0.01	1.15	-3.05	-1.36	0.53
HOW 5	0.02	1.02	-3.44	-1.34	0.54
Y25Q1	0.01	0.47	-2.67	-1.02	0.75
ABPW 5	0.04	0.85	-2.87	-0.8	0.81
ABPW 6	0.07	-2.43	-2.96	-0.38	0.87
BBPW 2	0.09	-1.79	-2.94	-0.79	0.78
BBPW 5	0.04	-2.2	-2.39	-0.68	0.17
BBPW 7	0.09	-1.58	-3.09	-0.4	0.87
Pe 72	-0.04	1.02	-2.88	-0.85	0.76

WELL IDENTIFIER	K/Cl MOL RAT	Ca/Mg WEIGHT RAT
DD33y1	0.16	33
FF32y1	0.25	31
GG32t4	0.22	8
SPPW 002	0.12	18
SPPW 003	0.15	17
BCPW 3	0.22	29
BCPW 5	0.21	24
BCPW 7	0.17	36
BCPW 15	0.28	44
BCPW 18	0.23	30
SFOW 1	0.32	19
SFOW 2	0.37	19
SFOW 3	0.1	9
SFOW 4	0.32	13
HPW 2	0.16	40
HPW 3	0.14	35
HOW 5	0.19	39
Y25Q1	0.13	18
ABPW 5	0.45	15
ABPW 6	0.49	7
BBPW 2	0.34	17
BBPW 5	0.05	10
BBPW 7	0.55	7
Pe 72	0.15	11

Appendix E: EDX analyses of glauconite

		Weight % Oxide					# of ions on the basis of 22 O equivalents, ignoring H_2O^+ 8.00=					
							Tetrahedral		Octahedral			
Sample	Depth (feet)	SiO_2	Al_2O_3	Fe_2O_3	MgO	K_2O	Si	Al	Al	Fe^{+3}	Mg	K
A1-unkn2	385-395	55	18	13	9	5	7.0	1.0	1.7	1.2	1.7	0.9
A1-unkn3		57	18	12	8	5	7.1	0.9	1.9	1.1	1.6	0.8
A1-unkn4		58	18	10	9	5	7.3	0.7	1.9	1.0	1.7	0.8
A1-unkn5		56	10	19	8	8	7.4	0.6	0.9	1.8	1.5	1.3
A2-unkn6	425-435	54	9	19	7	7	7.4	0.6	0.9	2.0	1.5	1.2
A2-unkn7		57	8	21	7	7	7.5	0.5	0.7	2.1	1.5	1.2
A2-unkn8		59	8	17	8	7	7.7	0.3	1.0	1.7	1.5	1.2
A3-unkn1	455-465	56	18	13	8	6	7.1	0.9	1.8	1.2	1.4	0.9
A3-unkn3		54	13	17	8	7	7.1	0.9	1.2	1.7	1.6	1.2
A4-unkn1	465-475	54	17	14	8	6	7.0	1.0	1.6	1.3	1.6	1.0
A4-unkn2		56	16	12	9	7	7.1	0.9	1.6	1.2	1.7	1.1
A4-unkn3		58	13	15	8	6	7.4	0.6	1.4	1.4	1.6	0.9
A5-unkn1	495-505	57	12	14	9	8	7.4	0.6	1.2	1.4	1.7	1.3
A5-unkn4		55	18	13	8	6	7.0	1.0	1.7	1.3	1.5	0.9
A5-unkn5		57	13	16	8	6	7.3	0.7	1.3	1.6	1.5	1.0
A5-unkn6		53	15	18	9	5	6.9	1.1	1.3	1.7	1.7	0.8
A8-unkn1	565-575	57	9	19	7	8	7.5	0.5	1.0	1.9	1.4	1.3
A8-unkn2		58	13	13	8	7	7.5	0.5	1.5	1.3	1.5	1.2
A8-unkn3		56	12	17	8	7	7.3	0.7	1.2	1.7	1.5	1.1
A8-unkn4		59	15	11	9	6	7.5	0.5	1.6	1.1	1.7	1.0
A8-unkn5		57	11	17	8	7	7.4	0.6	1.2	1.6	1.5	1.2
A9-unkn1	575-585	63	10	16	3	8	8.0	0.0	1.5	1.6	0.7	1.3
A9-unkn2		61	8	18	5	8	7.9	0.1	1.2	1.8	1.0	1.3
A9-unkn3		61	11	15	5	8	7.8	0.2	1.5	1.4	1.0	1.3
A9-unkn4		69	6	11	4	10	8.7	0.0	0.9	1.0	0.8	1.5
A9-unkn5		58	11	16	8	7	7.6	0.4	1.2	1.6	1.5	1.2

		Weight % Oxide					# of ions on the basis of 22 O equivalents, ignoring H_2O^+ 8.00=					
							Tetrahedral		Octahedral			
Sample	Depth (feet)	SiO_2	Al_2O_3	Fe_2O_3	MgO	K_2O	Si	Al	Al	Fe^{+3}	Mg	K
B1-unkn6	465-475	54	11	20	8	6	7.1	0.9	0.8	2.0	1.7	1.1
B3-unkn3	495-505	44	33	12	7	5	5.6	2.4	2.5	1.1	1.3	0.8
B3-unkn6		58	11	16	9	6	7.5	0.5	1.1	1.6	1.7	1.0
B3-unkn7		58	13	15	9	6	7.4	0.6	1.4	1.4	1.6	1.0
B4-unkn3	515-525	58	11	15	9	8	7.5	0.5	1.1	1.5	1.7	1.3
B4-unkn4		57	10	17	8	8	7.5	0.5	1.1	1.6	1.6	1.3
B6-unkn4	545-555	54	18	15	7	6	7.0	1.0	1.7	1.4	1.4	1.0
B6-unkn5		53	20	13	8	6	6.8	1.2	1.8	1.2	1.5	0.9
B6-unkn6		52	16	18	8	6	6.8	1.2	1.3	1.7	1.6	1.0
B6-unkn7		55	14	17	7	6	7.2	0.8	1.3	1.7	1.4	1.0
B7-unkn2	585-595	56	14	15	8	7	7.2	0.8	1.3	1.5	1.6	1.1
B7-unkn3		55	21	11	8	6	6.9	1.1	2.0	1.0	1.5	0.9
B7-unkn4		56	15	15	8	6	7.2	0.8	1.5	1.4	1.6	1.1
B7-unkn5		56	14	14	9	6	7.2	0.8	1.4	1.4	1.8	1.0
B7-unkn6		54	20	12	8	5	6.9	1.1	1.9	1.2	1.6	0.9
B8-unkn1	605-615	60	18	8	9	5	7.4	0.6	2.1	0.7	1.7	0.7
B8-unkn2		60	17	11	8	4	7.4	0.6	1.9	1.1	1.5	0.7
B8-unkn3		56	15	15	8	6	7.2	0.8	1.4	1.5	1.6	1.0
C2-unkn2	266-276	57	12	17	7	6	7.4	0.6	1.2	1.7	1.4	1.0
C2-unkn3		56	13	17	8	6	7.2	0.8	1.2	1.7	1.5	1.0
C2-unkn4		54	10	20	9	7	7.2	0.8	0.8	2.0	1.7	1.2
C2-unkn5		55	11	19	8	7	7.3	0.7	0.9	1.8	1.6	1.2
C2-unkn6		52	10	24	8	6	6.9	1.1	0.5	2.4	1.6	1.0
C2-unkn7		53	13	20	8	7	7.0	1.0	1.0	2.0	1.5	1.2
C11-unkn1	296-306	57	12	18	7	6	7.4	0.6	1.2	1.8	1.3	1.1
C11-unkn2		56	10	21	7	6	7.3	0.7	0.9	2.1	1.3	1.0
C11-unkn3		53	12	22	6	6	7.2	0.8	1.0	2.2	1.1	1.0
C11-unkn5		58	8	22	6	6	7.6	0.4	0.9	2.2	1.1	1.1
C11-unkn10		52	15	17	9	6	6.8	1.2	1.2	1.7	1.8	1.0

		Weight % Oxide					# of ions on the basis of 22 O equivalents, ignoring H_2O^+ 8.00=					
							Tetrahedral		Octahedral			
Sample	Depth (feet)	SiO_2	Al_2O_3	Fe_2O_3	MgO	K_2O	Si	Al	Al	Fe^{+3}	Mg	K
C11-unkn11	296-306	55	12	18	8	7	7.3	0.8	1.0	1.8	1.6	1.1
C12-unkn4	356-366	59	12	13	9	8	7.6	0.4	1.3	1.3	1.7	1.3
C12-unkn5		59	11	15	8	8	7.6	0.4	1.2	1.4	1.6	1.3
C6-unkn3	376-386	58	14	13	9	6	7.4	0.6	1.4	1.3	1.8	0.9
C6-unkn4		58	14	13	10	6	7.4	0.6	1.4	1.2	1.8	1.0
C6-unkn5		58	14	12	10	6	7.4	0.6	1.4	1.2	1.9	1.0
C6-unkn6		56	14	14	10	7	7.2	0.8	1.3	1.3	1.9	1.1
C6-unkn7		59	13	12	10	6	7.5	0.5	1.5	1.1	1.9	1.0
C6-unkn8		59	14	11	10	7	7.4	0.6	1.5	1.0	1.9	1.1
C6-unkn9		57	15	13	9	6	7.3	0.7	1.6	1.2	1.7	1.0
C6-unkn10		59	14	11	10	6	7.5	0.5	1.6	1.0	1.9	1.0
C6-unkn11		45	26	18	6	5	5.9	2.1	1.9	1.7	1.2	0.9
C7-unkn5	386-396	46	25	13	6	6	6.1	1.9	2.1	1.4	1.3	1.0
C8-unkn1	426-436	58	9	2	9	8	7.5	0.5	0.9	1.7	1.7	1.3
C8-unkn4		58	10	18	6	7	7.6	0.4	1.2	1.8	1.2	1.1
C9-unkn1	446-456	60	11	15	6	7	7.8	0.2	1.5	1.5	1.1	1.2
C1-unkn2	466-476	61	8	18	5	8	7.9	0.1	1.2	1.7	1.0	1.3
D1-unkn1	24-30	58	10	17	8	8	7.6	0.4	1.1	1.6	1.5	1.3
D1-unkn2		58	12	15	8	7	7.5	0.5	1.3	1.5	1.5	1.2
D1-unkn3		59	11	14	9	7	7.6	0.4	1.3	1.4	1.7	1.2
D1-unkn4		58	12	14	8	7	7.5	0.5	1.4	1.3	1.6	1.2
D2-unkn1	30-32	67	15	6	8	5	8.1	0.0	2.1	0.5	1.4	0.8
D2-unkn2		68	13	7	6	4	8.3	0.0	1.9	0.7	1.2	0.7
D2-unkn3		59	14	15	8	3	7.5	0.5	1.6	1.4	1.5	0.5
D4-unkn1	45-52	60	15	10	7	7	7.6	0.4	1.9	1.0	1.4	1.1
D4-unkn5		59	8	16	8	8	7.7	0.3	1.0	1.6	1.6	1.3
D4-unkn7		59	9	18	8	7	7.7	0.4	1.0	1.8	1.5	1.2
D4-unkn8		54	14	20	6	6	7.0	1.0	1.1	2.0	1.3	1.1
D5-Glauc1	52-62	65	9	17	0	8	8.3	0.0	1.4	1.7	0.0	1.4

		Weight % Oxide					# of ions on the basis of 22 O equivalents, ignoring H_2O^+ 8.00=					
							Tetrahedral		Octahedral			
Sample	Depth (feet)	SiO_2	Al_2O_3	Fe_2O_3	MgO	K_2O	Si	Al	Al	Fe^{+3}	Mg	K
D5-Glauc2	52-62	66	7	16	3	9	8.5	0.0	1.1	1.5	0.5	1.5
D5-unkn1		57	18	11	8	7	7.3	0.7	1.9	1.0	1.4	1.1
D5-unkn2		59	13	14	8	8	7.6	0.4	1.4	1.3	1.5	1.3
D5-unkn3		62	11	12	7	8	7.9	0.1	1.6	1.1	1.4	1.3
D5-unkn6		59	12	15	7	7	7.6	0.4	1.4	1.5	1.4	1.1
D5-unkn7		60	23	11	0	6	7.4	0.6	2.8	1.0	0.0	0.9
D5-unkn9		60	11	14	8	8	7.7	0.3	1.3	1.4	1.5	1.3
D5-unkn10		60	11	15	7	8	7.7	0.3	1.3	1.4	1.3	1.3
E3-unkn2	231-240	64	11	9	7	9	8.1	0.0	1.6	0.9	1.3	1.4
F3-unkn1	178-198	54	15	17	9	5	7.0	1.0	1.3	1.7	1.7	0.9
F3-unkn2		55	15	15	9	7	7.1	0.9	1.4	1.4	1.7	1.1
F3-unkn3		55	15	18	7	6	7.1	0.9	1.3	1.7	1.4	0.9
F3-unkn4		53	17	17	9	5	6.8	1.2	1.4	1.6	1.7	0.8
F4-unkn1	198-203	55	15	15	8	7	7.2	0.8	1.4	1.5	1.5	1.2
F4-unkn3		57	14	15	8	6	7.3	0.7	1.5	1.4	1.5	1.0
F4-unkn4		58	14	14	7	7	7.4	0.6	1.5	1.4	1.4	1.1
F4-unkn6		59	13	14	8	7	7.6	0.4	1.5	1.3	1.5	1.2
F4-unkn7		57	8	20	8	8	7.5	0.5	0.7	2.0	1.6	1.3
F4-unkn8		57	11	17	7	8	7.5	0.5	1.2	1.7	1.4	1.3
F5-unkn1	203-218	59	9	20	4	8	7.7	0.3	1.2	2.0	0.8	1.3
F5-unkn2		57	12	17	7	8	7.4	0.6	1.2	1.6	1.3	1.3
F5-unkn3		56	10	19	8	7	7.4	0.6	0.9	1.9	1.5	1.1
F5-unkn4		55	10	20	8	7	7.2	0.8	0.8	2.0	1.6	1.2
F5-unkn5		54	12	19	8	7	7.1	0.9	1.0	1.8	1.6	1.2
F6-unkn1	238-243	64	10	15	4	7	8.1	0.0	1.5	1.4	0.7	1.1
F6-unkn2		70	6	16	0	8	8.9	0.0	0.9	1.5	0.0	1.2
F6-unkn3		59	8	21	6	6	7.7	0.3	0.8	2.1	1.3	1.1
F6-unkn4		60	6	22	5	7	7.9	0.1	0.8	2.1	1.0	1.2
F6-unkn5		60	11	15	7	7	7.7	0.3	1.4	1.5	1.2	1.2

Sample	Depth (feet)	Weight % Oxide				
		SiO_2	Al_2O_3	Fe_2O_3	MgO	K_2O
F6-unkn6	238-243	61	4	24	4	6
F6-unkn7		61	11	14	7	7
F6-unkn8		60	7	21	6	6
F6-unkn9		62	4	21	6	7

# of ions on the basis of 22 O equivalents, ignoring H_2O^+ 8.00=

Tetrahedral	Octahedral				
Si	Al	Al	Fe^{+3}	Mg	K
8.1	0.0	0.7	2.4	0.7	1.1
7.8	0.2	1.5	1.3	1.3	1.1
7.8	0.2	0.9	2.0	1.2	1.0
8.1	0.0	0.6	2.1	1.1	1.2